The Mechanical Contact Behaviour and Tribology of Polymer Gears

by

Khalid Abdulkhaliq M. Alharbi

MSc (Eng.), BSc (Eng.)

A thesis submitted in partial fulfilment of the requirements
for the degree of
Doctor of Philosophy in Engineering

University of Warwick, School of Engineering

February 2018

Contents

List of Figures

List of Tables

Acknowledgments

The author would like to acknowledge the supervision and kind support of Prof Derek Chetwynd and Dr Ken Mao during the work on this research project.

Thanks go to the School of Engineering for the availability of research facilities.

Also, thanks go to Umm Alqura University for the scholarship and financial funding for this degree research work.

Finally, special thanks go to my family and friends for their valuable and endless support throughout the years spent in this work, especially, my mother, my father, my wife and my two sons.

Declaration

This thesis is submitted to the University of Warwick in support of my application for the degree of Doctor of Philosophy. It has been composed by myself and has not been submitted in any previous application for any degree. The work presented (including data generated and data analysis) was carried out by the author.

Parts of this thesis have been published by the author (by date sequence):

The wear and thermal mechanical contact behaviour of machine cut polymer gears, Wear 2015;332–333:pp822–826 (co-authored)

Polymer Gear Wear and Performance Prediction, Proceedings of the Fourth Annual Postgraduate Symposium 2016, School of Engineering, The University of Warwick, UK (first author)

Polymer Gear Wear and Failure Analysis: The Case of Acetal and Nylon Gears, Proceedings of the Ninth Saudi Students Conference 2016, Birmingham, UK (first author)

Wear and Performance of Polymer Gears, Proceedings of the Fifth Annual Postgraduate Symposium 2017, School of Engineering, The University of Warwick, UK (first author)

Wear and mechanical contact behaviour of polymer gears, ASME: Journal of Tribology, 2017, in press (first author)

Abstract

Interest in using polymer gears has been growing dramatically in the last decade. Increasing understanding of their working behaviour has improved appreciation of their advantages compared to their limitations when selecting appropriate applications. However, restricted knowledge still leaves many unfulfilled areas that might benefit from their valuable advantages and control of their limitations, for example, in replacing. their metallic counterparts in more applications. Given their very different materials properties, it is important to develop bespoke design and rating methods for polymer gears, with properly validated rules, that are not mere modifications to metallic gearing rating methods. A major aim of this thesis is to provide a new deeper understanding for use when designing and rating some technologically important types of polymer gears for wider applications.

Having identified an important research gap in polymer gearing theory and practice, this thesis covers mostly experimental studies involving continuously monitored wear and wear rate and microscopic evaluation of underlying tribologies. It examines the behaviour of polymer gears made of acetal, nylon (moulded and machine-cut) and polycarbonate, all common gearing materials, during and after running under different physically realistic conditions. Some modifications to test rigs uniquely designed to operate at a continually constant load enable study of surface thermal behaviour under dry and lubricated conditions and with simulations of moderate gear misalignments.

In dry-running cases, gear load capacity and wear behaviour of different polymers and variations in underlying tribology all presented important relations between the gear tooth wear rate, the applied load and the tooth surface temperature. Quite similar patterns were seen under oil lubricated conditions. Typically, though, there was a nearly three-fold improvement in gear load capacity, the wear rate and gear tooth surface temperature were decreased, and SEM showed some changes in surface tribology. Finally, deliberately introduced angular misalignments between gear pairs indicated a reasonable tolerance of small but practical levels, with different tribological behaviours between the left and right sides of the tooth surfaces. A severe increase in wear rate and tooth failure arose from misalignments above 0.8° yaw angle and 0.4° pitch angle.

After a unifying discussion, conclusions are drawn and further work is proposed for extended studies over different parameter ranges.

Nomenclature and Abbreviations

Nomenclature

A	Area of the gear housing	mm^2
a	Half contact width	
b	Gear face width	mm
c	Specific heat	
CD	Gear centre distance	mm
d	Gear pitch circle diameter	mm
e	diffusivity of air	
H	Transmitted power	W
K_2	Empirical values which depend on whether the polymer gear is paired with polymer or with steel	
K_3	Empirical values which depend on the design of the drive housing	
k	Thermal conductivity	
k_s	Specific wear rate	m^3/Nm
L_{ab}	The line of action	mm
m	Gear module	mm

m_c	Gear contact ratio	--
n	Number of teeth	--
N	Number of cycles	--
p	Circular pitch	mm
Q	Wear depth (as measured in the tests) at the pitch line	mm
q_a	Arc of approach	mm
q_r	Arc of recess	mm
q_t	Arc of action	mm
r	Reference radius	mm
r_a	Outside radius	mm
T	Torque transmitted	N
V_1	Sliding velocity for gear 1	m/s
V_2	Sliding velocity for gear 2	m/s
α	Yaw misalignment angle	Degrees
β	Pitch misalignment angle	Degrees
θ	Pressure angle	Degrees
θ_a	Gear ambient temperature	°C
θ_b	Gear body temperature	°C
θ_f	Gear flash temperature	°C

θ_{max}	Maximum body temperature	^{o}C
ε	Thermal emissivity	--
ρ	Specific gravity	
ω_1	Driving gear angular velocity	RPM
ω_2	Driven gear angular velocity	RPM

Abbreviations

CD	Gears Centre Distance
IDMS	Image Dimension Measurement System
LVDT	Linear Variable Differential Transformer
PA	Polyamide
PC	Polycarbonate
POM	Polyoxymethylene
RPM	Revolutions Per Minutes
STA	Simultaneous Thermal Analysis

Chapter 1
INTRODUCTION

1.1 Preamble

From their beginnings up to the present (and continuing), humankind has developed many different tools to help with, and overcome, their limited abilities and cope more easily, faster and more reliably with life's daily demands. One of the issues that they were faced with was transmitting and benefiting from the natural power they explored around them; for instance, the wind, flowing water and animals are all often potential sources of kinetic energy that could aid tasks, such as harvesting and grinding crops and seeds. This led them to invent different tools that are used for power transmission [1]. Among these tools were gears, which were thought to be firstly built in different shapes starting from triangle and pin shapes and ending up with a circular shape [2]. Gears were continuously being better practically developed and understood as craft objects (by skilled craftsman) until the 16th century, when the theory of gearing was formed. Then the involute curve theory followed in the 18th century, which formed the new generation of gear shapes that is still being used. Since being introduced, these gears have remained one of the fundamental classes of devices in the mechanical engineering field, especially useful in power transmission with the advantages of high efficiency, low losses and no slip.

After the emergence of steam turbines and the industrial revolution in the 19th century, the focus was on developing gears for higher power transmission at higher speed. This led to the requirement of understanding gear tooth strength calculations which were first developed by Wilfred Lewis in 1892 [3]. This method of gear rating is still being used for the calculations of gear tooth strength (with some modifications and

correction factors) and is known as the Lewis equation. This was followed by the requirement of using gears for torque amplification that required the development of gear rating techniques depending on gear strength, life and endurance. Some new rating methods took into account the surface durability in the case of wear and thermal factors [4]. Having these gear rating methods enabled the issuing of some common gear standards that are used over the globe to simplify the design and use of gears in the commercial sector [5–7].

Standardizing gears kept the evolution of tooth shape more stable for a while, with the involute profile as the most common gear tooth shape which uses a pressure angle of 20° (~0.35 rad). Further development was shifted to focus on trying different materials for the requirements of light weight, less noise and low cost, reflecting new policies for environmentally safer products. More attention was paid to the use of polymer materials in gearing applications for their suitability to these new requirements.

1.2 The background to polymer gearing

Given the requirement of finding new materials to be used in gearing for gaining different benefits, such as lower cost, noise and weight, polymer were one class of the potential materials to be used more widely in engineering applications. They offer many advantages, compared to metals, namely [8]:

- Low production cost (10-50% less than the cost of metal gears, especially when injection moulded in large batches, and cost can be reduced using multi-cavity moulds to produce multiple gears simultaneously [9]).
- Faster and easier to produce in complex shapes and different colours.

- Lighter and lower inertia.
- Some materials are quieter in operation than metal gears due to their internal damping and resilience.
- The ability to operate in low or no lubrication medium with high efficiency output.
- Higher resistance to environmental corrosion.

Beside these advantages, raw material production of polymers consumes less specific energy than metal production, making them more environmentally friendly. For instance, the process of producing one ton of plastic raw material requires around 1.2 barrels of oil and that produces less carbon footprint compared to one ton of steel production, which consumes around 3.1 barrels of oil leading to the emission of 1550 kg of CO_2. Although these figures are for 'commodity' plastics, they may also give a good prediction of how far polymers are more environmentally friendly than metals in the case of production processes [10,11].

Metal gears are not usually the preferable choice for medical or laboratory devices, because lubricants are always required for smooth and low noise running; both lubricants and the metals can be sources of contamination, bio-activity, etc. Similar arguments apply to the chemical industries. This is not the case with their polymer counterparts, where lubricants are not required in some cases or can be embedded in polymer materials as internal lubricants [9]. In addition, the light weight of polymer gears gives them good advantages in applications where weight is one of the crucial factors of functioning; a good example of this is aerospace applications [12].

For these reasons, polymer gears may take over from metal gears in applications that require such advantages, although they are traditionally used in low load motion transmission applications. Examples of polymer gears can be found in printers, household appliances, and even electric vehicles. Polymer gears are taking over from metallic gears in more applications as their advantages become more easily exploited. Two billion polymer gears are produced every year, and this number is

massively higher than the number of steel gears produced in the same year [13].

The automotive industry is one of the sectors that most benefits from these advantages, as they focus on improving their products. A recent study shows that using polymer gears in automotive industry reduces energy consumption by around 9%, as a result of decreases in gear weights by 70% and, consequently, gear inertias by 80% [14].

Despite polymer gears having all these advantages, their applications, are still limited because they have some limitations, which include:

- Their load capacity is limited to about 64 kW (for PEEK gears with 2 mm module, 30 teeth, 17 mm face width and 60 mm pitch diameter) due to their low stiffness [15,16].
- Low maximum running temperature, with risk of material softening.
- Low thermal conductivity.
- Relatively unstable shape dimensions (when produced), due to thermal effects and moisture absorption [17].
- The gap in knowledge for their design and rating methods, which are normally derived from the rating techniques used for metal gears [18,19]. This design and rating method is still employed by the British Standard 6168 and other standards, in line with designers and users in the commercial sector [5,6].

Optimum performance in polymer gears cannot be achieved using the current method of rating metal gears, which relies mostly on the Lewis formula [20] and calculates the stress concentration on the gear tooth root. Such a rating technique is not adequate with polymer gears because they have been found to be more affected by thermal factors [21], as well as various wear of materials phenomena (i.e. stiffens and creep) [4,22]. Currently, the effects of these parameters on polymer gear operation are still under investigation [23–26]. On the other hand, some other polymer gears standards attempt to involve the effect of thermal phenomena in the

design rules, but lack fully accurate temperature prediction [7], as an understanding of this topic is still under development [27]. Using metal gear ratings to rate polymer gears leads to failure in most mechanical systems and so generically limits non-metallic gear applications. For this reason, an understanding of polymer gear behaviour has become very important to understand and employ these mechanical devices more appropriately, to increasingly gain from their advantages and overcome their limitations.

Because of the wide disagreement between metal gear and polymer gears in case of manufacturing techniques and mechanical and chemical properties, it is required to develop specific rating methods that are appropriate for designing fully functional polymer gears.

These issues will be studied in greater detail in Chapter 2.

1.3 Research aim, questions and objectives

The longer-term aim of this research project is to investigate the behaviour of different types of polymer gears, under different running conditions using systematic testing and investigation methodologies, in order to provide a new, deeper understanding for such mechanical devices to be taken into account when designing and rating those gears for wider applications.

Achieving this aim requires considerably deeper understanding of the behaviour of polymer gears under realistic conditions, in term of both good quality experimental data and modelling.

The brief background above and literature review that follows in Chapter 2 highlights that there remain serious, unresolved research questions concerning durability. They also show that although some attempts have been made to study tooth temperature and manufacturing method, there is

not yet enough data, nor even adequately precise methods, for answering questions about the practical usefulness of current thermal models.

To achieve the aim of this research project, the following research questions were set out:

1. What is the practical load capacity of different types of polymer gears and what are their limitations?
2. What is the wear rate behaviour of those polymer gears with respect to load changes?
3. How is their surface temperature behaving while in continuous running?
4. What is the surface tribology of different polymer gear teeth that were running at different conditions?
5. What is the effect of oil lubrication on polymer gear wear behaviour, surface temperature and surface tribology?
6. What is the effect of different types of gear misalignments that might occur in real applications on polymer gear wear behaviour, surface temperature and surface tribology?

To answer those research questions, the main objectives of this thesis are:

(i) To review the relative literature about polymer gears.
(ii) To design a systematic research methodology that includes testing and investigating the targeted samples, during and after tests.
(iii) To improve the test rigs used to achieve the requirements of the designed methodology.
(iv) To test the targeted samples, with continuously logging of tooth surface wear, time and surface temperature parameters.
(v) To tribologically investigate the samples after the tests.
(vi) To study the load capacity of different types of polymer gears.

(vii) To investigate the tribological behaviour of the dry-running polymer gear teeth.
(viii) To measure the polymer gear teeth surface temperature while in dry-running.
(ix) To study the effect of oil lubrication on polymer gear wear, tribology and performance.
(x) To measure the polymer gear teeth surface temperature while in oil lubrication running.
(xi) To investigate the effect of different types of gear misalignment on the wear, tribology and performance of polymer gears.
(xii) To measure the polymer gear teeth surface temperature while in misalignment running.
(xiii) To analyse the result data, discuss it and link it with the reviewed literature.

It was anticipated that further research could be carried out to find the possibilities of improving durability and endurance of polymer gears. Such achievements might open up a new area of extending the use of polymer gears in more advanced applications that require more durable materials and mechanical parts in lighter weights.

Theoretical estimations of gear surface temperature are still under development and do not provide the required information for proper non-metallic gear design. Therefore, the current research was to focus more on failure modes and the wear rate of polymer gears, while further deep investigations would concentrate on heat build-up measurements and calculations.

1.4 Thesis outline

As stated above, the main aim of this research project is to investigate the behaviour of different types of polymer gears during testing and by after test investigation. Therefore, this thesis contains eight chapters, which

address the research questions in a logical order, starting with an introduction and ending by the conclusion. The chapter outlines are as follows:

Chapter 1 Introduction

The introduction provides a general background about polymer gears, including their advantages, limitations and their promises for future improvements. In addition, it illustrates the research aim, questions and objectives.

Chapter 2 Polymer gears and tribology: a review

Chapter 2 summarises the relevant literature around polymer gears, starting with the general terminologies of gearing, then moving to the research work trends on important topics. The review then covers the tribology and mechanical properties of polymer materials, focussing on gearing applications. In addition, the current practice of polymer gearing design is discussed, including polymer gear standards and the theoretical methods of calculating the gear contact ratio. The literature review then moves to the failure mechanisms and analysis of polymer gears, followed by one of the most important factors on those gears failure, which is the thermal effect. The effect of oil lubrication and gear misalignment on polymer gearing is also discussed. Finally, polymer gear testing methods are reviewed.

Chapter 3 Research methodology

This chapter illustrates the systematic methodologies that were used in this research project. It starts by defining the two polymer gear test rigs (dry running and oil lubrication) used and the measurements and data logging methods of wear, time and surface temperature. The chapter then talks about the properties of the tested samples. Finally, the after-test investigations using different methods are illustrated.

Chapter 4 Load capacity and wear behaviour of polymer gears

After reviewing the literature and illustrating the research methodology, this is the first chapter of the results and discussions. It presents the results of step-loading tests for different polymer gear types to define the wear rate at different load ranges, in addition to the gear load capacity.

Chapter 5 Tribology of dry-running polymer gears

Here some endurance test results are presented, analysed and discussed. The results cover the wear and wear rate at different loads and speeds, in addition to the gear tooth surface temperature. The chapter includes the after-test surface tribological investigations, analysis and discussions.

Chapter 6 Polymer gears and oil lubrication

In this chapter, the effect of oil lubrication on polymer gear performance is discussed. This includes the wear and wear rate change and surface temperature behaviour. Gear load

capacity change is also illustrated. More endurance experiments at different load levels are presented. And the after-test investigations are analysed and discussed.

Chapter 7 The effect of misalignment on polymer gears

In chapter 7, the most active misalignment types are modelled in experiments designed for this purpose. Polymer gear wear and wear rate are presented against the amount of misalignment angle and discussed. Surface temperature change is reported and discussed. The after-test surface tribological investigations are analysed and discussed.

Chapter 8 Conclusion and future work

A general conclusion to the whole thesis is provided, including general summaries for each result and discussion chapter. In addition, it gives recommendations for future works.

Chapter 2
POLYMER GEARS AND TRIBOLOGY: A REVIEW

2.1 Introduction

In the previous chapter, the importance of understanding polymer gears, as promising mechanical devices, was clarified and the research objectives of this work were defined. This chapter presents a comprehensive review of the literature around the topic focusing on the relevant materials. It includes a survey about the state of art of gears as mechanical devices, their terminologies, their applications, their current design and rating techniques, gear lubrication, and their different types of wear and failure mechanisms. In addition, it presents information about engineering polymer materials and their mechanical and tribological properties, including wear and surface damage behaviours. Important difference between metal and polymer gears are explored and, especially, thermal effects in polymer gears are discussed. Finally, through this critical analysis a research gap is defined and reflected by the objectives of this research.

This research project will cover some areas under the topic of the performance of polymer gears, which include failure and endurance of these gears. This research is aiming ultimately to propose a new design method for polymer gears.

A review of the literature related to the area of this research will be covered, including the mechanical properties of polymer materials and polymer gears as well as failure mechanisms and failure modes in polymer

gears. Then, the relation between the literature covered and the research objectives of this project will be stated.

2.2 Fundamentals of gearing

One of the main functions of gearing is to deliver the kinetic energy and the mechanical rotational movement between two or more shafts. Other functions including, speed change, shift of the motion angle and between angular and linear, fluid pumping applications and so on. The focus in this research will be on the first main function.

The earliest gearing system was claimed to be of two friction discs [20]. Many gear shape improvements have been made to increase the power capacity of such devices in addition to the increase of efficiency and motion stability (vibration reduction). The invention of the gear tooth involute profile was one of the most active improvements that has been used over since. Figure 2.1 shows the generation of the tooth involute profile from unwrapping a rope from a circle, while a point on the rope generates the curve [28]. Figure 2.2 shows the generation of the tooth involute profile from a belt that was attached to the base circles of two pulleys [29]. While rotating, both pinion and gear involute curves are continually normal to the belt line. This profile was classified as one of the conjugate gearing concepts, which claimed to provide a stable motion between the driving and driven gears, with constant velocity ratio fluctuations [3], even with the change of the centre distance between the mating gears, a feature that made it one of the most common profile that is used in gearing applications.

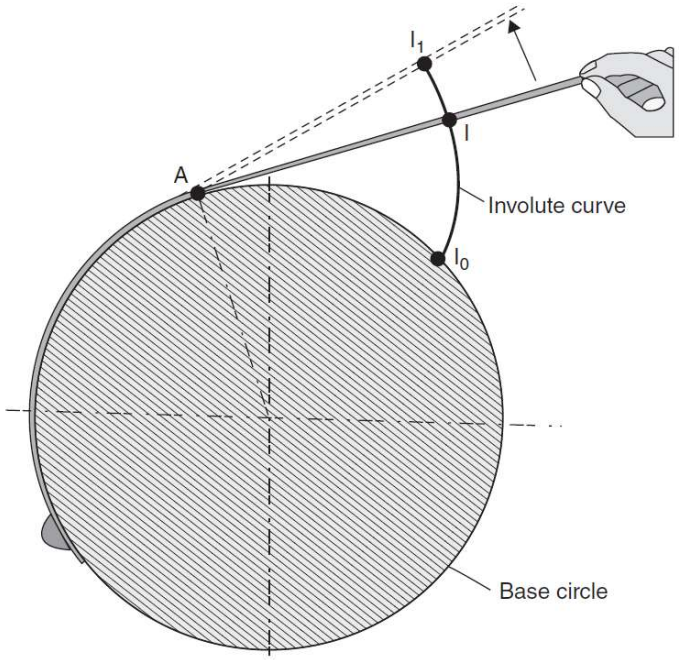

Figure 2.1 Involute profile generating from a wrapped rope [28].

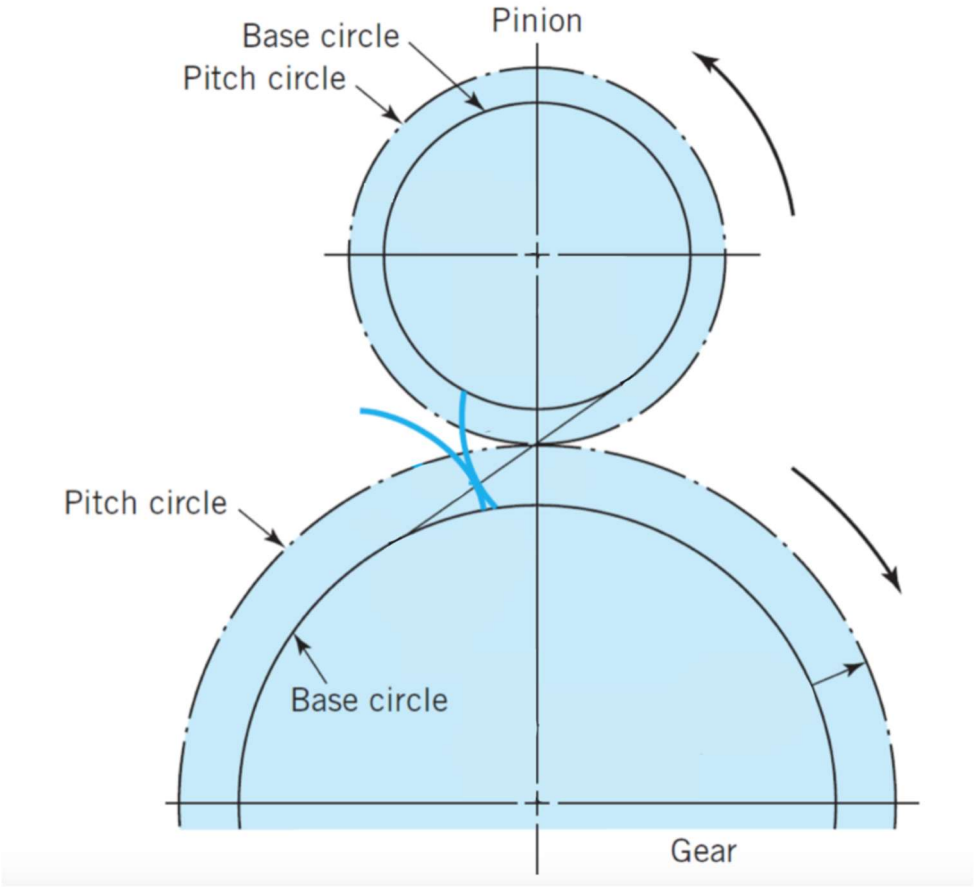

Figure 2.2 Involute profile generating from two pulleys and a belt [29].

Spur gears are the most common type that was increasingly used with the establishment of the conjugate theory, for their easily defined shape and manufacturing. Figure 2.3 shows a 3D view for part of a spur gear, with the important nomenclature illustrated [29]. These terminologies will be used as mentioned here, throughout this work, with the pair of gears assigned as driving and driven, because all the research work will be focused on the 1:1 ratio, as the limitation of the available test rig, although this case may not always reflect the real life applications where variable speed ratios differ the surface temperature between the mating gears, which affect the polymer gearing behaviour.

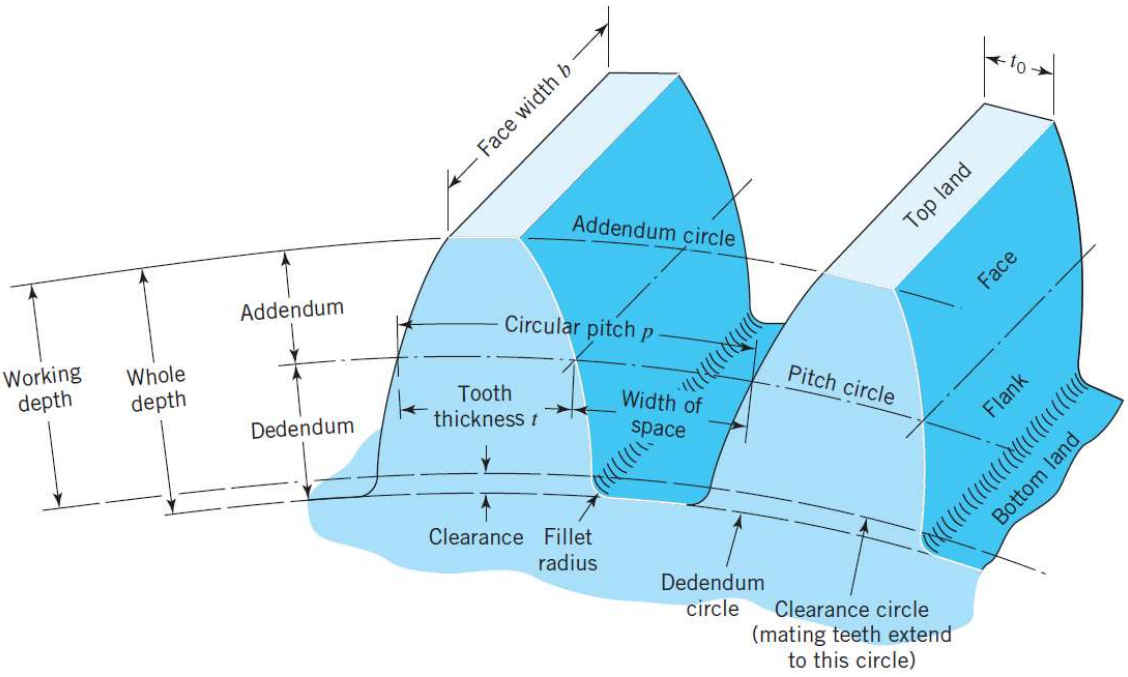

Figure 2.3 Spur gear nomenclature [29]

Mainly, spur gear teeth are geometrically classified by what is so called the gear module (m), which can be defined as:

$$m = \frac{d}{n} \tag{2.1}$$

where d is the pitch circle diameter and n is the number of teeth.

The circular pitch (p) in Figure 2.3 can be defined by:

$$p = \frac{\pi d}{n} \tag{2.2}$$

Most of the gear geometries can be defined in term of pitch circle diameter (d), which is a theoretical circle that intersects with the other meshing gear pitch circle in a point that is called the pitch point. The distance between the centres of the two circles is called the centre distance (CD), which is calculated as:

$$CD = \frac{d_1 + d_2}{2} \tag{2.3}$$

where d_1 and d_2 are the driving and the driven pitch circle diameters, respectively.

While in mesh, a gear pair goes through different engagement stages. Figure 2.4 shows the terminologies of a pair of spur gears in different places of contact, in addition to further spur gear nomenclature [29]. These nomenclatures will be used as here in all relative places in this thesis. Tooth profile that is located outside the pitch circle is called the addendum, whereas the inside part of the tooth is called the dedendum. The line n-n is commonly known as the common normal, which the ideal kinematic contact point always appears on. The line of contact lies between the two points of a and b. The angle between the common normal and the common tangent to the two pitch circles is known as the pressure angle (θ). The period between a and p is called the approach stage, while the period between p and b is the recess stage, and the corresponding angles are known as the angle of approach and the angle of recess, respectively.

As other mechanical devices, gears are subject to surfaces tribological contact, specifically, along the line of action. The contact occurs repeatedly between driving teeth and the driven teeth, and the contact ratio will change. The method of this engagement varies in type and direction, along the line of contact, between rolling and sliding contact. Figure 2.5 shows the type and direction of gear pair teeth contact at different stages

of mesh [30]. At the approach stage, the dedendum of the driving gear tooth and the addendum of the driven gear tooth are experiencing sliding contact. While at the pitch point stage, there is, theoretically, no sliding contact. On the other hand, at the recess stage, the addendum of the driving gear tooth and the dedendum of the driven gear tooth are experiencing sliding contact again. At all stages, the rolling contact is constant and in the same direction.

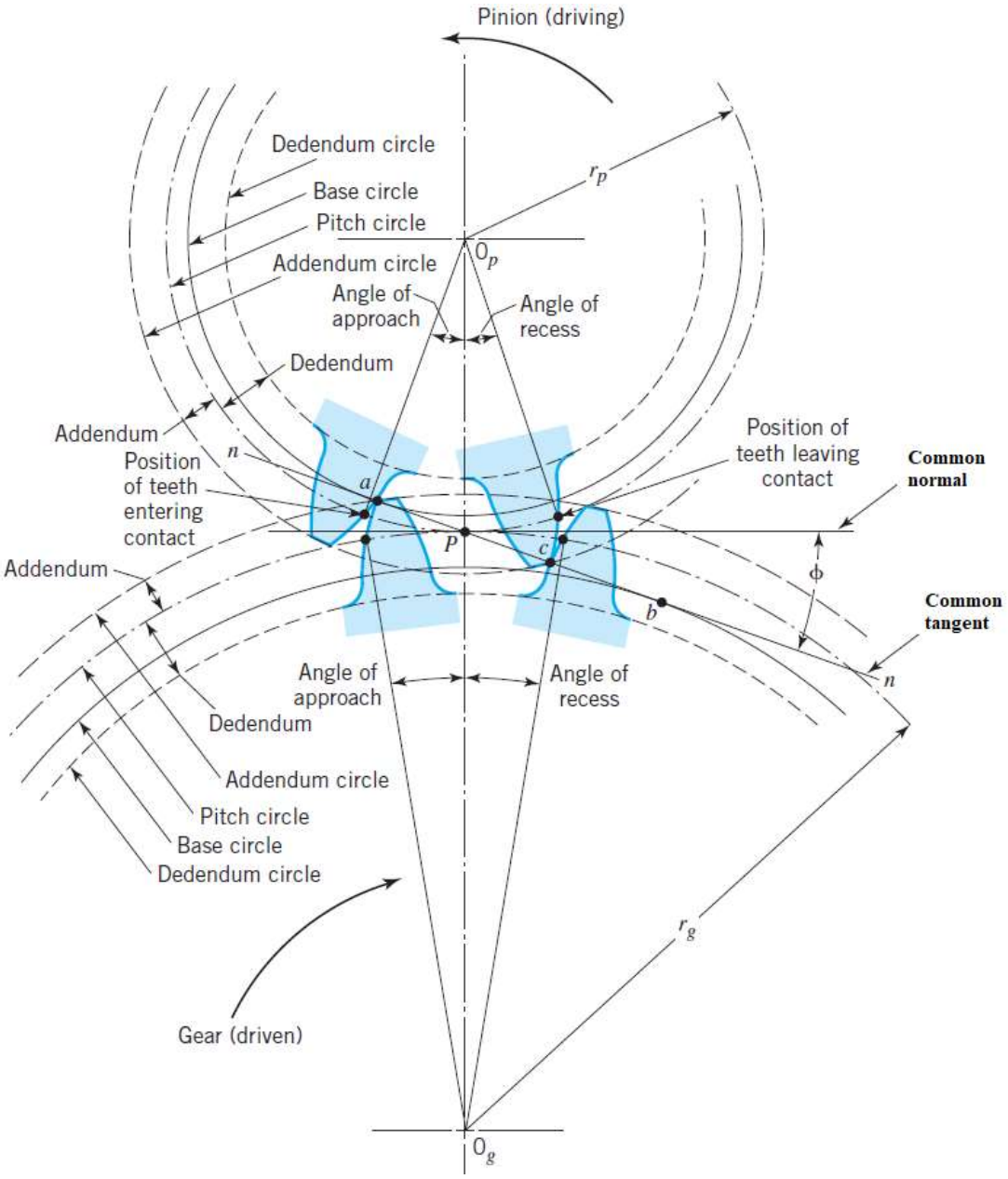

Figure 2.4 Further spur gear nomenclature and meshing terminologies [29]

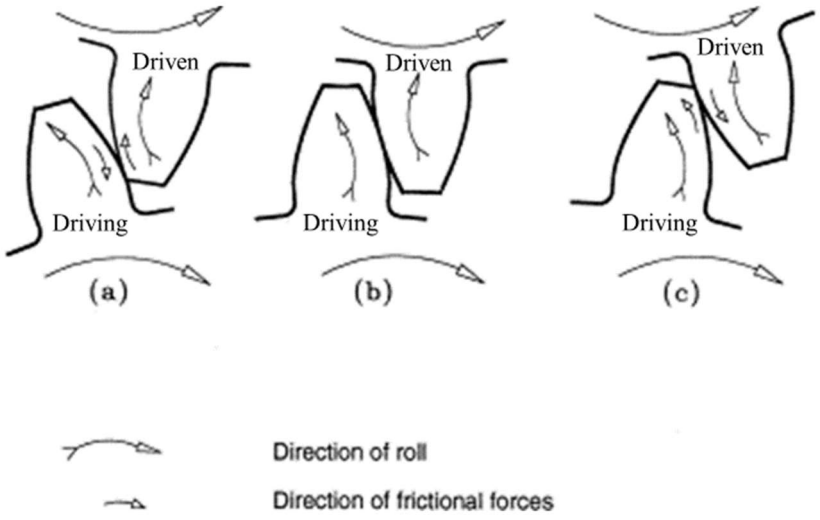

Figure 2.5 Gear tooth rolling and sliding contact, (a) at approach stage, (b) at pitch point and (c) at recess stage [30]

The sliding contact here is one of the important phenomena with respect to surface tribology, and therefore defining its velocity is worthwhile for this work. Figure 2.6 shows the schematic diagram of a driving gear tooth and a driven gear tooth in contact, with velocity vectors represented to analyse the sliding velocity calculation [29]. Here, the driving gear velocity is represented as V_g and the driven gear velocity is V_p. The surface tangent velocity component is defined as V_{gt} and V_{pt} for the driving and driven, respectively. The opposite normal components (V_{gn} and V_{pn}) are always equal, if in constant contact and with no deflections. The sliding velocity direction is always tangential to the surface contact and can be defined by finding the difference between the two tangent velocity components (V_{gt} - V_{pt}). It is continuously changing, with the maximum at the beginning of the approach stage and at the end of the recess stage and zero at the pitch point. Therefore, the sliding velocity can be defined as a function of the distance from the pitch point.

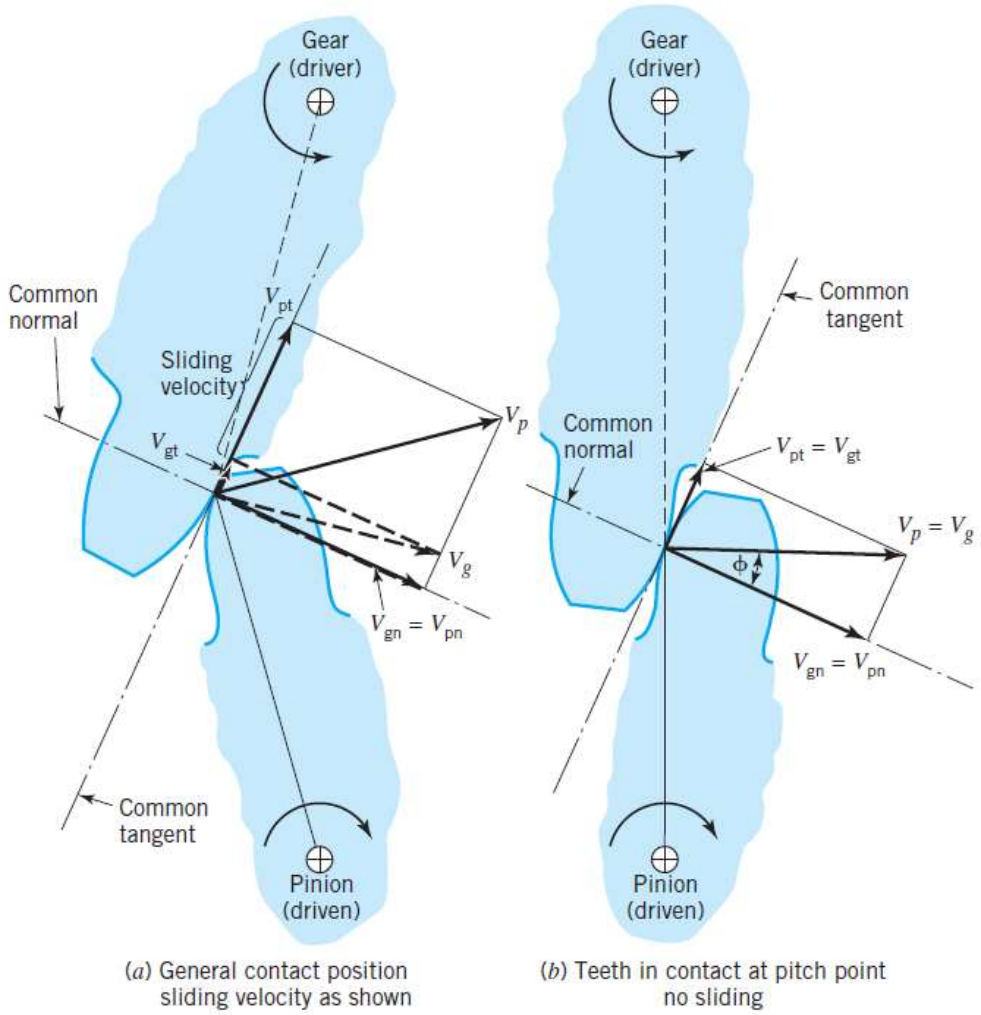

Figure 2.6 Schematic of two gear teeth in mesh to define the tooth sliding velocity [29]

Because the sliding velocity varies from the highest at tooth root and tip to zero at pitch, and for simplifying, the average sliding velocity (ΔV) can be defined, specifically for 1:1 gearing ratio, by multiplying the sum of the two gears' angular velocities by the half of the line of contact (*ab* in Figure 2.4),

$$\Delta V = (\omega_1 + \omega_2) \cdot \frac{L_{ab}}{2} \tag{2.4}$$

2.3 The progress of research work on polymer gears

It is well known that gears are used in mechanical equipment and machines to handle and transmit power or to deliver the rotational motion between shafts. The mostly used material is metal for the reason of heavy duty toleration that metal provides as a result of relatively higher mechanical strength and lower surface damage and wear rate.

The topic of polymer gears is still not well established due to the low amounts of models and data resulting from the low number of research projects on the topic during the last five decades. Singh et al [31] counted the number of articles across the years between 1959 and 2016. Figure 2.7 shows that the yearly number of published articles about polymer gears was most often just one for the period between 1959 to 1999, reaching three or four articles in a few years. Publication increased after 1999, indicating the increase of interest in those gear systems as their potential advantages and benefits were realised. Most of the publications (113 articles) were focused on spur gears, while only 9 articles were about helical, worm or bevel gears, with the amount of 4,3 and 2 articles respectively.

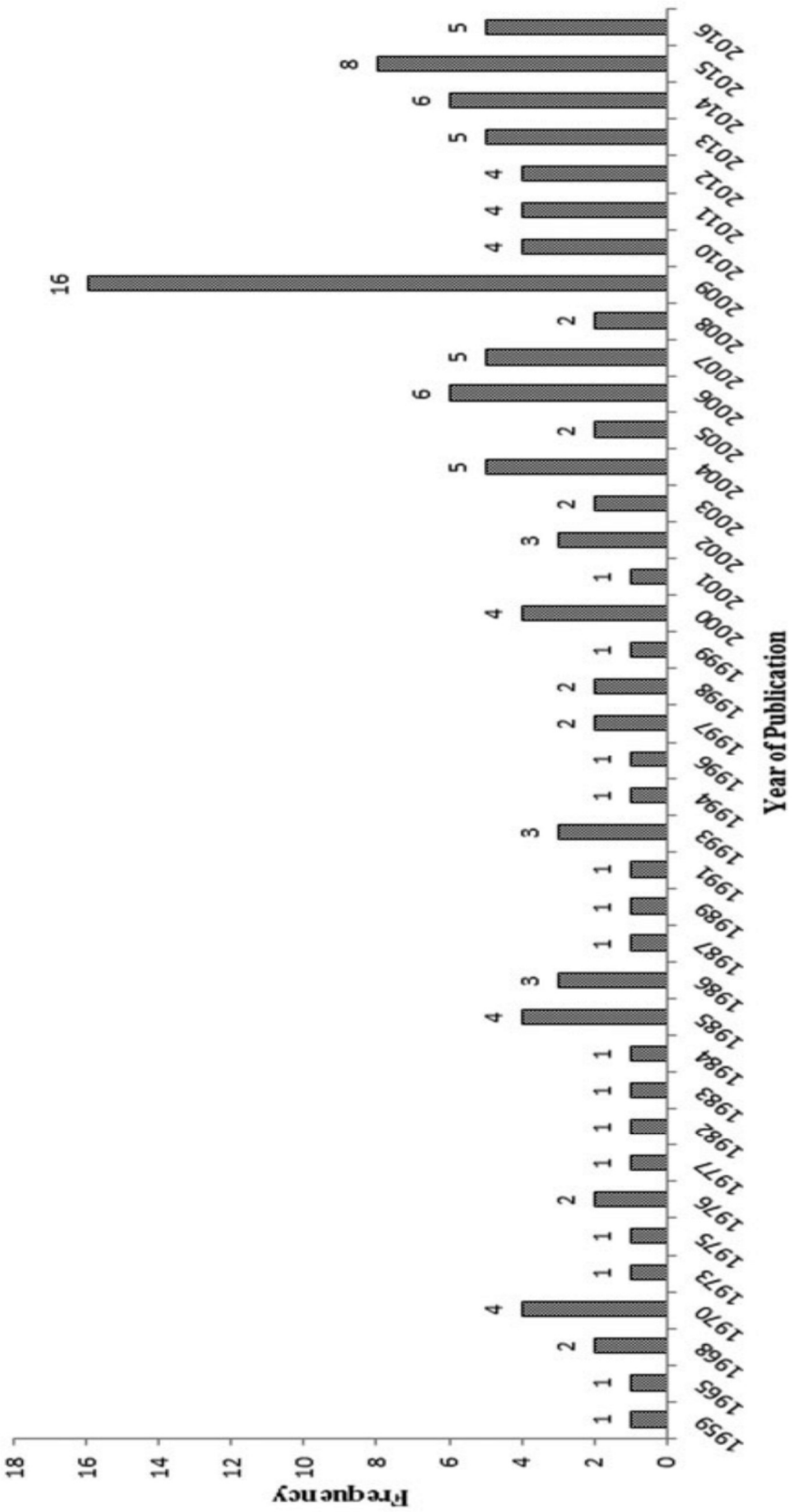

Figure 2.7 Number of articles on the topic of polymer gears across the period between 1959 and 2016 [31]

2.4 Tribology of polymers: mechanical applications

The British Department of Education and Science defined tribology as "the science and technology of interacting surfaces in relative motion and practices related thereto" [1]. One of the main purposes to study tribology on mechanical parts is to reduce or maintain the friction between rubbing surfaces [32]. Mostly, tribology deals with the friction, lubrication and wear concepts.

Friction force is a physical phenomenon that occurs as a result of the natural resistance of a body to moving over another for reason of the surfaces' contact. It has long been known experimentally that friction force is mostly proportional to the normal applied pressure and, therefore, forms a proportional relation between the two loads, that is commonly known as the coefficient of friction,

$$\mu = \frac{F}{P} \tag{2.5}$$

where, F is the friction force and P is the normal force pressure.

According to Menezes et al. [32], the two main mechanisms of friction in polymers are ploughing and adhesion, and the range of friction coefficient of polymer materials when in sliding contact with other polymers, metals or ceramics lies between 0.1 and 0.5, though, this coefficient of friction could go beyond these values with the effect of different conditions [33].

Mostly, metal mechanical parts rely on the strength of material in design and rating [34,35]. In polymers, other factors are more actively in effect [36,37]. The surface wear is first to mention in this list, followed by the thermal effect [38]. Both are affected by the lower values of the material properties of plastics, such as the strength of material, thermal conductivity and glass transition point. Most researchers [39–42] were focusing on the surface wear effect on polymer mechanical devices behaviour, while fewer attempts were focused on the thermal effect on the

performance of polymer machines [35,43–46]. This section will focus more on the wear, tribology and surface mechanical contact behaviour of polymer devices, while the thermal effect will be discussed later in section 2.12.

Wear was defined by the Institution of Mechanical Engineers (IMechE) as "the progressive loss of substance from the surface of a body brought about by mechanical action" [47]. It has increasingly become more important when designing polymer machines, because of the high effect it plays on such devices. The high unpredicted behaviour of their surfaces makes it high requirement to study the tribology to understand their wear phenomena [48].

2.5 Polymer gears' advantages and limitations

Polymer gears have become more popular in more applications nowadays as research has revealed some of their advantages. These advantages include, in comparison with metal gears [4]:

1) They can be operated in a dry condition without using any type of lubrication, including oil and grease;
2) They are cheaper to manufacture;
3) They are less noisy in operation because they have higher internal damping capacity;
4) They can be much lighter as they have lower density;
5) They offer more chemical corrosion resistance;
6) They are easier to manufacture in many ways and in more complex shapes.

Although, it appears that polymer gears have many potential mechanical advantages, which leads to interest in replacing metal gears to get more reliable and economical devices, they still have some limitations that need to be addressed satisfactorily to ensure the benefits from the above

advantages in most mechanical applications. Some of these limitations (comparing with metal gears) are [4]:

1) The power transition of polymer gears is still limited to around 22 kW (30 hp) comparing to around 20000 kW in metal gears [15];
2) Lower temperature resistance, which leads to limited operating temperatures;
3) Dimensional (shape) instability, especially for nylon, after manufacturing.

Trading off the limitations and advantages, it can be seen that, while polymer gears are ruled out of some applications, they often have more advantages than limitations. They can be more suitable for specific applications than metal gears. For example, they have a desirably large strength-to-weight ratio and yet are simple to produce [49].

In order to tackle these limitations and exploit the advantages, to benefit more advanced applications, much research has been done to study and understand polymer gears and to propose design improvements. In the early stages of research, polymer gear was tested in pair with metal gear for the purpose of finding the failure mechanisms of polymer gears [50,51]. This type of mating benefits the polymer gear by conducting heat away trough the steel gear. Then, some researchers began to study polymer gear pairs in mesh, once it was found that in real applications do not often run polymer gear against metal gear, and hence the results will be more accurate and realistic design guides. Some of these studies will be covered in the following sections [4,41].

2.6 Current practice in gear design

Using gears to transfer rotational movements between input and output shafts is one of the straightforward basic concepts of power and motion

transmission [20]. They are one of the first choices for a designer (others are chains and belts) when it comes to providing torque or speed changes, as a requirement of that transmission. Subject to small dissipative losses, gear systems conserve power (work-energy) when regulating speed and torque.

The designer of a gear train set should take into account several requirements if the final machine is to achieve the performance required for running in a specific environment. Those requirements include ones relating to gear tooth strength, durability, efficiency, temperature, noise, weight and cost [51,52]. Those elements can be arranged in terms of importance according to the environmental specifications that the designed set will be running in.

The weight of gears can be controlled to some extent by the type of material used (in line with the effect of size, which is governed by torque). Therefore, material choice in gear rating is one of the important factors to control the device weight. Cost can be governed by the materials choice, as well as by requirement to meet gear accuracy and standards. Similarly, noise can be controlled by the chosen material and the working environment.

The peak local temperature and its effect, which is one of the most important characteristics for many gear set applications, could be controlled to a certain extent by lubrication, but there is still something of a scientific race to find out more possible ways to control temperature. One of these possibilities is by using different materials [52].

All in all, it is not easy to set up a single design standard that satisfies all the design considerations mentioned above. There are always likely to be some compromises. For example, when trying to reduce the noise or increase the quality by changing some of the characteristics, there might will be an increase in cost. Indeed, one of the aims of this research project is to find ways to increase the quality without raising the cost by using

some new materials. This involved finding out their working ranges and advantages and so improving on the current designs. But always there is a minimum requirements that the gear set should survive fatigue or fracture and wear [52].

2.7 Polymer gear standards

Standards are required for every framework of services or technologies as helpful business tools to organise the designing, processing, production, operation and maintenance of those services and technologies [53]. Many were originally established to organise products more economically than technically, but these aspects are now highly inter-related. A recent report by Hogan et al. [54] claimed that standards contribute to the UK's productivity growth by 37.4%. As more standards developed, they became of growing interest for policies and legislation, e.g., starting to form guidelines for health and safety [55].

The basics of standards for metal gears were introduced and developed some hundreds of years ago (with the establishment of metallic gears). Polymeric gears started to be used around 70 years ago, and, therefore, their standards are quite recent and still under development. They continue to face the challenges of not unduly restricting potential users of polymer gears from the wide range advantages of this new technology. Effective standards must draw the right balance of guidelines to benefit from the advantages and avoid failures predicted from the limitations. Another challenge those standards face is the wider range of polymer materials and their composites, compared to metal, and the greater numbers of factors strongly involved in polymer gear design and rating. For instance, thermal effects can be very significant on polymer gears mechanical operation and they can be very sensitive to change of other factors (e.g., load or speed) [56]. In addition, polymer materials are not defined as constantly by

different suppliers, because there is no unified material prosperities standard, compared to metals' material standardization.

Different standards for polymer gears have developed in different parts of the world, yet they are still fewer than metal gears standards and they are very limited. The German standard “VDI 2545: Gear Wheels Made From Thermoplastics” [57] was the earliest standard for polymer gears and was introduced in 1981 and withdrawn in 1996. It was an amendment from one of the steel gears standards “DIN 3990: Calculation of load capacity of cylindrical gears; introduction and general influence factors” [58] that was introduced in 1970 and amended in 1987. This clearly establishes VDI 2545 as the first developed but therefore based on early technology (earlier issue). The standard focused on tooth stress concentration (as is common for metal gears) and was limited to two types on nylon material and acetal material gears [27]. Although VDI 2545 was withdrawn many years ago, it is still in use by the commercial sector. In addition, it is widely mentioned in the literature.

In 1982, the British Standards Institution introduced “BSI 6168:1987: Specification for non-metallic spur gears” [59] which was reproduced in 1987 and amended in 1991. This standard was developed from VDI 2545 with some fundamental amendments using Hachmann and Strickle’s gear bulk temperature calculations [60,61], which made the standard more advanced and more useful for designers by taking thermal factors into account.

In 2013, “VDI 2736 part 2: Thermoplastic gear wheels - Cylindrical gears - Calculation of the load-carrying capacity” [7] was introduced by the Association of German Engineers as a replacement of the VDI 2545, with the inclusion of new thermal effect calculations and a mention of gear tooth bending. This standard was modified in 2014. Recent studies [27,62] were conducted to verify the accuracy of the thermal model provided in this standard and their findings are discussed in section 2.12 on polymer gear temperature calculations. In brief, although a thermal framework was

added to this document, limitations are still clear in the accuracy of temperature predictions against different operational parameters.

During the late 20th and early 21st centuries, the American Gear Manufacturers Association (AGMA) introduced and developed three standards for polymer gears, each of which was focused on a certain aspect. The first standard was "AGMA 920-A01: Materials for Plastic Gears" [63] which was introduced in 1993 and modified in 2001. The standard talks about commonly used and suitable materials, from the range of plastics, for certain gearing applications. It links each type of plastic material to certain gearing applications based on its material properties. In addition, it mentions the preferred manufacturing method (injection moulding or machine cutting) for each material by taking account of the material mechanical properties and the shrinkage rate. In some cases, suppliers' materials data sheets provide different information for either or both of material applications and manufacturing techniques; this may be because they use different testing methods, which forms one of the drawbacks of this standard. Another limitation is that no one report can realistically cover more than a small fraction of the potentially available polymer types, beside resins and composites. Users of this document should treat it as a general guide, convenient for initial planning, but always consult specific data sheets at the detail design stage. This standard was reviewed and republished in 2015 as "AGMA 920-B15: Materials for Plastic Gears" [64].

The second of the AGMA documents to be published was "ANSI/AGMA 1006-A97: Tooth Proportions for Plastic Gears" in 1997 [5]. It was developed from two older standards: "AGMA 201.A2, Tooth Proportions for Coarse-Pitch Involute Spur Gears" introduced in 1968 [65] and "ANSI/AGMA 1003-G93, Tooth Proportions for Fine-Pitch Involute Spur and Helical Gears" introduced in 1992 [66]. The standard defined a basic rack that was specified for plastic gears. It is one of a range of AGMA standards that were specified for basic gear rack forming, but with an explicit focus on gears with lower material strength and higher gear

deformation. A similar standard, “ANSI/AGMA 1106-A97: Tooth Proportions for Plastic Gears” [67] was produced with metric units as its main units. The standard was reaffirmed in 2016.

In 2001, AGMA introduced “AGMA 909-A06: Specifications for Molded Plastic Gears” [68] which focused on a specific type of polymer gears manufacturing, that is injection moulding. The document was structured as a communication guideline between polymer gear designers and manufacturers by describing the important technical features involved in injection moulding procedures. One of the main limitations of this report is that it does not cover other methods of production or other gear shapes.

In general, none of the three AGMA standards takes account of the technical part of polymer gear behaviour in real-world applications in a way useful as a guide for designers to rate polymer gears accurately for their applications. This is in contrast to the VDI standard and the British standard already mentioned. Overall, there is still a lack of standards for polymer gears in the matter of life prediction and gear rating for the wider variety of polymer materials. According to Sheridan and Smith [56], manufacturers in the United States are still rating polymer gears using “ANSI/AGMA 2000-A88: Gear Classification and Inspection Handbook - Tolerances and Measuring Methods for Unassembled Spur and Helical Gears (Including Metric Equivalents)” [69], the standard also referred to as the “AGMA Q numbers”. This standard was developed specifically for metal gears, which is clear evidence for it being a generally unreliable standard for non-metallic gears. This implies that many other polymer gear providers design their products with no use of standard documents.

2.8 Plastic gear contact ratio

Gear contact ratio is formally defined as ‘the average number of pairs of teeth in contact during the course of action’[20,70,71]. It reveals the

amount of load applied on one tooth, while in mesh with other gear, as well as how many teeth are sharing the load at the same time. This information can be used to define the stress concentration on that tooth.

In theory, gear contact ratio (m_c) can be defined by dividing the length of arc of action (q_t) over the circular pitch (p)

$$m_c = \frac{q_t}{p} \tag{2.6}$$

From Figure 2.8, Equation (2.6) can be rewrite as:

$$m_c = \frac{L_{ab}}{p \cos\theta} \tag{2.7}$$

where L_{ab} is the reflection of the arc of action on the line of action and θ is the pressure angle.

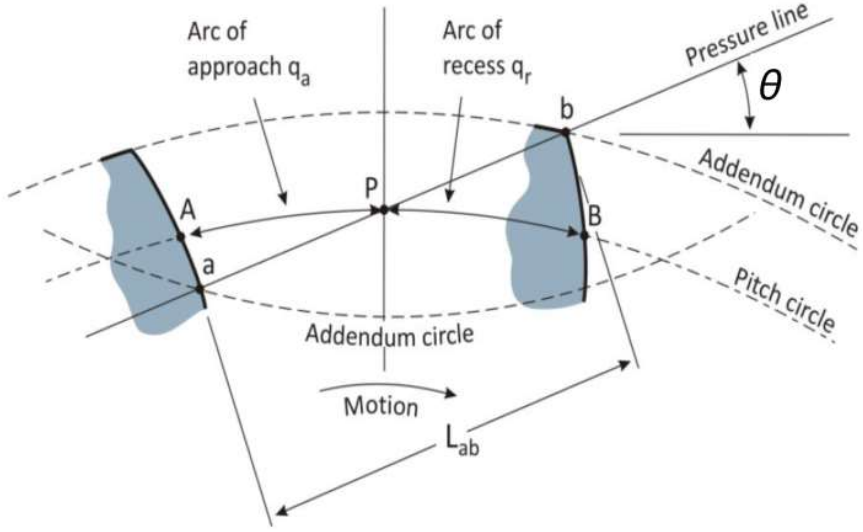

Figure 2.8 Explanation of gear contact ratio [71]

Teeth load sharing in plastic gears is one of the important physical parameters that needs to be understood for proper design and application, because it has an effect on the position of the most loaded point on a gear

tooth during the full mesh stage [18]. For instance, if the load sharing is one at a time, the highest loaded point is agreed to be at the tip point of the gear tooth, while if the contact ratio is around 1.5, then the highest loaded point will be positioned around the pitch line (middle of the gear tooth).

Theoretical calculations on acetal gears contact ratio by Cornelius et. al [72] revealed that more than one tooth carries the load during mesh time. Super-fast images were taken by Yelle and Burns [18] which supported this conclusion.

As polymer gears have quite similar failure propagation near the root side to metal gears, the Lewis equation is still usable for this kind of material [18]. However, there are some differences between polymer gears and metal gears that make this equation not fully applicable to polymer gears and lead to less accurate designs. Using the Lewis equation to rate polymer gears provides strength curves which show a large effect of gear module on gear running life. In reality, this parameter does not give an accurate gear rating, because the load sharing and module are both affected by plastic gear contact ratio [18]. Tooth load sharing and contact ration showed an increase of around 10% to 70% with polymer materials, compared to theoretical estimations [73,74]. Polymer gears have other different modes of failures that dictate gearing train design, for example, thermal failure and surface failure, as defined earlier. Defining real contact ratio might be also important to these failure modes as it is important with respect to tooth root bending stress. One of the objectives for this research project is to find out the effect of real contact ratio on this important behaviour.

The material flexibility of polymers leads to bending the loaded teeth in mesh, which causes the following tooth to be engaged in mesh earlier than the theoretical time. As a result of this phenomena, the contact ratio of polymer gears is higher than that of metal gears of the same dimensions and design. In addition, the contact ratio in polymer gears has a positive

correlation to load and a negative relation to gear module [72]. A theoretical calculation of the relations between real contact ratio and load and gear module was provided by Yell and Burns [18] and the effect on polymer gear rating using the Lewis method was illustrated by redefining tooth form factor.

Load sharing in polymer gears is different to that in metal gears because material viscoelastic behaviour leads to higher factors of tooth load sharing in polymers and that, consequently, makes polymer gears load handling smoother and gear vibration lower. In addition, higher load sharing factors lead to higher gear load capacity as a result of lower single tooth stress and Hertzian contact stress loads.

Yelle and Burns [18] claimed that the Lewis equation gives a curve that depends on gear module and running time, which is suitable for rating metal gears. They theoretically calculated the real contact ratio of plastic-plastic and plastic-steel gears using a gear mating mechanical model (Figure 2.9) and by defining the amount of tooth deflection affects theoretical gear contact ratio through their equation

$$D_v = \left[\frac{W_n}{EF} + \sum_{j=1}^{m} \frac{\Delta S_j}{w_j}\right] \frac{1}{\sum_{j=1}^{m} \frac{1}{w_j}} \tag{2.8}$$

where:

D_v: vertical deflection of the cam model (Figure 2.9) caused by a unit normal load W_u

W_n: total transmitted normal load = $W_t/cos\theta$

E: dynamic (storage) modulus

F: gear face width

ΔS: separation distance

w_j: non-dimensional compliance of the tooth or tooth pair = $EF/k`$

k`: single tooth spring stiffness

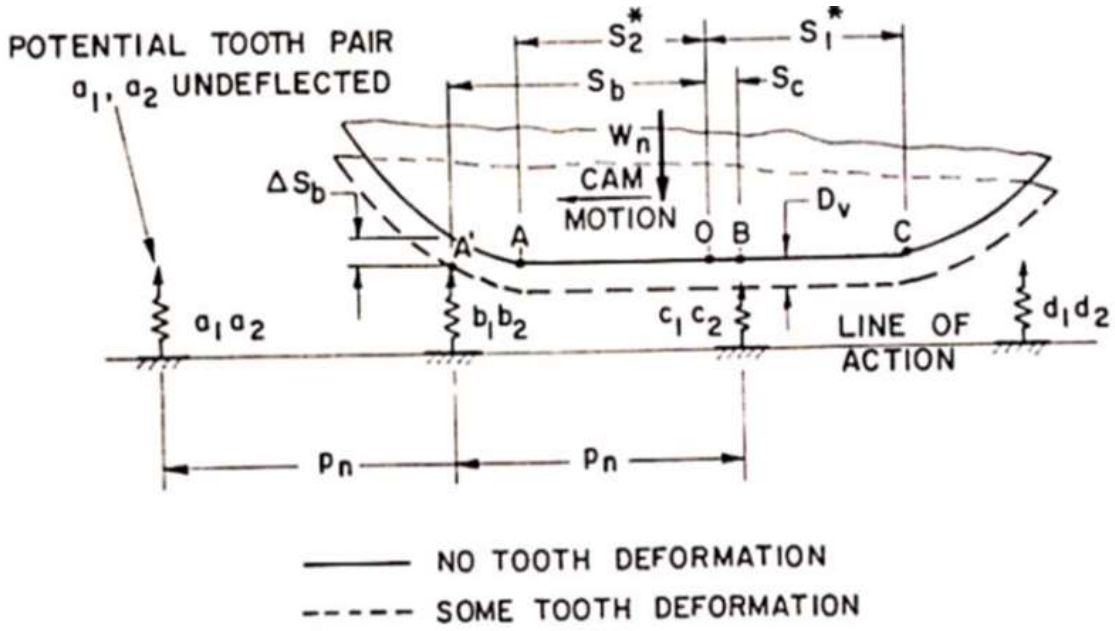

Figure 2.9 Yelle and Burns's real gear pair model (plastic/plastic pair) [18]

From their theoretical calculations they concluded that the polymer gear contact ratio depends on load and gear module. In addition, they claimed that the Lewis equation gives an improper rating when used for polymer gears. Their contact ratio is higher than their counterpart metal gears, which affects the strength curve and should be taken into account in polymer gear rating. This may be done by redefining the form factor in the Lewis equation by adding a material-specified correction factor to it, hoping that this could reduce the model dependence of root bending fatigue on gear module only, as in metals.

2.9 Failure mechanisms of polymer gears

Polymer gears have different failure mechanisms to metal gears, which leads to the requirement of different gear rating for proper design and functionality. In polymer gears, failure modes are more varied than are seen in metal gears. To date, therefore, most manufacturers rely more on their experience as an art for designing and manufacturing polymer gears

than on science and theoretical calculations. This happens because current plastic gears rates and standards do not predict gear life and endurance properly. For example, it is often noticed that polymer gears designed by manufacturer's art may last longer than was indicated by standards' rating and running time calculations [4,21,22,40,75,76]. Therefore, more understanding of polymer gear failure mechanisms and gears' life and endurance are urgently needed so as to predict polymer gears life more precisely.

Several different types of failure modes for polymer gear teeth are discussed in the literature in some detail. Some of them are similar to metal gear failure modes, while others occur uniquely with polymer gears. After extensive experimenting on a wide range of materials for polymer gears, Hachmann and Strickle [60] stated the four most common modes of failure at plastic gears to be: cracking at tooth root; cracking at pitch circle; excessive tooth flank wear; and tooth surface pitting that occurred with gears tested in lubricant medium (Figure 2.10). Apart from wear, Walton and Shi [21] classified the other three modes of failure as forms of tooth fatigue failure.

Bravo et al. [77] added static, thermal and fatigue damage modes to the modes of plastic gear failure (Figure 2.11). They explicitly emphasised thermal failure as one of the main failure modes for polymer gears, because thermal behaviour is one of the main factors that affect the function of many polymer gears. Also, hub and rim failures were reported in other literature [16,29,70,78] as modes of polymer gear failure.

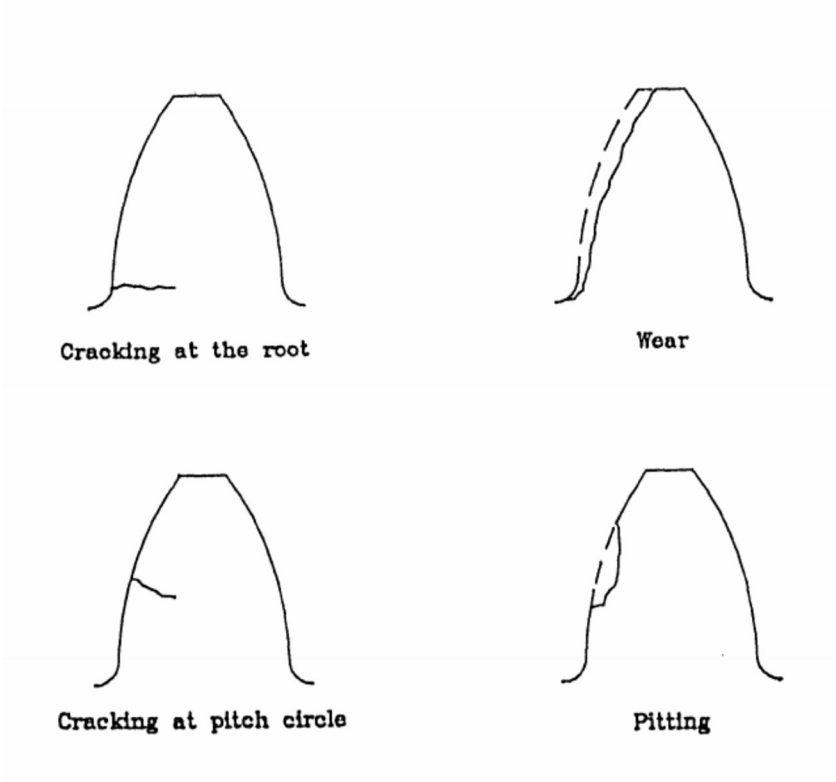

Figure 2.10 Some of the polymer gear tooth failure types [60]

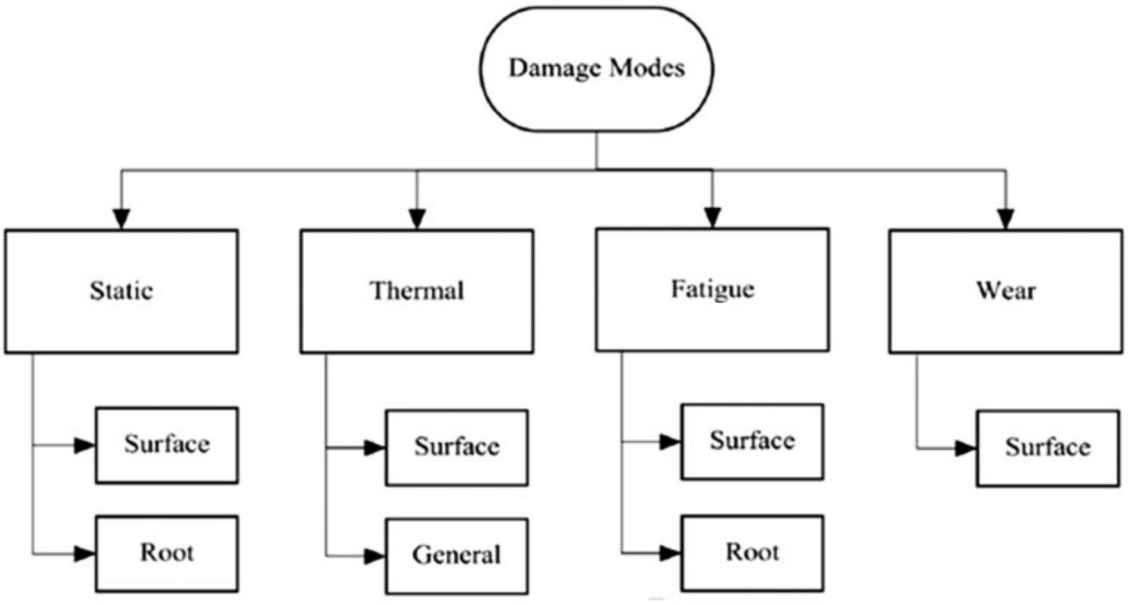

Figure 2.11 Damage modes of polymer gears [77]

All these modes of failure are significantly affected by thermal behaviour, as are tooth deformation due to bending stress, tooth surface scuffing, and plastic flow. It is thereby one of the most important factors for polymer gears design and rating. From the journey of exploration into these modes of failure, some (at least partly empirical) polymer gears standards were established to provide guidance in such gears rating, although such standards are still under improvement depending on research data to predict life and endurance more accurately.

Because of the wider range of failure modes in polymer gears than in their metallic counterparts, it is more difficult to develop a single failure prediction model to rely on for rating polymer gears, under all reasonable operating condition. Each one of these failure modes, and the mechanism associated with it, will be explained in the following sections.

2.9.1 Fracture

Tooth fracture mostly occurs either at the root point or around the pitch point of polymer gear teeth. Mao et al. [41] claimed that the location of this fracture could be predicted once locating the formation micro cracks. One of the possible solutions to delaying the occurrence of the fracture is to reinforce the polymer material and keep the fibre direction parallel to the surface of the gear tooth, by controlling the moulding process [26].

Some studies asserted that the main cause of fracture is the Hertzian contact stress that occurs with the change of load distribution from one to two or more teeth [51,79]. One of the proposed solutions is, therefore, to control the pressure changes over the gear tooth curve by changing the face width along the curve from the root to the tip [79,80].

Gear tooth surface microcracks are claimed to be more active at the tooth root and around the pitch line surface in nylon material. This phenomenon was referred to be as one of the tooth failure initiations, by the formation of tooth fracture [4].

2.9.2 Wear

Gear tooth wear is a surface phenomenon in which layers of material are removed or worn away, more or less uniformly, from the contacting surfaces of the gear teeth [81]. Wear rate can be defined as the amount of tooth thickness reduction per rolling cycle [41,49]. Polymer gear wear has been studied in many aspects. It was found that the wear rate is affected by many different variables, such as, load value, operation time, slip ratio, temperature, and so on. Figure 2.12 shows different types of surface wear [82].

One of the solutions for controlling the wear behaviour is to fibre reinforce the polymer gear. This method could decrease the wear rate in the reinforced gears by ten times of the unreinforced gears wear rate. While in the case of non-reinforced polymer gears (polyamide nylon 66), slip ratio was required not to exceed the value of 0.11 (as a critical value) to be able to control the wear at low reasonable rate [49].

2.9.3 Pitting

Pitting is one of the failure modes that occurs mainly in nylon gears. The phenomenon starts by the formation of some micro cracks and the their propagation. When two close cracks get deeper, they may also get closer to each other until they meet and form a small material fracture particle that leaves the body [49,81]. The removed material leaves behind a pit in the surface. Over time existing pits tend to widen and more are formed [4]. As with fracture, some studies described that the main reason of this pitting is the Hertzian pressure that occurs for the reason of the change of load distribution from one to two or more teeth [51,79]. Again, one of the proposed solutions is to control the pressure changes over the gear tooth curve by changing the face width along the curve from the root to the tip [79,80].

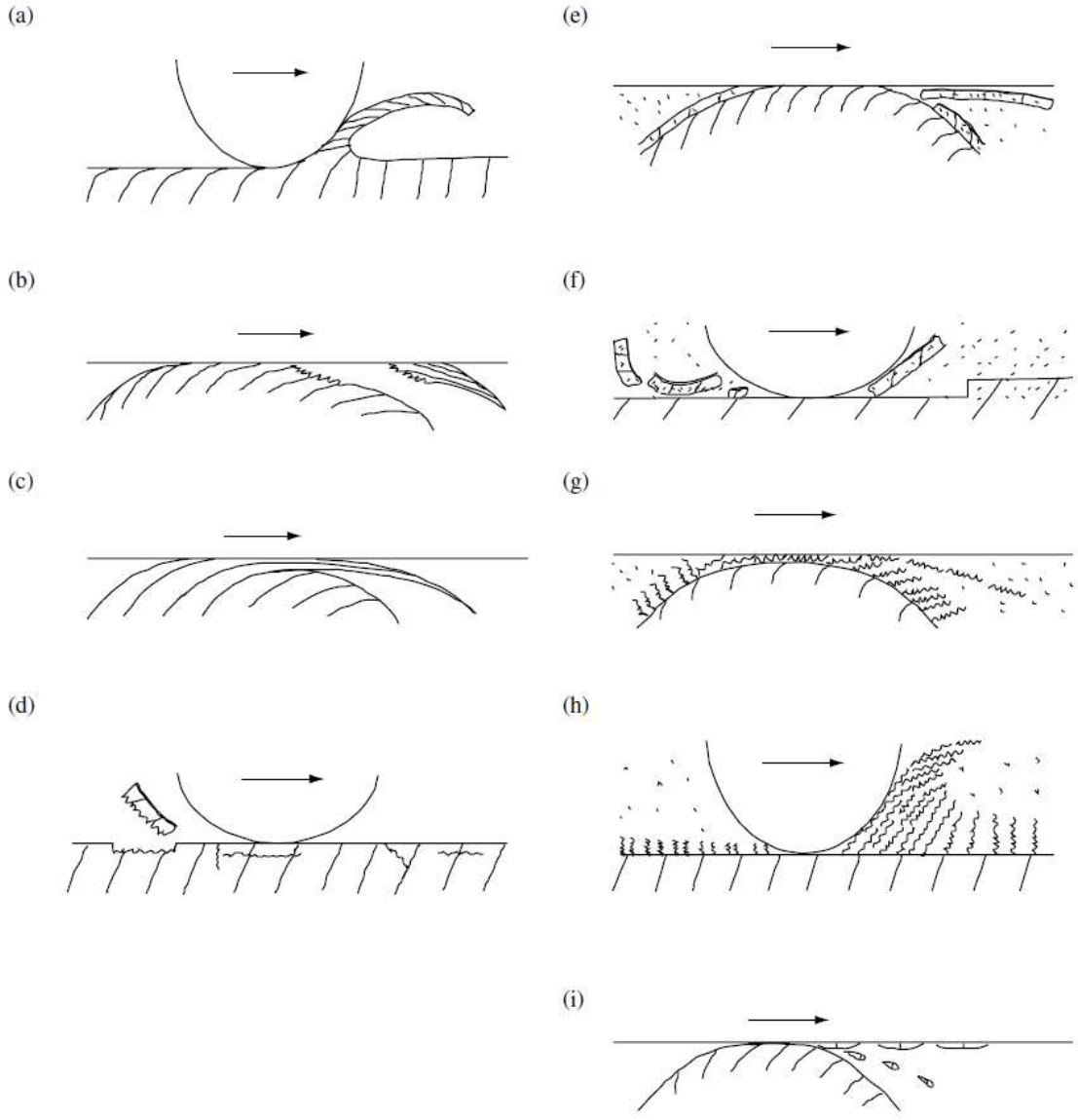

Figure 2.12 Wear types: (a) abrasive, (b) adhesive, (c) flow, (d) fatigue, (e) corrosive by shear, (f) corrosive by delamination, (g) corrosive by accumulated plastic shear flow, (h) corrosive by shaving, and (i) melt wear [82]

2.9.4 Scuffing

Scuffing is a result of two surface temporarily welding and being torn apart that causes a small amount of the surface material to be removed [83]. This type of welding occurs as a result of the friction between the two surfaces, with energy dissipation getting higher as load increases and resulting in local overheating [4].

It is important to note that, if the amount of material that is removed from the surface does not cover the entire surface, i.e. not all of the surface area appeared to be damaged, then this type of failure is usually described as pitting or scuffing. Otherwise it tends to be described as wearing [4].

2.9.5 Plastic flow

Unlike most metals, polymeric materials can quite readily redistribute across surface through plastic flow. They also soften considerably at modest temperature. Thus the failure of polymer gears can arise from gear tooth flow encouraged by the thermal softening caused by high friction between the surfaces [4].

2.9.6 Thermal

As stated by Bravo et al. [77], thermal was added to the modes of plastic gear failure, because of the low thermal conductivity of polymers and low critical temperatures for material state transitions. The glass transition point and melting temperature of thermoplastics are relatively low. Once the operating gears reach these temperatures, tooth shapes are deformed leading to significant changes to gear smooth mesh by the conjugate function, in addition to the change in the pressure angle. Another form of failure caused by exceeding the critical temperatures is the high increase on wear and surface failure, which lead to an instant tooth failure as a result of high surface plastic flow caused by frequent surface contacts [84]. Thermal expansion could be counted as thermal failure, because of the tooth form changes it may function that could affect the other forms of tooth failure.

2.10Wear mechanisms in polymer gear and the effect of different variables

Many studies have been done to understand the wear mechanisms of polymer gears by running a pair of polymer gears, of similar or different materials [26,42,60,75,79,85,86], under different conditions and by changing different operational variables, such as load and running speed. Most collected experiment data focused around assessing the amount of surface wear by measuring the reduction in tooth thickness during the running of the gears [41]. Some work focused on measuring the gear temperature using an infrared camera [44].

In a comparison of two different materials, using similar pairs of gears, it was found that acetal gears normally failed as a result of thermal effects, while the major effect of failure in nylon gears was tooth fracture [41].

2.10.1Load variable

Regarding the load variable, Mao [41] concluded that, in acetal gears, a critical point was found (typically around 7 Nm), where the wear rate showed a rapid change, i.e. a low wear rate at lower torques and very high wear rates at higher torques. The study used only one size and design of polymer gears, regarded as representative of those used in the higher power region of polymer gear applications. The wear at lower torques could be matched with the wear rate equation defined by Friedrich [87]. On the other hand, the different wear rate phenomenon at higher torques was ascribed to the rise of the temperature of the material to its melting point [88].

At low loads, one can apply the wear volume formula developed by Archard [89] and modified by Friedrich [90] using a thrust bearing testing method. The wear volume V_w was represented, as

$$V_w = k_s F s \tag{2.9}$$

where k_s is the specific wear rate, F is the normal force, and s is the sliding distance.

Equation (2.9) was reformed by Mao [75] for the tooth profile of the spur gear, as gear tooth specific wear rate k_s (m^3/Nm):

$$k_s = \frac{Qbd}{2TN} \tag{2.10}$$

where Q is the wear depth (as measured in the tests), b is the gear face width, d is the gear pitch circle diameter, T is the torque transmitted, and N is the number of cycles corresponding to the wear depth Q.

One of the limitations of this equation is that it does not include the material properties, although they may play an important role in wear behaviour.

2.10.2Speed variable

Data concerning the effect of speed on reinforced and unreinforced polymer gears is limited [91]. However, the effect is known to depend on the load variation. When the load exceeds a certain limit associated with a certain material, a gear will show a different response, which includes high effective heating and high mechanical deformation. Thus, the rotational speed of that gear will have a noticeable effect on that gear life, i.e. increasing the speed will decrease the gear's life, expressed as number of cycles. In general, most wear and failure mechanisms associated with thermal softening will be made worse by higher frictional power dissipation, which depends directly on the product of load and sliding speed.

2.11Wear rate of polymer gears

Mao [75] linked the wear rate of acetal gears and their maximum surface temperature by assigning a critical value where the wear rate changes dramatically. The critical value was assigned to the melting temperature for the specified material (acetal). A theoretical equation was developed to predict the gear surface maximum temperature, which was tested against some experimental tests to measure wear rate and surface temperature under different conditions. The paper concluded that good agreement was found between the theoretical and experimental approaches, and that the melting temperature is indeed the critical point for wear rate transition. This transition point idea and equation may not be generalised for other polymer materials, as there has been no attempt found in the literature to investigate its validity for other materials.

2.12Thermal effect on polymer gears

According to Gauvin et, al [19] thermoplastics are less heat conductive than metals. One of the first models to calculate the polymer gear temperature (while in continuous running) was developed by Hachmann and Strickle [60,61]. This model was focusing on the heat generation from the slide contact (without looking at the other sources of heating). They defined the polymer gear body temperature as:

$$\theta_{max} = \theta_a + H\mu \frac{u+1}{N+5u}\left[\frac{K_2\ e^{3/4}}{Nbk(Vm)^{3/4}} + \frac{K_3}{A}\right] \tag{2.11}$$

where θ_{max} is maximum body temperature, θ_a is ambient temperature, H is transmitted power, e is diffusivity of air, A is area of the gear housing, K_2 is empirical values which depend on whether the nylon is paired with nylon or with steel, and K_3 is empirical values which depend on the design of the drive housing.

A theoretical model to calculate the maximum teeth temperature of a pair of gears in mesh was developed by Mao [75]. This maximum surface temperature (θ_{max}) is expressed as the combination of three different types of temperature, namely gear ambient temperature (θ_a), gear body temperature (θ_b) and gear flash temperature (θ_f) (°C), which depend on energy dissipated and thermal properties of the materials, i.e.

$$\theta_{max} = \theta_a + \theta_b + \theta_f \tag{2.12}$$

or

$$\theta_{max} = \theta_a + k_1 T + k_2 T^{3/4} \tag{2.13}$$

where

$$k_1 = \frac{3.927\mu}{bc\rho Z(r_a^2 - r^2)} \tag{2.14}$$

and

$$k_2 = 1.11\mu \frac{\left(V_1^{1/2} - V_2^{1/2}\right)}{2r^{3/4}b^{3/4}\sqrt{k\rho c}} \left(\frac{\pi E}{R}\right)^{1/4} \tag{2.15}$$

Here, T is transmitted torque, ρ is specific gravity, k is thermal conductivity, c is specific heat, a is the half contact width, r_a is the outside radius, r is the reference radius, b is the tooth face width, V_1 and V_2 are the sliding velocities for gear 1 and gear 2 respectively.

It is inferred from the literature that polymer mechanical properties and tribological characteristics are more largely affected by temperature change than metals [37,92]. Therefore, some effort has been made to measure the surface temperature of a gear while it is running, using different methods of measurement, and to compare these figures with theoretically derived temperature calculations [19,22,37,93]. Although progress has been made in this sector, there is still some limitations especially under high speed running and high loaded conditions, to provide temperature limits that polymer gears can reach before failure [94,95], and

which designers could rely on while rating polymer gears. Theoretical estimations of gear surface temperature are still under development and do not provide the required information for proper non-metallic gear design. As a result of this, the research here will focus more on failure modes and the wear rate of polymer gears. Further deep investigations are made which concentrate on heat build-up measurements and calculations. The new design of a useful testing method needs to be implemented and validated.

Mao [43] developed a numerical approach to predict the flash temperature of polymer gears using a finite element analysis method to model Blok's flash temperature equation [96], as it was considering the Hertzian contact mainly applies in gear meshing and does speed variation effect more than heat conduction (in polymer gears), but with considering gear's tooth meshing position. Figure 2.13 shows the theoretical flash temperature distribution of a gear tooth, while in mesh, that was compared with the Blok's theory.

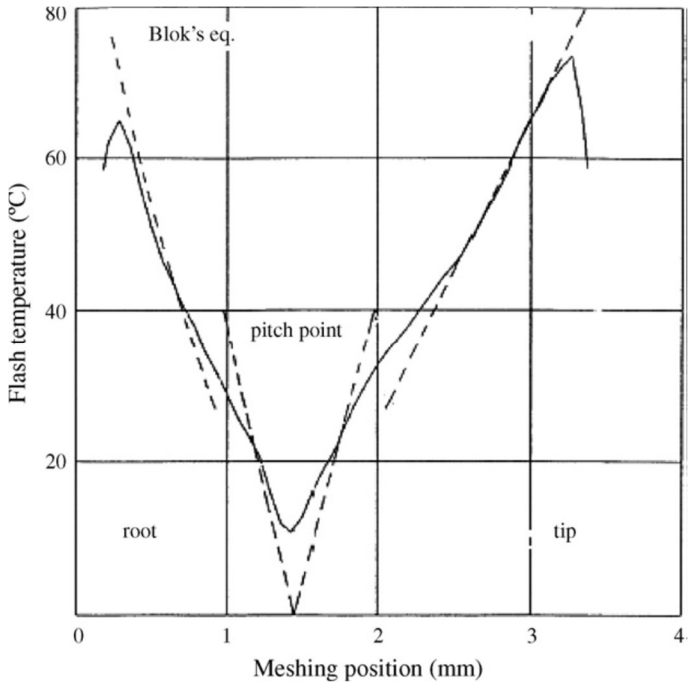

Figure 2.13 Mao's theoretical flash temperature distribution compared to Blok's theory [43].

In polymers, the flash temperature is always much higher than the average body temperature, because of the low thermal conductivity of those materials [87,97]. The sliding speed showed higher effect on the flash temperature than the surface pressure [88].

2.13The effect of lubrication on polymer gears

Lubrication is beneficial for mechanical devices to reduce friction between rubbing surfaces and, in consequence, decrease the drawbacks of thermal effects. In addition, it reduces the wear and wear rate of the rubbing surfaces. Lubricating polymer components, which are in continuous contact function, increases their running time by around five-folds [98].

Polymer materials can work in no lubrication environment, because of the property of the materials that allows them to function with a self-lubricant (internal lubrication). Therefore, polymer gears are mostly used in applications that requires dry-running gearing. Examples of these applications can be found in office and medical machines. Although, as discussed earlier, polymer gears are more highly affected by the thermal factor than their metals counterpart, and, in that case, lubrication may be a good alternative to control this factor.

Two main benefits can be gained from operating polymer gears in a lubricant medium [1,84]. Firstly, it controls the friction coefficient to lower limits, which decreases the tooth instant flash temperature while in gear mesh. Secondly, it functions as a fluid coolant and reduces the tooth surface temperature.

2.14Effect of manufacturing technique on polymer gears

Friedrich [87] illustrated that when a polymeric disc was tested against a metal pin using a tribometer device, nylons showed some dependence on the manufacturing method, either an extruded or a cast disc. Figure 2.14 shows the specific wear rate of different polymer discs running against a metal pin, with the increase of nominal contact pressure. The label 100 in the graph represents nylon 6 (extruded), while 102 represents the nylon 6 (cast). In addition, 101 in the figure represents nylon 66. It can be seen that the cast nylon 6 showed less load capacity than the extruded nylon 6.

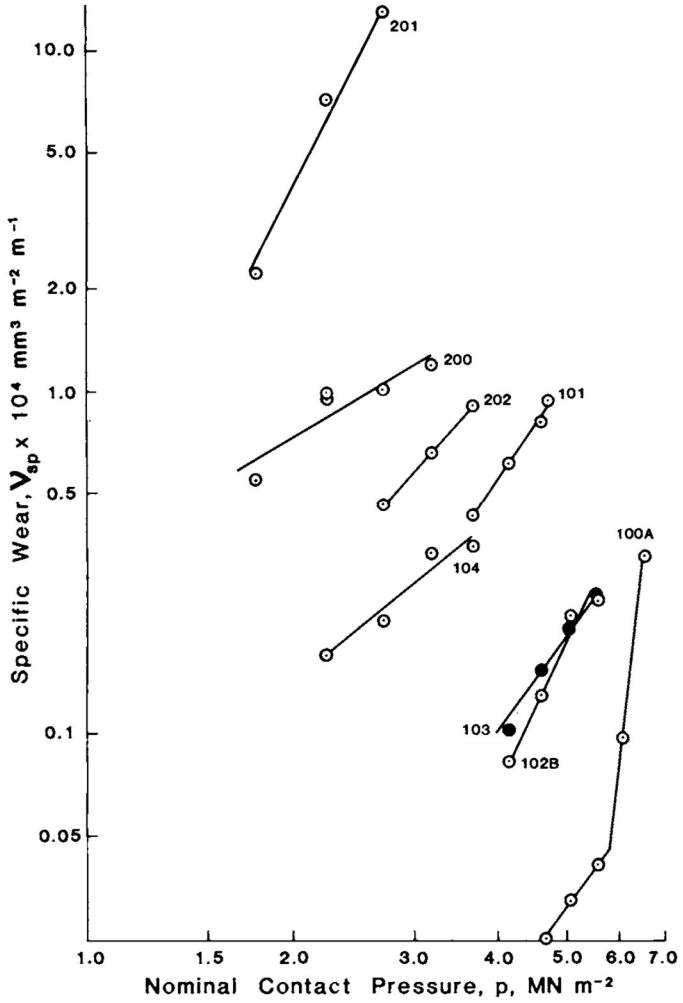

Figure 2.14 Specific wear rate of different polymers against contact pressure (sliding speed = 0.1 m/s) [87]

Gordon and Kukureka [99] measured the wear rate of two discs running in non-conformal condition. They were made of different polymers and polymer composites. The tests were conducted under a range of loads and speeds. Figure 2.15 shows their results for the steady-state wear rate vs. pressure × velocity for different samples with a 2% slip ratio. It can be seen that the fibre reinforcement increases the discs' load and speed.

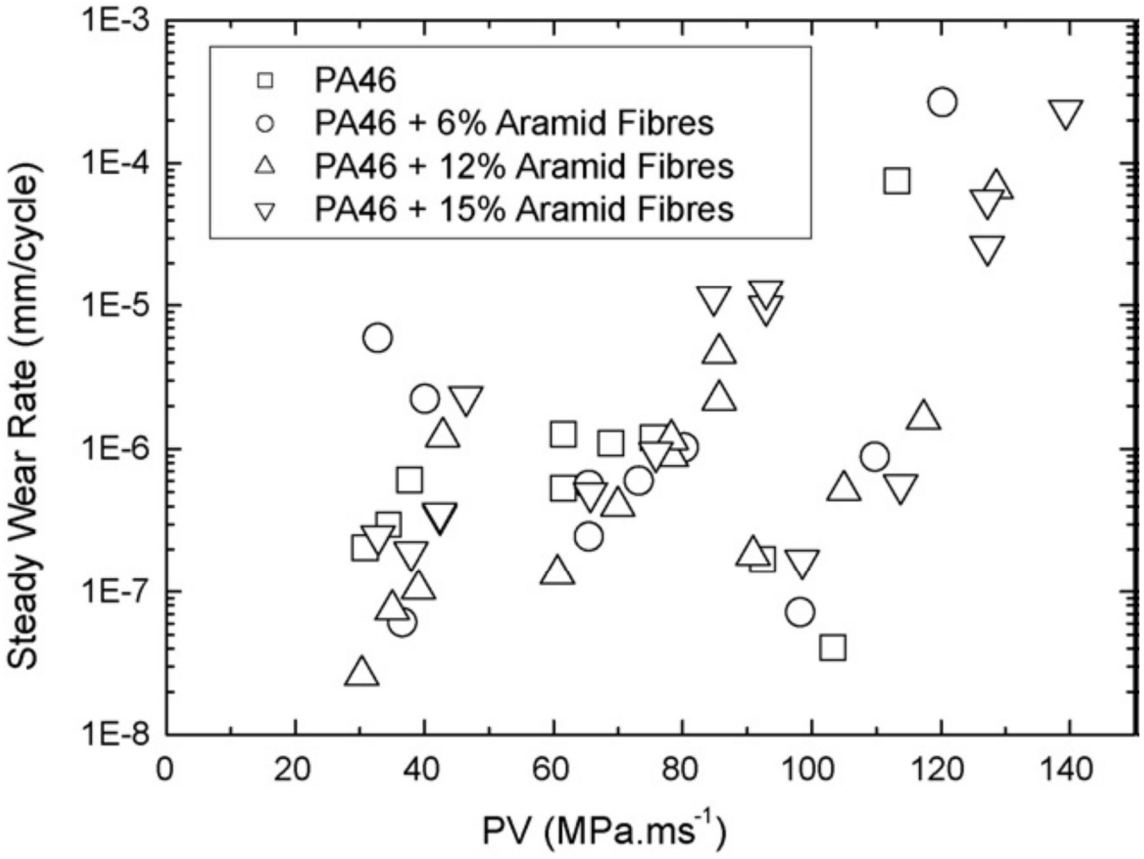

Figure 2.15 Steady-state wear rate vs. pressure × velocity for different samples with a 2% slip ratio [99]

2.15The effect of gear misalignment

Searching through the literature, it was difficult to find any studies concerning the misalignment of polymer gears, although some works were found on metallic gear misalignment.

2.16Material variation between driving and driven

It has been found that the there is an effect on the wear rate when using different materials for the driver and driven gears [41]. This raises an interesting point of research, to study how selecting different materials as a driver or driven gear affects the design and potential applications of polymer gears. It was noted that failure always occurred in the driving gear as a result of the load direction that made the stress concentration higher on that gear. A finite element method study showed that the pressure force at the initial engagement or access point is higher than the pressure force at the end of engagement or recess point. Generally, a dramatic decrease in wear rate was obtained by meshing an acetal driving gear and a nylon driven gear, for the same reason [42].

2.17Durability improvement by shape control

There is some research that focused on improving the durability and performance of polymer gears by controlling the gear tooth shape in different ways. In this section some of these studies will be mentioned.

Because two of the limitations of polymer gears are low heat conduction and a weakness in high temperature working, some studies have tried to reduce the operational temperature by modifying the tooth shape by inserting some specified holes to act as teeth cooling system (Figure 2.16) [100]. The work was based on the idea that a reduction of 10 ºC in gear operation temperature leads to a 5-10% increase in nylon tensile strength and fatigue life [101]. The modification reduces the heat generation from the gears in two ways: firstly by reducing the hysteresis effect and secondly by increasing heat dissipation by increasing the surface area in contact with air. As a consequence of reducing the temperature, the wear rate in the teeth will be reduced.

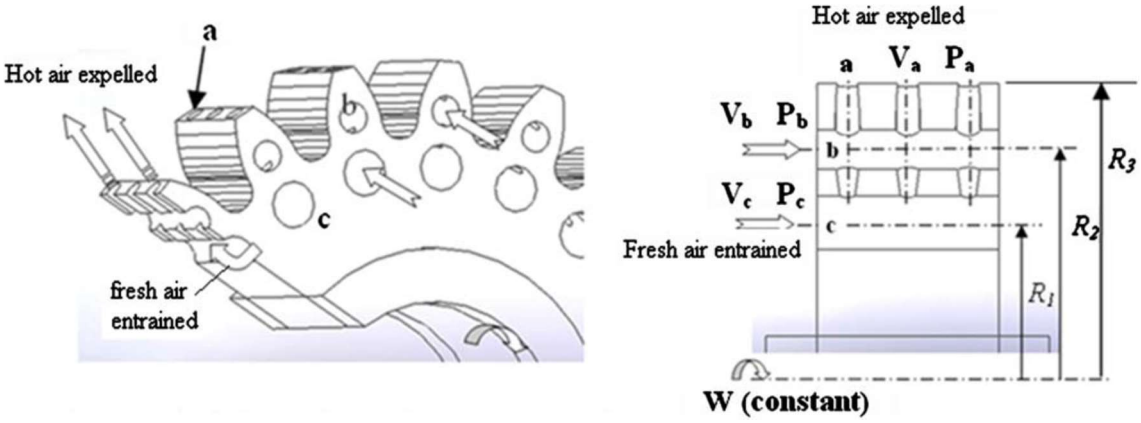

Figure 2.16 Gear tooth-cooling model [100]

Another study [80] suggested that face width modification (Figure 2.17) can help to stabilize the effect of the Hertzian pressure on a single tooth by equalizing the pressure over the face width ratio. Their modification lowered the effect of the Hertzian pressure, so reducing pitting formation around the pitch line, lowering the wear rate during the main stage of gear life and increasing the overall life of the gear.

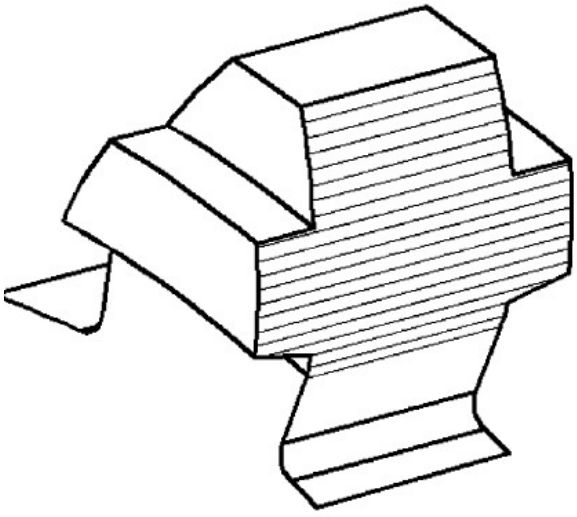

Figure 2.17 Imrek's modified tooth profile model [80]

2.18Summary

This chapter has reviewed the literature most directly related to the current research topic. It gives a summary and critique about the main concepts, observations and techniques that were covered by previous research, which form the base for the new work.

Several different types of failure mode have been shown to occur when running polymer gears under various load pressures. However, although these modes of failure were studied in some details in the previous work, none of the studies covers all the design parameters, operating conditions and materials required to devise a specific design standard or guideline method for polymer gears.

Finally, the main aim of this PhD research project was mentioned under the relevant sub-topics and discussed in relation to the current literature review in order to confirm the research questions and objectives.

Chapter 3
RESEARCH METHODOLOGY

3.1 Introduction

It is clear from the Introduction (Chapter 1) and the Literature Review (Chapter 2) that there is a wide distinction between standards and industrial sector rating techniques for polymer gears. Accordingly, the best way to answer the research questions is by following specific testing methods and observations. This chapter explains the research methodology design and procedures that were set up to satisfy the research objectives described in chapter 1.

This experimental programme relies mostly on employing unique test rigs, designed at the University of Warwick [35] with the aim of measuring gears wear under controlled variation of geometric parameters and running conditions. The basic system, which exploits the back-to-back concept, was improved at different stages of this project, in line with other measurements improvements, in order to satisfy measurement accuracy requirements and different test conditions. This chapter gives more details of the test rigs parts, properties and functions. Then the specific methods and techniques used consistently in this research will be explained.

As gears come in different materials, specifications and geometry, the current test rigs are specifically designed for testing gears that made of polymer materials and composites and with some pre-specified geometries (here, centre distance of 60 cm and face width of 15 mm). Accordingly, the load and speed conditions were designed to match the applications for these materials, namely lower loads and speeds compared to metal gears.

3.2 Polymer gear test rig I

The ‘polymer gear test rig I’ provides continuous measurement of polymer gear wear and endurance in dry running conditions, so determining the wear rate of tooth flank surfaces. A broadly similar test rig concept was used previously at The University of Birmingham [1,4,78], although this newly designed test rig is more developed, allowing for modelling and testing of different parameters that occur in real applications, namely operational speed, load, sample material, thermal effects and gear misalignment. In addition, four different parameters can be measured using the new device, which are continuous gear wear, gear surface temperature, time to failure and ambient temperature. A main and unique function of this rig is that it allows for constant applied load over the whole running time.

The design of the rig follows a back-to-back setup, whereby a pair of steel gears (with typical geometry similar to the tested gears and lubricated by oil) drive the two polymer gears using two parallel shafts, one of which has a conical clutch to allow for the initial position adjustment of the tested pair of gears and the torque setting arm. Figure 3.1 shows test rig I with its main parts labelled. The test rig is classified as one of the power recirculation mechanism family, where the electric motor is only required to balance test rig losses that occur from the friction of the bearings, belt, gears and other parts.

One of the main advantages of this test rig is that it was designed to continually measure the wear of gear pairs with good precision, while no load changes are caused by the wear of the running tested gears. When using other well-known test rigs, where an electric motor is used to apply the load and an electric generator is employed to handle that load, the experiment cannot assure that precisely set and continually constant load is applied. Controlling the load throughout a test is very crucial for the current work as it is one of the main parameters that affects the wear rate

of gears. Also, the other testing techniques cannot measure the wear progression of the tested gears very precisely or accurately; the only direct approach is by measuring the number of rotations of each gear of the pair and inferring wear from the difference, which is not a reliable measurement method (especially at short running times), because the difference in the number of rotations (or rotation angle) will be very small. Kono [16] designed a test rig to measure the wear of polymer gears indirectly, by stopping the test each time and measuring the thickness of the tooth before rerun the test again. The current test rig is carefully designed to precisely control the load in accordance with gear dimensions changes arising from wear and so to more accurately measure the wear and wear rate of the polymer gears.

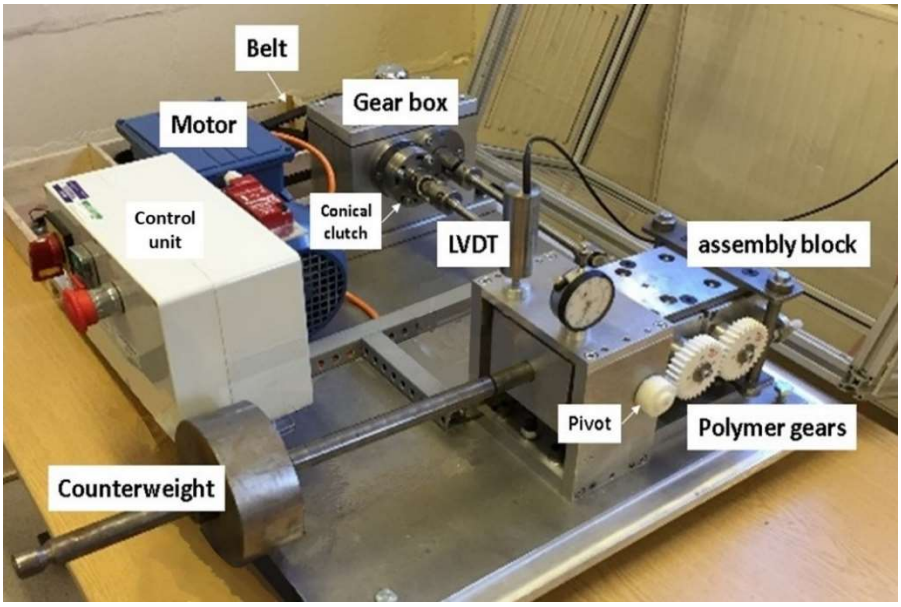

Figure 3.1 Polymer gears test rig I

Tested gears are continually loaded by a constant amount of torque, using a dead-weight system comprising an adjustable counterweight on a (manually adjusted) horizontal torque setting arm (Figure 3.1). Applying this constant weight, with the ability of the assembly block to move around a holding pivot, allows the system to maintain a constant torque on the

tested gears, even with the continuous reduction in the thickness of teeth as a result of surface wear.

A cut-off switch is attached under the assembly block to automatically stop the test when a pre-set level of wear is reached or immediately after gear teeth fracture or suffer other complete damage. The maximum wear allowed is controlled by the two hard-stops below the mounting block and they were adjusted to allow the movement of 1.50 mm above and 1.50 mm below the horizontal position.

While the test is running, moments around the block pivot (which is free to rotate) are equal, which means that the torque of the loaded arm is always balanced by the load carried by the tested gears, and the load on these gears is thereby known and under control. This technique provides a continually constant load on the tested gears, irrespective of the amount of reduction of gear tooth thickness. By ensuring a stable torque on the gears, their wear rate can be defined with respect to the number of cycles at each specified load. The movement around the pivot relates directly to the amount of tooth thickness reduction (and very small comparatively tooth deflection), so measuring the amount of block movement reveals the amount of tooth surface wear in real time. Some factors, including tooth deflection and thermal expansion, may contribute to the wear results, which may not be eliminated from the wear results using the available test rig.

The wear is monitored by measuring the vertical component of the movement of the block using a Linear Variable Differential Transformer (LVDT) (contact displacement transducer) calibrated to an accuracy of 1 µm (device and calibration is described in section 3.5.1). Because of the continuous running of the electric motor and the dead-weight loaded arm, speed and torque are constant throughout the duration of the experiment, while wear, and so time to failure, is recorded simultaneously during the test at regular time intervals.

3.2.1 Principles and specifications for test rig I

Test rig I was built for dry running polymer gears test. Figure 3.2 illustrates the main sub-assemblies, layout and operational principles of the new gear test rig. Drive power is provided by an AC electric motor running at constant speed. A toothed v-belt drive using interchangeable pulleys then provides drive to a gearbox at the rotational speed specified for a particular test.

This test rig is currently driven by a TEC single-phase and dual permanent capacitor asynchronous AC electric motor [102] providing a maximum power of 0.55 kW and running nominally at 1500 RPM. Checks with a precision tachometer confirmed that it maintained this speed to within about 1%. Belt-pulley systems were available to provide testing speeds of 500, 1000, 1500 and 2000 RPM.

The dead-weight loading mechanism can hold the load applied to the test gear pair to within the accuracy of 0.8% of that nominally set. The minimum applied load is governed by the inherent weight of the torque setting arm itself. The maximum load that can be driven is governed by the motor power and running speed to cope up with gear friction losses (in addition to other parts' losses), which is very small in this test rig and, therefore, the maximum torque is limited by the amount of load that the load setting arm can handle in the current configuration.

All tests operated on this test-rig configuration were under dry running conditions and without any gearbox cover. The ambient temperature around test gears was therefore room temperature, typically 22°C to 23°C.

Test rig I allows four different types of misalignments (axial, radial, yaw and pitch misalignments) to model real gear applications misalignment problems that occur mostly by gear box cases or shaft deflection due to different parameters, like thermal expansion and load strain. The test rig I misalignment mechanism will be discussed in the next section (3.2.3).

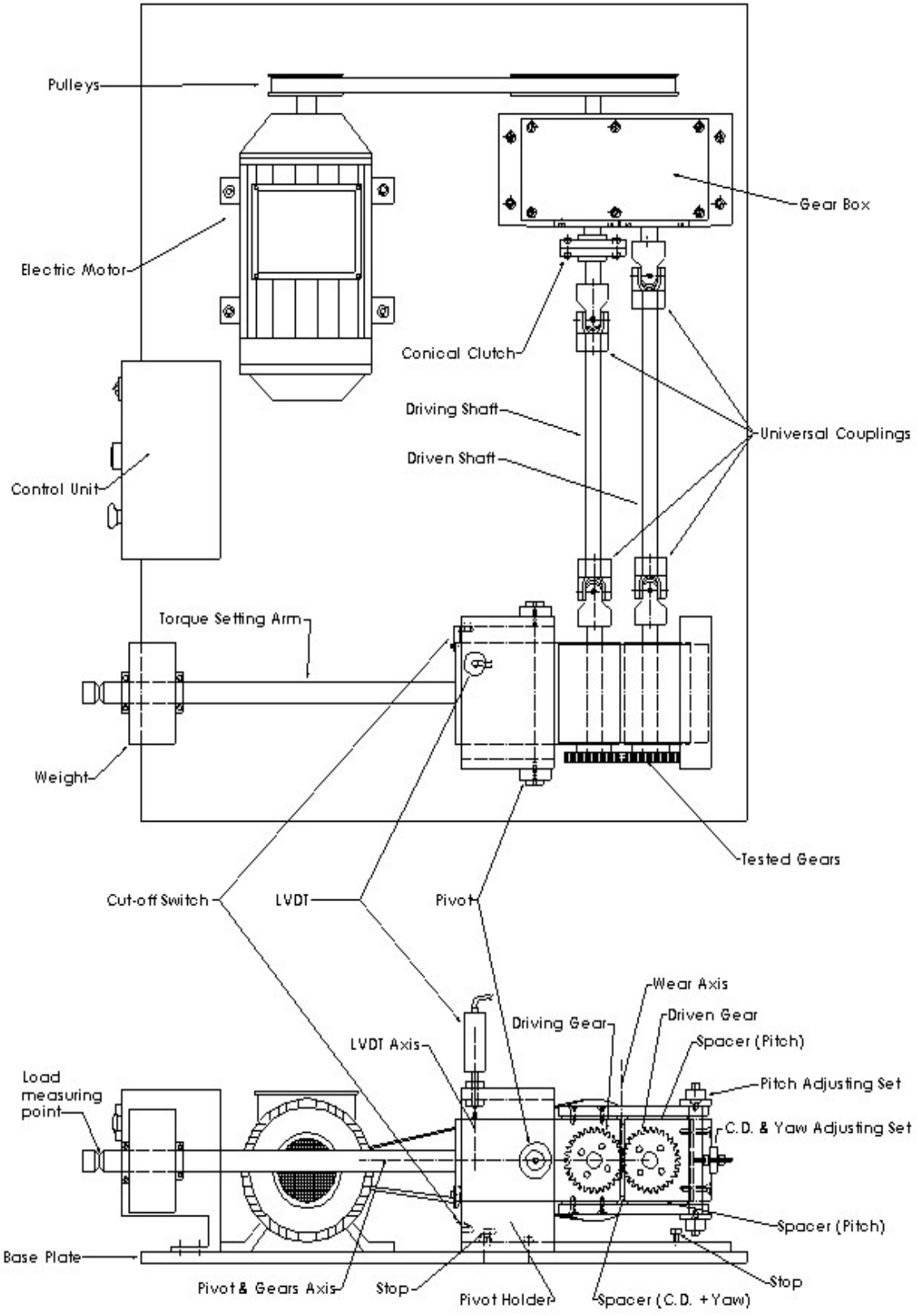

Figure 3.2 Schematic of test rig I layout

3.2.2 Backlash adjustment

All tested polymer gears were designed with the same outer diameter of 64 mm (as used by previous authors). These gears were produced using two different manufacturing methods, namely injection moulded polymer gears and machined cut polymer gears. Both methods result in a small amount of gear dimensional instability, leading to some differences in outer diameter of up to around 0.3 mm. To make sure gears are tested in the right conditions, one of the requirements is to adjust the centre distance for each couple of gears to maintain the right backlash to a standard amount.

Test rig I has the function of centre distance changing, which leads to control the amount of backlash. The gear holding block was made of two parts, each of which carries one of the two gears. A centre-distance (CD) spacer was placed in between these two halves (Figure 3.2), which can be replaced after loosening the CD adjusting nuts. Therefore, the space between the two gears can be changed by controlling the size of this spacer. To ensure an acceptable accuracy, the final CD and backlash was checked using a Vernier calliper for the first and feeler gauges for the second.

3.2.3 Misalignment modelling

Test rig I was designed to model four different types of misalignments (axial, radial, yaw and pitch misalignments). It was intended to reflect some real gear running problems, one of which is misalignments that occur mostly through gear box case or shaft deflections caused by various different parameters, such as thermal expansion and load strain.

Figure 3.3 shows the four types misalignments that can be set by the current test rig I. The mechanism can be adjusted by moving the two gear mounting blocks relative to each other by adjusting the size and shape of misalignment spacers (shown in Figure 3.2).

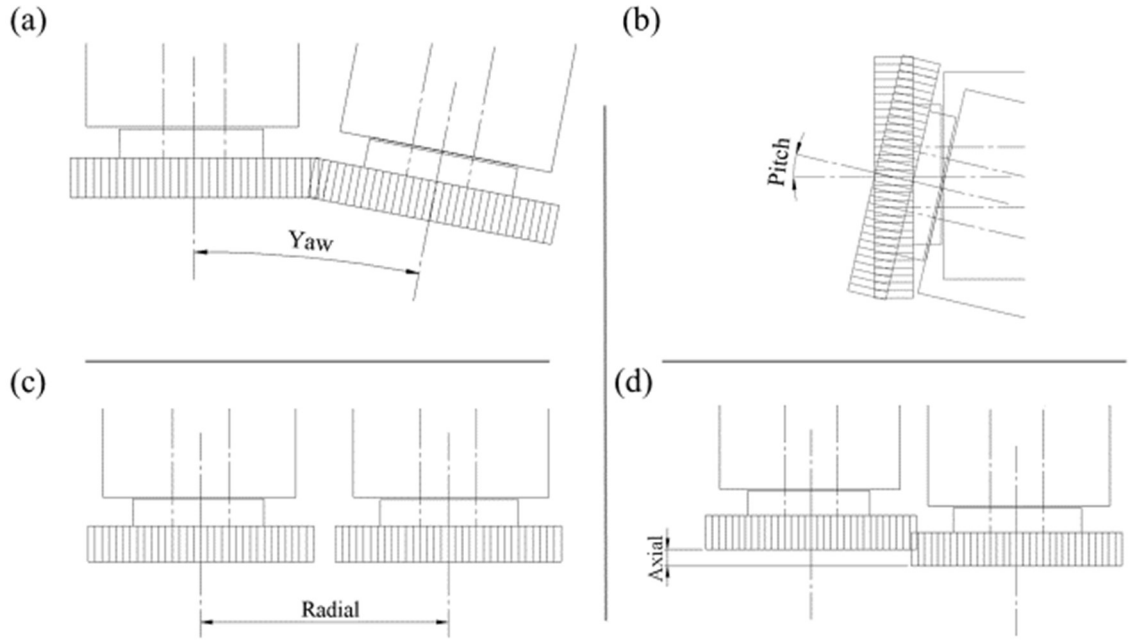

Figure 3.3 The four types of misalignments allowed by test rig I: (a) yaw misalignment, (b) pitch misalignment, (c) radial misalignment and (c) axial misalignment

3.3 Polymer gear test rig II

Similar to test rig I, 'polymer gear test rig II' continually measures wear and endurance for polymer gears, but in a lubrication medium. It has the similar function of applying constant load across the running time of the test, regardless the amount of gear teeth damage. By measuring gear tooth surface wear as a function of running cycles, wear rate can be defined for polymer gears in oil or grease medium. The main concept of this test rig is similar to the concept of test rig I. The new improvement here is the addition of oil bath that covers the test gears and provides a controlled volume to apply any kind of lubrication to the tested gears. To the present, no other test rig is available that provides this unique function, which is continually measuring surface wear for polymer gears under lubrication. In addition to this new function, test rig II provides the control of four other parameters, namely: operational speed, load, sample material and thermal effects. The variables that can be measured and logged using this

test rig include: continuous rear tooth wear, time to failure, gear surface temperature and ambient temperature.

Figure 3.4 shows the layout test for rig II and its main parts (labelled). As in test rig I, the setup is a 'back-to-back' configuration. A pair of steel gears (with typical geometry similar to the tested gears and lubricated by oil) drive the pair of test gears using two parallel shafts with four universal couplings. One of the two shafts contains a conical clutch to control the adjustment of the initial position for the test gears and the torque setting arm. The test rig is classified as one of the power recirculation mechanism family, where the electric motor is only required to balance test rig losses that are occurred from the friction of the bearings, belt and other parts. This test rig is designed to run at higher speeds than the previous one for the reason that gear lubrication allows the capability to run faster.

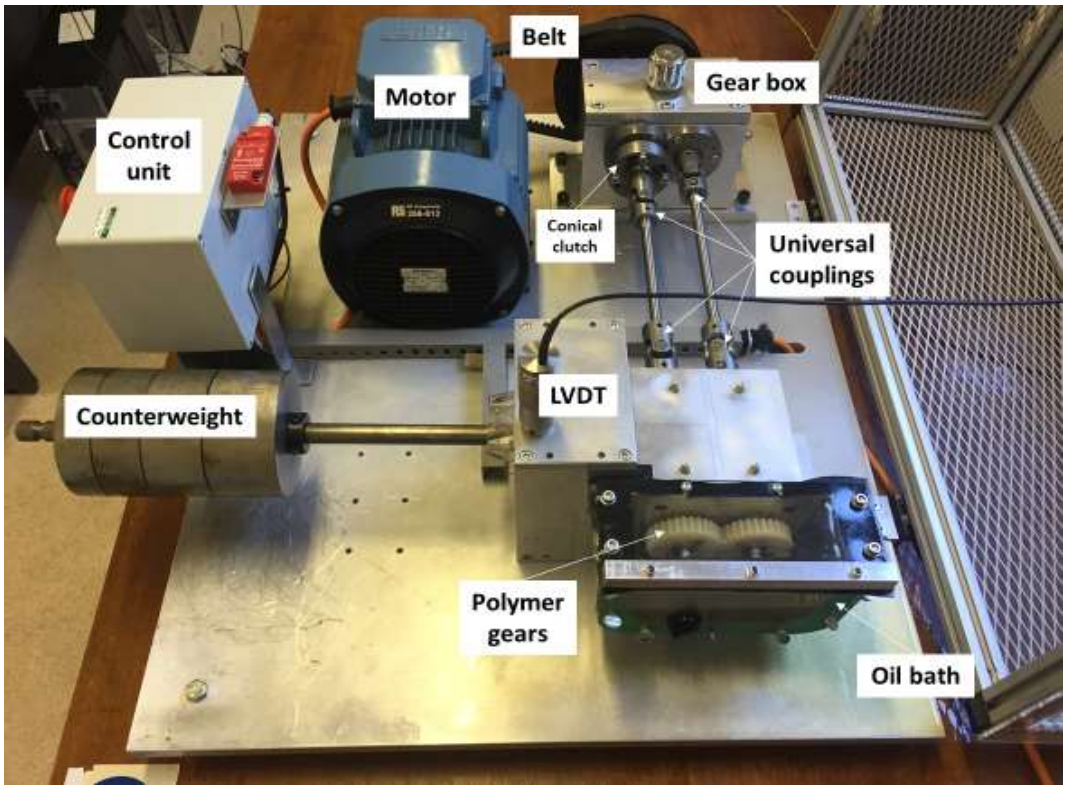

Figure 3.4 Polymer gears test rig II

While test gears are running under lubrication, load is not affected by the change of gear teeth thickness, although the position of the load setting arm will be changing accordingly. This load stability is important in this research, because it is one of the main parameters to be tested against wear rate of polymer gears, making this test rig (as the previous test rig) the most suitable device for obtaining the required data.

Other test rigs have been used to test polymer gears in oil lubrication, but to measure different parameters other than wear and wear rate. For example, Cropper [78] measured torque difference between input and output to get the transmission efficiency.

As in the previous test rig, the tested gears are loaded continually using the load setting arm. With the ability of movement of the assembly block, the counterweight and the mounted oil bath around the pivot, the system ensures that the constant required amount of load is stabilized throughout the running time, regardless of the change of gear shapes. When reaching gear teeth failure point, the assembly block touches the mounted micro switch, so stopping the electric motor. The free rotation pivot ensures equal torque between the load setting arm and the load of the test gear pair and consequently allows the measurement of wear of tested polymer gears at a specified torque. Measuring this rotation around the pivot represents the teeth thickness reduction (wear) and a small amount of teeth deflection. This measurement is done using an LVDT and the measurement method will be explained in section 3.4.

3.3.1 Principles and specifications for test rig II

Figure 3.5 illustrates the main sub-assemblies, layout and operational principles of gear test rig II. It was built for polymer gear tests in a lubrication medium. An aluminium container is attached to the front of the assembly block to function as a gear case and to keep lubrication fluid. The front and top sides of the container was made of transparent plastic

thick sheet to visually monitor the polymer gears while running under test (Figure 3.4).

A three phase AC electric motor drives the test rig at a constant speed to overcome mechanical losses at different parts. Test running speed is set using the interchangeable toothed v-belts and pulleys. The set speed is then stable across the steel gear pair and the test gear pair.

This test rig is currently driven by an ABB three-phase and dual permanent capacitor asynchronous AC electric motor [103] providing a maximum power of 4.6 kW and running nominally speed at 3000 RPM. Checks with a precision tachometer confirmed that it maintained this speed to within about 0.6%. Belt-pulley systems were available to provide testing speeds of 500, 1000, 1500, 2000 and 4500 RPM.

Similar to test rig I, the dead-weight loading mechanism in test rig II can hold the load applied to the test gear pair to within the accuracy of 0.8% of that nominally set. The minimum applied load is governed by the inherent weight of the torque setting arm itself. The maximum load that can be driven is governed by the motor power and running speed to cope up with gear friction losses (in addition to other parts' losses), which is very small in this test rig and, therefore, the maximum torque is limited by the amount of load that the load setting arm can handle in the current configuration.

All tests operated on this test-rig configuration were under oil lubrication running condition using aluminium and plastic gear box to contain the liquid. The ambient temperature around test gears was therefore the temperature of the air and oil around the test gear pair.

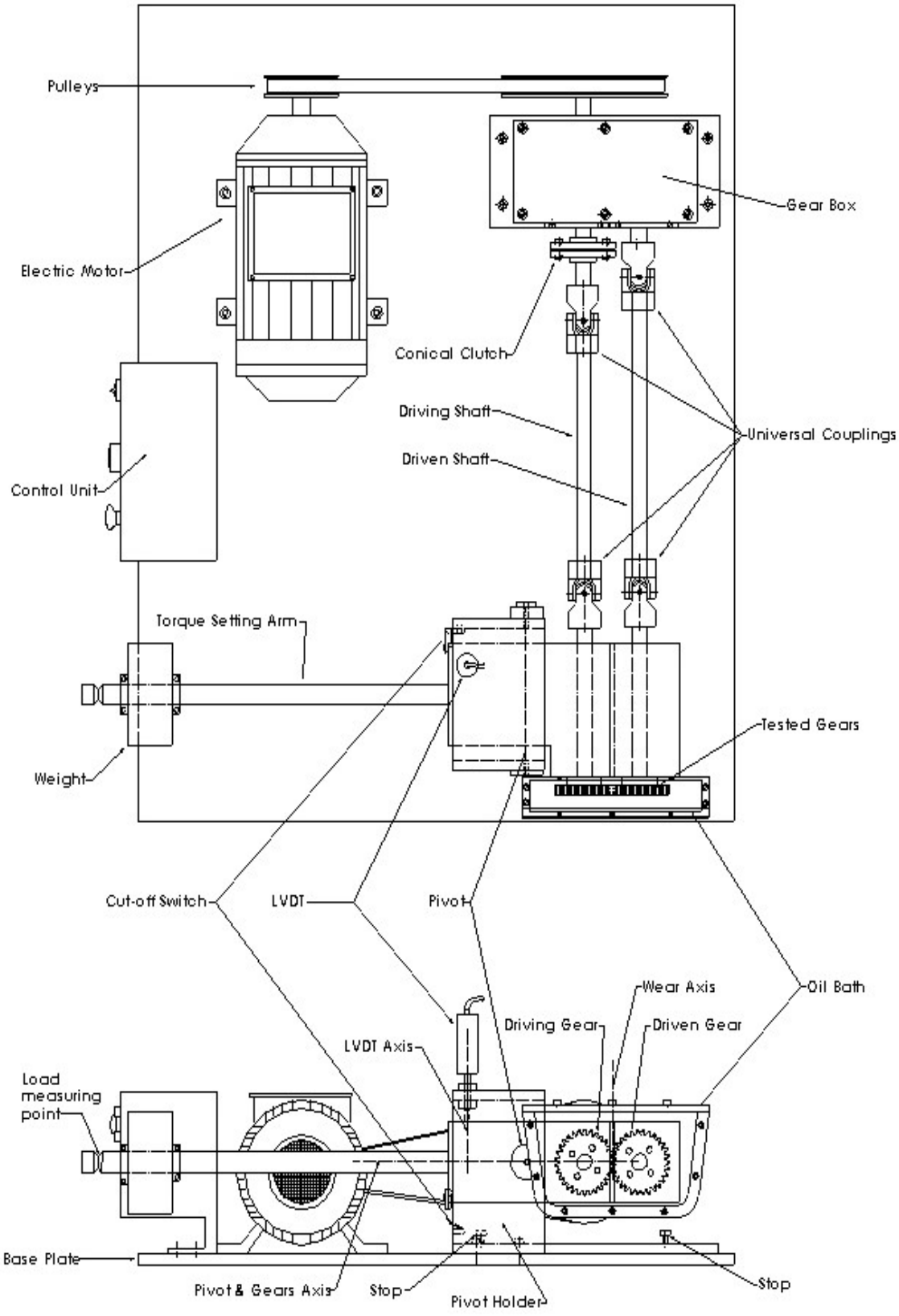

Figure 3.5 Schematic of test rig II layout

3.4 Loading method

Both test rigs use the same loading method, which follows the torque balancing technique around the free rotating pivot. Figure 3.6 shows the schematic diagram for the gear loading mechanism of both rigs. As the loaded arm is balanced by the torques at the two shafts. Therefore:

$$WL = T1 + T2 \tag{3.1}$$

where, W is the equivalent force measured at the load measuring point (Figure 3.2 and Figure 3.5), L is the horizontal distance between the measuring point and the pivot, and $T1$ and $T2$ are the applied torque on shaft 1 and shaft 2.

Neglecting the friction in system (as friction forces cancel each other's because of the opposite direction rotation of the shafts), equation (3.1) can be rewritten as:

$$WL = 2T$$

where, T is the applied torque on the tested gears.

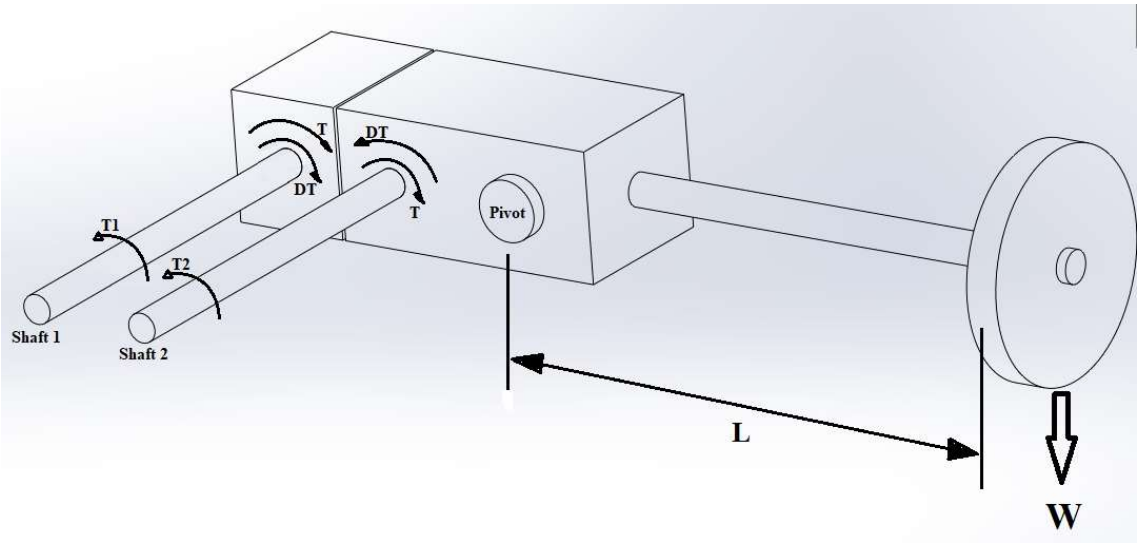

Figure 3.6 Gear loading system

3.5 Wear measurement method

In both test rigs, polymer gear wear is measured and logged across the running time using an LVDT fixed at certain location on the gear block. The design of these test rigs allows the movements of the block to represent the amount of reduction in gear teeth. Therefore, measuring the amount of displacement of this block from its original location is a straightforward method to monitor gear teeth wear. In the following sub-sections, the wear measuring method will be discussed and critically analysed.

3.5.1 Linear Variable Differential Transformer (LVDT)

The used LVDT (type DCTH400AG/1430 from RDP Electronics) [104] has a range of 25 mm and useful resolution of ±0.25%. It was calibrated using calibration-quality gauge blocks with an accuracy of 0.1 µm (see Figure 3.7). The calibration was repeated three times to increase accuracy and eliminate errors. For each gauge block placed in the calibration set, the LVDT output voltage was logged for half an hour. The mean of the logged voltage (volt) was then plotted (neglecting the earlier and final set of data) against the gauge block thickness (mm), as in Figure 3.8. When using the LVDT to measure wear of polymer gears, the output voltage should replace the x value in the equation in Figure 3.8 to get the amount of displacement in mm.

Because of the 2:1 lever fraction, the LVDT resolution of 60 µm (0.25% of the 25 mm range) leads to 30 µm resolution of gear wear depth reading. In addition, because of the rapid sampling rates, averaging of the output signals is possible leading to more increased resolution. Therefore, the corresponding minimum change (wear) at the tooth contact (for the present positioning of the LVDT) can reach up to 1 µm, with the maximum considerably larger than the 3.00 mm maximum wear allowed by the hard-stop function. The LVDT system, which represents an excellent

compromise between sensitivity, robustness, reliability and cost, was incorporated specifically for the needs of the current test programme.

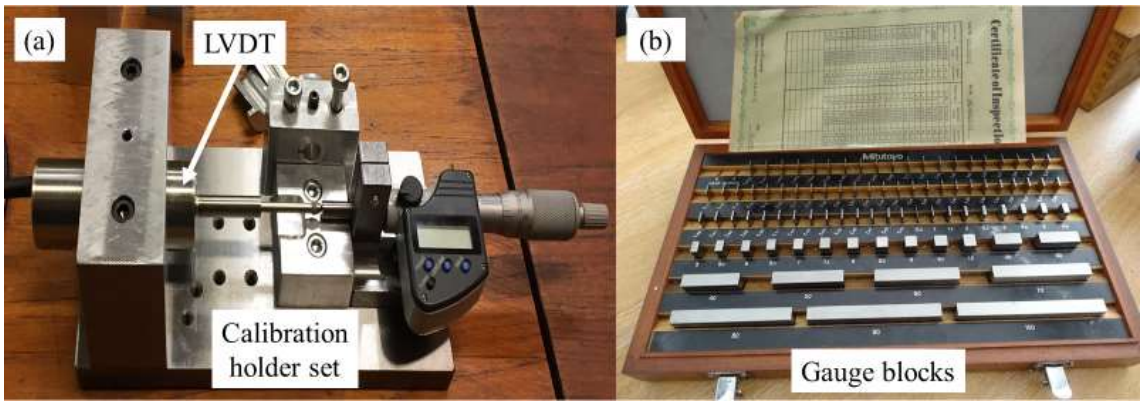

Figure 3.7 (a) LVDT and calibration holder set, and (b) gauge blocks

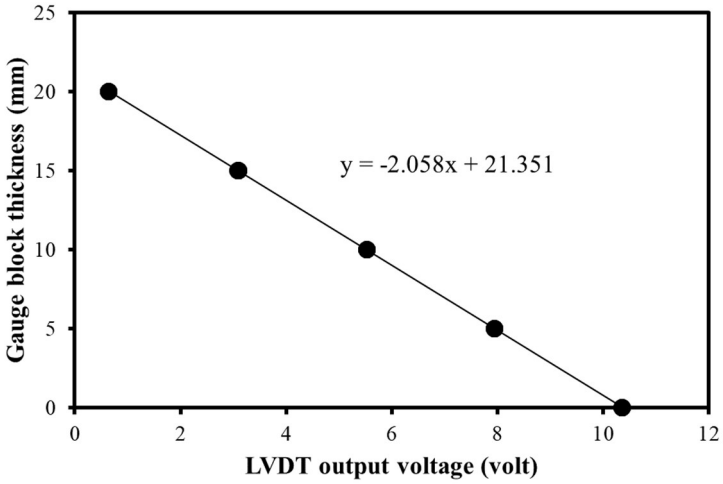

Figure 3.8 LVDT calibration curve

3.5.2 Wear measuring location

Movements of the gear holder block represent the thickness of the amount of material taken from the teeth flanks multiplied by two (the ratio of the distance between the pivot and the displacement transducer measurement axis over the pitch radius of the test gear) (Figure 3.9). This means that wear is measured as a tooth thickness reduction in units of length,

measured across the gear pitch line. This contrasts with the more common method of assessing tooth volume reduction, gear mass reduction, or even off-line tooth thickness reduction measurements all of which require the test is stopped and the test gears (temporarily) removed. The LVDT connector is connected to a microcomputer to log the displacement change (wear depth) in μm as a function of time in milliseconds, allowing a high quality continuous record of wear rate to be defined at any period of the running time.

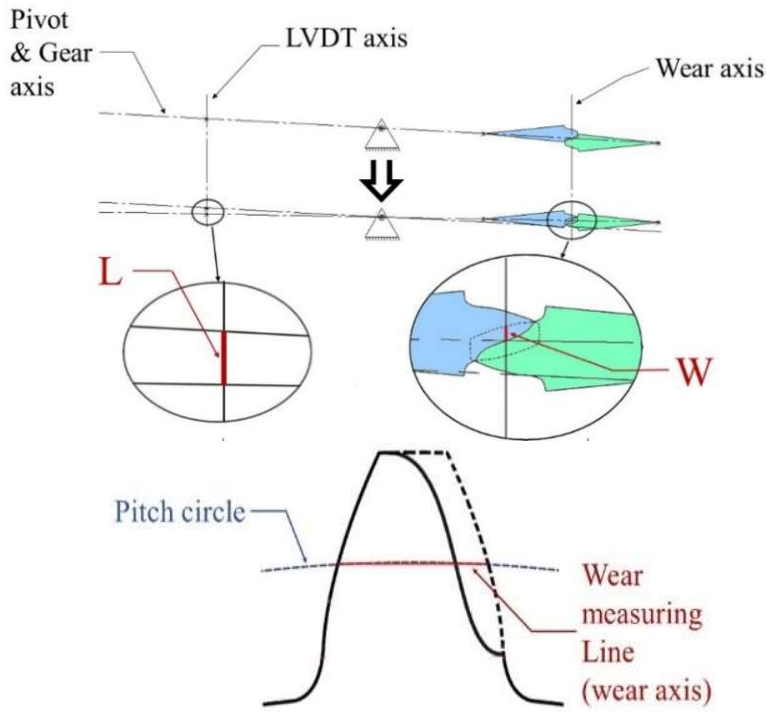

Figure 3.9 Wear measurement (a) method and (b) location

3.5.3 Current method compared to other testing methods

The tribological behaviour of polymers has often been studied using rolling-sliding disc test rigs to represent the measurement of wear rate and failure of different mechanical parts, for instance gears, cams, bearings, etc. such data could be used to represent the tribological behaviour of gears in a way because meshing gears also have both rolling and sliding

surface contact. However, this technique does not predict the unique tribological behaviour of the gear tooth flank, which involves a changeable rolling and sliding behaviour across the tooth flank. The sliding is high around the tooth root and tip while there is almost no sliding around the gear pitch point. Moreover, the load distribution across the gear tooth varies depending on the gear geometry. Generally, the load is higher around the gear pitch line and lower around tooth root and tip, which affects the tooth flank temperature variation and consequently various wear phenomena, including wear rate. This load variation does not occur in rolling-sliding disc tests. The current test rigs both reduce these drawbacks and at the same time increase the result accuracy by more closely modelling the real conditions of gear train device.

3.5.4 Measurement accuracy analysis

For both test rigs, measuring the vertical component of the block movement to determine the amount of gear tooth wear may have some limitations. Inevitably, some error factors apply to this kind of gear wear measurement, as to others. The next sections will discuss these error factors in more detail.

Vibration

The free moving cantilever arm with a loaded end may increase the amount of vibrations on the tested gears, which may form a potential drawback to this testing method. Therefore, during all test runs, the fluctuation in wear readings was measured over certain amounts of time at a rate of milliseconds in order to capture any dynamic behaviours. The amplitude of such local fluctuation was found less than 0.01 % of the overall wear readings, which does not have much effect on measurements, especially with the normally long times of running. In consequence, it was judged to have no effect on gear wear rate calculations for the present work.

Gear teeth deflection

It was observed during the very first tests that when the tested gear pairs were being loaded and the rig adjusted at the start of the running stage, the tooth deflected to some extent. This led to the measuring of higher displacements during the first few minutes of a test, which is explained as a bedding-in stage in terms of the overall cycle-wear curves. This type of deflection could not be separated explicitly from the actual wear displacement measurements in this particular design of the rig. Therefore, the first sub-set of the data was neglected and the wear rate was defined accurately only using the following stage of nearly-linear data, when the wear rate settles to a relatively low and nearly constant value. This was consistent with one of the main targeted objectives of the current research, to infer the required wear rates of the tested polymer gears. Further investigations should be considered as a follow-up stage to better understand the tooth deflection effect on the wear rate of polymer gears.

This tooth deflection may be affected by thermal behaviour changes during the running period. Thermal effect varies depending on the tested material properties. Figure 3.10 shows the stress-strain curves for the acetal (Delrin 500) at different temperatures. In addition, Figure 3.11 shows he stress-strain curves for the nylon (PA) at different temperatures. It can be seen that the material stress capacity reduces with the increase of the temperature.

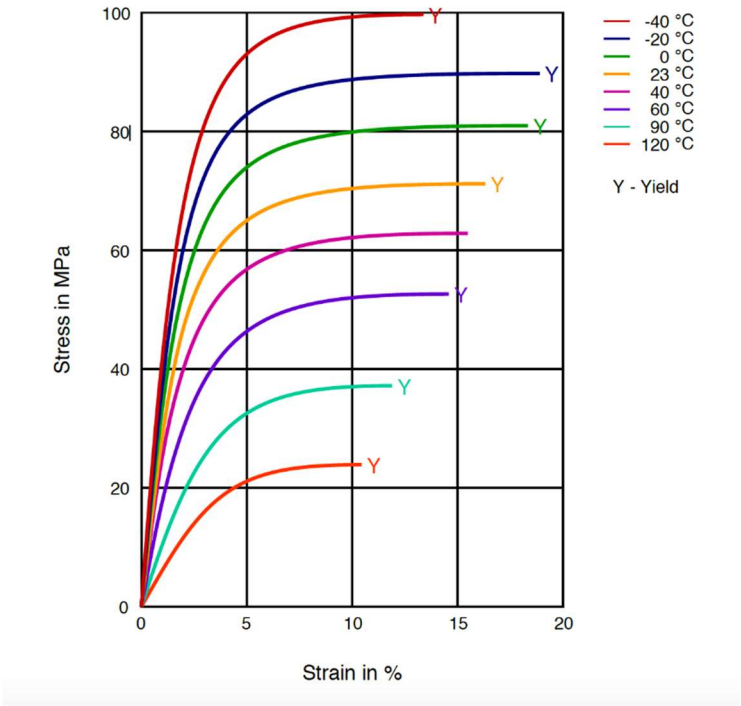

Figure 3.10 The stress-strain (dry) curves for the acetal (Delrin 500) at different temperatures [105]

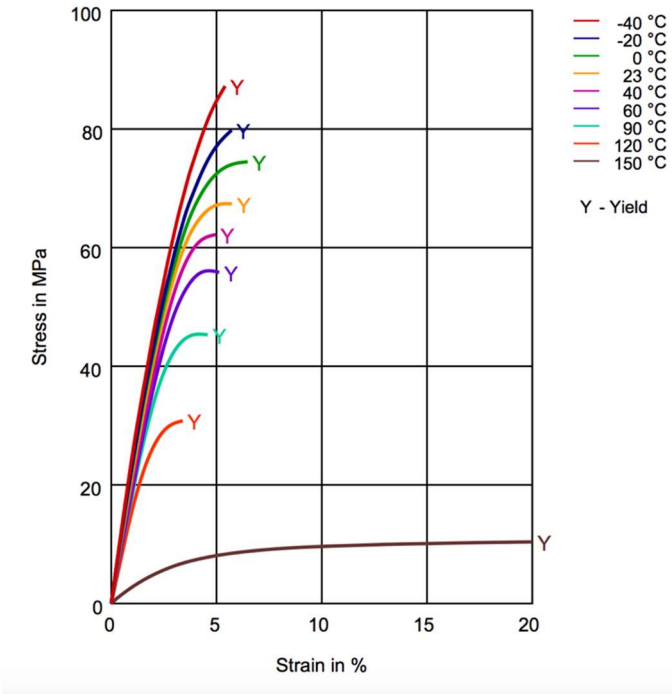

Figure 3.11 The stress-strain (dry) curves for the nylon (PA 66) at different temperatures [106]

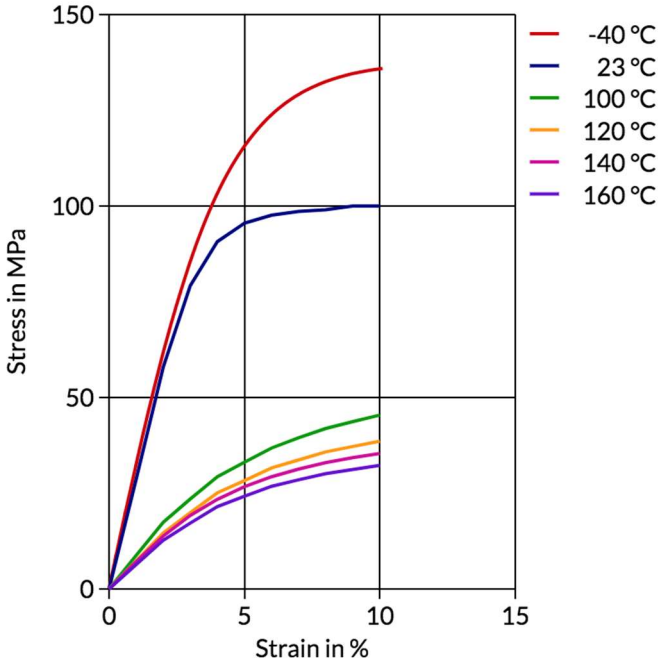

Figure 3.12 The stress-strain (dry) curves for the nylon (PA 46) at different temperatures [107]

3.6 Temperature measurements

Because of the high variation of wear rate phenomenon with load changes in nylon gear tests, a method of measuring gear temperature was required. Measuring gear tooth surface temperature after stopping the teats was not very accurate, because of the fast decrease in temperature. Therefore, it was required to measure the temperature while the gears are running. Two types of temperature were measured. Firstly, ambient temperature around the gears was measured using thermocouples. Then, gear tooth surface temperature was measured using a high definition thermal imaging camera. The following two sub-sections will highlight the methodology for each of these methods.

3.6.1 Ambient temperature measurement

Consideration of local temperature falls within the objective of understanding the wear and failure behaviour of different materials in different test conditions. High precision calibrated S-type thermocouples were used to measure the temperature around, and close enough to, the tested gears (1 mm from tooth tip surface) at different times during the running period. Figure 3.13 shows the locations of temperature measurement points around the tested specimens. Air flow circulation around the teeth flank surfaces can be treated as turbulent flow. Therefore, the measured air temperature at the specified distance may be taken as being close enough to the surface temperature. The measured temperatures were recorded and analysed alongside wear rate, and later combined with a theoretical model to obtain better understanding of it.

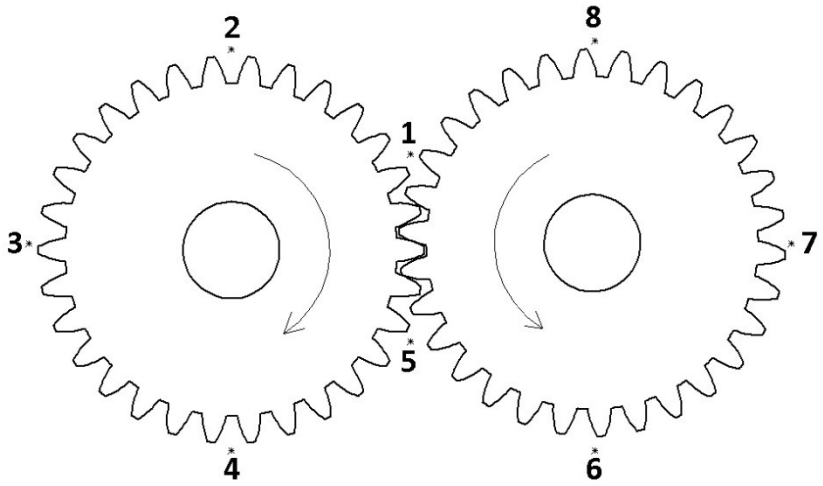

Figure 3.13 Temperature measurement locations using S-type thermocouples, (1) before access, (2), (3) and (4) around the driving gear, (5) after recess, and (6), (7) and (8) around the driven gear

3.6.2 Gear tooth surface temperature measurement

It was noted that the nylon gear wear rate phenomenon is highly sensitive to load with a slightly different pattern than other materials. For this

reason, a high definition thermal imaging camera (FLIR T425) [108] was used in some specified tests to measure the tooth flank temperature, and to highlight its effect on such changing phenomena. The camera has a high-speed record function of up to 1000 frames per second, which helps in the special case of high speed running gears. This infrared camera measures temperature within the range of -20 to 1200 ^{o}C, with a thermal sensitivity of less than 0.05 ^{o}C (at room temperature) and a temperature measurement accuracy of ±2 %, which makes it the suitable device for the required application. In addition, there is the capability of connecting the devise to a computer to log the temperature readings to the provided software (FLIR Research IR) at the rate of 1000 frames per second.

At test rig I, where gears run in dry condition, the camera was fixed above both gears (Figure 3.14). The gear teeth flank temperature was measured for both the driver and driving gears simultaneously. After setting up the camera and connecting it to the computer, some of the preliminary parameters were entered in the 'FLIR Research IR' software as in Table 3.1. Temperatures were recorded in milliseconds and plotted against gear running cycles.

Figure 3.14 Thermal imaging camera location

Table 3.1 Thermal camera preliminary parameters

Thermal emissivity (ε)	0.96
Temperature range	0 - 120°C
Object distance	0.4 m
Atmospheric temperature	22 - 23°C
Calibration	On
Frame rate	1000 Hz
Relative humidity	30 %
Focus	Auto
Digital zoom	1x
Quality	High
Palette	Iron
Image colour adjustment	Auto

In the case of tests running in oil, the thermal camera cannot measure gear surface temperature; because of the gear cover. Therefore, test rig II was modified to be able to measure gears' temperatures by adding two tubes with flat conical ends as in Figure 3.15. To the lower edge of the tubes, a pair of rails were inserted to guide the oil dripping from the top surface of the bath to the sides of the gears to prevent temperature measurement disruption. This modification allows surface temperature measurement with acceptable accuracy (Figure 3.16). Because of the complicated shape of these tubes, they were produced using 3D printing method. Using this manufacturing method allows producing these tubes as one part, i.e. without the need of assembly or welding processes. The material used to produce these parts was tested to ensure the thermal capability beyond our gear running limitations.

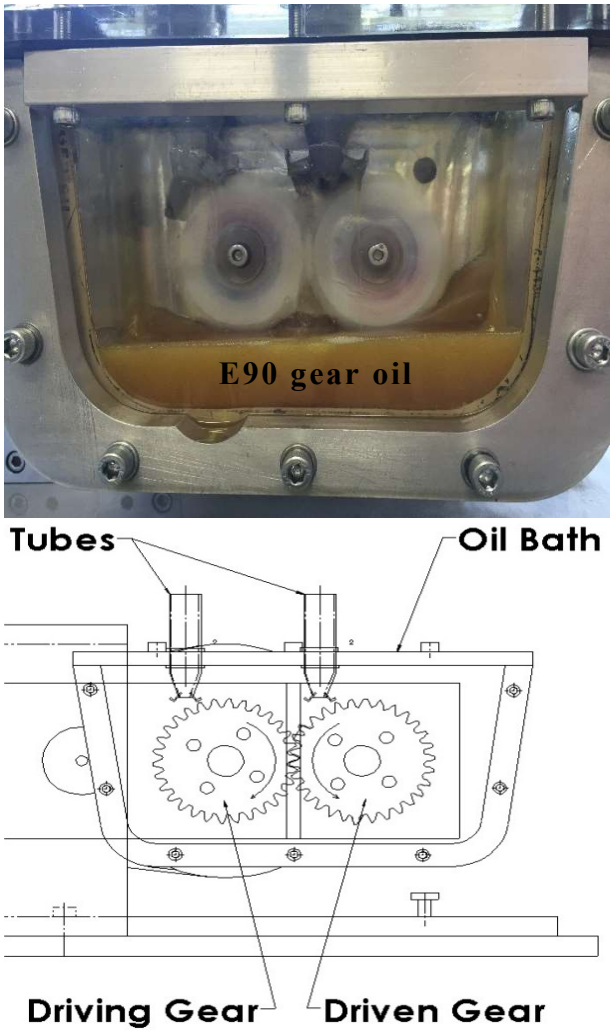

Figure 3.15 Test rig II, oil bath modification

Figure 3.16 Thermal imaging camera position at test rig II

Figure 3.17 shows the thermal images as they appear in the software, where (a) represents the dry running condition in test rig I and (b) represents the oil lubrication condition in test rig II. In both cases, the two red triangles on the driving and driven gears represent the maximum surface temperature. Close contours were drawn on both driving and driven gears and the maximum surface temperature was plotted with respect to running cycle. Results are presented in contrast to wear graphs to be analysed together.

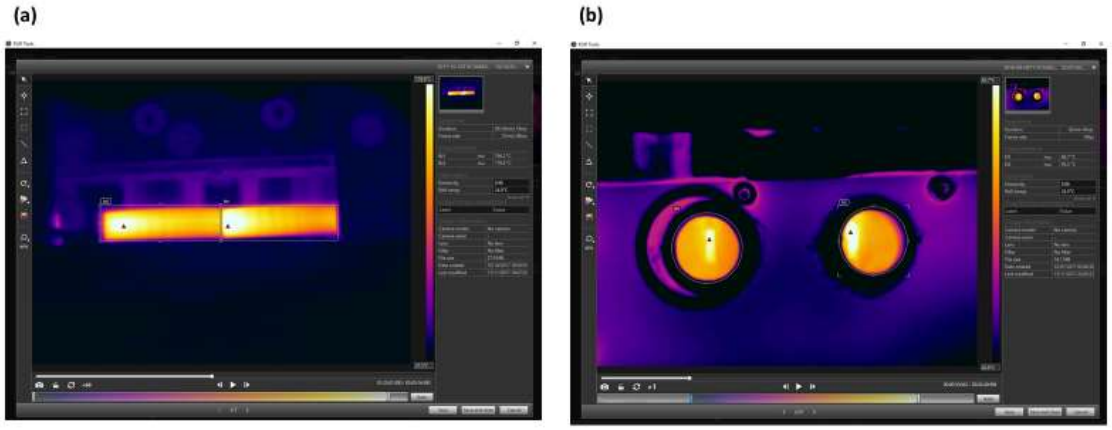

Figure 3.17 Thermal image in FLIR Tools software, a) dry and b) oil lubrication

In both test rigs, surface temperature measuring location is at the tooth surface flank, where the highest temperature is expected to occur, according to many researchers (as illustrated in chapter 2). Figure 3.18 shows temperature measurement locations for driving and driven gears in accordance to the running directions.

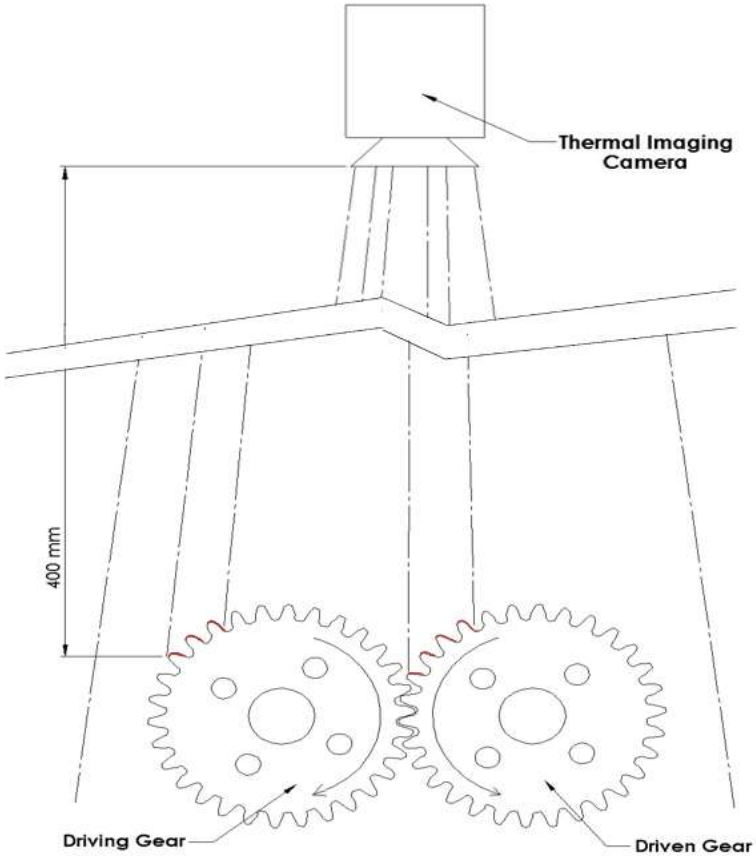

Figure 3.18 Gear tooth surface temperature measurement location

3.7 Test gear specifications

This research used four different sets of gears: the first two sets were nylon 66 and acetal gears, manufactured using a machine cut process, while the second two sets were nylon 46 and polycarbonate (PC) gears produced by injection moulding (materials properties are presented in Table 3.3). They were chosen to be of practical relevance and also for easy comparisons with previous works on polymer gears, as well as previous tribology studies on polymer surfaces operated in non-conformal rolling and sliding contact and pin on disc studies. It is worth clarifying here that, when large numbers of gears are produced, injection moulded gears are very low in cost compared to machine cut gears, as their cost mostly depends on the manufacturing of the mould itself. Typically, moulded gears are 10-20% of the cost of machine cut gears. On the other hand,

when a small batch is required, machined cut gears will be lower in cost, because the cost of designing and manufacturing a mould is avoided. The machine cut gears were manufactured by uniform cuts on extruded bars of nylon (Polyamide 66) and acetal (Delrin 500, POM) using a uniform cutter to shape the required involute profile following the standards for polymer gears manufacturing [6]. Similarly, injection moulded gears were manufactured using a mould that was designed to the same standard. Spur gear samples were designed to a module of 2 mm, 30 teeth and a face width of 15 mm. The tooth flank forms an involute profile with a pressure angle of 20 degree. The calculated theoretical contact ratio is 1.67 (Table 3.2). however, polymer gears are soft enough to deform and mostly increase this amount [18], which might cause changes to the teeth load sharing and pressure angle and consequently affect the contact pressure and Hertzian contact stresses on gear teeth.

Table 3.2 Gear geometry specifications

Module (mm)	2
Tooth Number	30
Pressure angle (deg)	20
Face width (mm)	15
Tooth thickness (mm)	3.14
Contact ratio	1.67
Root fillet (mm)	0.5

Table 3.3 Tested gears' material properties [109–112]

	Machine cut nylon 66	Machine cut acetal	Injection moulded nylon 46	Injection moulded polycarbonate
Supplier	In house	Ondrives	Protolabs	Protolabs
Density (g/cm^3)	1.15	1.41	1.18	1.2
Tensile strength (MPa)	85	67	100	64.8
Flexural modules (MPa)	3100	2200	3000	2340
Static coefficient of friction	0.20	0.10	0.20	0.31
Dynamic coefficient of friction	0.28	0.30	0.28	0.42
Melting temperature (ºC)	258	165	295	144
Real gear shape and colour				

All the polymer gear batches tested conformed to the AGMA polymer gears standard [67], with an outer diameter of 64 mm (±0.3 mm) and a shaft diameter of 16 mm (±0.01 mm). All gears were to the same geometry, therefore all tests were set to gear ratio of 1:1. All produced test gears were checked to ensure gear tooth profiles adequately satisfied the standard involute profile. Figure 3.19 shows one of the samples being checked under the measuring profile projector to be magnified ten times and reflected against the standard gear profile.

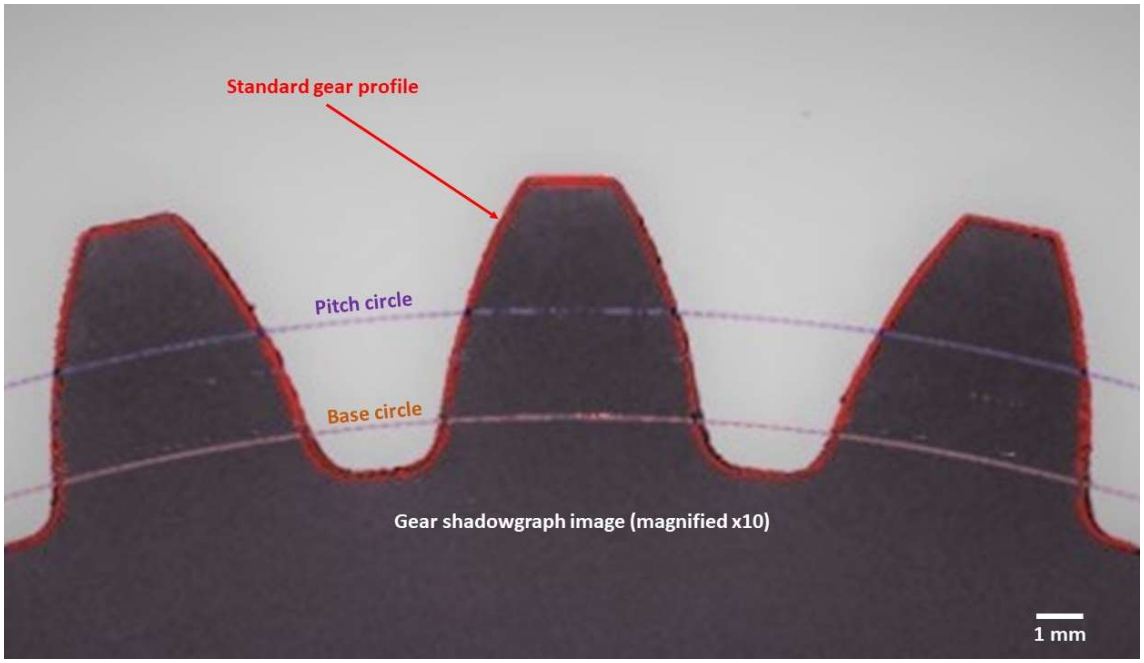

Figure 3.19 Test gear tooth profile compared to the theoretical profile (magnified x10)

Both manufacturing methods lead to some dimensional instability due to material shrinkage as a consequence of manufacturing process, although it is lower in machine cut gears than in injection moulded gears. For the current research samples, the outer diameters of machine cut acetal gears shrank by an average of 0.18 mm from the original diameter (64 mm) (Figure 3.20), while it was reduced by an average of 0.43 mm in the injection moulded nylon 46 gears. On the other hand, the outer diameter of injection moulded polycarbonate gears was increased by the average of 0.83 mm above the theoretical one. Only machine cut nylon 66 gears dimensions were stable enough to satisfy the designed dimensions to around 0.01 mm. These dimensional changes could lead to changes in pressure angle, contact ratio (theoretically 1.65) and set backlash that reduce the noncomparability between individual tests. The centre distance adjustment feature of the test rigs was used to minimise the reaction for each gear pairs. Note that it was confirmed after a number of tests that these amounts of shrinkage do not affect wear rate results, because they are insignificant compared to the wear and deflection measurements.

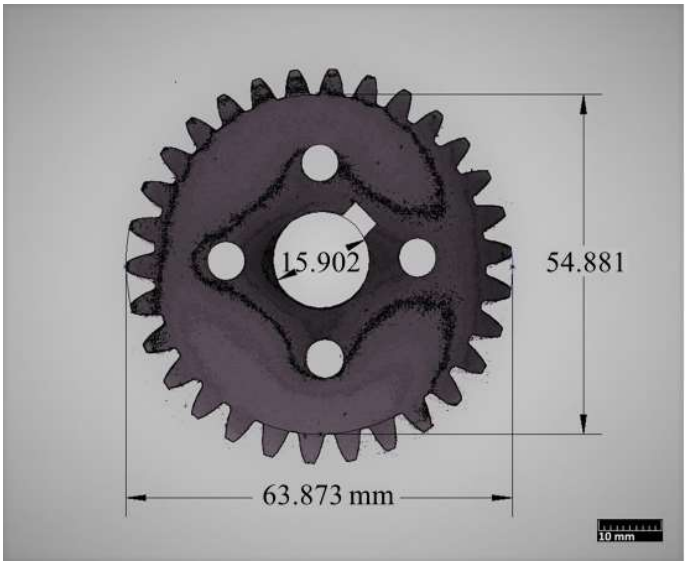

Figure 3.20 Test gear dimensions, measured by profile projector (magnified x10)

Some nylon gears tests had been run previously [4,37], and the results led to the conclusion that nylon gears are the most complicated non-metallic gears, especially for failure modes where fractures occur mostly around the pitch circle, but sometimes at the roots of gear teeth. Also, nylon materials can form small micro cracks when under Hertzian contact stress that lead, after propagation and connecting together, to form large cracks, which progress to tooth fracture failure. Removing the root fillet from the injection moulded nylon gear sample might, therefore, clarify the form, mode and location of failure.

3.8 Test gear investigation

During and after running of a test using either of the two test rigs I and II, all tested gears were investigated using different methods. Firstly, visual observations were made of the gear pairs while running to record the time, status and location of any surface colour changes, and to record the amount and size of debris falling and its time intervals and periods. Further visual inspection of the gears was done after running to investigate the general

status of gears and their teeth in case of shape changes and to note the amount and location of any damage. Secondly, the gears were weighed after testing and compared to their original weights to obtain an independent estimate for checking the total wear. Thirdly, a shadowgraph was used to study the final gear teeth surface profiles in comparison with the initial profiles and to measure the amount of tooth thickness reduction. Fourthly, there was deeper investigation of the tooth surfaces using an optical microscope and an SEM.

When running the tests, some of the tests reached the fracture points, where gears' teeth experience severe damage, while others are stopped before the fracture point or somewhere at the middle of the wear stage. This stop is intentionally done to have the gear tooth surfaces tribologically investigated before they are damaged.

The following will explain the methodologies and used tools for each one of the followed investigations.

3.8.1 Visual investigation

During each test, records were taken for the visual status of the test. The records were assigned to time and time periods using a clock and a stopwatch. Observations includes different variables on the tested gears, as well as the general status of the test including test rig situation and running behaviour. More record notes were taken once the rig was stopped including the stop time, general status of test gears and the amount of debris. A high definition camera (Nikon D5500 [113]) was used to take some pictures of test gears and debris during and after tests. A lens of 18-55 mm focal length was used to picture important events during tests to get wide angle standard images. High shutter speed was used, because the running speed is high. On the other hand, a long focal length (300 mm) lens was used to picture test gear teeth after running to get more detailed images of surface topography. Low shutter speed was used in these photos

to get more detailed images, because both camera and specimen are in stationary status.

3.8.2 Measuring profile projector

After a test stopped, test gears were weighed before being further investigated using a measuring profile projector (or image dimensions measurement system, IDM). The device magnifies the reflected image 10 times, increasing the accuracy of measurement to around 0.01 mm.

A pre-test gear tooth profile was reflected using this IDM and one test gear sample of each batch. The reflected images were then printed and marked on transparent sheets to be used as reference profiles for comparison with after-test samples.

Each after-test gear was attached to the pre-test profile sheet and placed in the IDM to reflect both before and after profiles at the same time. Investigations include gear tooth profile to study the effect of load, speed and other parameters on tooth surface shape. In addition, tooth thickness reduction at the pitch circle was measured to be compared with tooth wear measured using each of the test rigs.

3.8.3 Microscopy

When running the tests using both test rigs I and II, some of the tests reached the fracture point, where gears' teeth experience severe damage, while others were stopped before the fracture point or somewhere at the middle of the wear stage. This stop was intentionally done to have some gear tooth surfaces in an under-running condition (before they are damaged), so that they can be tribologically investigated.

After gears had gone through the three previous types of investigation, they then were taken to the microscopy lab to be investigated under different types of microscopes. In this lab, gear teeth went through two

stages of preparation to the standard for each one of the microscopes. Specimens were then investigated using three types of microscopes, namely: a stereo microscope, a higher resolution optical microscope and a scanning electron microscope (SEM).

The first stage of preparation process is common for all microscopes. It starts with choosing a suitable tooth (of the thirty teeth) of the gear to be cut and separated. The tooth was then cleaned of any excess material from the cutting process. Further cleaning was done using a methanol solution to make sure no debris was left on the tooth surface that could distort the microscope image of the viewed surfaces or damage equipment. Specimens were then left to dry for half an hour. The second stage of preparation process depends on the type of microscope used. It will be explained in each of the following sections.

Stereomicroscope

A stereomicroscope (Nikon SMZ-2T, with a magnification resolution of up to 6.3x) [114] was used for an initial investigation and to help with the selection of the suitable tooth for further investigation (Figure 3.21). This type of microscope functions at low magnification ranges, but its magnification can be increased up to 416x if an auxiliary objective is used. In addition, Clarity of images can be increased by using the attached halogen light. Because of the wider specimen area (field of view) and around 120 mm working distance, a test gear could fit in full without cutting for first observation. The prepared tooth was then examined again using this device to check it was clear of any small particles prior to insertion in the SEM chamber.

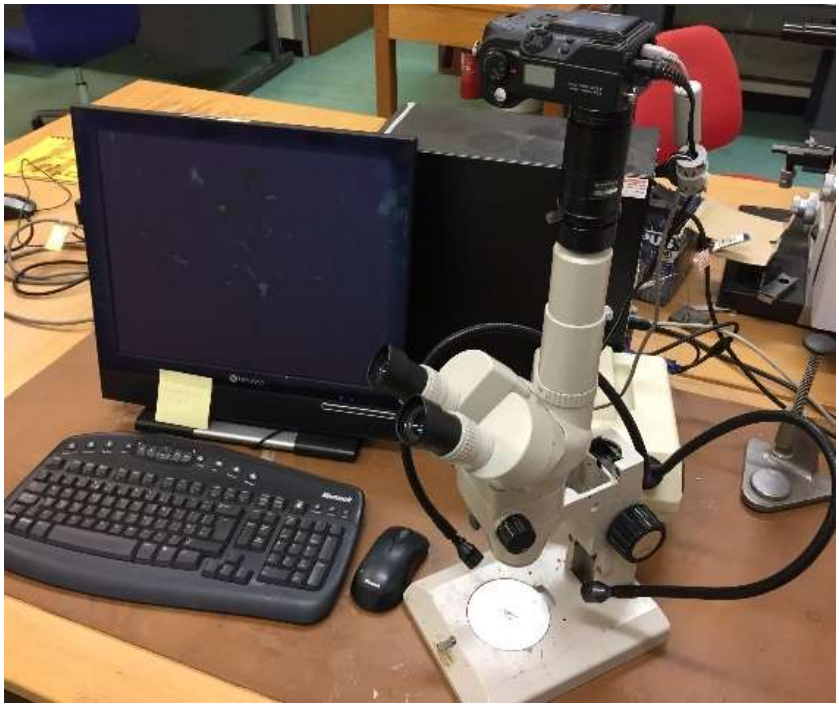

Figure 3.21 Stereo microscope

Higher resolution optical microscope

A higher magnification range optical microscope was used to investigate gear teeth to find out the occurrence of microcracks. A Reichert POLYVAR Met [115] with transmitted light function was used (Figure 3.22 (a)). Micro-thin slices (Figure 3.23) of the tooth side were required, so needing more processing on the previously prepared tooth to take place. First, the tooth was embedded inside a cast support of standard Bakelite resin in a cylinder shape with a diameter of 6 mm. Then, micro-thin slices were cut using the ultra-microtome (Leica-Reichert, ULTRACUT E) [116] (Figure 3.22 (b)). Slices were then placed on slides to be placed and studied under the microscope.

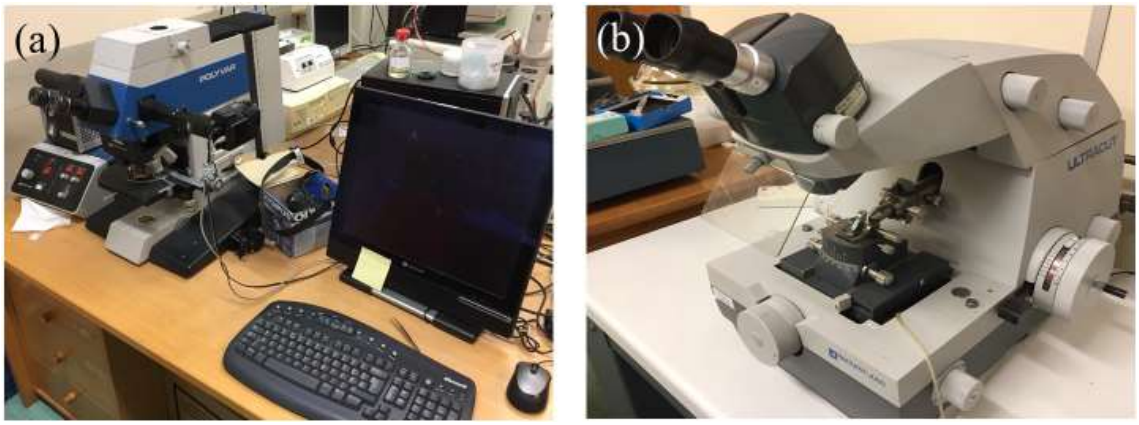

Figure 3.22 (a) Reichert POLYVAR Met high resolution optical microscope and (b) Leica-Reichert ULTRACUT E ultra-microtome

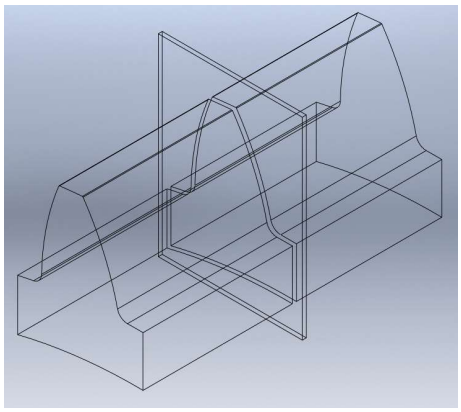

Figure 3.23 Slicing location

Scanning Electron Microscope (SEM)

More tribological advanced investigation was required to understand the function of gear tooth surfaces and damage type at different loads and speeds. For this reason, the scanning electron microscope (Philips, XL30 ESEM) [117] (Figure 3.24) was used to magnify gear tooth surface to reach the nanometre scale. It has the capability of magnification of up to 50,000 times. To prepare a sample to be investigated using this device, the cleaned and dried gear teeth were placed on standard SEM specimen holders and gold coated using a gold coating machine (BIO-RAD SEM Coating System) (Figure 3.25 (a)). Then, a silver (diluted with methanol) was applied on an area that covers both the edge of the tooth and the

specimen holder using a special brush, to act as an electric field connector (Figure 3.25 (b)). The prepared specimen was placed in the SEM chamber, which was then evacuated less than 5 x 10^{-5} mbar. At this vacuum pressure, the accelerating voltage can be applied and image appears on the screen. The accelerating voltage was set to the range of 5 to 12 kV to avoid the heating and melting of the gear tooth surface, because of the hardness properties of polymer materials.

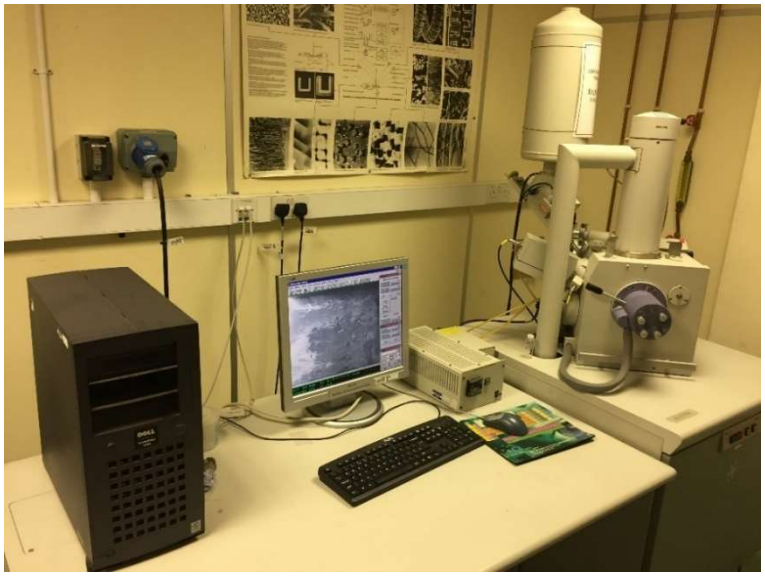

Figure 3.24 Philips XL30 ESEM

Figure 3.25 (a) BIO-RAD SEM Coating System and (b) gear tooth prepared for SEM

3.9 Simultaneous Thermal Analysis (STA)

Simultaneous thermal analysis (Figure 3.26) was done for each one of the tested polymer materials to get real time measurement of weight change with heat. The resulted curve of heat flow against time was analysed and the energy required to melt the material or to recrystallize it was defined. In addition, a more specific melting temperature was defined for each material. Samples were tested at heat rate of 10°C/min and temperature was increased to about 20 °C higher than material data sheet melting point and then cooled down to around the room temperature again. Results were analysed and compared with the temperature measurements done on test rigs I and II.

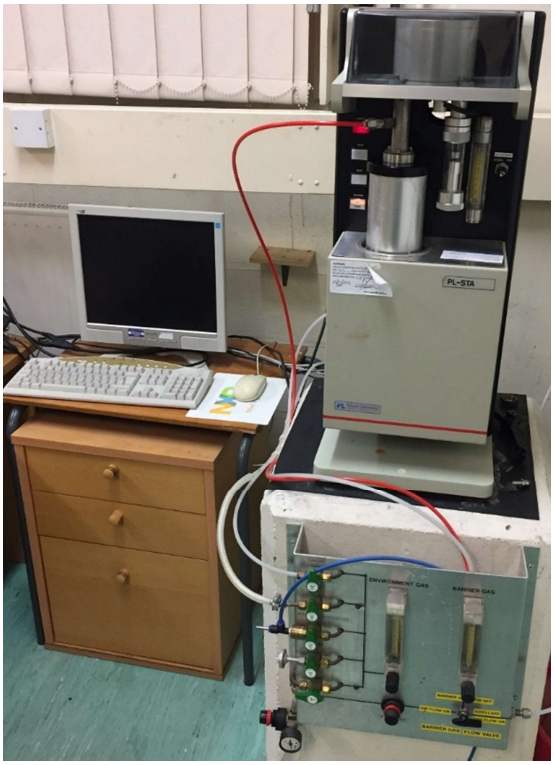

Figure 3.26 Simultaneous thermal analysis (STA)

3.10Summary

This chapter illustrates and explains the research methodologies used for this research project. The two main test rigs are introduced, and their main parts and functions illustrated. The main measured parameters using these test rigs are defined, namely polymer gear wear assessed in continuous measurement using the LVDT device and gear surface temperature in continuous measurement using a thermal imaging camera. In addition, the continuous measurement method of ambient temperature around the gears is discussed.

Different test gear samples were used in this research project. Test gears parameters are explained, including the effect of the manufacturing method and material type on gear dimension stability. Four different material types are included.

Finally, this chapter explains the methodology for gear observations, during and after tests. Those observations include: visual investigation, measuring profile projector and microscopy investigation. In addition, the use of simultaneous thermal analysis for the four polymer materials is introduced.

The following chapters will include the results of tests and their analysis and discussions.

Chapter 4
LOAD CAPACITY AND WEAR BEHAVIOUR OF POLYMER GEARS

4.1 Introduction

As discussed in Chapter 2, the first thorough study of injection moulded acetal gear capacity and wear behaviour was done by Mao [4]. It considerably increased understanding of the phenomena involved in the actual contact behaviour of acetal gears. Therefore, a first set of tests following a similar general approach was designed to discover the overall patterns of wear phenomena and gear capacity for different polymer materials and for two different manufacturing methods.

This chapter starts by presenting results on directly-measured gear tooth wear and under-running test observations using equipment and methods introduced in Chapter 3. Second, it presents and discusses the wear rate of each test and their more notable changes with load. Third, it goes on to discuss the microscopic observation of the teeth and debris in order to better understand the failure mechanisms. Finally, it discusses in some detail how the experimental data relates to analytic modelling. This study involves four polymeric materials and two manufacturing methods.

4.2 Step-loading tests

To measure the total wear and wear rate of pairs of gears under sets of different loads and certain speeds using the current test rig, it would be ideal to run a pair of gears continuously to record wear until failure at each specified load and speed. However, this leads to the consumption of a large amount of gears. Because of the high price of precision gears, an alternative strategy was adopted: to run one pair of gears once at a selected speed, with the load increased by a set amount at set intervals of running time for each load and to measure the tooth surface wear at each load step. This relatively new testing method is called the gear step-loading testing method.

Any set of gears made from specific material has its load and speed endurance capabilities, i.e. maximum load and maximum speed limits. These two capabilities may be determined using the current test rig by running an incremental load test. Initially, one pair of gears was run at a certain low load, which was then increased by the set amount (0.5 Nm in the current experiment) after each specified time interval (half an hour here). In addition, this type of test could reveal the amount of wear rate per cycle for each applied load, which led to a reduction in the number of tests required to reveal such data, and as a result saved more time and cost.

Previously, each load had to be examined by running a separate full test using a pair of polymer gears; this meant consuming a higher amount of test samples to clarify the wear rate value of each load. Using the incremental load test method reveals the required wear rate of polymer gears for each amount of load and, at the same time, saves time, effort and cost by reducing the required number of samples and tests.

4.2.1 Machine cut acetal gears

Figure 4.1 shows the step-loading test result for a machine cut acetal gear running at 1000 RPM, with an initial load of 5 Nm, step-load of 0.5 Nm and final load of 9.5 Nm. It can be seen from the chart that there are some jump steps in wear readings at load transition points. This is because when the load is increased, there was a very small amount of increase in tooth deformation, which could not be separated from wear readings using the current design of the test rig. Although this limitation does not affect gear wear rate (mm/cycle) that is derived from this plot, some improvements could be applied to eliminate tooth deformation from wear readings, which requires the availability of more time and facilities. For instance, tooth thickness across pitch line could be measured at each stage and gear deflection may be theoretically calculated, then both results could be compared with wear readings.

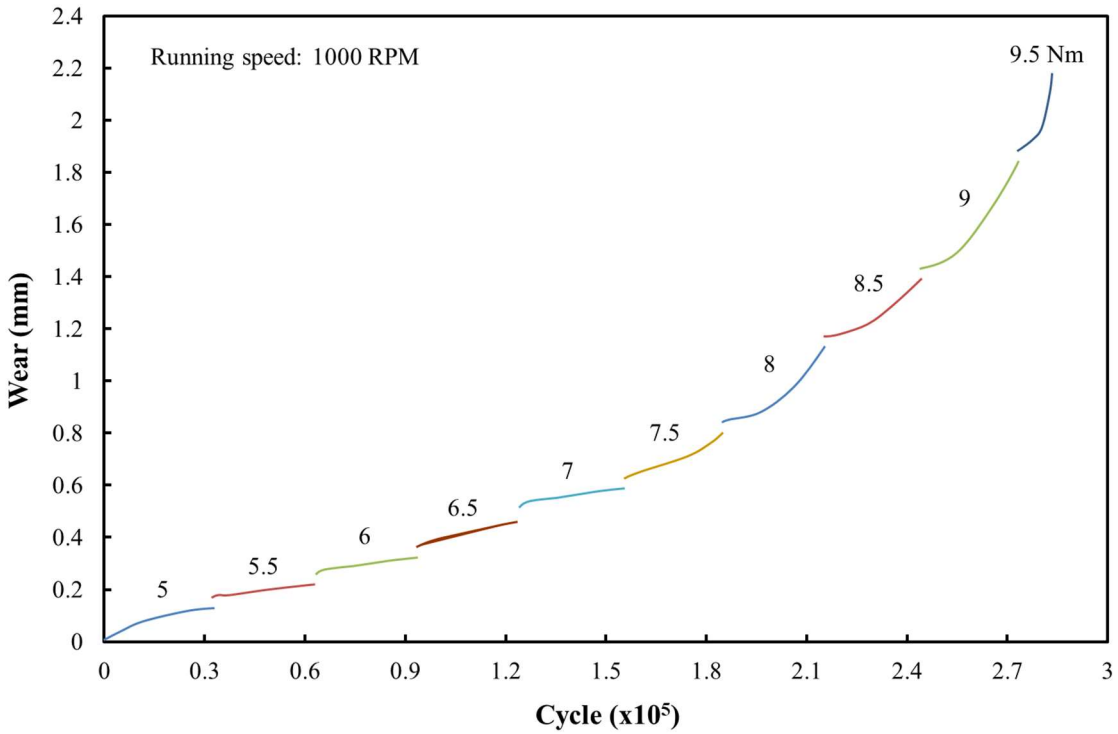

Figure 4.1 Step-loading wear of machined cut acetal gear pair

At the end of the plot, the final jump in wear indicates the gear teeth fracture point, where the test rig's loaded arm drops down and stops the test automatically by touching the cut-off switch. In this test, the gear pair was fractured at the highest capacity load it could reach, therefore the practical highest load capacity was taken as the load increment prior to the one of which fracture occurred. It may be seen from Figure 4.1 that the load capacity of the machined cut acetal gear was 9 Nm. Gear load endurance can be found using this test method for different materials and ranges of speeds, leading to a rapid identification of the ranges of loads and speeds likely to be acceptable for general application and so the ranges most in need of larger-scale study. Therefore, the approach is ideally suited for scoping trials used to specify sensible parameter ranges for larger-scale, specific studies (next chapters). Figure 4.2 shows the after-test machine cut acetal gears.

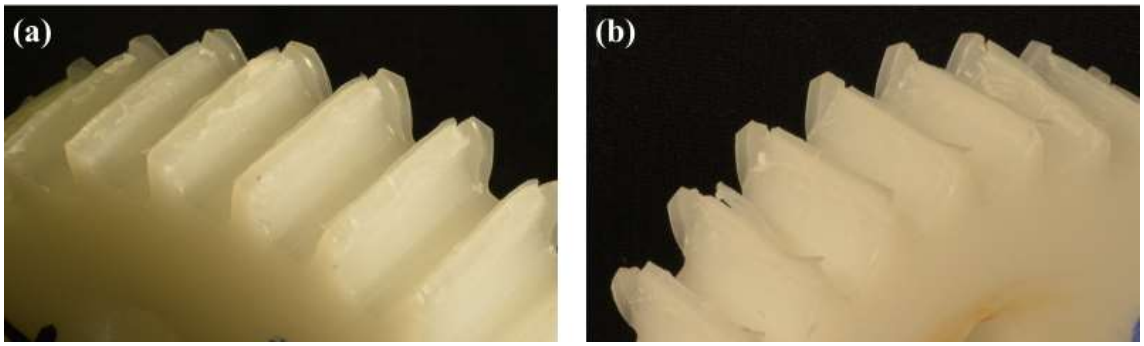

Figure 4.2 The after-test machine cut acetal gears (step-loading test), (a) driving and (b) driven

The wear rate (as a function of number of cycles) for each load was determined from the slope of the least sequence trend line fit to the final ten minutes of data at each stage of loading. In all cases fits were of high quality, with a squared correlation coefficient (R^2) above 99%. Figure 4.3 summarises the values that were obtained from Figure 4.1 for machined cut acetal gear pair.

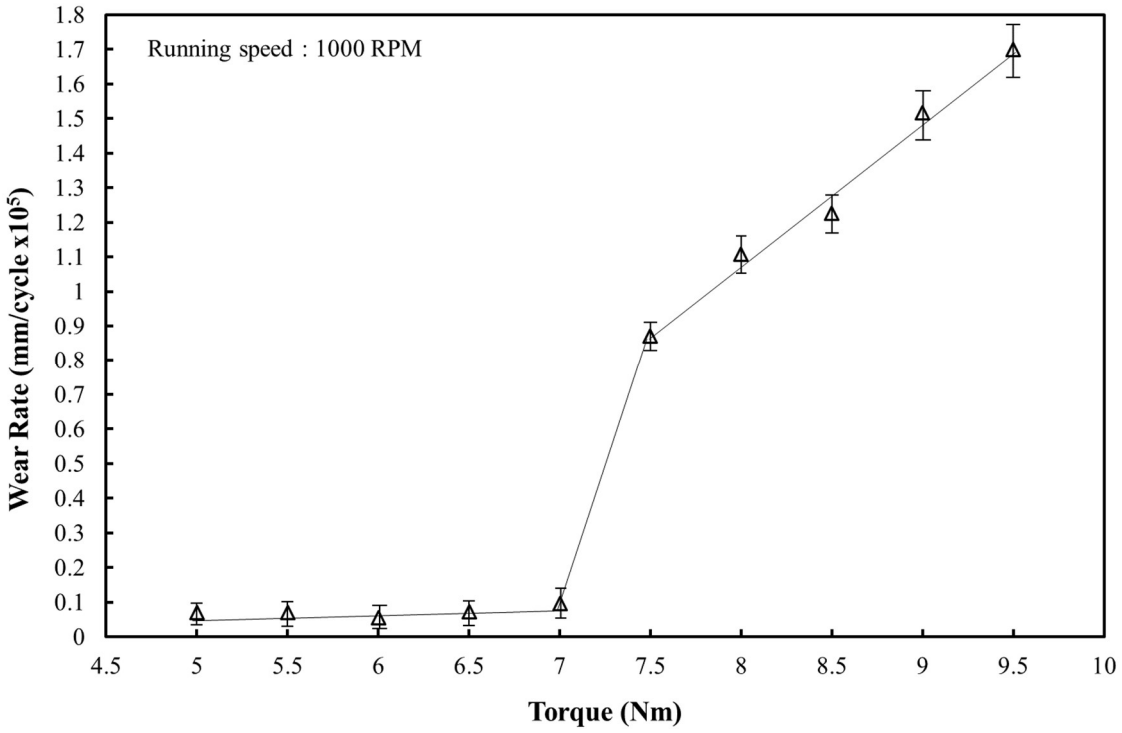

Figure 4.3 Wear rate of machined cut acetal gear (with error bars and typical regional trend lines shown for illustration)

It can be seen from Figure 4.3 that the acetal gear wear rate is relatively low at applied torques below 7 Nm, but this rate increases dramatically afterwards to relatively high values. Therefore, the value of 7 Nm has been assigned as a critical value, along with advice that it is preferable for the load not to exceed this limit to ensure longer life gear running. Moreover, it appeared likely that the reason for the sudden increase after this point was that the gears' surface temperature reached the melting point of acetal (165 ºC). A similar conclusion was reached in other research [75,88]. Comparing the wear rate of these machine cut acetal (Delrin 500) gears with the wear rate of injection moulded acetal (Delrin 100) gears (with similar dimensions and specifications, apart from the face width) found by Hooke et. al. [22] strongly suggests that the wear rate of acetal gears is independent of the manufacturing technique used to produce them. The wear rates and transition points of the two samples with different manufacturing methods nearly match, with the transition points happening

at 7.5 Nm load because they relate to the gear surface reaching its melting point.

4.2.2 Injection moulded nylon gears

The same procedure just applied to an acetal gear pair was then used to assess the load-wear characteristics of other types of gear. Figure 4.4 shows the incremental load test results for an injection moulded nylon gear pair. It can be seen that there was again a jump step in wear reading at a load transition point, for the same reason as in Figure 4.1. The final jump in wear indicated the gear teeth fracture points. From Figure 4.4, the maximum load capacity for the injection moulded nylon gear is 9.5 Nm. Figure 4.5 shows the after-test injection moulded nylon gears.

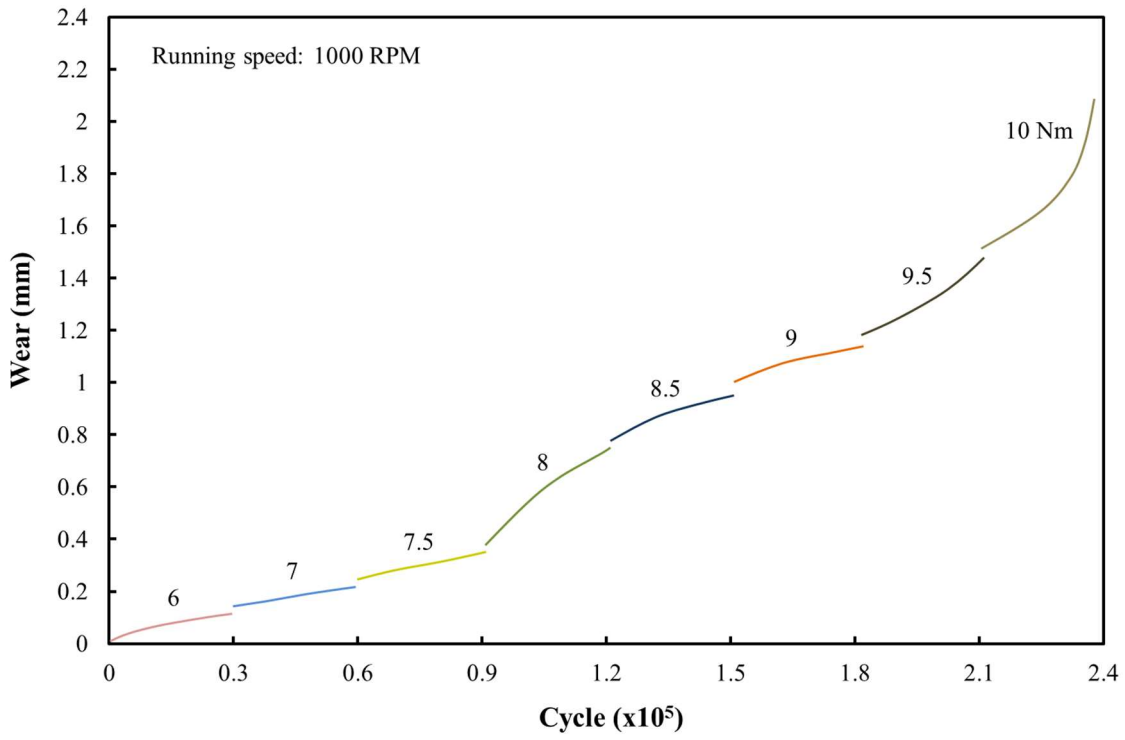

Figure 4.4 Step-loading wear of injection moulded nylon gear pair

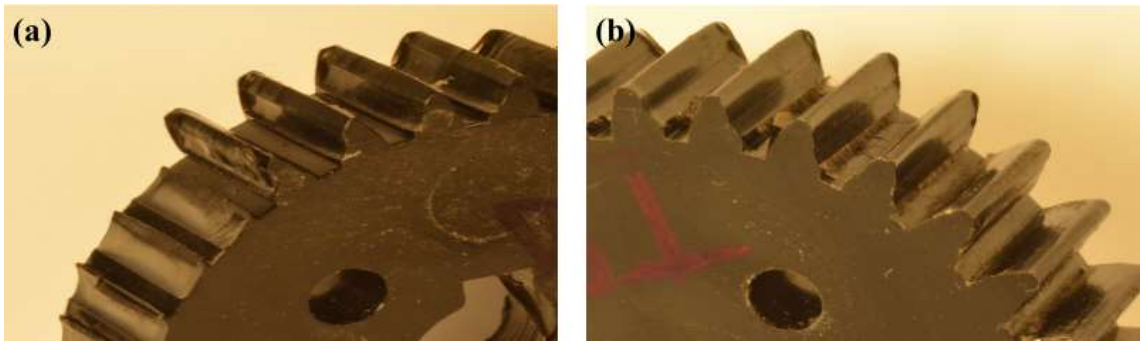

Figure 4.5 The after-test injection moulded nylon gears (step-loading test), (a) driving and (b) driven

Injection moulded nylon gears showed different wear rate behaviour in the torque incremental test. It may be seen from Figure 4.6 that the wear rate is relatively low at the loads of 7.5 Nm and lower. This wear rate suddenly reached a peak when the torque reached 8 Nm before returning to wear rate values similar to those in the early stage. This event was followed by a dramatic increase at loads of 9.5 Nm and afterwards. This wear rate trend was found to be repeatable for many tests that were done, with similar observations found each time. Moreover, this pattern closely matches that seen for the wear rate of two nylon discs running in non-conformal contact [37], where the authors identified the same wear rate trend with respect to load increase.

In the current test, it was observed that on reaching the load of 8 Nm, a brown colour film covered the working teeth surface flanks. This was thought to be some molten material from the gears' surfaces that functioned as an internal lubricant, which was taken to be the reason for the sudden decrease in wear rate after reaching a peak at that point. A similar conclusion was reached by Hooke [37] using twin nylon disc.

The earlier low load range wear rate was occurring at relatively low gear surface temperature, and showed the same behaviour as acetal gears, where wear rate increased slightly with load increase. Increasing the load afterwards led to an elimination of the surface film created at 8.5 Nm torque. This phenomenon revealed the reason for the sudden decrease in

wear rate at a certain load, followed by a dramatic increase. The tested injection moulded nylon gears were fractured at a load of 9.5 Nm and the fracture normally occurred at the root of the driver gear teeth.

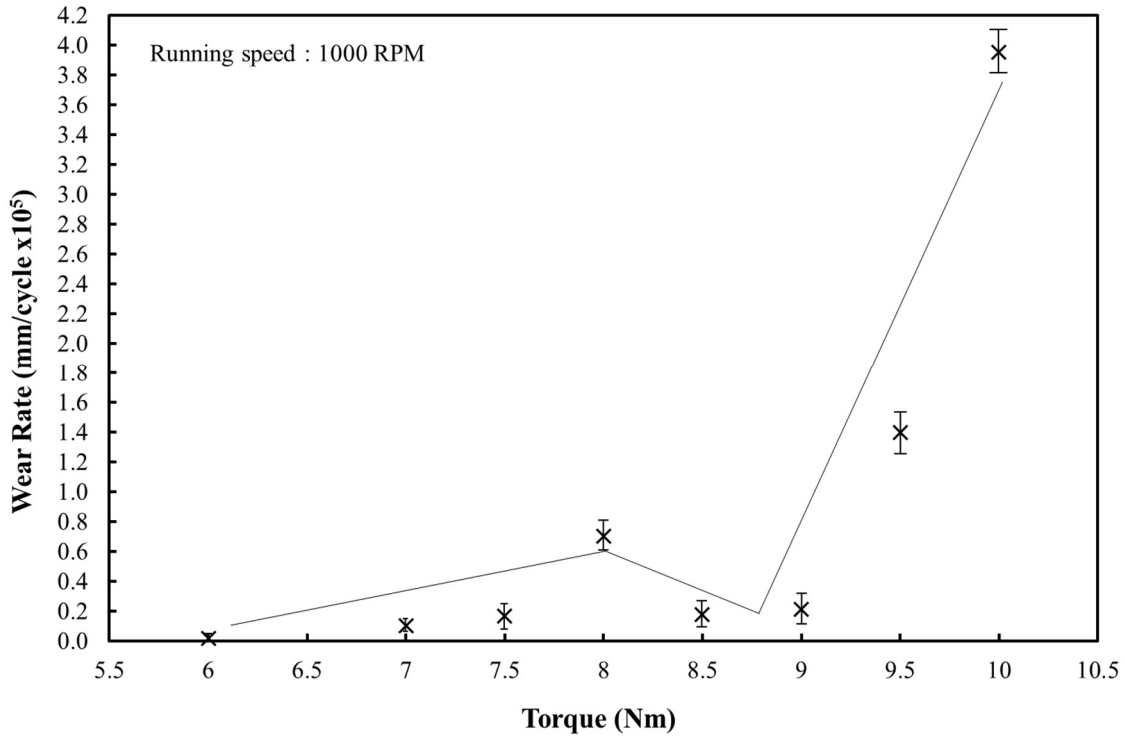

Figure 4.6 Wear rate of injection moulded nylon gear (with error bars and typical regional trend lines shown for illustration)

4.2.3 Machine cut nylon gear

A closely similar pattern was seen when testing machine cut nylon gears (Figure 4.7). Figure 4.8 shows the after-test machine cut nylon gears. The wear rate was generally low at lower loads and then became relatively high with a dramatic increase at a torque of 10 Nm, but with two clear dips at loads of around 6.5 Nm and 9 Nm (Figure 4.9). The reason for these wear rate decreases is the same as for the injection moulded nylon gears. Although they have the same gear dimensions, similar friction coefficients and melting temperatures, injection moulded nylon gears fractured at load of 9.5 Nm, while machined cut nylon gears were able to carry the load for

up to 11 Nm. This difference in load capacity was thought to be because of different material crystallinity that leads to different structural stiffness and strength. Two researches by Hook et. al [118] and Kukureka et. al [92] confirmed the variance of material crystallinity by the manufacturing techniques.

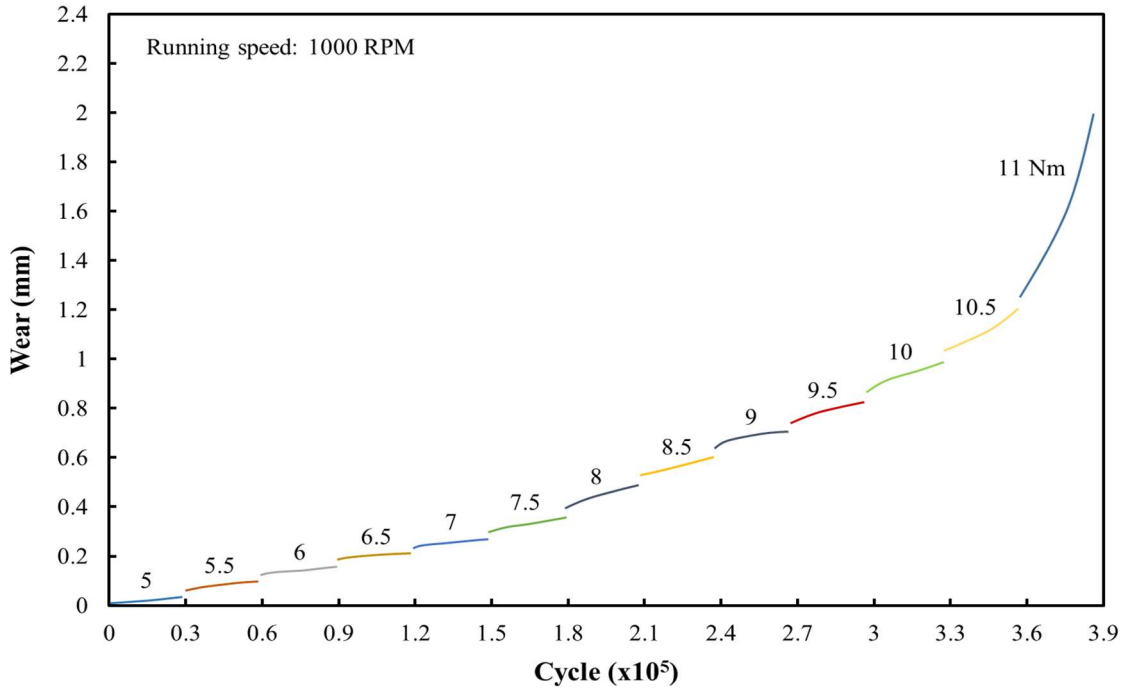

Figure 4.7 Step-loading wear of machined cut nylon gear pair

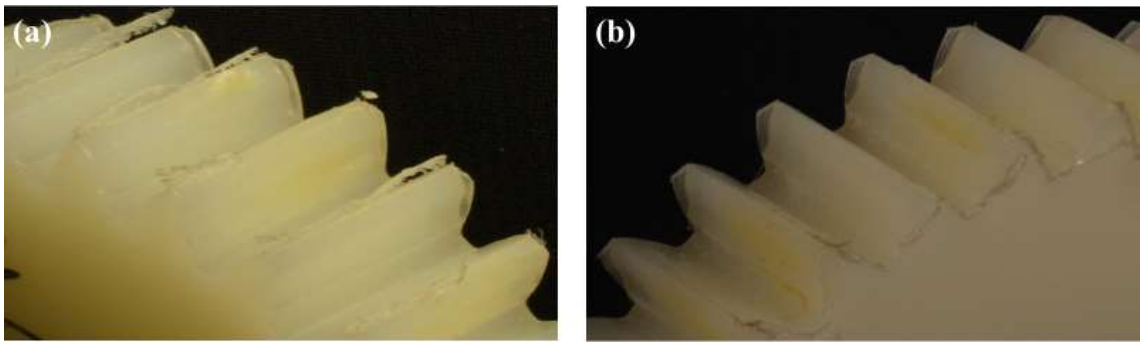

Figure 4.8 The after-test machine cut nylon gears (step-loading test), (a) driving and (b) driven

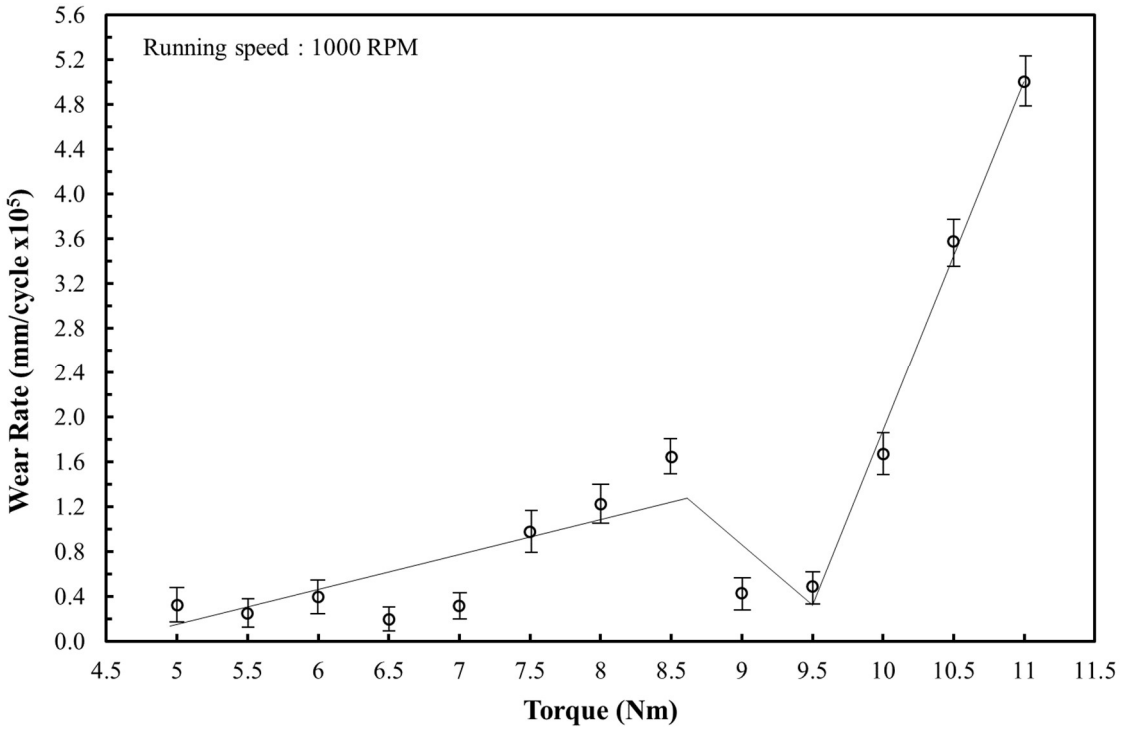

Figure 4.9 Wear rate of machined cut nylon gear (with error bars and typical regional trend lines shown for illustration)

Visual observation to this test revealed the similar interesting phenomenon that on reaching the load of 8.5 Nm the working teeth surface flanks was covered by a yellow coloured film. At values around this critical load, some molten material covered the tooth surfaces and acted as an internal lubricant, which was thought to be the reason for the sudden decrease in wear rate after reaching a peak at that point. Therefore, when designing nylon gears by considering running time and life, one should take into account, especially, any wear rate quoted for nylon at loads around the peak transition area. It might be unwise to rely on operation continuing consistently in this window.

4.2.4 Injection moulded polycarbonate gears

A similar wear rate phenomenon was observed by running pairs of injection moulded polycarbonate (PC) gears (Figure 4.10), where wear rate

(Figure 4.11) was fairly at constant increase at loads below 4.5 Nm before jumping to a relatively high wear rate, which was followed by a sudden failure by teeth fracture around the dedendum side and mostly close to the root of the driver gear teeth. Moreover, the wear rate of PC is relatively high at low applied loads, compared to other tested materials, while load endurance is very low (3 to 5 Nm), which is below the starting load used for the other materials. This is likely to occur because of the higher coefficient of friction of this material compared to others, as well as the low durability of wear and fatigue strength (Table 3.3), which leads to higher surface temperatures.

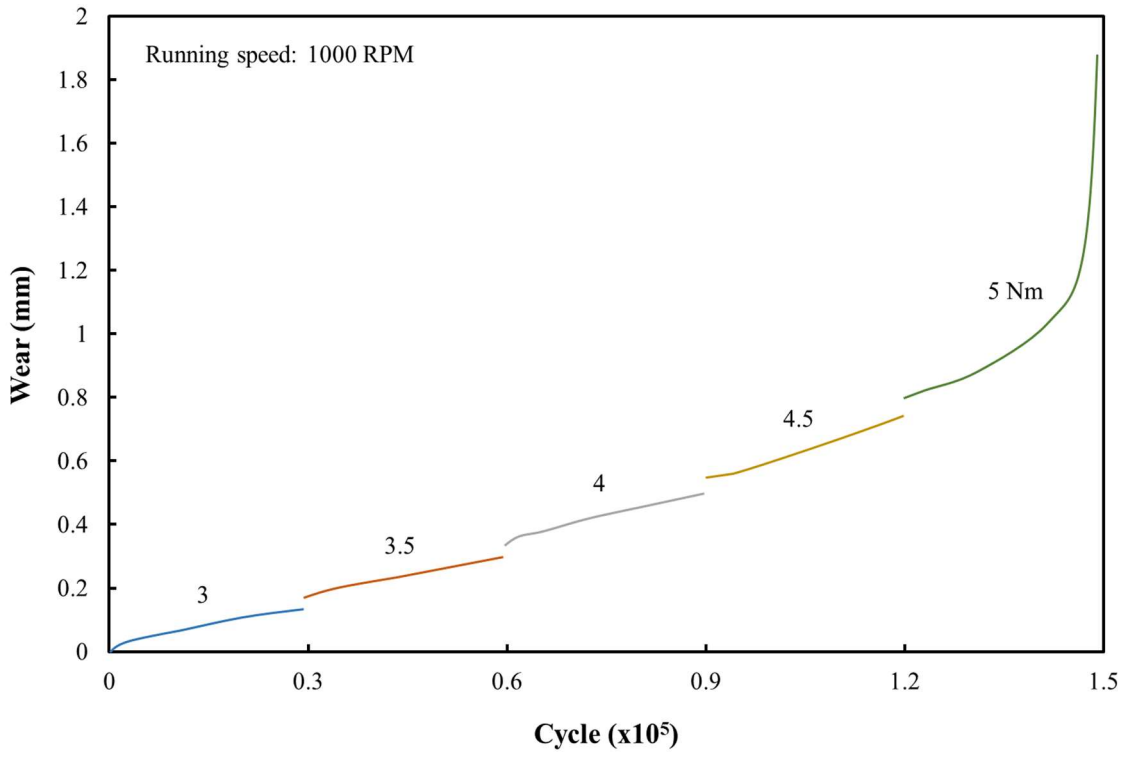

Figure 4.10 Step-loading wear of injection moulded polycarbonate gear pair

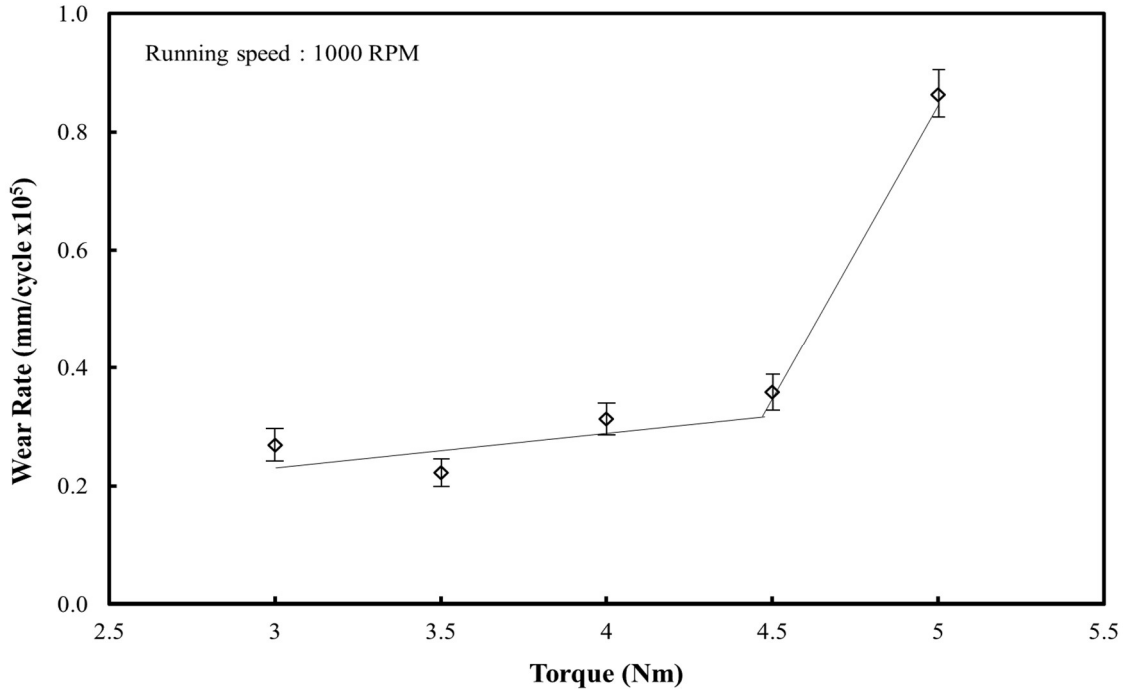

Figure 4.11 Wear rate of injection moulded polycarbonate gear (with error bars and typical regional trend lines shown for illustration)

It was observed with this specific material that when the fracture point was reached and the test stopped, some melted and re-solidified material could be seen at the front of the driven gear teeth flanks, towards the root side. After stopping the rig, this molten material was observed to suddenly gain rigidity and to shape into some material clots at the dedendum circle. The after-test gear tooth surfaces can be seen in Figure 4.12.

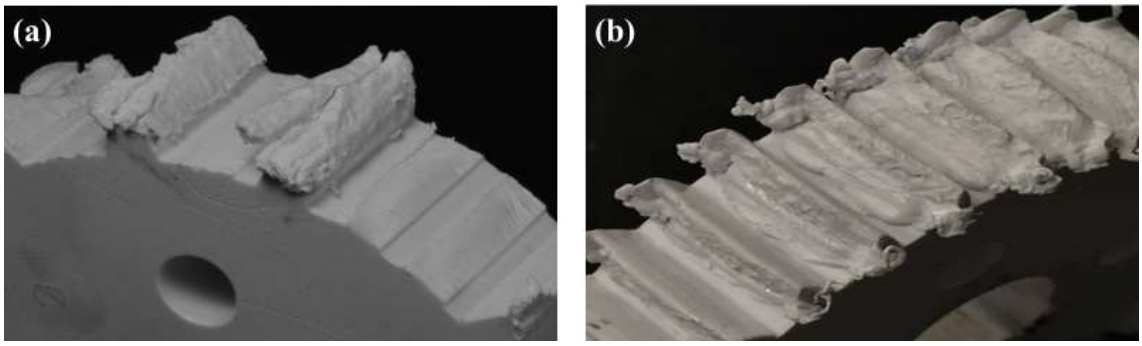

Figure 4.12 The after-test injection moulded polycarbonate gears (step-loading test), (a) driving and (b) driven

4.3 STA results for the four polymer materials

A small sample of around 10 mg of each tested polymer material was examined using the Simultaneous thermal analysis (Figure 3.26) to find the glass transition temperature, the melting temperature and the recrystallisation temperature for each sample. Experiments were set up to apply a heat rate of 10°C/min on the tested sample, until reaching the targeted temperature (20°C above the given highest temperature from the material data sheet) and then cooled down at the same heat rate until returning to the room temperature again. The heat flow and temperature were plotted against time. The area under and above the high transition parts were calculated to find the required energy to melt the material or to recrystallize it.

Figure 4.13 shows the STA curve for the machine cut acetal material. The tested sample size was around 12.5 mg.

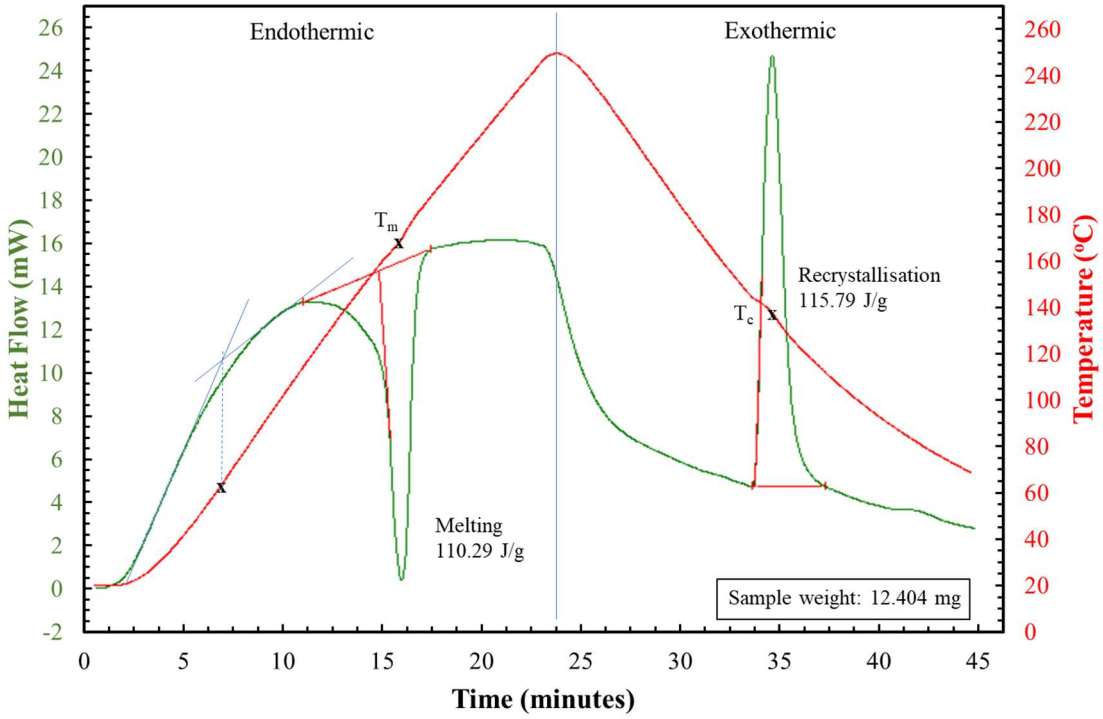

Figure 4.13 STA curve for acetal (machined from an extruded bar)

It can be seen that there is a slight bend in the curve at the temperature of 63°C, which thought to be the deflection point as compared to the supplier datasheet (76°C temperature of deflection [119]). In addition, the curve shows the melting temperature of the material as 168°C. The recrystallisation temperature was around 137°C. Also, the curve revealed the amount of energy that was required for melting the sample and to recrystalising it, as 110.29 J/g and 115.79 J/g, respectively.

Figure 4.14 shows the STA curve for the nylon (PA46) sample that was made by an injection moulded process. The tested sample size was around 9.3 mg.

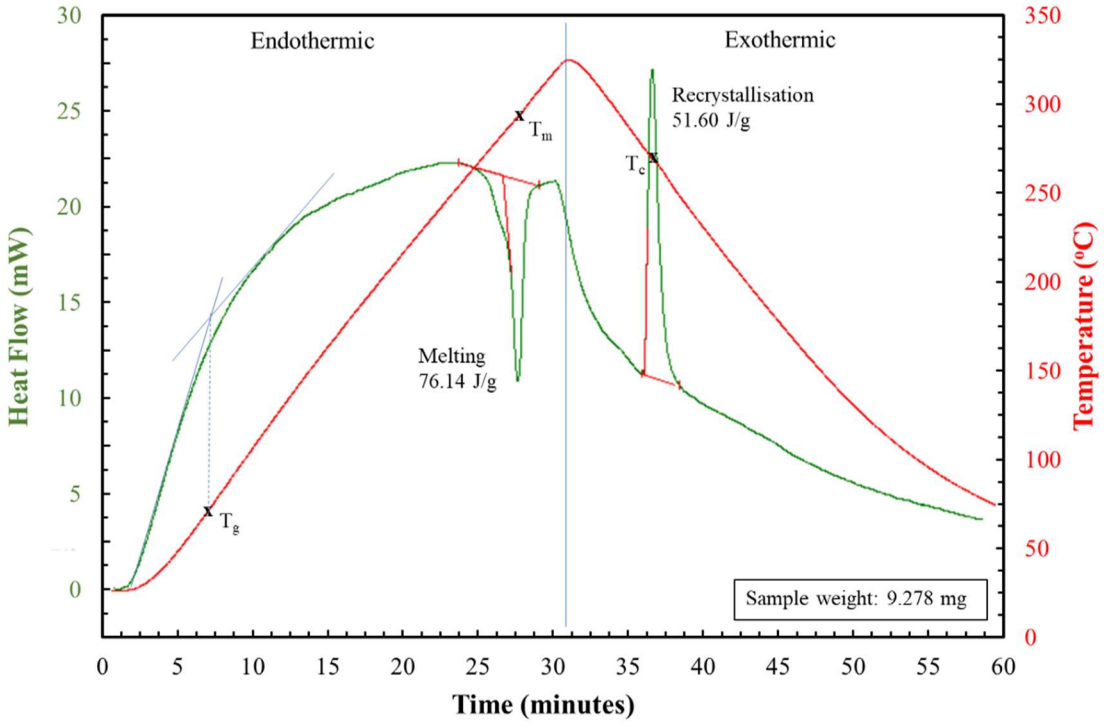

Figure 4.14 STA curve for nylon (PA46) (injection moulded)

The figure revealed the injection moulded nylon (PA46) glass transition temperature as 71°C (75°C from the supplier datasheet [107]), the melting temperature as 293°C and the recrystallisation temperature as 269°C. In

addition, it showed the energy required to melt the sample as 76.14 J/g and the energy required to recrystalise the sample as 51.60 J/g.

Figure 4.15 shows the STA curve for the machine cut nylon (PA66) sample of around 11.5 mg.

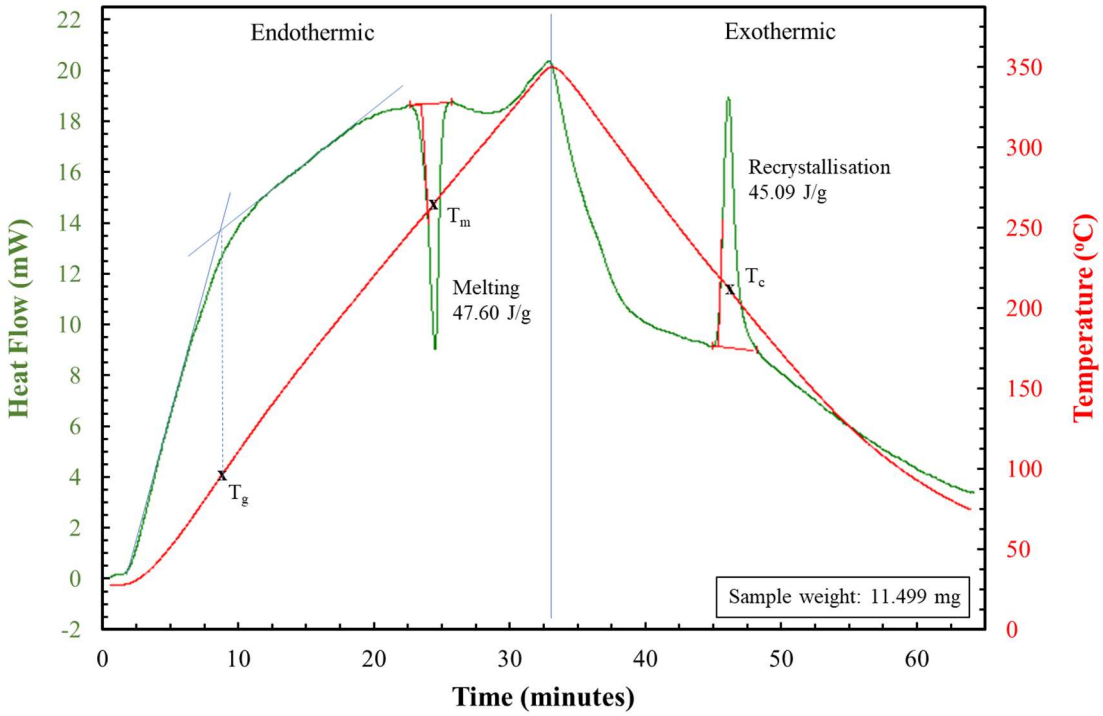

Figure 4.15 STA curve for nylon (PA66) (machined from an extruded bar)

It can be seen that the required energy to melt the sample is 47.6 J/g, while the energy that was required to recrystallise the specimen is 45.09 J/g. Also, the curve showed the glass transition temperature for the material as 98°C (47°C from the supplier datasheet [120]). The melting temperature and the recrystallisation temperature of the material was found at 263°C and 212°C, respectively.

Figure 4.16 shows the STA curve for the injection moulded polycarbonate (6555) sample of 9.8 mg.

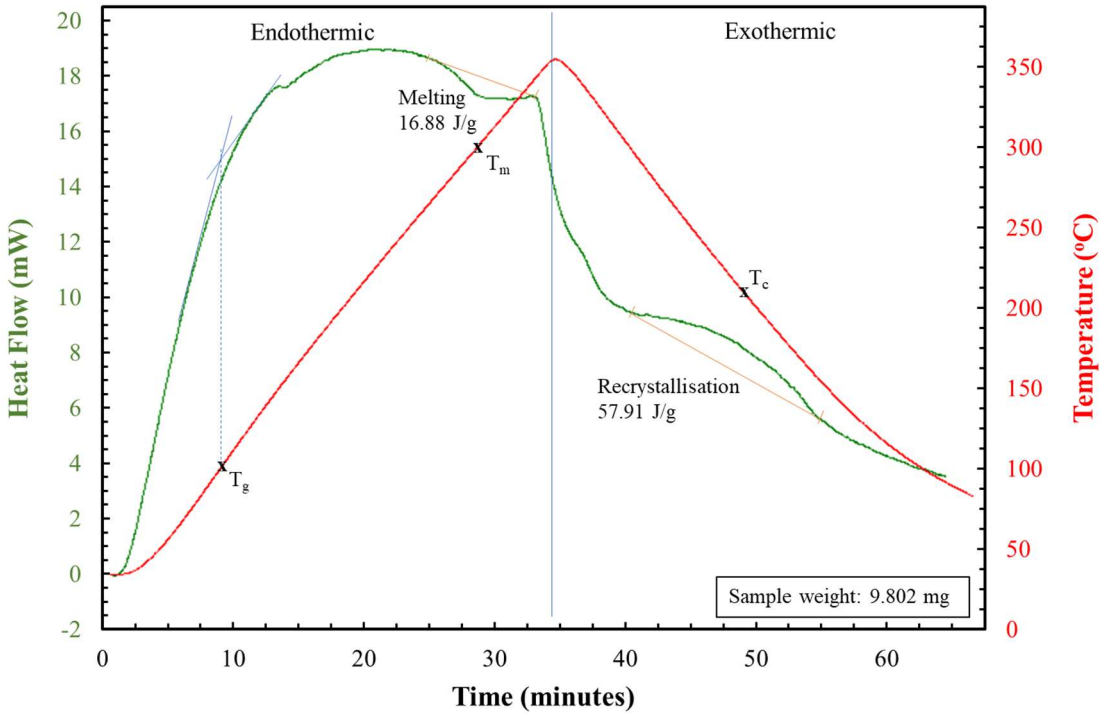

Figure 4.16 STA curve for polycarbonate (6555) (injection moulded)

The glass transition temperature for the injection moulded polycarbonate (6555) was found at 110°C (145°C from the supplier datasheet [112]). In addition, the melting temperature and the recrystallisation temperature of the material were recognised at 299°C and 210°C, respectively. The figure illustrated the amount of energy that was required for melting the sample as 16.88 J/g, while the required energy to recrystalise it as 57.91 J/g.

4.4 Polymer gear wear rate phenomena

The lower wear rate ranges in Figure 4.3, Figure 4.6, Figure 4.9 and Figure 4.11 (before the dramatic increases) may be compared with the wear volume formula developed by Archard [89] and modified by Friedrich [90] using a thrust bearing testing method.

Inserting the current test data into equation (2.10) gives a specific wear rate of 5.14×10^{-15} m^3/Nm for machine cut acetal gears, 4×10^{-13} m^3/Nm for injection moulded nylon 46 gears and 4.1×10^{-13} m^3/Nm for machine cut nylon 6 gears. Friedrich [90,121] reported values of specific wear rate for polymer materials running against steel, with a very comparable 3×10^{-15} m^3/Nm for acetal. However, his specific wear rate for cast and extruded nylon 6 (1.05×10^{-15} m^3/Nm and 4.32×10^{-7} m^3/Nm, respectively) are very different to those found here. This divergence may reflect the complicated behaviour patterns seen here with nylon gears.

It should be emphasized that equation (2.10) will apply only for the low wear rates seen before the transition point, while the after-transition, wear rate is not predicted, where a high temperature occurred and affected the physical and mechanical properties of the polymers. The formula reflects an inverse relationship with the number of cycles and the (assumed constant) torque, a condition not strictly followed in the step-loading wear rate tests. Moreover, the formula does not capture any effects of running speed, which is in reality likely to affect temperature significantly in poor conductivity materials. Thus, considerably more research, including constant load tests of polymer gear pairs, is needed to establish the usefulness of the current specific wear rate equation as a tool for gear predictions.

For most polymer materials undergoing tribological actions, there is a transition point where the wear rate is suddenly greatly increased. This phenomenon was thought to be the result of polymer surfaces under friction heating reaching their melting temperature.

Figure 4.17 shows gear wear rates for the four tested materials. Applying equation (2.13) to the four different materials polymer gears tested at the running speed of 1000 rpm and the specified gear geometry and specifications (Table 3.2 and Table 3.3), the theoretical maximum load that intersects with the maximum surface temperature of each material may be defined and compared with the experimental results in Figure 4.17.

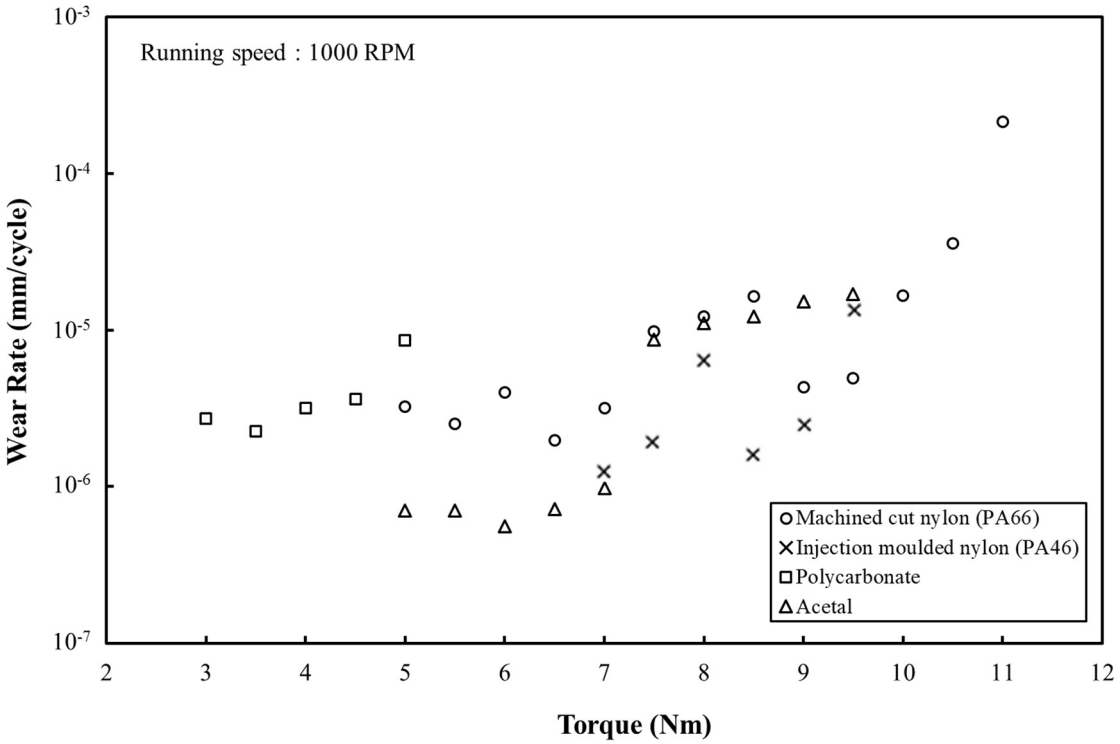

Figure 4.17 Gear wear rates for the four tested materials (wear rate in log form)

From equation (2.14) and (2.15), k_1 and k_2 are defined for each tested polymer gear, as in Table 4.1:

Table 4.1 Theoretical calculations for k_1 and k_2

	$k_1 = \frac{3.927\mu}{bc\rho Z(r_a^2 - r^2)}$	$k_2 = 1.11\mu\frac{(V_1^{1/2} - V_2^{1/2})}{2r^{3/4}b^{3/4}\sqrt{k\rho c}}\left(\frac{\pi E}{R}\right)^{1/4}$
Machine cut nylon (PA66)	0.016	0.281
Injection moulded nylon (PA46)	0.008	0.240
Polycarbonate	0.008	0.253
Acetal	0.013	0.232

Applying k_1 and k_2 in the gear maximum temperature equation ($\theta_{max} = \theta_a + k_1 T + k_2 T^{3/4}$) (eq. 2.13) and solving for the critical torque at the theoretical melting temperature as θ_{max} (from section 4.3).

Table 4.2 shows the theoretical and experimental load capacity comparison of different materials for polymer gears. Close agreements were achieved between the maximum tested load capacity of the different polymer gears and the theoretical calculations that predict the load capacity of a gear at the maximum surface temperature point. The larger variation between the two results for the injection moulded nylon 46 gears is thought to be caused by the absence of tooth root fillets on these samples, which leads to tooth fracture at the root side before reaching the maximum capacity of this material. All in all, one can conclude that polymer gears mostly fail at the highest torque due to thermal wear effects. Loading gears at torques below the specified critical load capacity leads to a reduction in wear rate and consequently increases the running life of such mechanical devices.

Table 4.2 Theoretical and experimental load capacity comparison of different materials for polymer gears

Polymer gear	Tested load capacity (experimentally defined at the transition point (Figure 4.17)) (Nm)	Theoretical load capacity (theoretically defined at the melting point (equation (2.13)) (Nm)
Machined cut nylon 66	10.5	9.8
Injection moulded nylon 46	9	11.4
Injection moulded polycarbonate	4.5	4.4
Machined cut acetal	8.5	8.2

4.5 Summary

Acetal gears showed the lowest wear rates during the early, slowly increasing stage of testing. Polycarbonate gears showed the highest wear rate with large values even at low loads, which confirms that it is not a functional material for high loaded gearing applications. Also, nylon gear wear rates showed more complicated patterns, which need to be more closely understood before the material is ranked for quality and employed in mechanical tribology applications.

Several tests have been set up for different types of material with the aim of getting wear measurements at certain loads and speeds to extensively understand wear rate behaviour as a function of load and speed change, as well as understanding the surface behaviour of each material under rolling and sliding contact (gears in mesh) by investigating the tooth worn surface using both optical microscopes and a scanning electron microscope (SEM). For this aim, more tests were conducted on acetal and nylon gears at a constant applied load. The results and discussions will follow in the next chapters.

Chapter 5
TRIBOLOGY OF DRY-RUNNING POLYMER GEARS

5.1 Introduction

After running the step-loading tests discussed in the previous chapter, it was concluded that more single-load tests were required to establish a thorough understanding for polymer gears wear rate and failure modes. In addition, such results will provide further validation for the step-loading wear rate results. Therefore, this chapter will focus on providing test results of single-load runs for three types of polymer material. These are the materials that provided more interesting results in the step-loading tests: machine cut acetal, injection moulded nylon and machine cut nylon.

All the results reported in this chapter were obtained using the test rig configuration discussed in section 3.2. In every case, the test gear holder block was adjusted to set the gear pair to a practical level of closeness to ideal alignment.

Further investigations of the tested gears were carried out after each single test using different methods, such as tooth surface profiling using the shadowgraph and examining the worn surface condition behaviour using SEM. Such investigations will be presented during this chapter.

5.2 Machine cut acetal gears

Figure 5.1 shows the result of a wear test on acetal gears at the load of 7 Nm and the speed of 1000 rpm. It is known from previous work [4] that there are three wear stages over the full life of a test (running in stage,

steady (slow increase) stage, and rapid wear and fracture stage). The longest and most important stage, which shows the working polymer gear wear rate and wear phenomena, is the middle steady stage. Therefore, to better understand the wear and surface tribology of this important stage, tests were stopped intentionally during this middle steady wear stage, and the gears taken for further surface investigation. The current test method allows this steady wear period and associated wear rate to be easily defined using the continuous record of wear across the running time. Gears were weighed and compared to the actual mass before the test to obtain the mass loss precise to 0.001 mg for comparison with the directly measured wear as a way of validation and to get a rough idea about the effect of tooth deflection on the wear measurement curve.

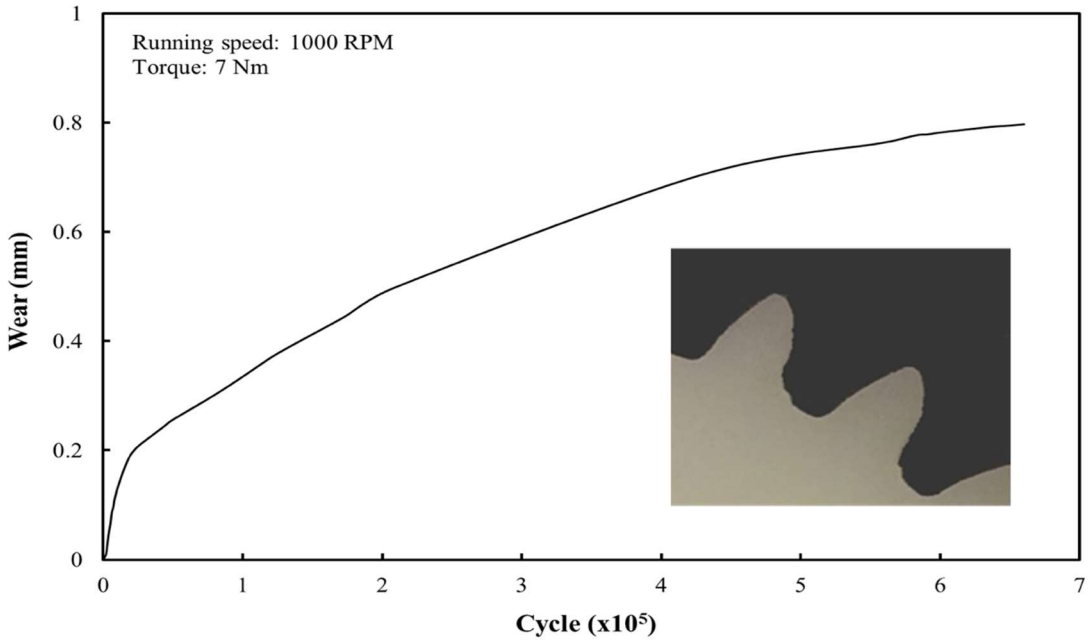

Figure 5.1 Tooth surface wear for machine cut acetal gear pair, loaded by 7 Nm torque and run at 1000 RPM speed

Machine cut acetal gears showed wear rate result of 9.66 x 10^{-7} mm/cycle at the load of 7 Nm of the step-loading test (Figure 4.3), while they revealed a wear rate of 8.55 x 10^{-7} mm/cycle at a constant load of 7 Nm in

the long-run test. Both results showed reasonably good agreement, with the minor difference between the results of the two methods proving that step-loading testing method could be useful for acetal gears load capacity measurement. One of the reasons of these differences could be the running time of the test. Because it is shorter at the step-loading test, it may not allow enough occurrence of the nearly-linear wear stage. Here in machine cut acetal gear test, this stage was starting to appear at around 3×10^4 cycles and more stabilized after running for 3×10^5 cycles. Therefore, the step-loading test could be an acceptable initial and rapid testing method that shows, to a satisfactory level, a good initial wear and wear rate data for polymer gears. This initial data could be useful for further investigation and long-run testing plan. In case of acetal gears, if the loading period was extended to around 5×10^4 cycles, the results will get more accurate, because gear wear behaviour is left longer to stabilize.

Monitoring the acetal gears test over the running time revealed that wear debris was falling from them in very small amounts during both the running in and steady stages of wear (Figure 5.2). Similar behaviour was observed with injection moulded acetal gears in previous work [75]. Some gear teeth and samples of the debris collected were investigated under the SEM, and pictures taken. Figure 5.3 shows the after-test machine cut acetal gear pair.

Figure 5.2 Debris falling from machine cut acetal gear test under 7 Nm load and at 1000 RPM

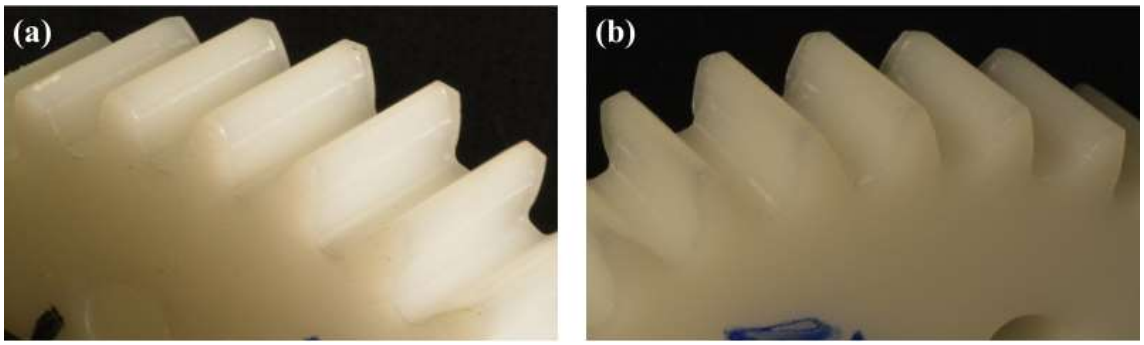

Figure 5.3 The after-test machine cut acetal gear pair, tested at 1000 RPM and under 7 Nm load, (a) driving and (b) driven.

After the test was stopped, gears were taken off and attached to a transparent film that had the original tooth profile (before testing) printed on it and wear thickness was measured using the measuring profile projector as in Figure 5.4. It is clear that driven gear has more wear (expressed as loss of thickness at the pitch circle) than the driving gear, but, in general, the average wear is 0.60 mm, which when compared with the measured wear in Figure 5.1, reveals a difference of 0.20 mm that represents the amount of tooth deflection. The after-test flank profile proves the sliding direction effect on the worn surface shape.

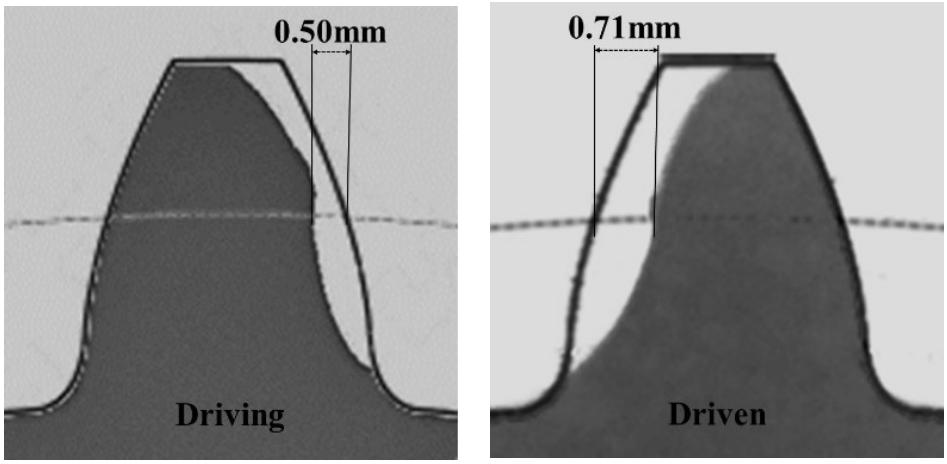

Figure 5.4 Wear thickness (using IDMS) for machine cut acetal gear test under 7 Nm load and at 1000 RPM

As revealed from Figure 5.5 (c) and (d), there was some friction at the pitch point of the driving and driven machine acetal gears which does not agree with the theoretical assumption that friction at the pitch point is zero (where the only motion is rolling and there is no sliding). All real gears have finite contact areas and so deviate a little from this ideal, with polymeric materials expected to show more sliding because they are less strong and less stiff than metals; some gear tooth bending while at mesh with the other gear in addition to the relatively high Hertzian contact could be two reasons for the slightly change in the rolling and sliding motions from gear theoretical motions.

Figure 5.5 (e) and (f) indicate that some thin chips are starting to separate from the tooth surface and then their edges are forming narrow long pieces of debris. They are starting to rotate as a result of the friction and so forming scratches on the whole tooth surface along the tooth profile from pitch point to tooth root (in the friction direction). These are seen in Figure 5.5 (g) and (h), where debris gathers before being thrown out of the gear mesh. Most of the debris collected from below the tested gears had a long and twisted shape.

Much the same phenomenon happens to the other side (addendum side) of the tooth face and friction direction. SEM investigations suggest that the friction is higher along the tip side of the acetal driving gear. It may be seen from Figure 5.5 (a) and (b) that debris formed at the pitch point has been moved in the direction of the tip, but some of it has been pressed along the way as a result of the higher pressure than at the root side, making them flat in shape rather than long and twisted in shape (as on the root side). Some flat chip debris was collected from below the tested gears.

In contrast to the root, the tooth tip edge is an open end that cannot collect debris being moved outwards, which means that the debris drops straight away out of the mesh.

Overall, Figure 5.5 reveals that scratch wear is the most prevalent form of wear that occurred over the whole tooth profile of the tested driving acetal gear. It was caused by moving debris between the two rubbing surfaces. In addition, some micro pitting wear was discovered as a result of repetitive Hertzian loading on the gear teeth throughout the test running time.

The acetal driven gear shows different wear phenomena to the driving gear, see Figure 5.6. This is because the sliding directions are different (from tip to pitch and from root to pitch). This gives the opposite direction of debris movements, but the same type of scratch wear as a result of debris rubbing between the two surfaces. In addition, some adhesive wear was observed at the tip side of gear teeth (Figure 5.6 (a) and (b)) as a result of thermal effects. More severe wear happened at the addendum side of the tooth, in line with the movement direction from top to bottom (tip to pitch). Figure 5.6 (c), (d) and (f) show that debris gathered around the pitch point as a result of motion direction, while (e), (g) and (h) show abrasive wear along the dedendum side of the tooth, in line with the interpretation that some debris moves over the surface from root to pitch line.

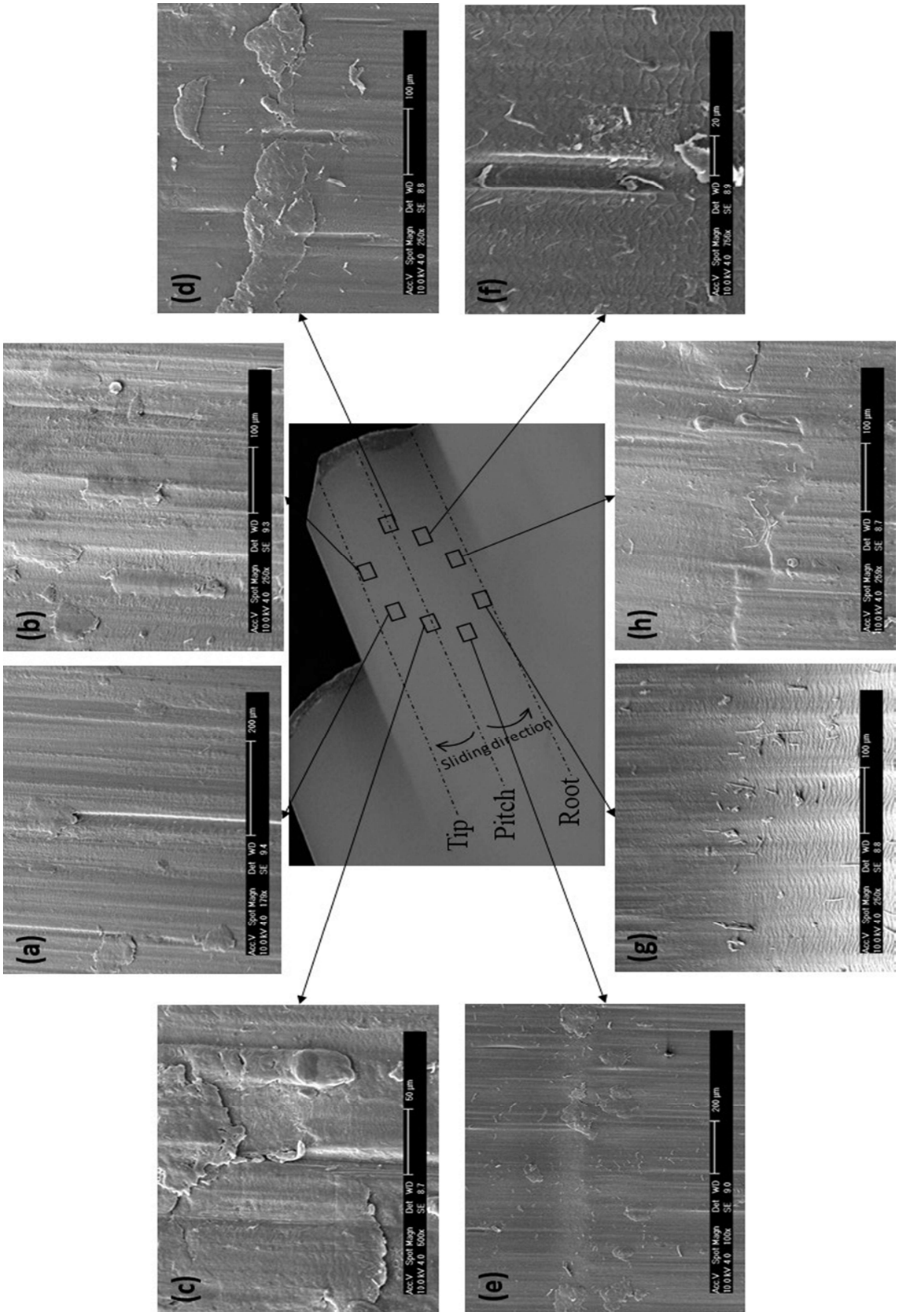

Figure 5.5 SEMs of machine cut acetal driving gear tooth (7 Nm, 1000 RPM)

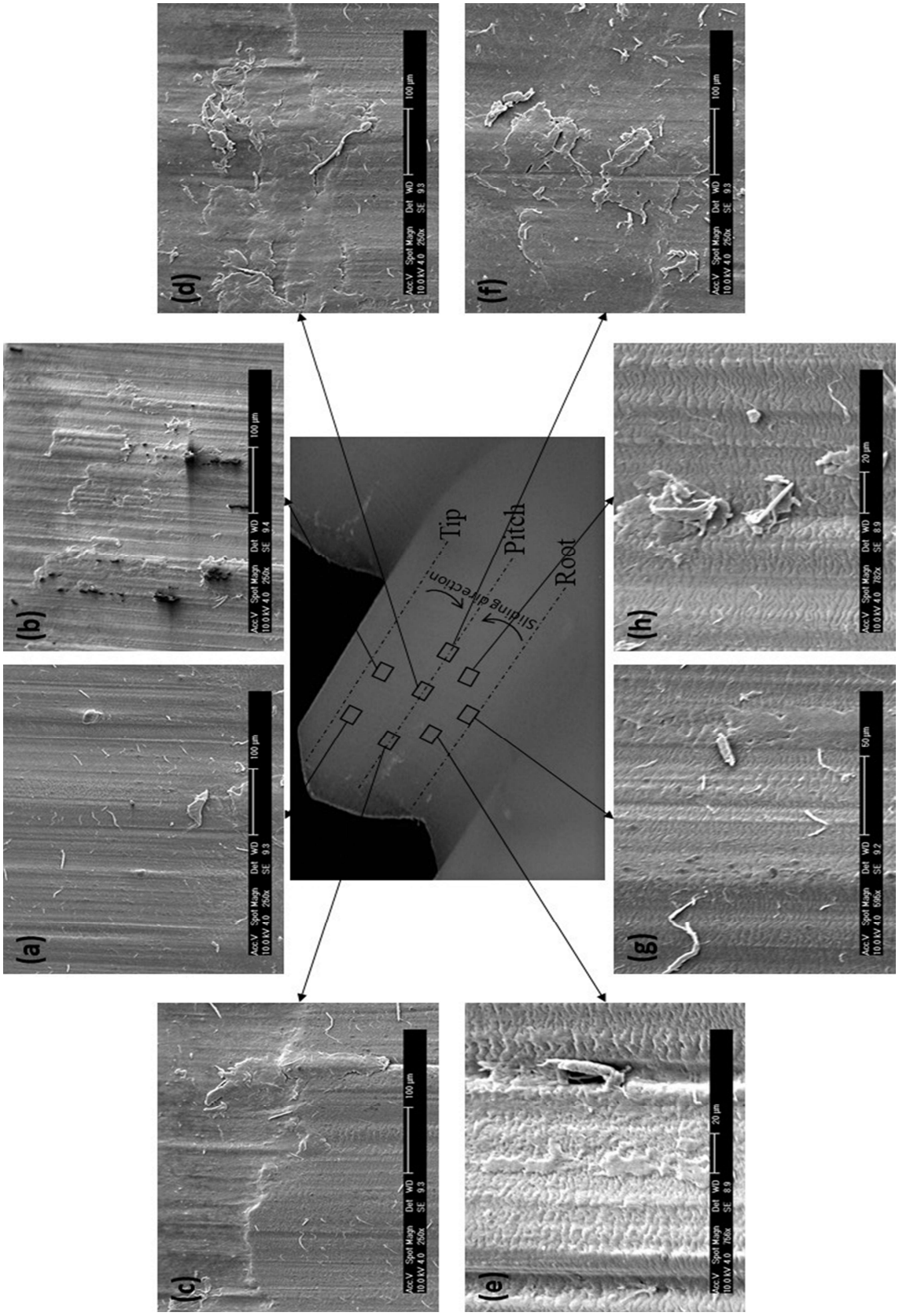

Figure 5.6 SEMs of machine cut acetal driven gear tooth (7 Nm, 1000 RPM)

5.3 Injection moulded nylon gears

As was seen in Figure 4.6 and Figure 4.9, the wear rate of nylon gears does not increase steadily with increasing load. Therefore, more investigations were needed to gain a greater understanding of how this wear transition occurs and to improve nylon gearing applications.

Figure 5.7 shows the wear trend of injection moulded nylon gears through around 5 x 10^5 cycles, which were loaded by 6 Nm and run at a speed of 1000 RPM. Observation of the nylon gears during the test revealed that almost no wear debris collected during the running in stage, which might lead to the conclusion that most of the measured displacement at this stage is the result of tooth bending by the applied load. This is consistent with the early high increase of the wear curve in Figure 5.7, followed by a very low slope in the steady wear stage. The amount of debris started to increase in the steady stage, although it was still a very small amount.

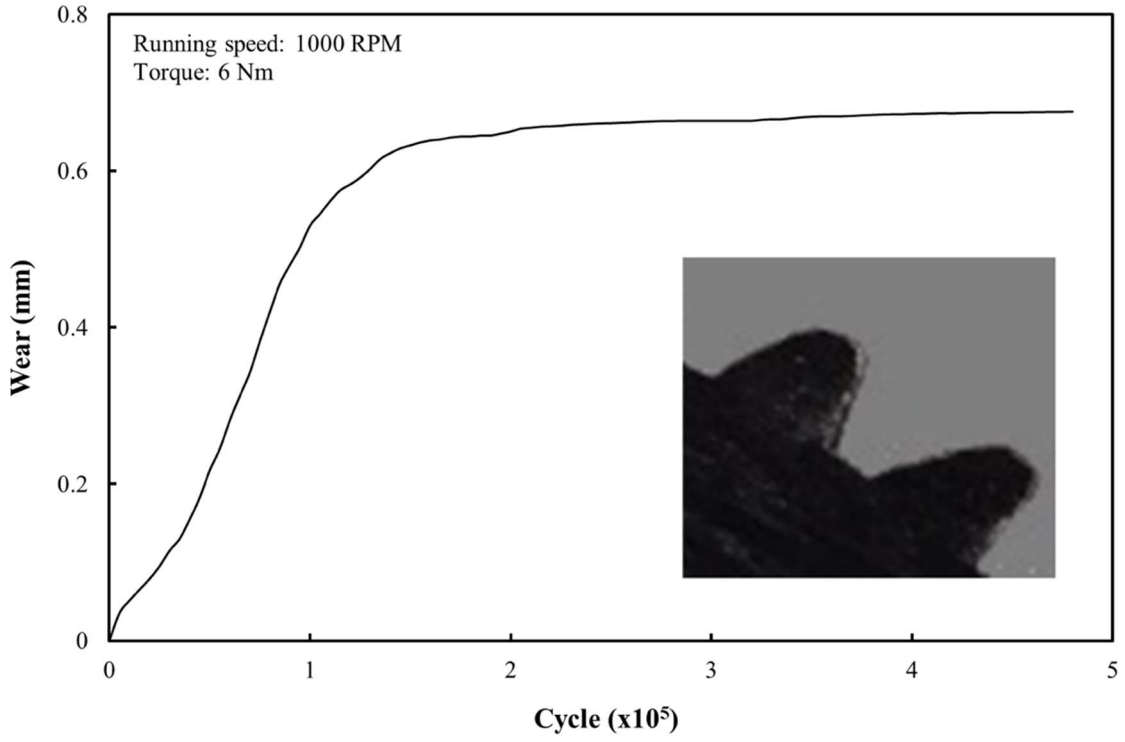

Figure 5.7 Tooth surface wear for injection moulded nylon gear pair, loaded by 6 Nm torque and run at 1000 RPM speed

Figure 5.8 shows the after-test injection moulded nylon gear pair.

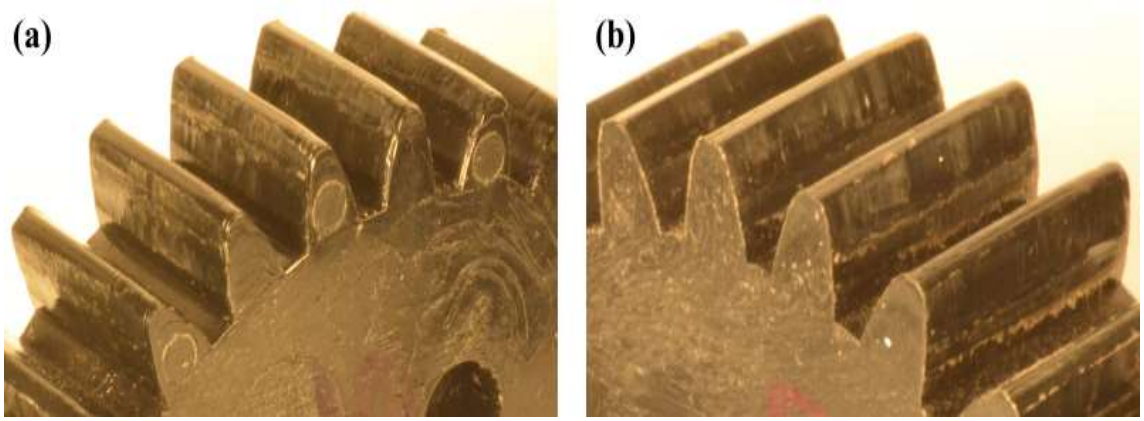

Figure 5.8 The after-test injection moulded nylon gear pair, tested at 1000 RPM and under 6 Nm load, (a) driving and (b) driven.

After stopping the test, gears were attached to a transparent film that had the original tooth profile (before testing), and wear thickness was measured using the measuring profile projector as in Figure 5.9. similar to the acetal gear, driven gear has more wear (expressed as loss of thickness at the pitch circle) than the driving gear, but, in general, the average wear is 0.31 mm, which when compared with the measured wear in Figure 5.7, reveals a difference of 0.33 mm that represents the amount of tooth deflection. The after-test flank profile proves the sliding direction effect on the worn surface shape.

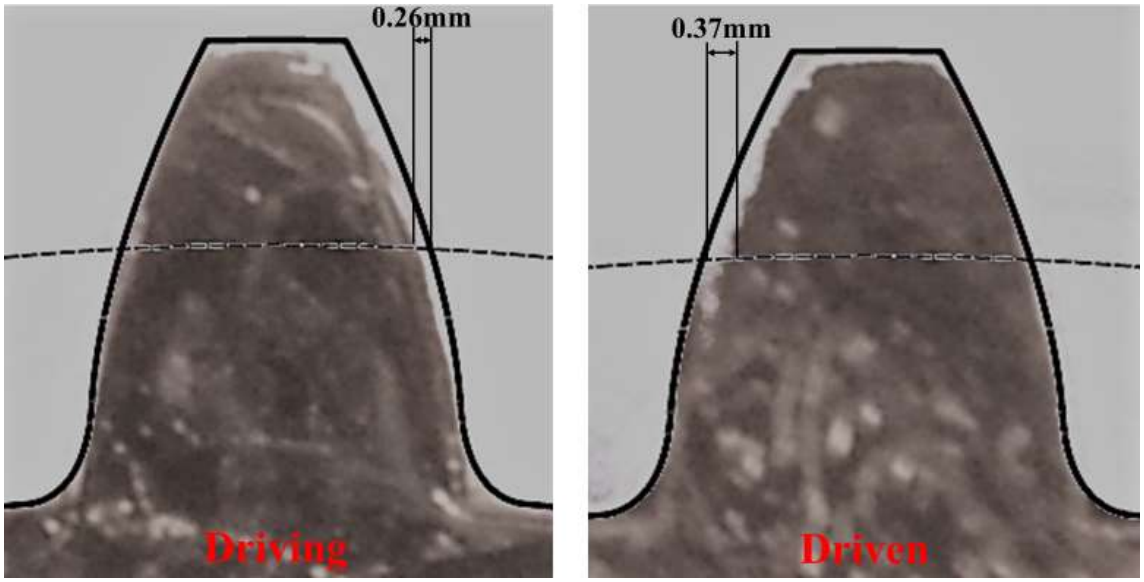

Figure 5.9 Wear thickness (using IDMS) for injection moulded nylon gear test under 6 Nm load and at 1000 RPM

Figure 5.10 presents the tooth surface wear result for injection moulded nylon gear pair that was tested at the running speed of 1000 RPM and under the torque of 10 Nm. Gears run for 4.3 x 10^4 cycles before the driving gear teeth were fractured at the root side. Tooth wear rate was low at the running-in stage of 1.5 x 10^4 cycles. This stage was followed by a highly increased wear rate at the running period between 1.5 x 10^5 cycle and 3 x 10^4 cycle. This increase was thought to be for the reason of tooth deflection as a result of the high load (the highest load at the previous step-loading test). Wear rate then decreased and stabilized of the next 1 x 10^4 cycles. One of the reasons of this decrease could be from the increase of gear contact ratio as a result of the wear and tooth deflection, which, in consequence, increases tooth load sharing between two to three teeth. Then, a gear teeth fracture was happened leading to the high increase in wear reading at around 4 x 10^4 cycle and afterwards. Test rig was stopped automatically immediately after the fracture. Observation of the test revealed that wear debris was dropping through all the running time, with an increased amount of debris at the nearly-linear stage and the final fracture stage.

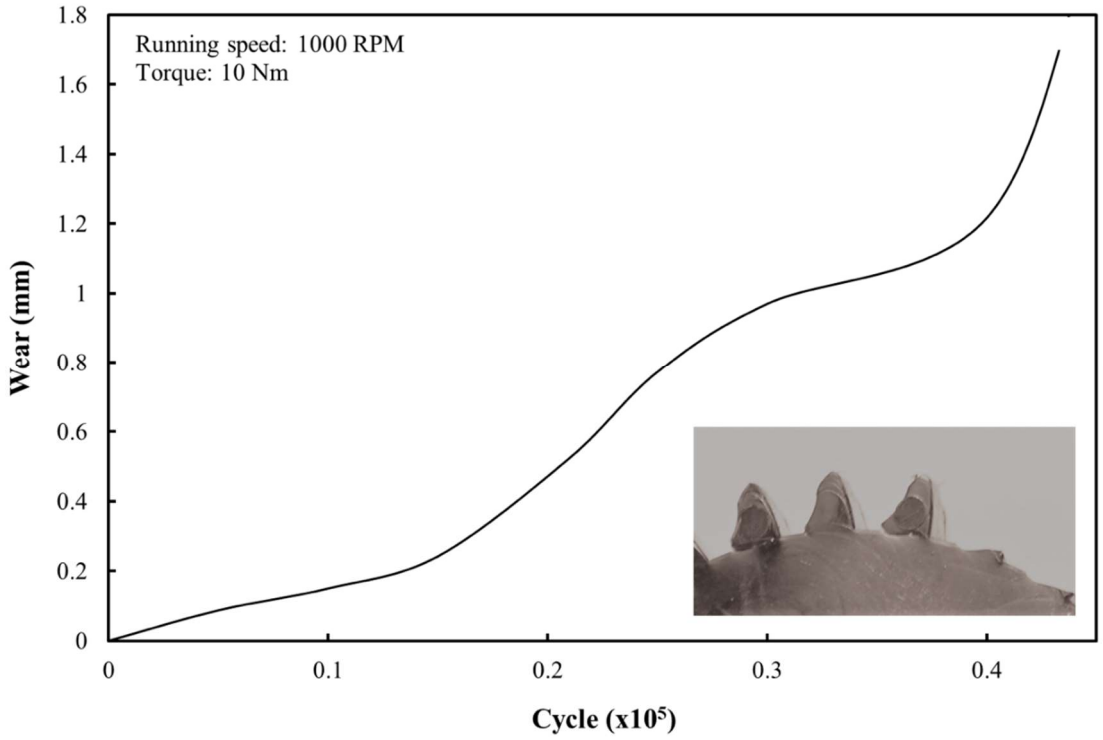

Figure 5.10 Tooth surface wear for injection moulded nylon gear pair, loaded by 10 Nm torque and run at 1000 RPM speed

Figure 5.11 shows the after-test injection moulded nylon gear pair.

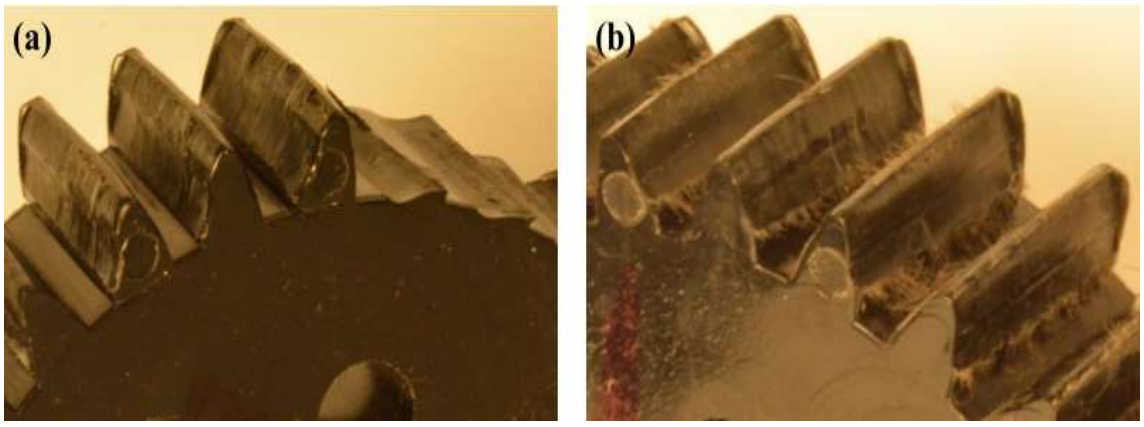

Figure 5.11 The after-test injection moulded nylon gear pair, tested at 1000 RPM and under 10 Nm load, (a) driving and (b) driven.

After stopping the test, gears were attached to a transparent film that had the original tooth profile (before testing), and wear thickness was measured using the measuring profile projector as in Figure 5.12. similar to the acetal gear, driven gear has more wear (expressed as loss of thickness at the pitch circle) than the driving gear, but, in general, the average wear is 0.46 mm, which when compared with the measured wear in Figure 5.10 (before fracture), reveals a difference of 0.53 mm that represents the amount of tooth deflection. The after-test flank profile proves the sliding direction effect on the worn surface shape.

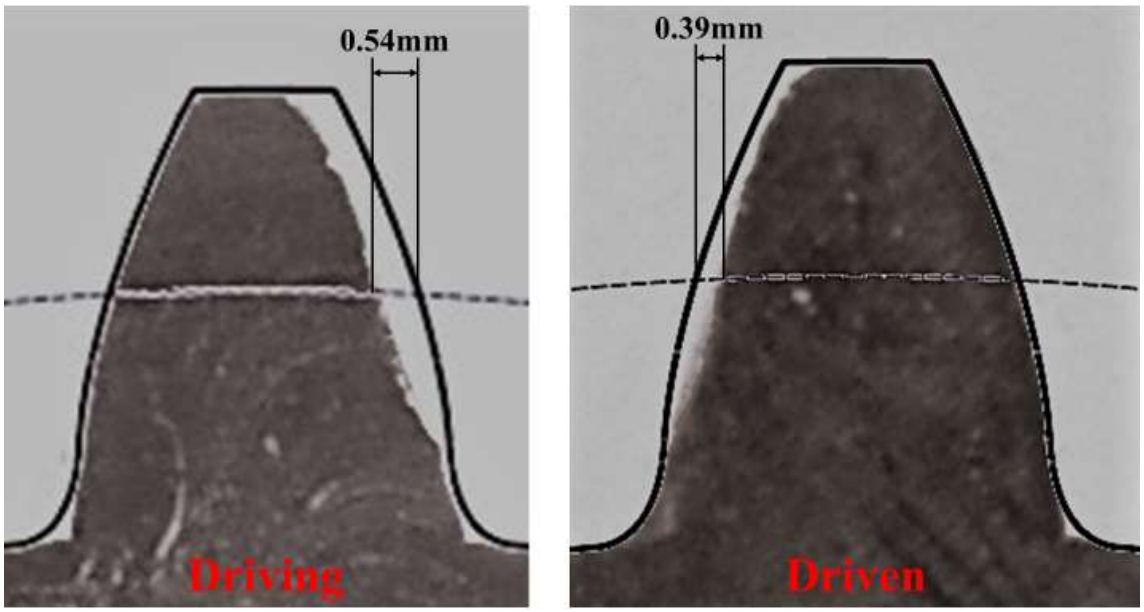

Figure 5.12 Wear thickness (using IDMS) for injection moulded nylon gear test under 10 Nm load and at 1000 RPM

Injection moulded nylon gear wear results showed some differences between the two methods. At 6 Nm load, wear rate was 1.75 x 10^{-7} mm/cycle at the step-loading test, but the number was dropped by about two times to 7.2 x10^{-8} mm/cycle at the long-run test. Similarly, the data showed the wear rate of 3.95 x 10^{-5} mm/cycle at the step-loading test, at the torque of 10 Nm, while the result slightly decreased to 2.47 x 10^{-5} at the long-run test for the same load. The difference between the two results

could be because the earlier method allowed gears to run for shorter amount of cycles than the later method. In the long-run test, injection moulded nylon gear wear behaviour seemed to establish the nearly-linear stage after longer running period (up to 2 x 10^5 cycles) than acetal gears. This seems to not allow the gear teeth to stabilize enough and to establish the nearly-linear wear stage until later. Therefore, it is recommended to run test gears for a longer time at each stage for injection moulded nylon gears. In these early tests, the surface temperature was not measured.

Wear tests were done by Hooke et. al. [37]using two rolling discs made of injection moulded nylon and running under different slip ratios and a similar conclusion was reached. Their results showed that the wear of nylon discs with respect to cycles was nearly-linear throughout the whole period of the test run. Their results reasonably match the nearly-linear wear stage of a pair of nylon gears shown in Figure 5.7. The early running in stage did not appear in their results because of the differences in specimen body shape (gear shape compared with disc). In the disc results, they found an initial negative reading of wear which they explained as disc expansion as a result of body temperature increase due to surface friction. The results in this work reveal an early stage high increase in displacement reading that is the result of tooth deflection. Similarly, the wear rate has a high sudden increase in the final stage of the life of polymer gears, while it is not always the case in polymer discs and the nearly-linear stage time is relatively shorter in gears than in discs, for the same shape related reasons. Therefore, the nearly-linear stage of polymer gear wear is the only stage that can validly be compared with polymer disc results. This stage shows good agreement. In contrast with disc results, dry running nylon gears showed relatively low wear rate results compared with other polymeric materials when running at low loads. This means that they are functionally well rated for low torque applications. Therefore, nylon materials show good promise in mechanical applications, although also having some drawbacks, which this research is intended to explore.

Electron microscopic analysis was carried out on the dry tested nylon gears at a load of 6 Nm and a speed of 1000 RPM. Results showed different wear and failure modes to those of dry running acetal gears. Figure 5.13 shows an SEM general view for the driving gear tooth surface after running at a speed of 1000 RPM for 8 hours and under an applied torque of 6 Nm. Generally, the most common failure mode is scuffing and plastic flow along the contact direction, where friction-induced temperature rises and direct loads cause the surface to soften and weld to the contacting surfaces. In contrast to acetal gears, there was smaller amount of debris sliding between the two rubbed surfaces, which had caused high wear.

The debris in nylon gears formed mostly at the edges, but sometimes from the middle, of contact surfaces towards the directions of the plastic flow (Figure 5.13 (a), (b), (g) and (f)). As can be seen, some of the contact surfaces are trimmed away as a result of scuffing, so forming some wear debris. The collected debris were in two shapes: small chips and rounded fibres (Figure 5.14). The small chips had fallen from the edges. The long-rounded fibres were initially taken off as chips and then rounded as they passed through the two rubbing surfaces.

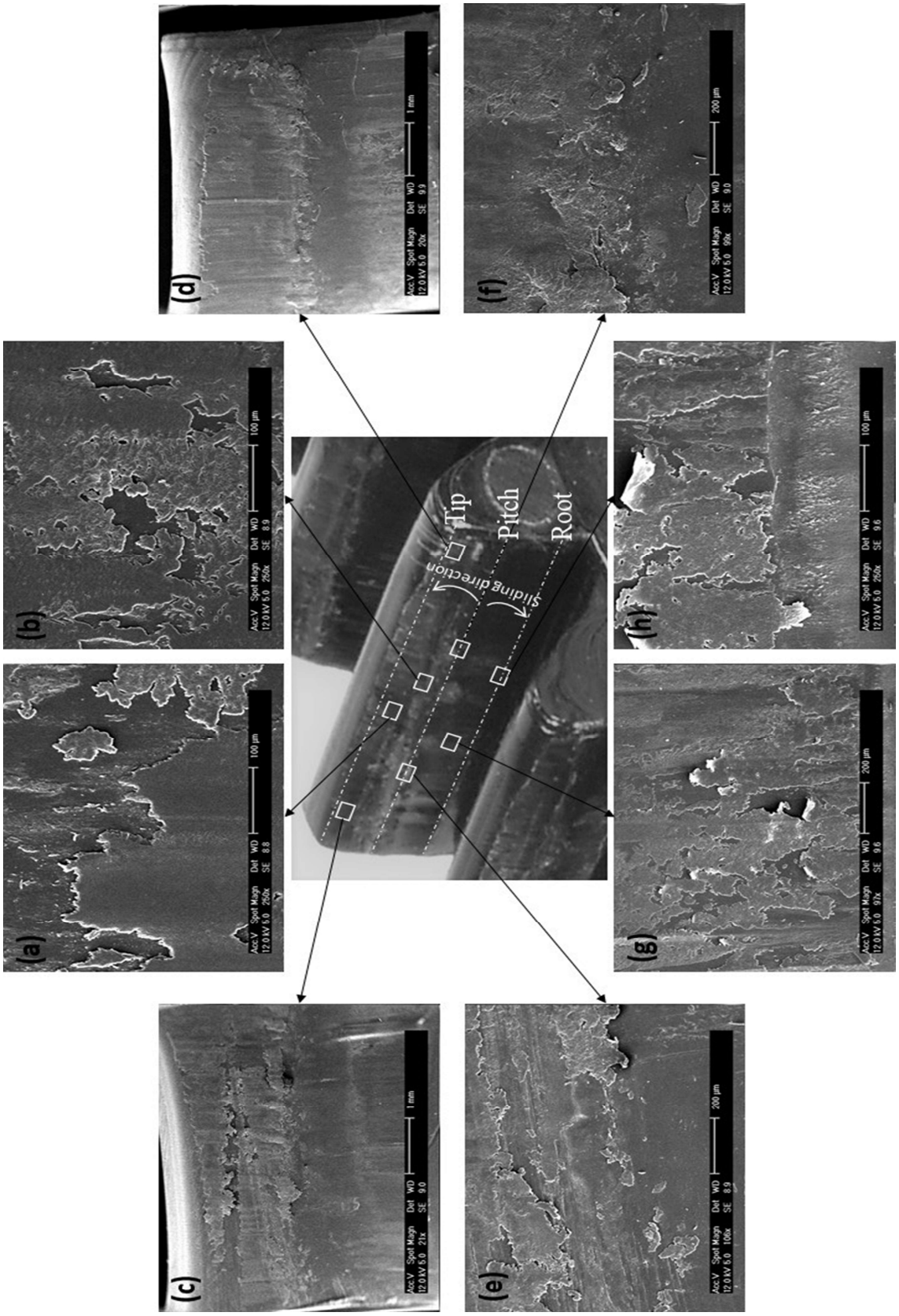

Figure 5.13 SEMs of injection moulded nylon driving gear tooth (6 Nm, 1000 RPM)

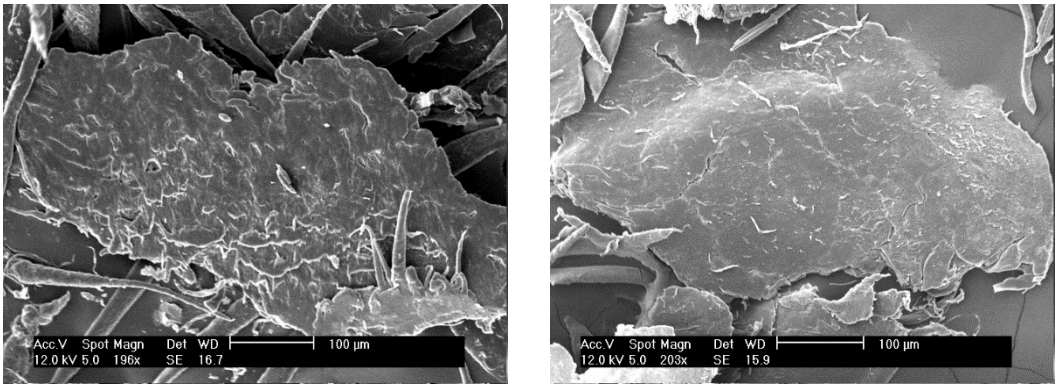

Figure 5.14 SEMs of debris collected from the test of injection moulded nylon gear (6 Nm, 1000 RPM)

At the pitch point of the driving nylon gear (Figure 5.13 (e) and (f)), there appeared to be less scuffing and plastic flow, because surfaces slide at lower relative speed near this point. Some micro cracks or pitting were expected around this area, caused by the high Hertzian stresses and later forming larger cracks that lead to the gear failure by pitch point fracture. However, none was found in this area. The fracture point at nylon gears was still unpredictable, as it varied between pitch point and tip of the teeth. Some other tested gears had fractured at the root point, leading to the conclusion that, in these tested gears, pitting and micro cracks were not the reason for gear tooth failure, as was concluded for nylon discs [37], although the nylon gears were run under closely similar load and sliding speed conditions.

Further investigations were carried out by slicing one of the teeth to look at its side under the SEM (Figure 5.15). No micro cracks can be seen at the pitch point or anywhere else on the contact surface, which leads to the conclusion that injection moulded nylon gears may not fracture because of micro crack formation, but for thermal reasons.

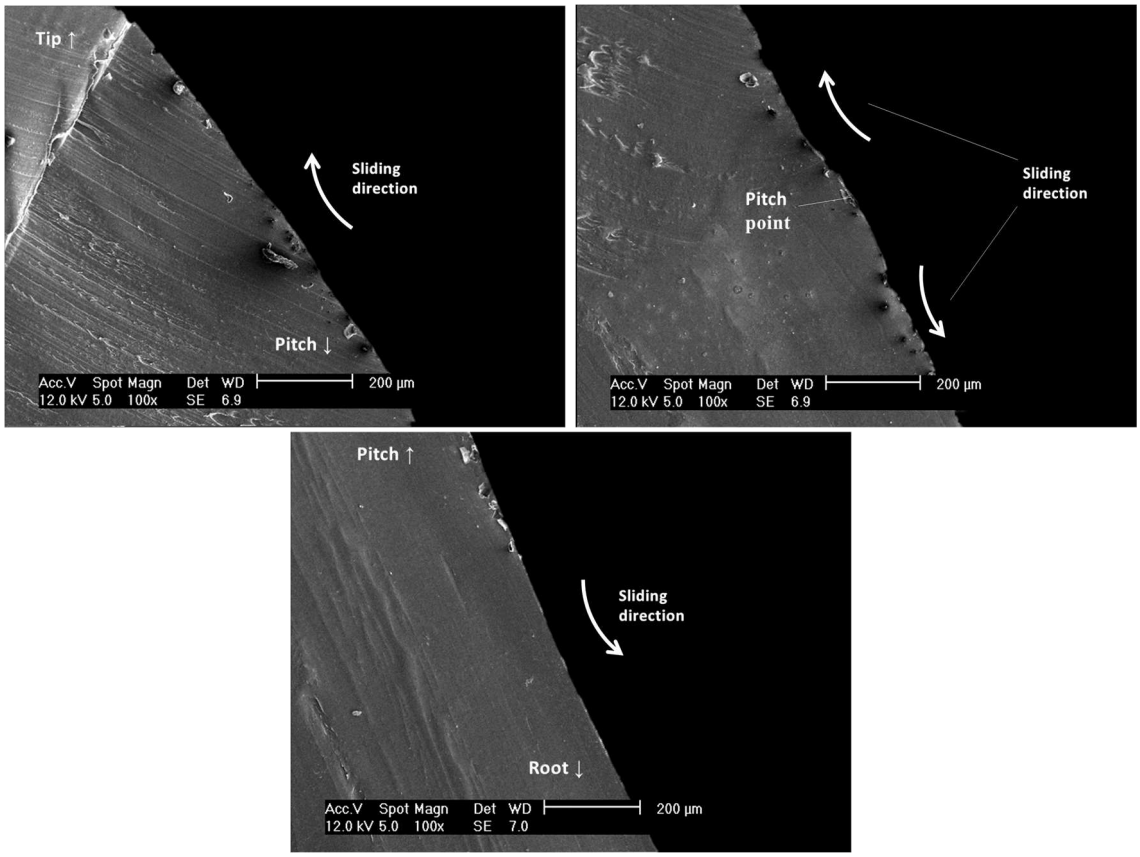

Figure 5.15 SEMs of the side of the driving gear tooth (6 Nm, 1000 RPM)

The SEM of the driven injection moulded gear tooth in Figure 5.16 shows very similar wear characteristics to the driving gear. A thin surface film covers most of the contact surface, which was formed as a result of thermal effects and high contact pressure, leading to some surface scuffing and plastic flow, but now towards the pitch point. Therefore, the detached chips from the surface travelled toward the pitch point and could be rotated and formed into rounded debris before they gathered at that point (Figure 5.16 (d) and (e)). This gathering is due to the teeth sliding direction (as seen in Figure 2.5 [30]).

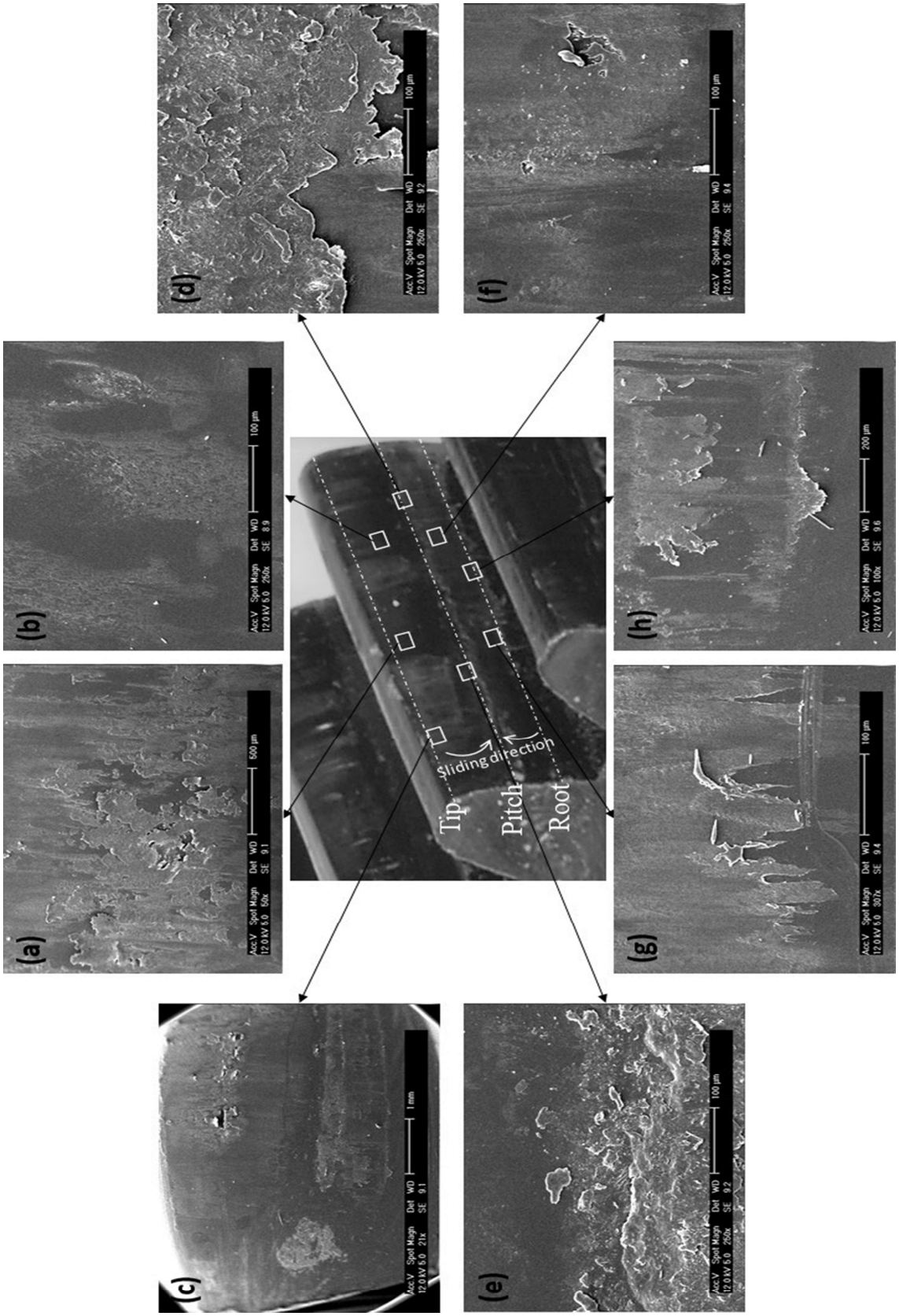

Figure 5.16 SEMs of injection moulded nylon driven gear tooth (6 Nm, 1000 RPM)

Again, no micro cracks were found in the driven nylon gears when investigated under the SEM, as shown in Figure 5.17.

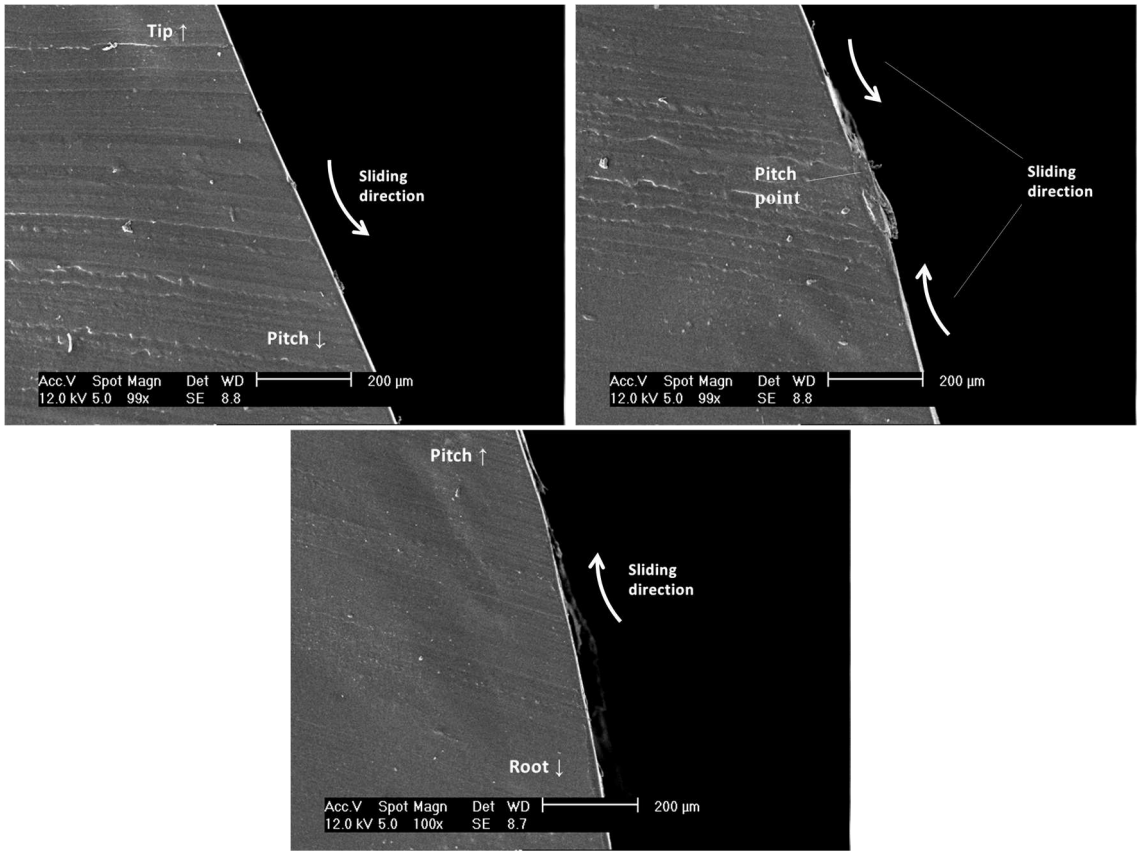

Figure 5.17 SEMs of the side of the driven gear tooth (6 Nm, 1000 RPM)

Further SEM investigations were carried out to the 10 Nm test. Figure 5.18 shows the SEM images for the tooth surface of the injection moulded nylon driving gear that was tested at the speed of 1000 RPM and under the applied load of 10 Nm. Abrasive wear was the common type of surface damage across the tooth surface, because of the highly loaded gears. The taken-out surfaces were rounded, as the two surfaces continue to slide, and taken towards the tip and root of the tooth. On its way, debris functions as an abrasive material that increases the wear rate of the surface. It was found here that the amount of debris was much higher than the 6 Nm injection moulded gear test. At the addendum side of the tooth surface (Figure 5.18 (a), (b) and (c)), more debris can be seen heading towards the

sliding direction. At the start of the sliding (near the pitch line), there was very little debris, while the abrasive wear was clearly seen. This amount of debris was increased during the contact of the two surfaces reaching the maximum amount near the tip of the tooth, which makes this side the highest worn surface region.

Moving to the pitch line area there was nearly no debris to be found. It was believed that this part of the surface was the debris generation area, as it is the initial sliding point. Two types of wear can be found in this area, namely adhesive wear (Figure 5.18 (d)), and wear abrasive (Figure 5.18 (e)).

At the dedendum side of the tooth surface (Figure 5.18 (f), (g) and (h)), similar wear behaviour to the addendum side can be seen. The abrasive wear was observed across the surface with lower amount of severity than the addendum side. Debris was again shaped by a similar method. Starting at the pitch line side, parts of the surface were taken out, as a result of the high pressure surface contact and the adhesive and abrasive wear, and rounded with the sliding of the two contacted surfaces towards the sliding direction. In its way, debris takes more material from the surfaces, which increases the wear severity. To the root of the tooth, debris was found with a higher amount. Some of it was still attached to the surface of the tooth root. This proves that debris was formed across the surface from the pitch line to the root edge.

The driven gear tooth showed the opposite direction of wear behaviour. Figure 5.19 illustrates the SEM for the tooth surface of the injection moulded nylon driven gear that was tested at the speed of 1000 RPM and under the applied torque of 10 Nm. It can be seen that the most common type of wear is the abrasive wear, with a higher severity at the tip side of the tooth. Debris was more focused around the pitch line side.

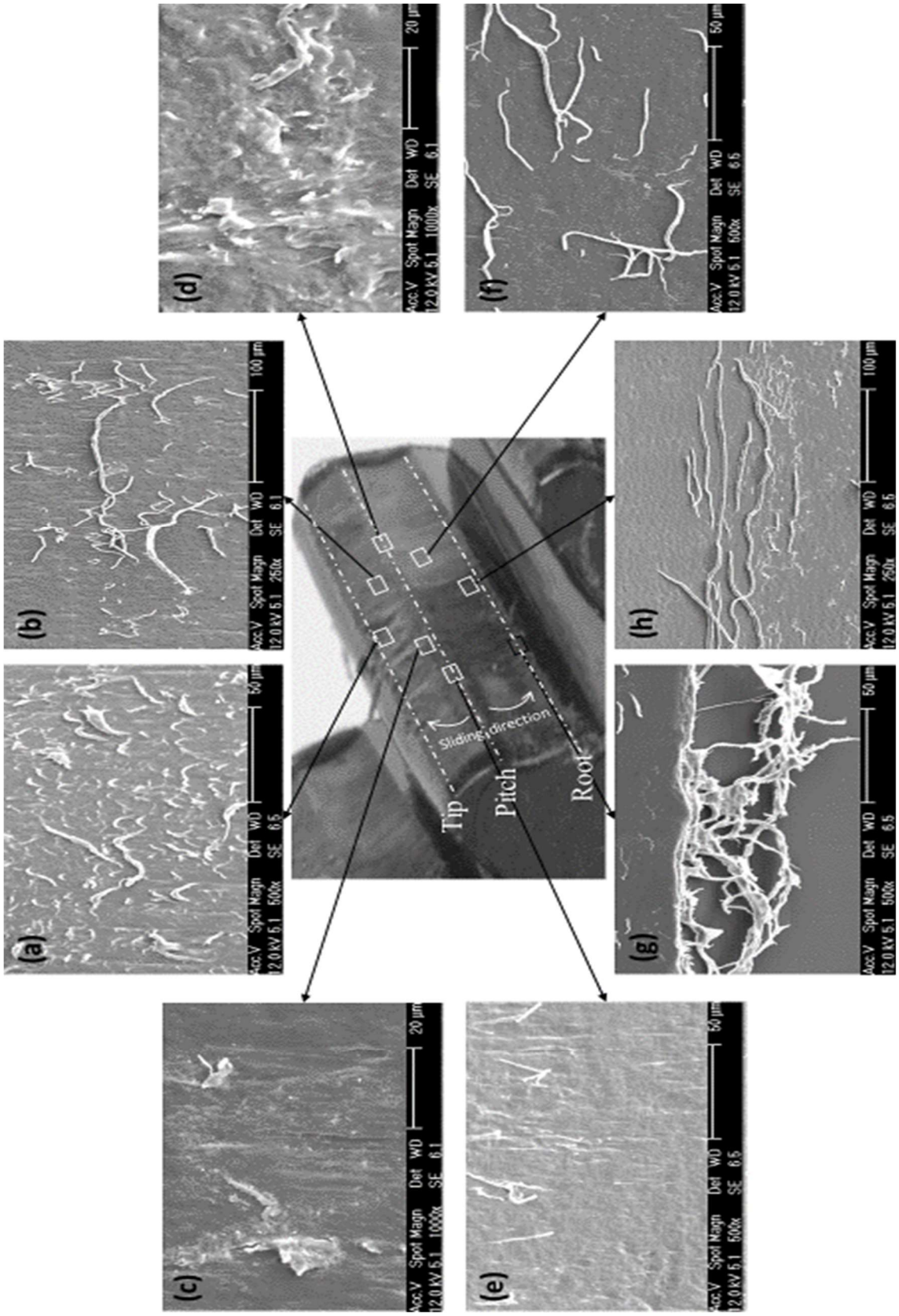

Figure 5.18 SEMs of injection moulded nylon driving gear tooth (10 Nm, 1000 RPM)

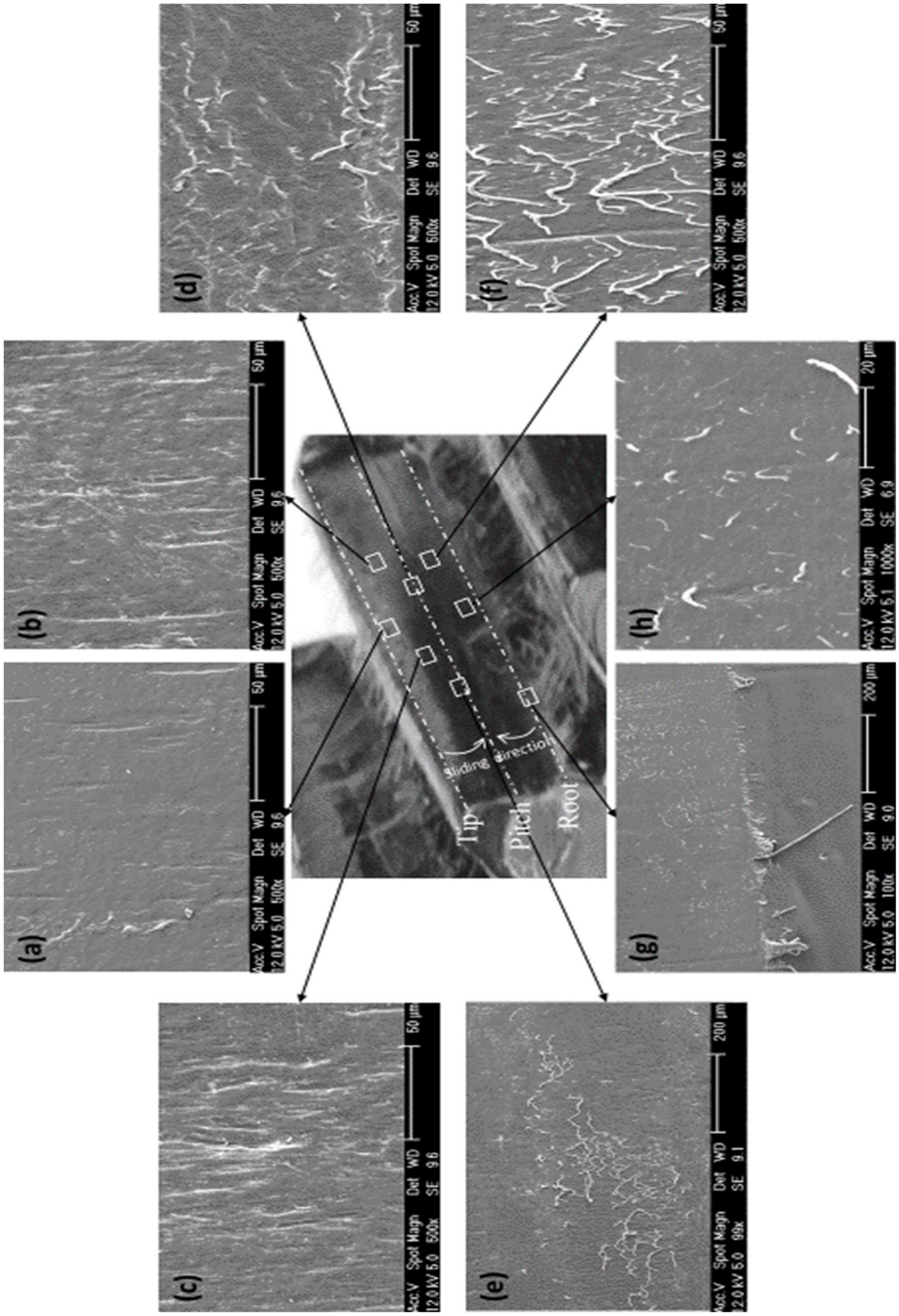

Figure 5.19 SEMs of injection moulded nylon driven gear tooth (10 Nm, 1000 RPM)

On the surface between the tooth pitch line and the tip (Figure 5.19 (a), (b) and (c)), the initial high pressure contact, at the start of the gear mesh, caused higher wear severity, especially towards the tip side. Abrasive wear is common here, with some scoring wear. Scoring tends to stretch towards the sliding direction making some surface vertical grooves. It was thought that this scoring and grooves were made by the wear debris of the driving gear teeth, which was classified as fretting wear type. This part of the gear was the highest worn part of the surface, with a high tooth thickness reduction.

Around the pitch line (Figure 5.19 (d) and (e)), a good amount of wear debris was gathered, as the direction of sliding drives it from the root and the tip. Debris was shaped in long-rounded particles because of the sliding contact between the two surfaces. A larger amount of debris was found at the top part of the pitch line than the lower part. During the rolling action, at the pitch line, some of the debris was hard pressed to the surface, due to the high pressure, and formed a flat partial cover on the surface. Abrasive wear was the common type in this area.

At the deddendum side of the tooth surface (Figure 5.19 (f), (g) and (h)), abrasive wear was functioning throughout the area. Some long grooves were formed by the moving debris, as fretting wear. It was observed that part of the debris was generated at the root side of the tooth surface, typically at the start point of the contact, due to the hard pressure of the surface contact by the tip of the driving gear tooth, which leads to extruding the surface materials forming some long tubes. These tubes, in addition to the surface sliding debris, act in a cumulative way to increase the amount of debris. The amount of debris was higher near the pitch line than the root. They scratch this area of the driven tooth surface as a fretting wear.

Figure 5.20 shows the SEM of the debris that was collected from below the running gears at the 10 Nm test. It can be seen that most of the debris

was shaped as long-rounded material. The thickness of these tubes ranged from 20 µm to 70 µm.

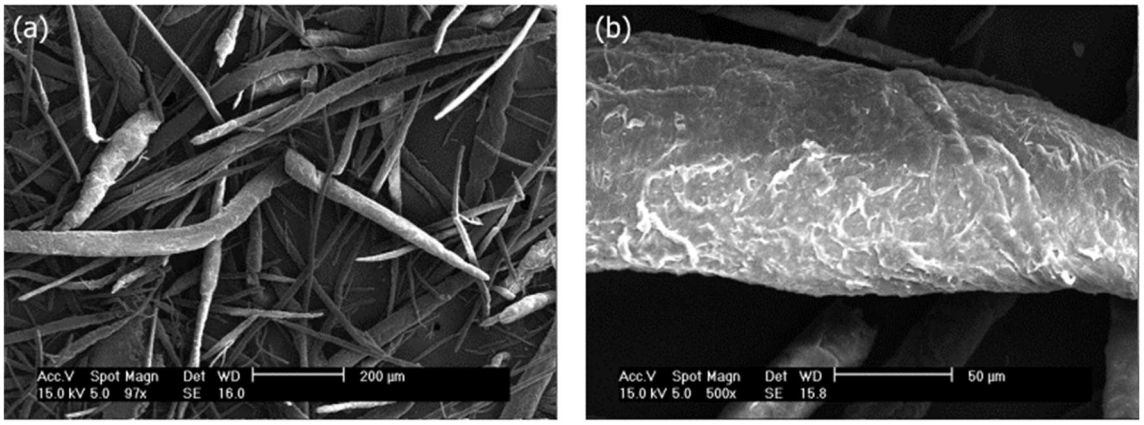

Figure 5.20 SEMs of debris collected from the test of injection moulded nylon gear (10 Nm, 1000 RPM)

5.3.1 The effect of the running speed

A number of tests were carried out under the control running speed, to study the effect of this variable on wear rate of injection moulded nylon gear teeth. It was aimed to compare the results with the previous load variable results to gain more understanding of the tribology of these gear teeth at different running speeds.

Figure 5.21 shows the wear of injection moulded nylon gear pairs running continually at a speed of 500 RPM and under two different loads of 6 Nm and 10 Nm. It was found from the two curves that wear rates (at the nearly-linear stage of wear) were 5.7×10^{-8} mm/cycle for 6 Nm and 2.91×10^{-6} mm/cycle for 10 Nm. The wear rate at 10 Nm is around 50 times higher than the wear rate at 6 Nm. Therefore, we can claim that at the running speed of 500 RPM, nylon gears loaded by 10 Nm will experience a high wear rate beyond some critical point. The first test (at 6 Nm) was stopped before gear tooth fracture or major damage, while the second test (at 10 Nm) was fractured after 217,000 cycles.

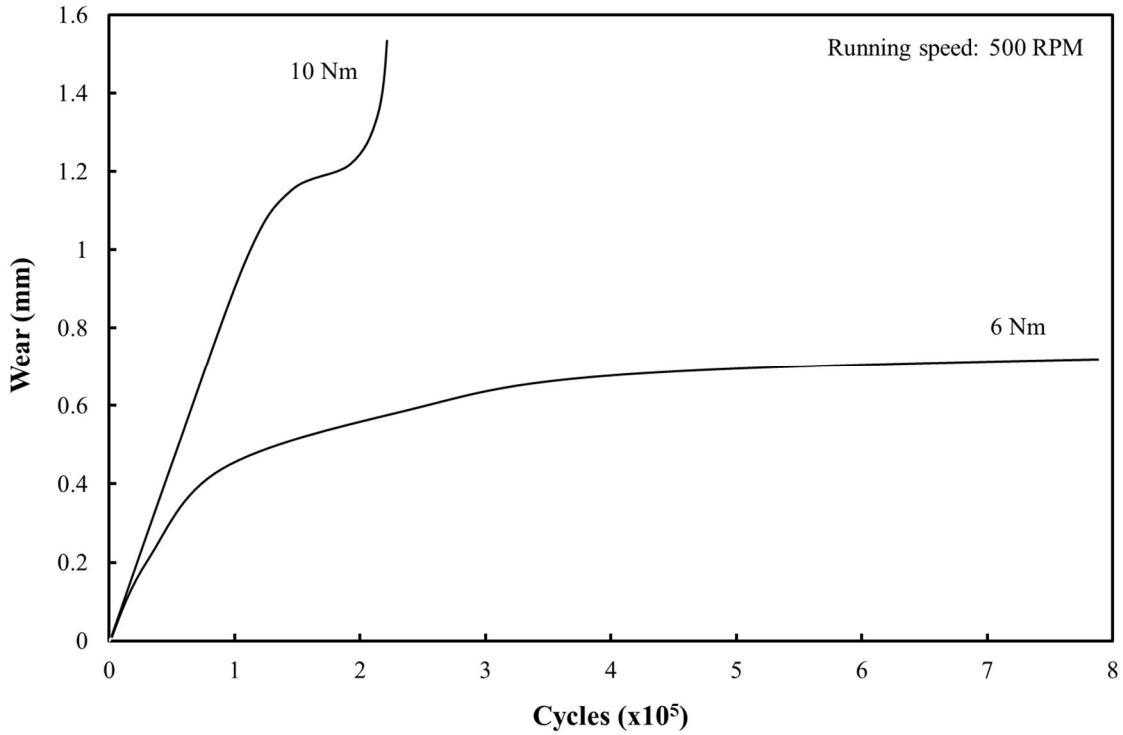

Figure 5.21 Tooth surface wear results of two tests for injection moulded nylon gear pairs, run at 500 RPM speed and loaded by 6 Nm and 10 Nm torques

Figure 5.22 and Figure 5.23 show the after-test injection moulded nylon gear pairs that were running at 500 RPM and under the load of 6 Nm and 10 Nm, respectively.

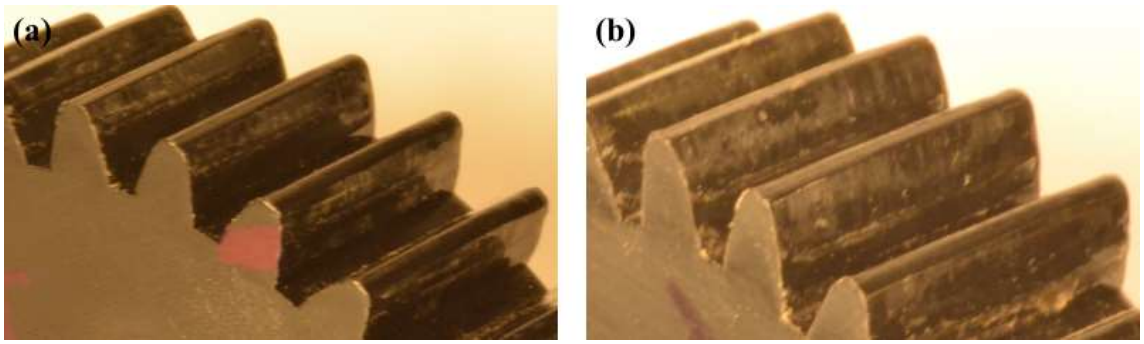

Figure 5.22 The after-test injection moulded nylon gear pair, tested at 500 RPM and under 6 Nm load, (a) driving and (b) driven.

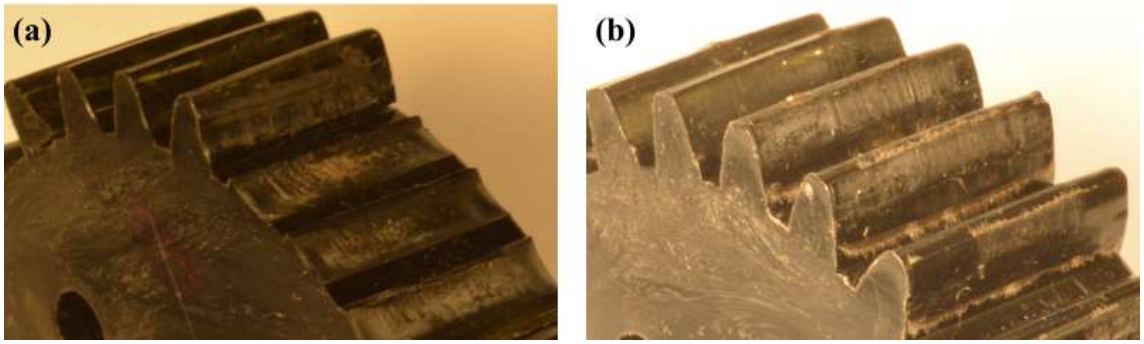

Figure 5.23 The after-test injection moulded nylon gear pair, tested at 500 RPM and under 10 Nm load, (a) driving and (b) driven.

Figure 5.24 shows the wear of injection moulded nylon gear pair at the speed of 1000 RPM and three different loads, namely: 6 Nm, 10 Nm and 13 Nm. The wear rate of the nylon gear tooth in these tests was defined at the nearly-linear (lowest) stage of the wear trend. For the 6 Nm test, wear rate was relatively low and stable around 7.2×10^{-8} mm/cycle, while the wear rate for both 10 Nm and 13 Nm tests were relatively high at around 3.95×10^{-5} mm/cycle and 6.75×10^{-5} mm/cycle respectively. These results validate the step-loading result for injection moulded nylon gear in section (4.2.2), which claimed that load critical point for this material is around the load of 9 Nm and provided similar wear rate values at similar loads. The status of gear running supports this conclusion, as 6 Nm test gear did not fracture or suffer major damage, but the two higher load cases fractured after relatively small numbers of running cycles (less than 50,000 cycles).

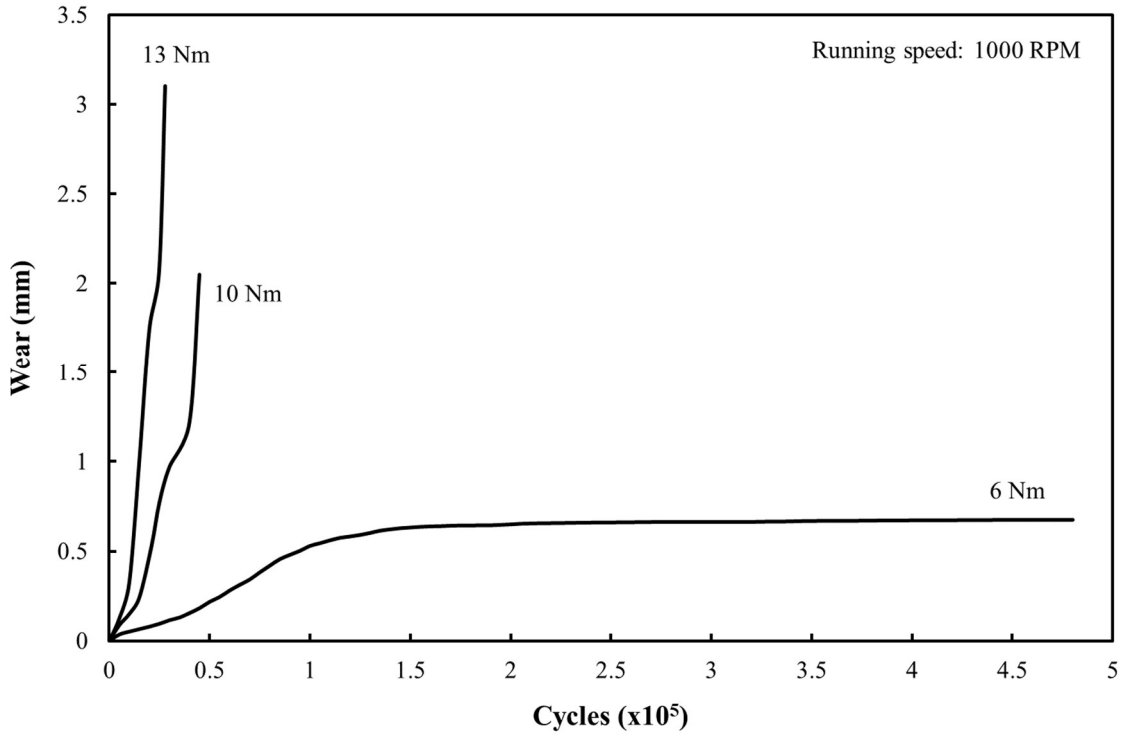

Figure 5.24 Tooth surface wear results of three tests for injection moulded nylon gear pairs, run at 1000 RPM speed and loaded by 6 Nm, 10 Nm and 13 Nm torques

Figure 5.25 shows the after-test injection moulded nylon gear pair that was tested at the speed of 1000 RPM and under the load of 13 Nm.

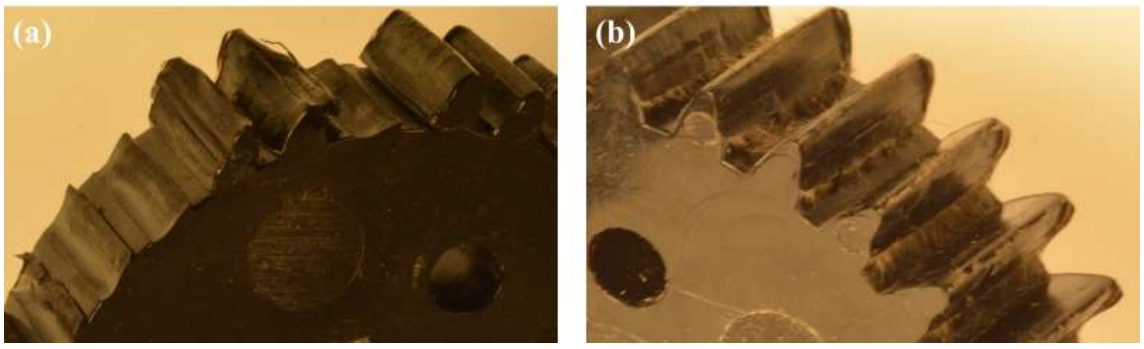

Figure 5.25 The after-test injection moulded nylon gear pair, tested at 1000 RPM and under 13 Nm load, (a) driving and (b) driven.

Running a pair of injection moulded nylon gears at higher speed showed similar phenomena. Figure 5.26 shows the wear trend for pairs of gears running at the speed of 2000 RPM and under two loading amounts. As speed increased, the applied load needed to be decreased in order to get the same wear trend and assign the location of the transition point. It can be seen from Figure 5.26 that at the load of 3 Nm, the wear rate was relatively low, at 1.1×10^{-8} mm/cycle. In contrast to the previous two speeds, the wear rate of nylon gear teeth at the load of 6 Nm and speed of 2000 RPM was relatively high at 2.4×10^{-7} mm/cycle. In addition, the gear teeth experienced root fracture in this test after running for less than 500,000 cycles.

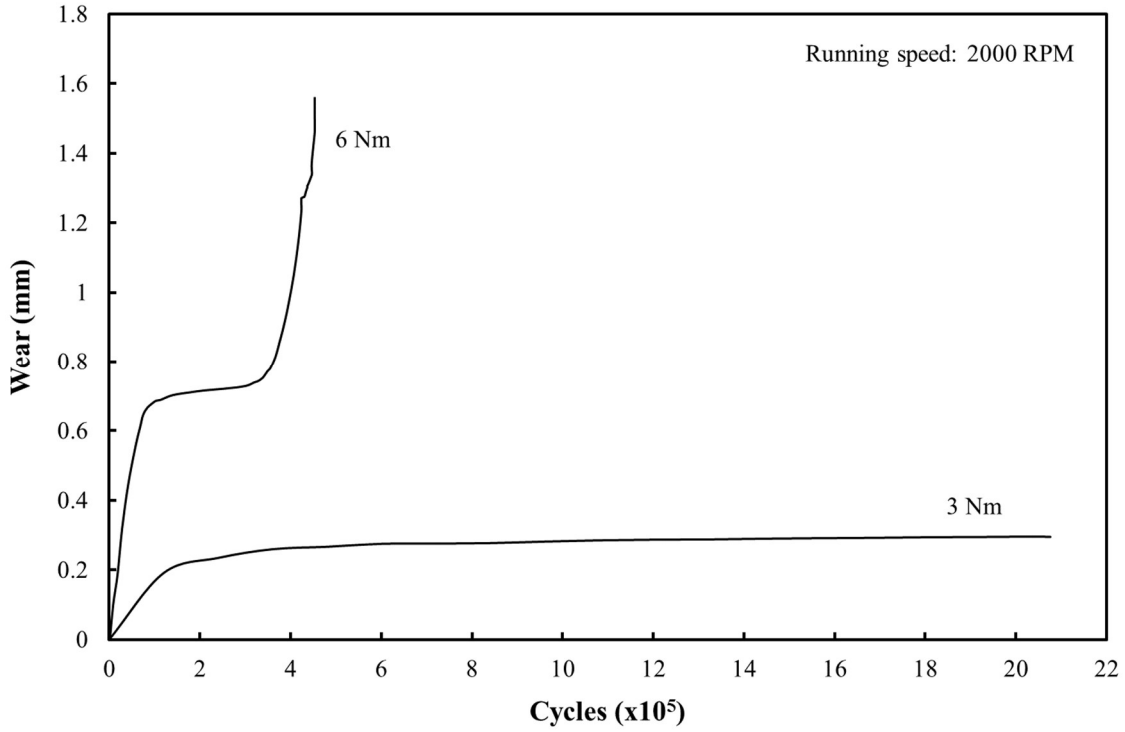

Figure 5.26 Tooth surface wear results of two tests for injection moulded nylon gear pairs, run at 2000 RPM speed and loaded by 3 Nm and 6 Nm torques

Figure 5.27 and Figure 5.28 show the after-test injection moulded nylon gear pairs that were running at 2000 RPM and under the load of 3 Nm and 6 Nm, respectively.

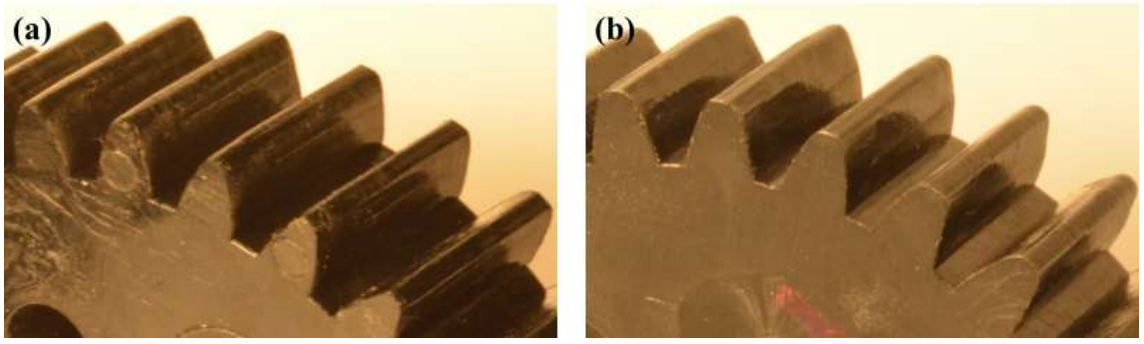

Figure 5.27 The after-test injection moulded nylon gear pair, tested at 2000 RPM and under 3 Nm load, (a) driving and (b) driven.

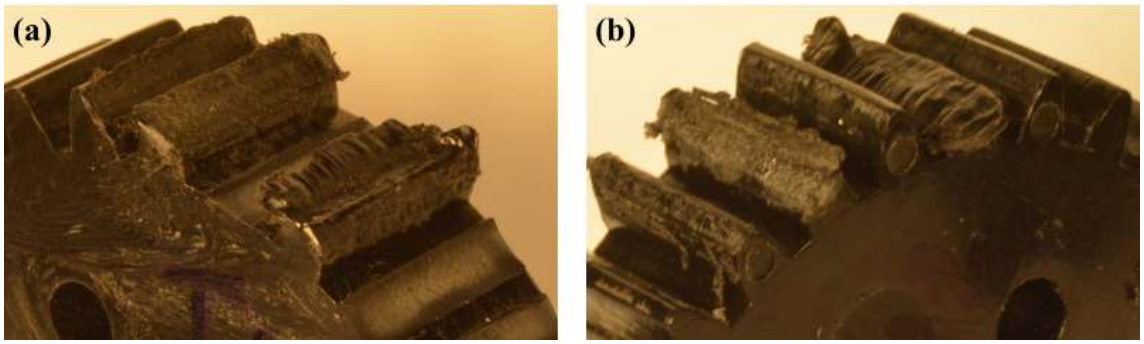

Figure 5.28 The after-test injection moulded nylon gear pair, tested at 2000 RPM and under 6 Nm load, (a) driving and (b) driven.

The general conclusion can be drawn that there is a positive relationship between gear running speed and gear teeth wear rate, as shown in Figure 5.29. Because of the high variance in wear rate, it is plotted in log form (base 10).

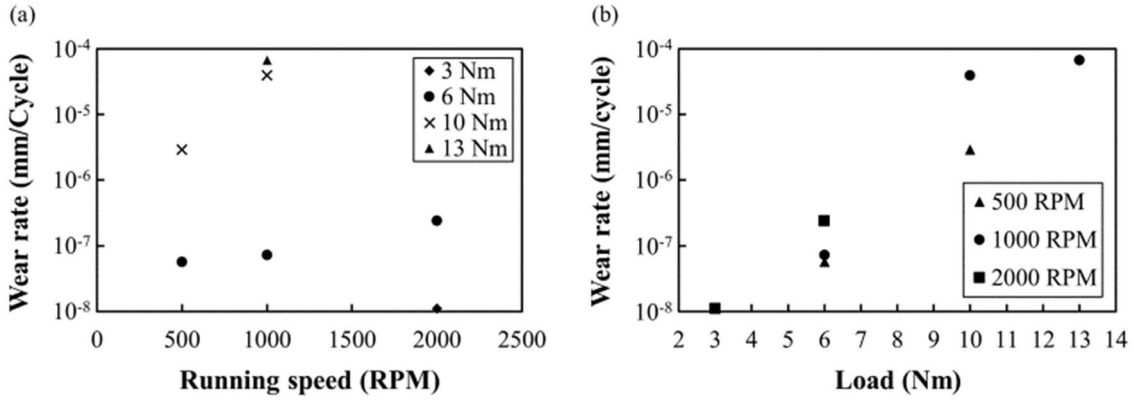

Figure 5.29 Wear rate of injection moulded nylon gear with respect to (a) running speed and (b) load

It can be seen from Figure 5.29 that at each speed there are two ranges of wear rate: high and low. Polymer gears mostly demonstrate these two types of wear rate phenomena dependent upon a critical of applied load. On the other hand, the wear rate did not show this phenomenon of high variance with respect to running speed. In general, wear rate showed a stable and steady increase when nylon gear running speed was increased. In addition, the gear load capacity is highly decreased with the running speed increase.

5.4 Machine cut nylon gears

The step-loading test for machine cut nylon gears (section 4.2.3) showed an important phenomenon, which was the negative relationship between the wear rate and the increase in the applied load at a certain value of load. This exceptional trend needed further investigation to reveal some of its causes. In this section, two of the long-run tests for machine cut nylon gear will be illustrated and discussed.

Figure 5.30 shows the wear curves for machine cut nylon gear teeth under the load of 5.5 Nm and 9 Nm and at the speed of 1000 RPM. Gears were run for 3.6 x 10^5 cycles before they were intentionally stopped during the steady stage of wear in order to tribologically investigate their teeth. The

steady stage of wear was easily defined during the test because of the function of continuously recording gear wear for this test rig. After both tests were stopped and gears were left to cool down from the high running temperature, the gear teeth appeared to recover from their deflected shapes. It can be seen from Figure 5.30 that the wear rate of machine cut nylon gears under the load of 8.5 Nm was higher than the wear rate under the load of 9 Nm, which confirms the wear rate transition phenomena at Figure 4.9. By the later stage of running of the 8.5 Nm test, the wear rate had slightly reduced, which is thought to be the result of the increase of either the pressure angle or gear contact ratio; as a result of highly worn out teeth. In addition, gears were running more smoothly at 9 Nm than at 8.5 Nm, where higher sound and vibration were recognised. Tested gears were weighed and compared to the pretested weight to get an estimate of the amount of weight loss and to validate wear results.

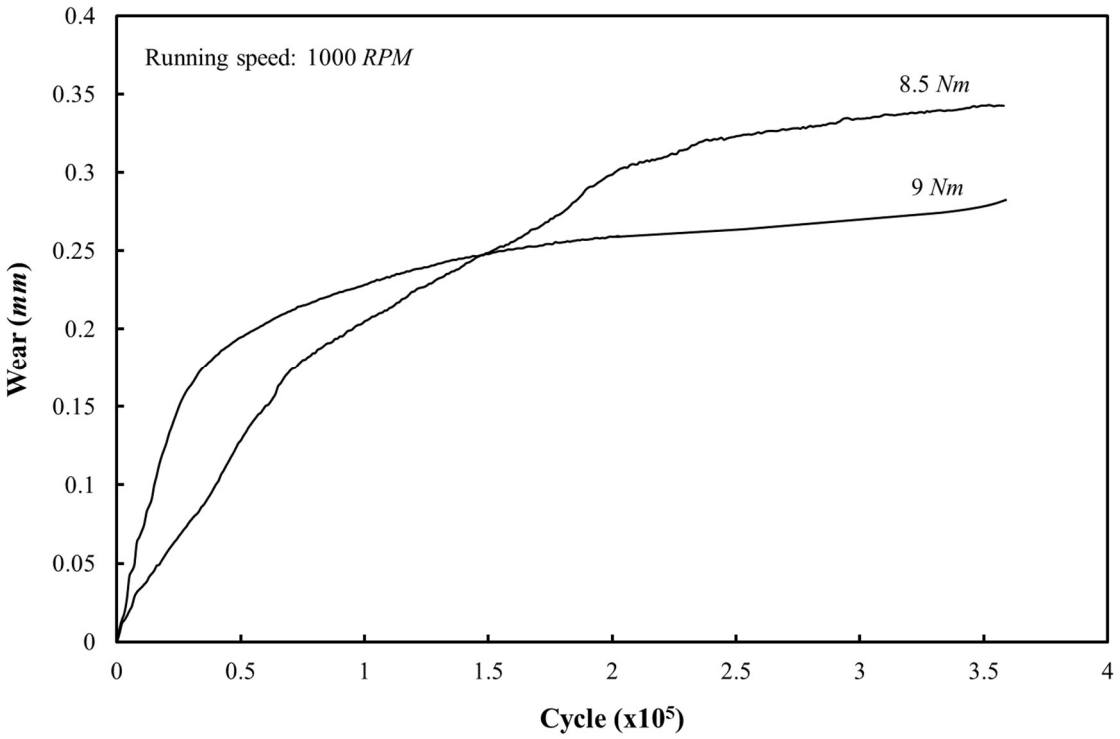

Figure 5.30 Tooth surface wear results of two tests for machine cut nylon gear pairs, run at 1000 RPM speed and loaded by 8.5 Nm and 9 Nm torques

Figure 5.31 shows the amount of after-test debris for both tests. In the 8.5 Nm test, debris started to fall from the beginning of the run (during the running-in stage) in small amounts. This was followed by a greater amount of debris in the nearly-linear stage, but the debris was much thinner in this test. On the other hand, there was much less debris at the running-in stage at the 9 Nm test. This was followed by a higher amount of debris with thicker shape in the nearly-linear stage. The colour of the debris here was different to the gear material colour, with some yellow texture that is thought to be the result of molten surfaces that were acting as an internal lubricant. Debris from both tests were collected and investigated under microscopes for more understanding of nylon gear wear behaviour, especially the changed colour. All in all, it was observed throughout the running time of the two tests that the amount of debris at 9 Nm was less than at 8.5 Nm.

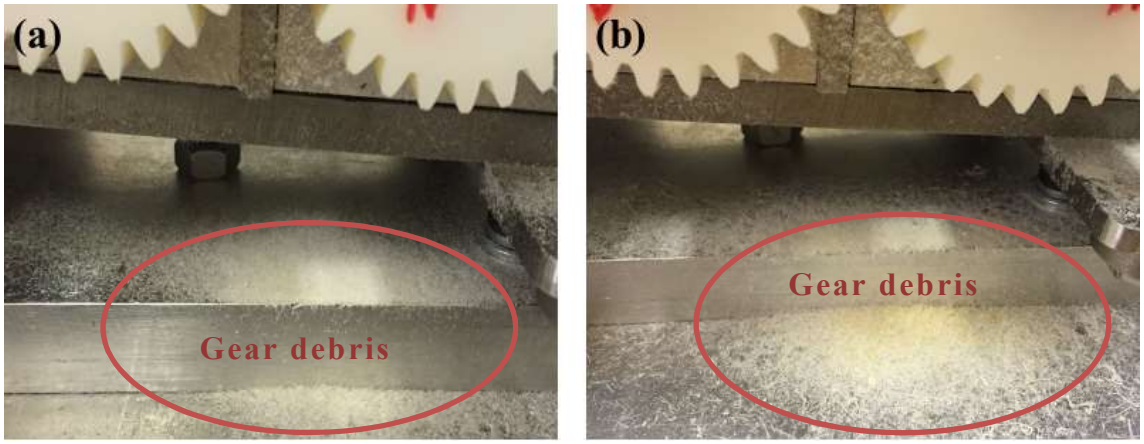

Figure 5.31 Gear debris of machine cut nylon gear at running speed of 1000 RPM and (a) 8.5 Nm and (b) 9 Nm

Figure 5.32 and Figure 5.33 show the after-test machined cut nylon gear pairs that were running at 1000 RPM and under the load of 8.5 Nm and 9 Nm, respectively.

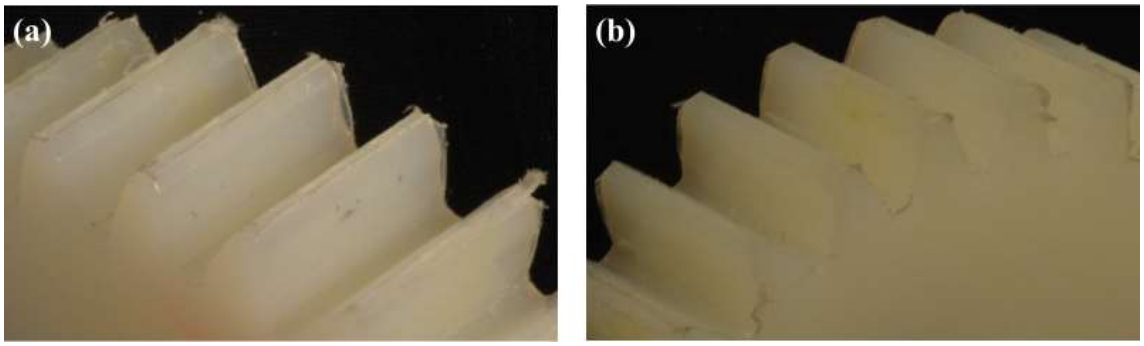

Figure 5.32 The after-test machined cut nylon gear pair, tested at 1000 RPM and under 8.5 Nm load, (a) driving and (b) driven.

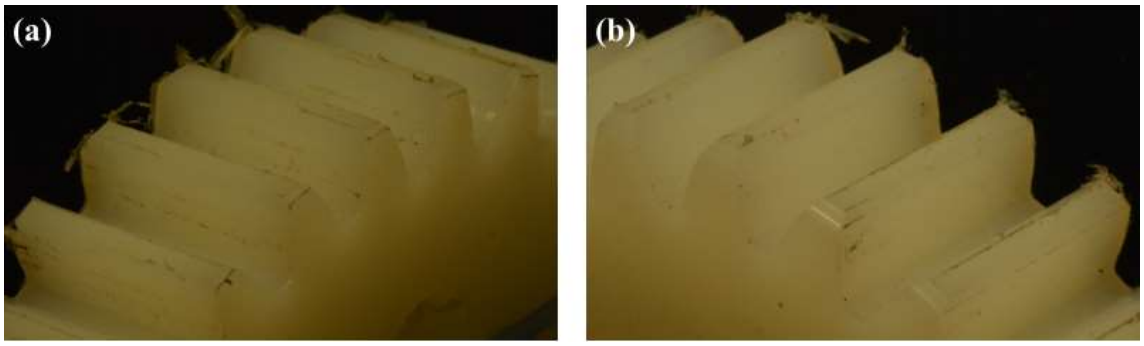

Figure 5.33 The after-test machined cut nylon gear pair, tested at 1000 RPM and under 9 Nm load, (a) driving and (b) driven.

Hooke et. al [37] discovered a decrease of wear rate in relation to the increase of either slip ratio or load for two nylon 66 discs running in non-conformal contact mode. The relation showed a general increase of wear rate with regards to the increase of load, apart from at a critical point where wear rate was changing dramatically. They measured the friction between the two discs and theoretically calculated the maximum surface temperature (including mean and flash temperature) and concluded that this sudden fluctuation in wear rate was the result of a thermal factor. For this reason, and for the aim to understand the decrease in wear rate of nylon gears with regards to load increase, surface temperature measurements were made for both the 8.5 Nm and 9 Nm tests using the thermal imaging camera.

Figure 5.34 shows gear teeth maximum surface temperature for machine cut nylon gears running at 1000 RPM and loaded at 8.5 Nm. It can be seen that maximum surface temperature was increasing quite rapidly in the running-in stage (the first 7 x 10^4 cycles), with the maximum surface temperature of both driving and driven gears at similar levels, until reaching 80°C. This was followed by a general increase in the maximum surface temperature between 7 x 10^4 cycles and 2 x 10^5 cycles, when the maximum surface temperature reached 120°C. Temperature values showed higher fluctuations in this period of running. Maximum surface temperatures for both gears then stabilized around the maximum value of 120°C with around 6°C of temperature fluctuation. In addition, at some stages of the running time, the surface maximum temperature of the teeth of the driving gear was around 5°C higher than for the driven gear. Once a test was stopped, gear maximum surface temperature showed a rapid decrease, reaching the initial running temperature value of 40°C within 30 minutes.

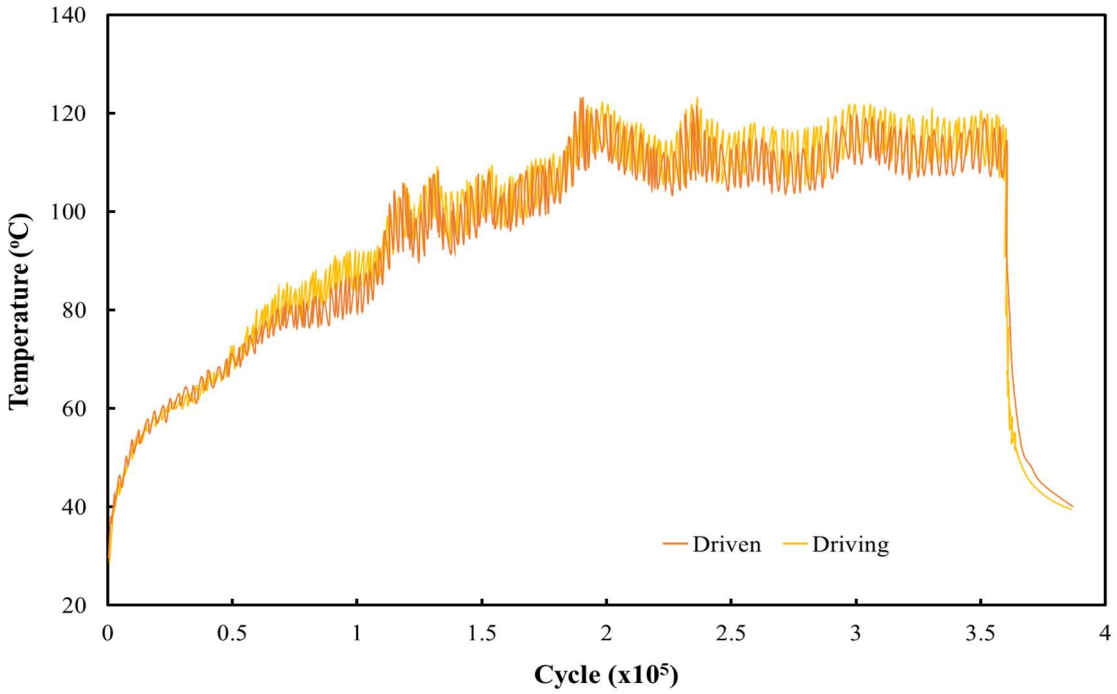

Figure 5.34 Surface maximum temperature of machine cut nylon gear (8.5 Nm, 1000 RPM)

Nylon gears tested at a load of 9 Nm showed a different thermal phenomenon. Figure 5.35 shows the maximum tooth surface temperature for a machine cut nylon gear pair at the running speed of 1000 RPM and under the applied load of 9 Nm. It can be seen that in the first 2 x 10^4 cycles, the maximum surface temperature was dramatically increasing at higher rate than for the 8.5 Nm test, reaching the value of around 75°C. This sudden increase was followed by a stable maximum surface temperature between 70°C and 75°C for the period between 5 x 10^4 cycles and 2.2 x 10^5 cycles. Tested gears then experienced an increase in tooth surface maximum temperature during the running period between 2.2 x 10^5 cycles and 3.5 x 10^5 cycles, with a higher amount of temperature fluctuation, until reaching 110°C. The test rig was stopped at 3.5 x 10^5 cycles and the gears were left to cool down for 30 minutes, when the maximum surface temperature rapidly decreased to 40°C. Generally, during the test, the driven gear showed a tooth surface maximum temperature that was around 5°C higher than the driving gear.

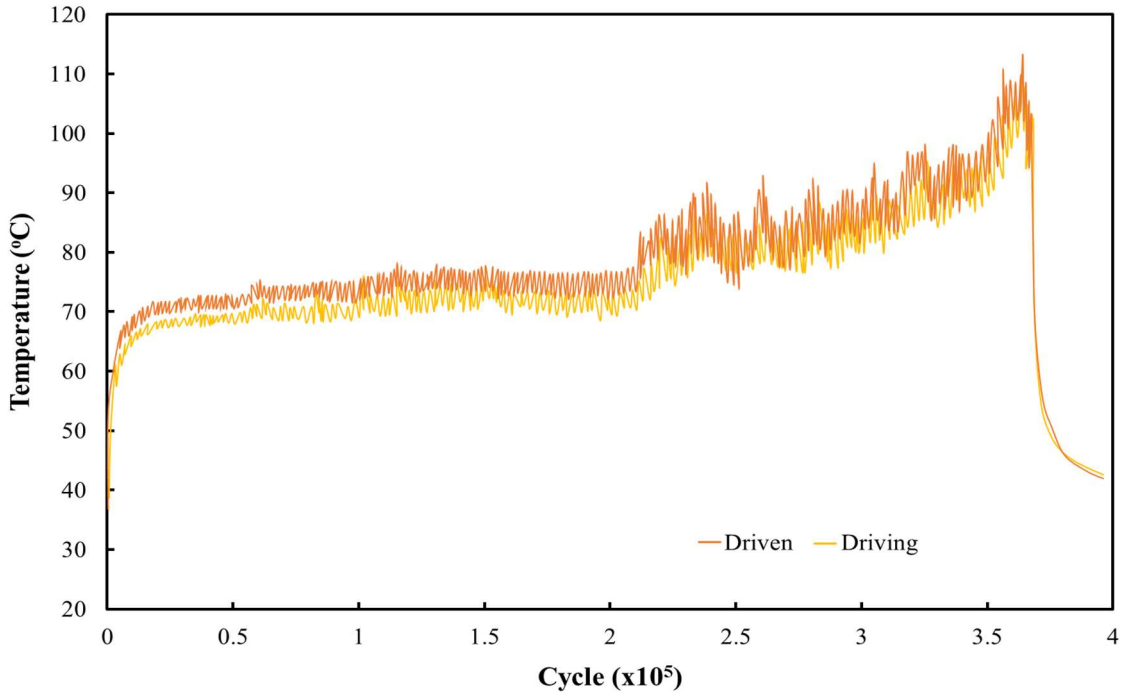

Figure 5.35 Surface maximum temperature of machine cut nylon gear (9 Nm, 1000 RPM)

For the 8.5 Nm test (Figure 5.34), the surface temperature reached the glass transition temperature for this material (see Figure 4.15) after running for around 1.15 x 10^5 cycles. This was thought to be one of the reasons for the increase in wear in Figure 5.30 during and after the same period and prevent the wear from establishing the nearly-linear stage in that time. On the other hand, 9 Nm test (Figure 5.35) showed stable temperature during the nearly-linear wear stage up until reaching 2.2 x 10^5 cycles, where the surface temperature started to increase slightly, although the value did not reach the glass transition temperature until later (around 3.5 x 10^5 cycle). This may explain the slight increase in wear readings in Figure 5.30 after this running time, but because of the stop of the test afterwards, we could not explore the continuing wear behaviour.

To further understand this wear rate and temperature changes with respect to load change, some investigations were carried out, using the SEM, on the tooth surfaces of the tested gear pairs.

Figure 5.36 shows the SEM images for the tooth surface of the machined cut nylon driving gear that was tested at the speed of 1000 RPM and under the applied load of 8.5 Nm. Different surface tribology and wear phenomena can be seen at different places.

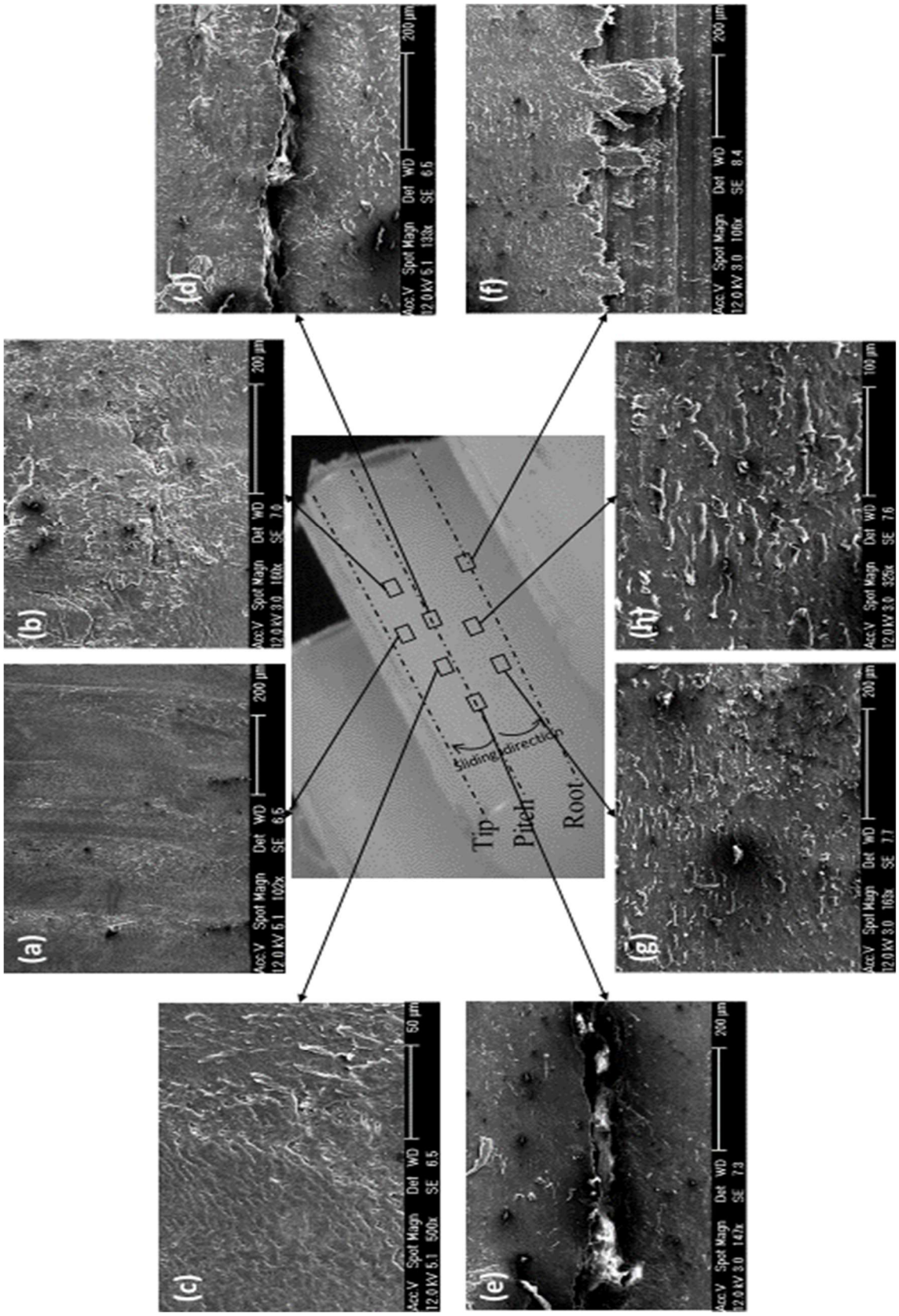

Figure 5.36 SEMs of machine cut nylon driving gear tooth (8.5 Nm, 1000 RPM)

At the addendum side of the tooth surface (Figure 5.36 (a), (b) and (c)), adhesive wear was the common type of surface damage, especially towards the pitch line. Debris started to form in this area. Towards the tip of the tooth, as the debris builds up, there were some surface scratches leading to the form of fretting wear. The surface was experiencing the highest severity wear at this part of the tooth, especially near the tip side. Due to the high surface temperature that was reaching above the glass transition point of the tested material, parts of the addendum area experienced some forms of plastic flow.

Around the pitch line (Figure 5.36 (d) and (e)), there was a clear crack formation across the tooth surface. It was thought that this crack is the result of the sliding direction. Some debris was found to be formed at this area, especially towards the dedendum side of the tooth. The wear mechanism was mostly abrasive and sometimes adhesive wear.

Figure 5.36 (f), (g) and (h) show the SEM for the dedendum side of the tooth surface. It can be seen that more debris can be found here than on the addendum side. Adhesive wear and surface plastic flow were the most common types of wear on this part of the gear. It was observed that parts of the surface were welded to the driven gear tooth (the addendum side), which pulled a large amount of micro-chips from the driving tooth surface towards the sliding direction. This phenomenon increased the wear rate and the tooth thickness reduction at this part of the gear.

On the other hand, the driven gear tooth showed different wear phenomena, due to the opposite sliding direction. Figure 5.37 shows the SEM images for the tooth surface of the machine cut nylon driven gear that was tested under the applied load of 8.5 Nm, while running at the speed of 1000 RPM. Less wear severity was found here than on the driving gear tooth.

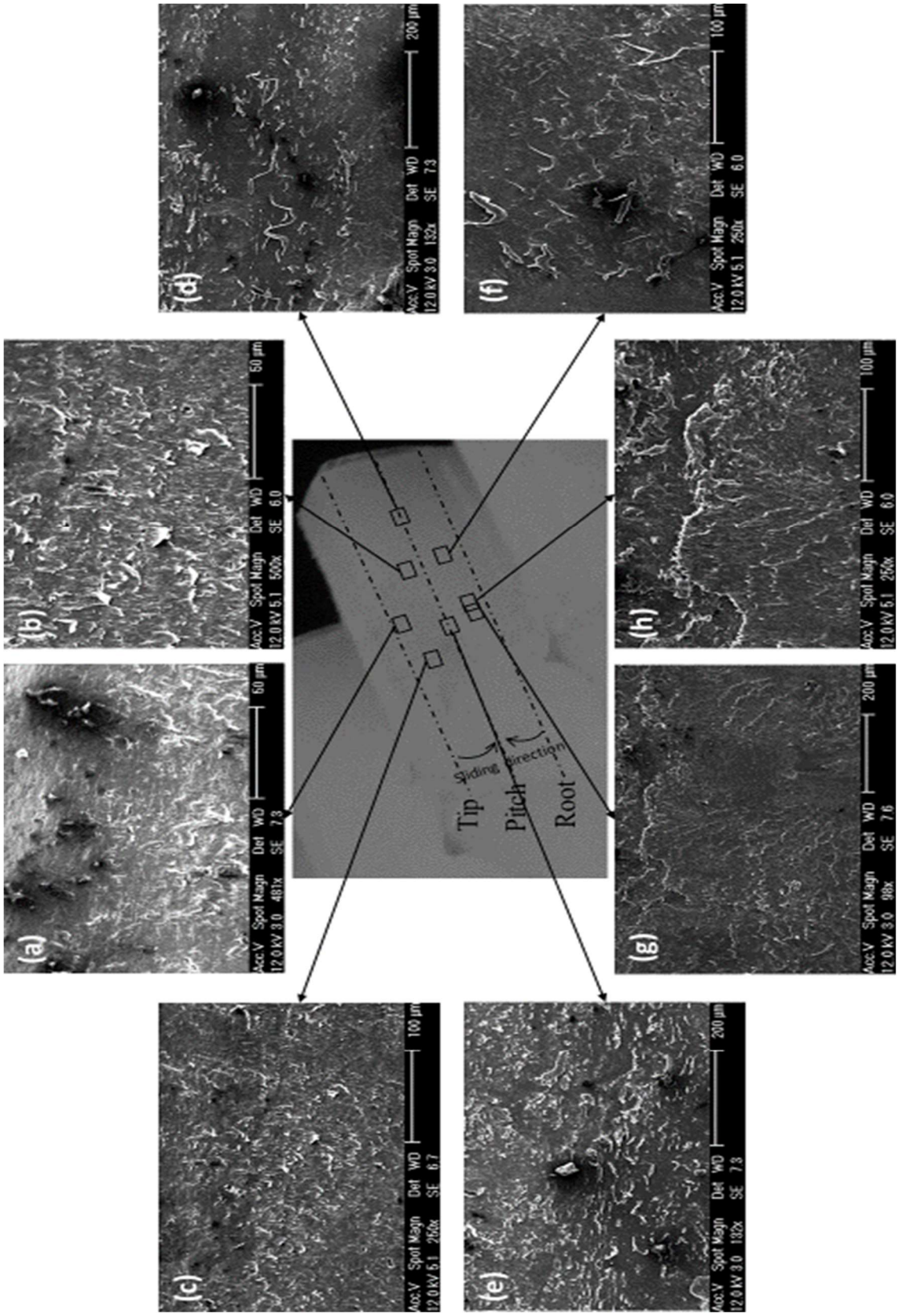

Figure 5.37 SEMs of machine cut nylon driven gear tooth (8.5 Nm, 1000 RPM)

At the addendum side of the surface (Figure 5.37 (a), (b) and (c)), adhesive wear and plastic flow were active towards the sliding direction. The amount of debris was cumulative towards the sliding direction. Some softened material was found on the tooth surface, as the temperature exceeds the glass transition point and the tooth was subject to high initial contact pressure from the driving tooth tip.

The area near the pitch line (Figure 5.37 (d) and (e)) was collecting the debris from both upper and lower parts of the surface, because of the sliding direction. Two forms of debris were found, namely long-rounded particles and chip particles. The chips were the likely to be the result of the adhesive wear, while the tubes could be formed from the chips as a result of the rolling between the two surfaces. No microcracks were found at this area of the driven gear tooth.

Between the root and the pitch line of the tooth surface (Figure 5.37 (f), (g) and (h)), adhesive wear was found to be active. Some larger chips can be observed on the surface. This could be from the high pressure contact with the addendum part of the driving gear tooth, which was highly worn out and could be subject to high surface temperature rates. Most of the debris in this side was in the form of thin chips. Some long-rounded debris was found near the pitch line, which is thought to be the result of the sliding contact between the two surfaces that leads to reform the chip debris. No microcracks were observed at this area.

A torque increase for 0.5 Nm leads to some wear rate and surface temperature decreases. Therefore the after test investigations could reveal some useful data to understand the surface behaviour changes. Figure 5.38 shows the SEM plates for the tooth surface of the machine cut nylon driving gear. The gear was tested at the speed of 1000 RPM and under the applied torque of 9 Nm. Tooth root fracture was about to initiate for this investigated specimen, due to the highly loaded gears. In general, different surface tribology can be seen in this test compared to the previous one.

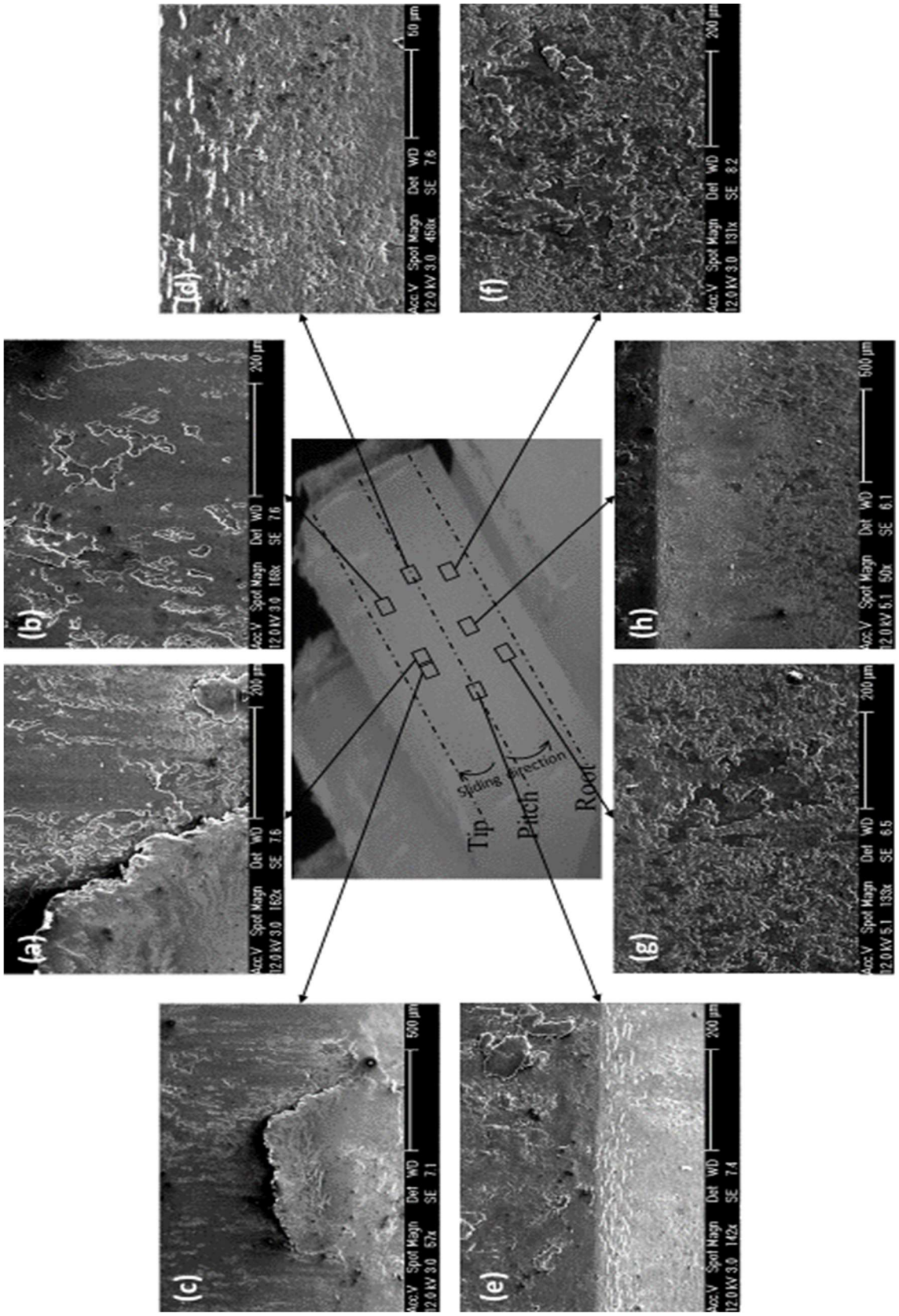

Figure 5.38 SEMs of machine cut nylon driving gear tooth (9 Nm, 1000 RPM)

At the addendum side of the tooth surface (Figure 5.38 (a), (b) and (c)), one can see some adhesive wear at some parts of the area. Interestingly, a larger part of the surface was covered by a softened material layer. This material was thought to be acting as a surface internal lubricant, which reduced the wear rate and surface temperature. The appearance of this phenomena in this test was not predicted but thought to be because of some specific conditions. For example, it might be the increase in surface pressure to an optimum level that causes the surface or the debris to spread along the contacting area. No form of debris was recognised at this part of the tooth.

Around the pitch line (Figure 5.38 (d) and (e)), the area tended to form two parts, with different surface characteristics at each. The top part had some shaped surface layer similar to the addendum side of the surface, but with a smaller covered area. The lower part was more of adhesive wear, with some chip debris taken out the surface towards the sliding direction. Interestingly, compared to the 8.5 Nm test, no crack or microcrack formation were observed here.

Forms of adhesive wear were more common towards the dedendum side of the tooth surface (Figure 5.38 (f), (g) and (h)). Similar phenomenon to the addendum side of the tooth surface were found here, where some softened material from the surface and the debris were layered across the surface of some parts of the area. This layer was, again, acting as a surface internal lubricant that reduces the tooth wear rate and surface temperature. The cause of this behaviour might be the increase in the contact pressure to an optimum point. No microcracks were observed at this part of the tooth.

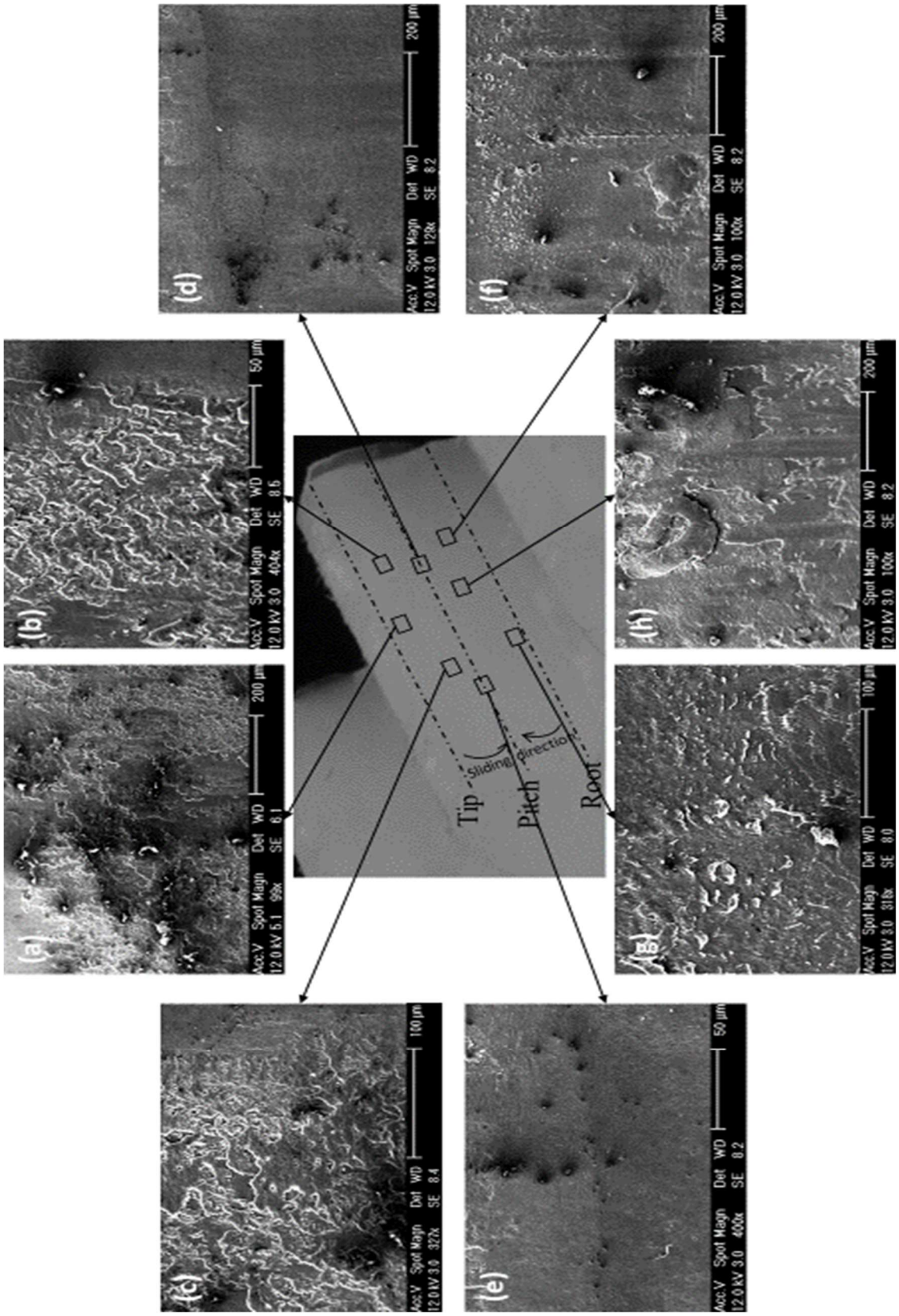

Figure 5.39 SEMs of machine cut nylon driven gear tooth (9 Nm, 1000 RPM)

Figure 5.39 shows the SEM images for the tooth surface of the machine cut nylon driven gear that was tested at the speed of 1000 RPM and under the applied load of 9 Nm. No fracture was observed at this driven gear.

The area between the pitch line to the tip of the tooth (Figure 5.39 (a), (b) and (c)) showed similar surface characteristics to the driving gear tooth. Adhesive wear was more common in this area, but with the same surface layering phenomenon covering most of the area. Some softened surface and debris were layered on top of the surface and acted as a surface internal lubricant. This behaviour reduced the surface wear rate and temperature.

Around the pitch line of the tooth surface (Figure 5.39 (d) and (e)), abrasive wear was more active. Interestingly, no wear debris was found at this area of the tooth, compared to the driven gear of the 8.5 Nm test, which may give an indication that most of the debris was pressed and layered on top of the addendum and dedendum surfaces before arriving to the pitch line by means of the sliding directions.

At the dedendum side of the tooth surface (Figure 5.39 (f), (g) and (h)), both abrasive and adhesive wear can be seen in different places of the area, but again with the surface layering function in action at most places. Some softened surfaces and debris wear layered on top of the surface act as an internal lubricant, which reduces the wear rate and surface temperature. No microcracks were observed at this part of the tooth surface.

To conclude, the main difference between the 8.5 Nm test and the 9 Nm test that could explain the wear rate and surface temperature to decrease with the load increase was a function of the surface tribology at each pair of gears. The surface layering behaviour at the 9 Nm test was thought to be one of the causes of these tribological changes.

5.5 Long run test

A long run test of the machine cut nylon gear pair under a lower applied load was undertaken to study the endurance of this material and its compatibility with gearing applications. Figure 5.40 shows gear tooth wear for machine cut nylon gear running continuously for about 1.2 x 10^7 cycles (one week) at the speed of 1000 RPM and under the applied load of 6.5 Nm. The test was stooped intentionally after one week. The early running-in stage wear caused a depth reduction of 0.2 mm after running for about 4 x 10^5 cycles. Wear then showed a stable period at a small rate between 4 x 10^5 cycles and 23 x 10^5 cycles. A higher wear rate was recorded between 23 x 10^5 cycles and 40 x 10^5 cycles, with a recognised jump in the wear readings. Then, for the rest of the running cycles, wear showed a nearly stable increasing gradient and the wear rate was nearly constant at a higher value than the previous stable period. By the end of the test, the gear wear curve showed the total amount of 0.34 mm of gear tooth width reduction and tooth deflection.

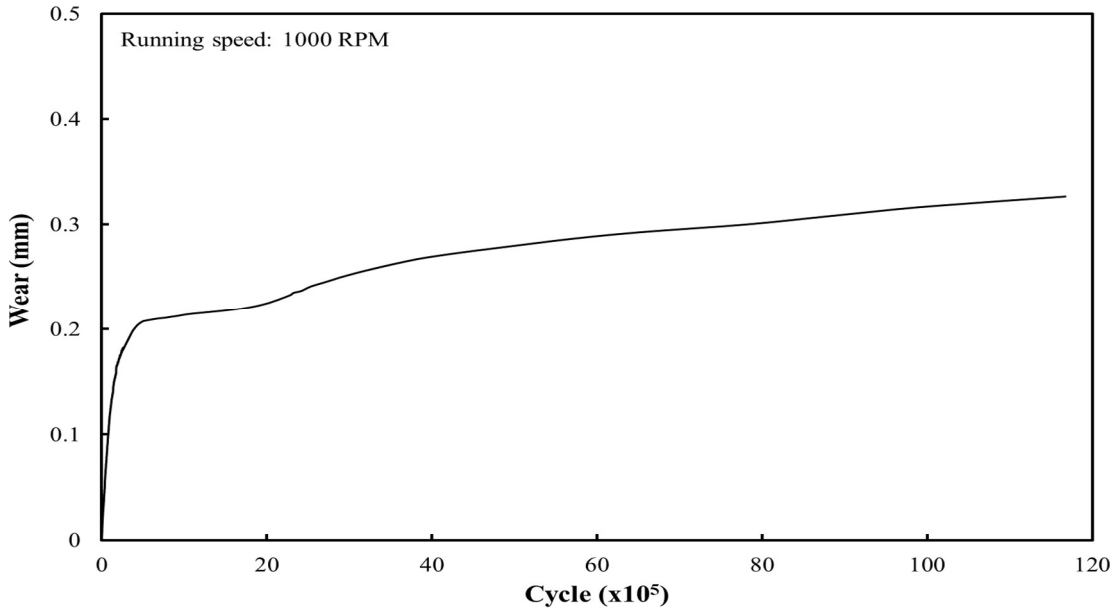

Figure 5.40 Tooth surface wear result of long run test (one week) for machined cut nylon gear pairs, run at 1000 RPM speed and loaded by 6.5 Nm torque

Figure 5.41 shows the after-test machine cut nylon gear pair that were running at 1000 RPM, under the load of 6.5 Nm, and for a long run period.

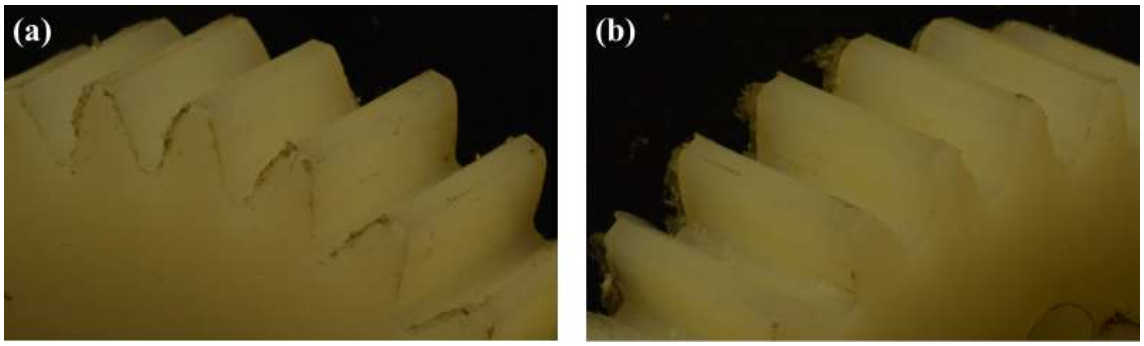

Figure 5.41 The after-test machined cut nylon gear pair, tested at 1000 RPM, under 6.5 Nm load and for a long running period, (a) driving and (b) driven.

The wear rate was found to be around 4 x 10^{-9} mm/cycle during the early stage of wear (between 4 x 10^5 cycles and 23 x 10^5 cycles). For the later wear stage (between 40 x 10^5 cycles and 120 x 10^5 cycles), wear rate increased to about 7 x 10^{-9} mm/cycle. The reason for this jump in wear rate was thought to be because of nylon material viscoelasticity. In general, viscoelastic behaviour for polymers tends to be greater than for metals. This means applying continuous load on a polymer specimen for a long time could lead to continuous amount of deflection. The test here used gears that were machined from a PA66 extruded bar, for which a flexural test (at the load of 10 N and deflection rate of 2 mm/min) showed a modulus of elasticity of 3100 MPa [120]. This relatively low value of modulus of elasticity could be one of the limitations for gearing applications for this particular material. Similar values of flexural modulus for acetal material could lead to the same amount of deflection after a long run for polymer gears. A similar test was done by Mao [4] for injection moulded nylon and acetal gears, but for a running speed of 500 RPM. His results showed quite similar wear behaviour, but with the wear transition phenomenon only occurring for acetal.

Surface maximum temperature of the gear teeth was measured using the thermal imaging camera. Figure 5.42 shows the maximum surface temperature for a machine cut nylon gear pair at the running speed of 1000 RPM and under the load of 6.5 Nm. The running time was one week, with the running amount of 1.2 x 10^7 cycles. During the running-in stage (0 to 4 x 10^5 cycles), gear maximum surface temperature jumped to an average value between 70°C and 80°C, with the maximum temperature for the driven gear about 3°C higher than the driving gear. Within the lower wear rate period in Figure 5.40 (from 4 x 10^5 to 23 x 10^5 cycles), the maximum surface temperature increased from 80°C to 95°C. Then, maximum surface temperature was fluctuating around 95°C for the last extensive period of higher wear rate.

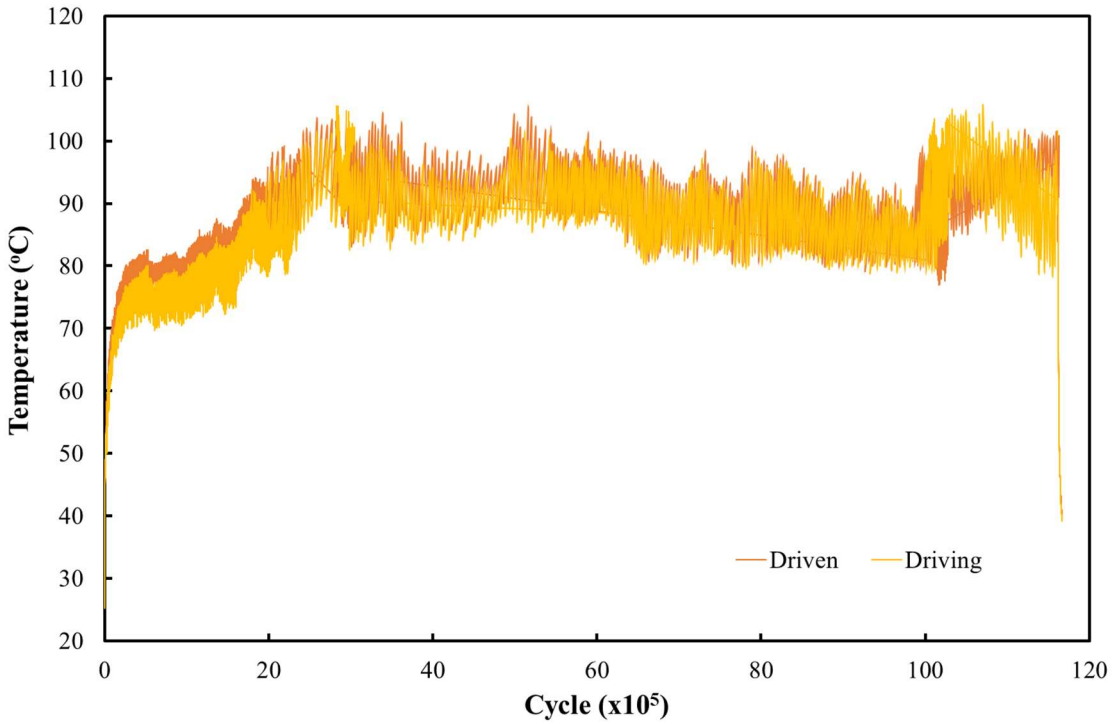

Figure 5.42 Surface maximum temperature of machine cut nylon gear (6.5 Nm, 1000 RPM)

Gear surface temperature measurements revealed that the glass transition temperature (98°C, from Figure 4.15) was reached during and after the 2.2 x 10^5 cycle for a couple of times. This may provide the reason of the sudden increase in wear in Figure 5.40 at that period of running time.

After-test investigation was carried out to further understand the wear mechanisms of the tooth surfaces. Figure 5.43 shows the SEM images for the tooth surface of the machine cut nylon driving gear that was tested at the speed of 1000 RPM and under the applied torque of 6.5 Nm. No tooth fractures were experienced by this tooth during the test.

At the addendum side of the tooth surface (Figure 5.43 (a), (b) and (c)), a large amount of surface scratches can be seen, with the appearance of some microparticle debris. Fretting wear can be classified as the common surface damage type in this area. Some surface pitting can also be discovered in some parts of the surface.

Around the pitch line of the tooth surface (Figure 5.43 (d) and (e)), a good amount of surface microcracks can be seen. This could be because of the sliding direction, as well as the Hertzian contact stress, as the gear was running for a long time (120 x 10^5 cycles). Adhesive wear was the most active type at this side of the gear. Some debris particles were found in small amount.

Moving to the dedendum side of the tooth surface (Figure 5.43 (f), (g) and (h)), fretting wear was found to be active again. With the help of microparticle debris, the surface was severely scratched. Some micro-pits can be seen across the surface. No microcracks were found on this part of the surface. Towards the root of the tooth (by the end of the surface contact), some surface plastic flow was observed and thought to be because the temperature increased above the glass transition point of the tested material.

The tooth of the machine cut nylon driven gear showed very similar surface tribology characteristics. Figure 5.44 shows the SEM of that tooth

after testing at the speed of 1000 RPM and under the applied load of 6.5 Nm. No tooth fracture was experienced at this part.

At the addendum side of the tooth surface (Figure 5.44 (a), (b) and (c)), the high initial contact surface pressure at the start of the gear mesh severely affected this area. With the long running time, a tip crack was formed along the tooth top side. Abrasive wear can be largely seen in most parts of the surface. Other parts were experiencing adhesive wear and plastic flow. Debris was hardly found here.

Moving to the pitch line side of the tooth surface (Figure 5.44 (d) and (e)), it can be seen that plastic flow was the most common type of wear at this area. Small amount of debris was found here and microcracks were observed.

The dedendum side of the tooth surface (Figure 5.44 (f), (g) and (h)) showed more abrasive wear activity. Scratches were observed in some places as a result of the fretting wear caused by surface debris. No microcracks were found at this side of the tooth surface and debris was hardly seen.

Figure 5.45 shows the SEM for the collected debris from below the tested gears. Most debris were formed in a long-rounded particle shape, while others were as microchips.

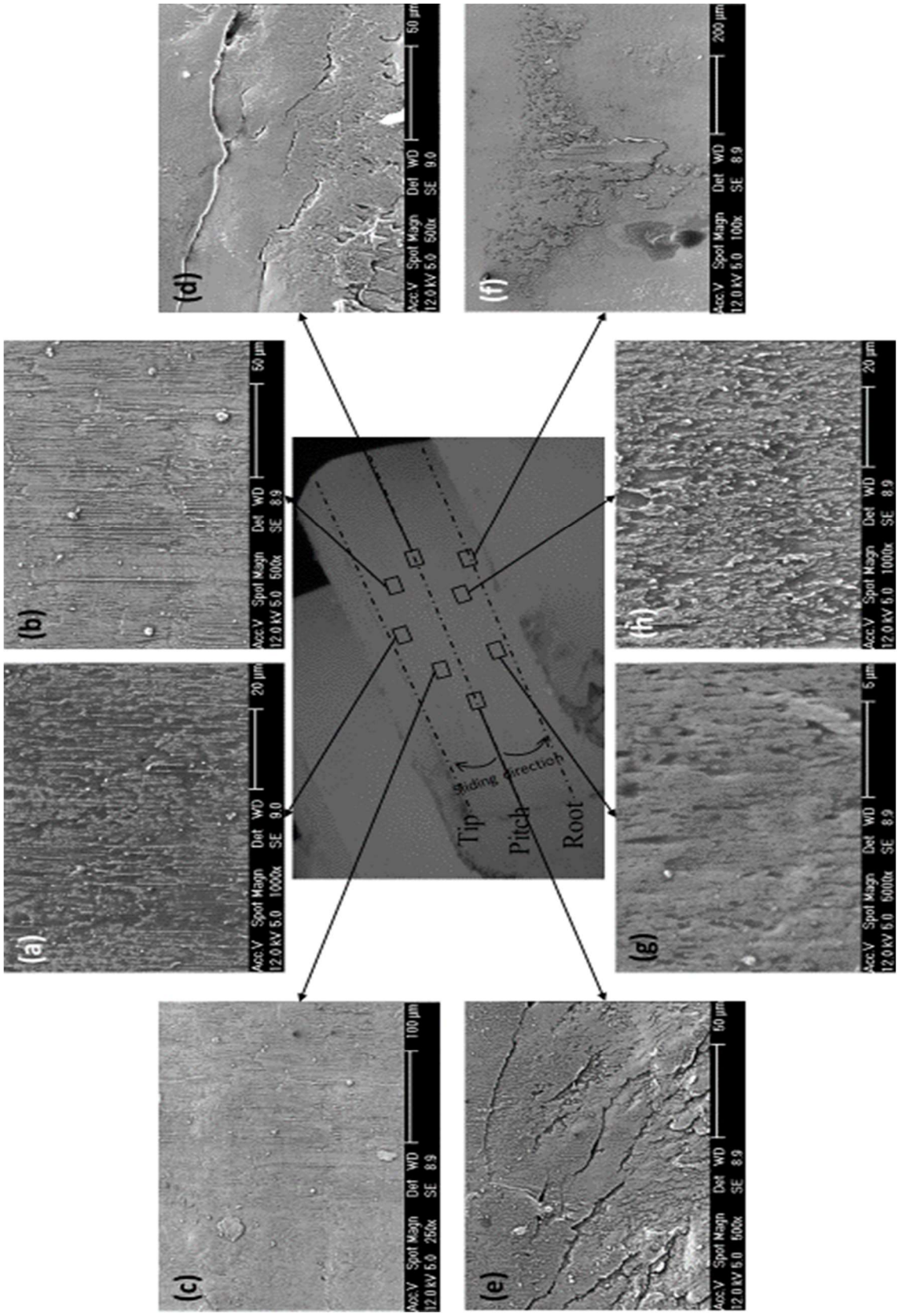

Figure 5.43 SEMs of machine cut nylon driving gear tooth (6.5 Nm, 1000 RPM)

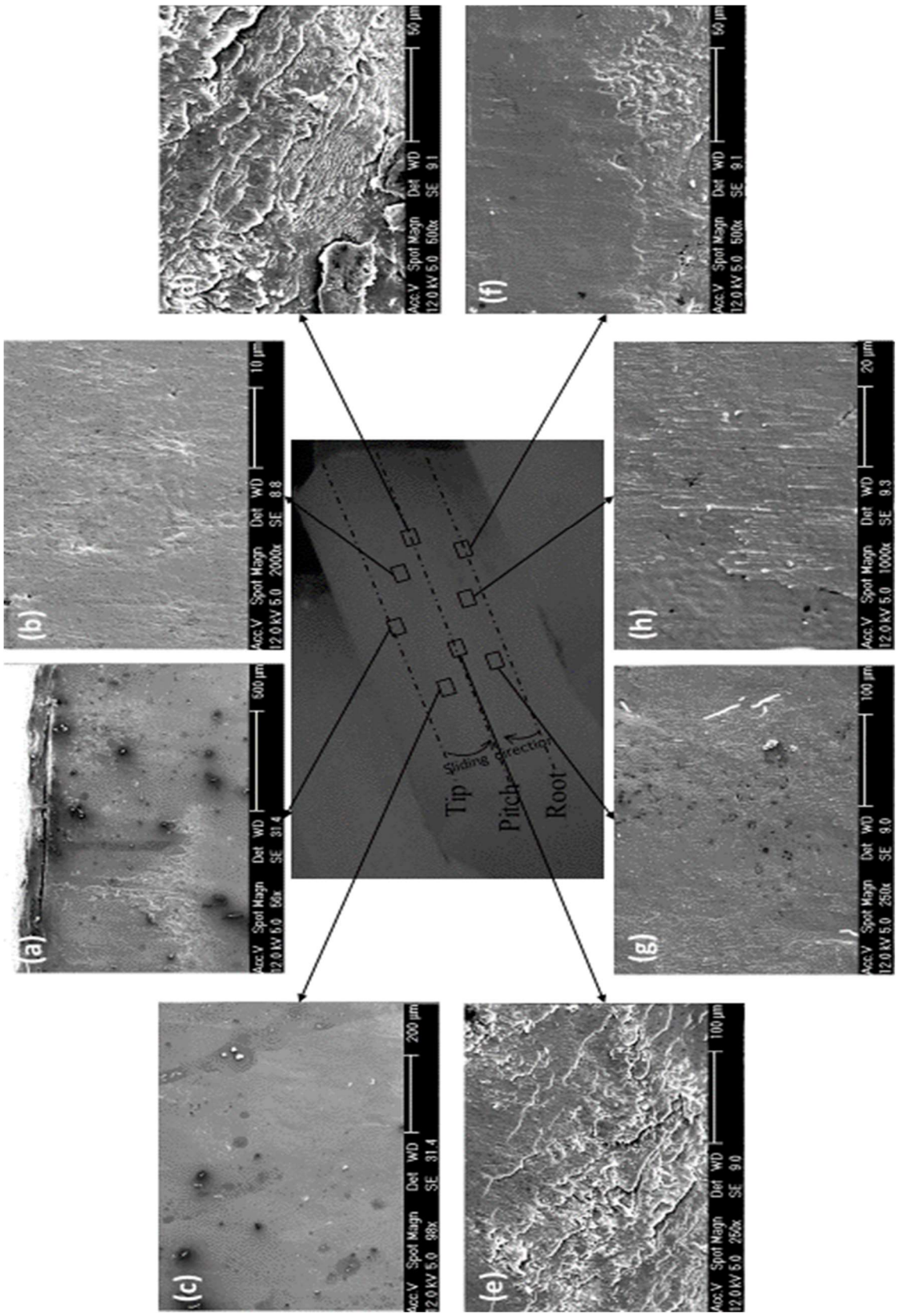

Figure 5.44 SEMs of machine cut nylon driven gear tooth (6.5 Nm, 1000 RPM)

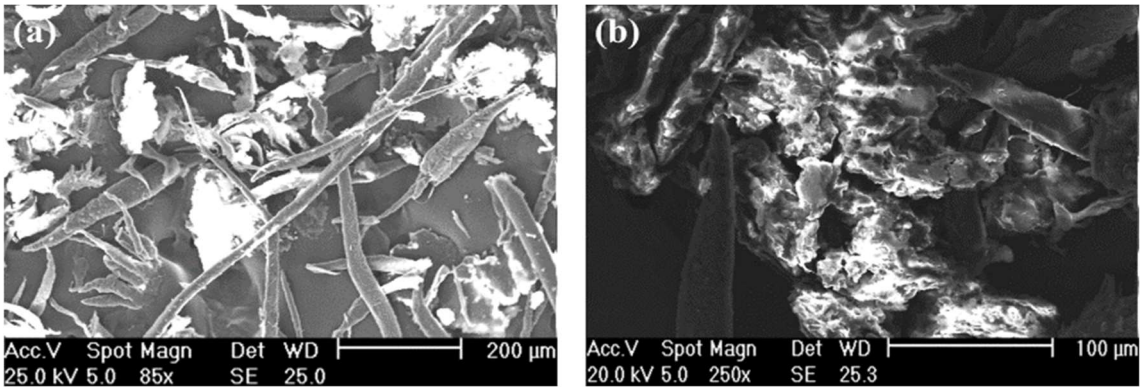

Figure 5.45 SEMs of debris collected from the test of machine cut nylon gear (6.5 Nm, 1000 RPM)

5.6 Summary

Gears made of different materials, using different manufacturing process, were tested in a dry-running condition and at different applied torques and speeds. Test rig I was used in all testing in this chapter. The aims were to understand the gear tooth wear phenomena at different running conditions and to further investigate the surface tribological behaviour of those gears.

The wear and wear rate of all tested conditions were defined, which confirmed close agreement with the step-loading tests. Further test validation was done by tooth thickness measurement using the image dimension measurement system. The after-test investigations revealed some indications for the failure modes of tooth surface for different polymer gears.

In machine cut acetal gears, abrasive wear was most common on the rubbing tooth surfaces, especially at the driving gear. Some adhesive wear was observed on the driven gear tooth surface. In injection moulded nylon gears, adhesive wear was more active than with the acetal gears. Uniquely, some chip debris was found in this type of gear.

The effect of running speed change was investigated. A positive relationship was found between the wear rate and the gear running speed.

A similar relation was found with respect to load increase, except at some critical loads, when some surface material functions as an internal lubricant.

Further investigations were made into the critical loads that were found in the machine cut nylon gear in the step-loading test. Close agreement was found when running long tests at those loads. The after-test investigations revealed that the reason for the decrease in wear rate with the load increase was that the surface material was functioning as an internal lubricant.

Finally, a long run test was carried out to investigate the endurance of the machine cut nylon gear in continuous long running. It was found that the wear rate of the gear teeth was further increased after a certain number of cycles, correlating with the increase in gear surface temperature. The after-test investigations revealed larger amounts of surface microcracks because of the long-time effect of the Hertzian pressure.

Chapter 6
POLYMER GEARS AND OIL LUBRICATION

6.1 Introduction

After investigating machine cut nylon gears in dry running conditions at both mechanical and tribological levels, and as previously illustrated in Chapter 2 that the effect of oil lubrication on nylon gears performance is still under investigation, it is beneficial to study the effect of lubricants on the performance of these gears. This chapter illustrates and discusses the results from machine cut nylon gear tests in an oil lubrication medium. The surface temperature was measured during tests and results are shown and discussed. Further post-test investigations using different methods are provided.

All tests in this chapter used polymer gear test rig II (discussed in section 3.3), which was designed for oil lubrication test purposes.

Starting with the step-loading test, nylon gears wear behaviour was defined and maximum working loads were found. This was followed by a number of long-run tests for further investigations.

6.2 Load capacity and wear behaviour of nylon gears in oil lubrication

It was previously demonstrated that polymer gear step-load testing is a useful way to define the load capacity of specific materials. It saves time

and cost by reducing the number of tests and samples required (to save the high costs of precision gears). In addition, this method provides an initial understanding of wear and wear rate behaviour of this gear. Although, it is ideal to test a gear pair at each load for full running time to record gear wear, this testing method provides initial understanding of wear phenomena and helps in the design of rigorous gear tests. Step-loading test is done by running a gear pair at a certain speed and under a specified load for a period of time (half an hour here), and then by increasing the load by a certain amount (0.5 Nm in the current test) for the next running period. Wear rate (per cycle) can be defined at each load by calculating the slope of the trending line of the wear curve of that load.

Step-loading test was done for a pair of machine cut nylon gears in oil lubrication. Because of the large number of loading steps in this test, the results are spread to four charts (from Figure 6.1 to Figure 6.4) for more clarity.

Figure 6.1 shows the wear result of the machine cut nylon gear running at the speed of 1000 RPM, in oil lubricant medium and under step-loads from 7 Nm to 11.5 Nm. Figure 6.2 shows the wear result for the same pair of gears, but under applied loads from 12 Nm to 16.5 Nm. Similarly, Figure 6.3 provides the wear results for the pair at the step-loading period between 17 Nm and 21.5 Nm. And Figure 6.4 shows the wear results for the nylon gears for loads from 22 Nm to 29 Nm. The step-load was 0.5 Nm for the loads between 7 Nm and 23 Nm. Because of the long time and close wear phenomena between steps, this step-load was increased to 1 Nm for the loads from 23 N to 29 Nm. Sudden jumps in wear reading between steps can be seen at all wear graphs. This is claimed to be because of the increase in torque at each step, which leads to an immediate increase in tooth deflection. This amount of deflection can not be separated from wear reading using the current testing method and devices, though this limitation does not affect the calculation of gear tooth wear rate at the final end of each step.

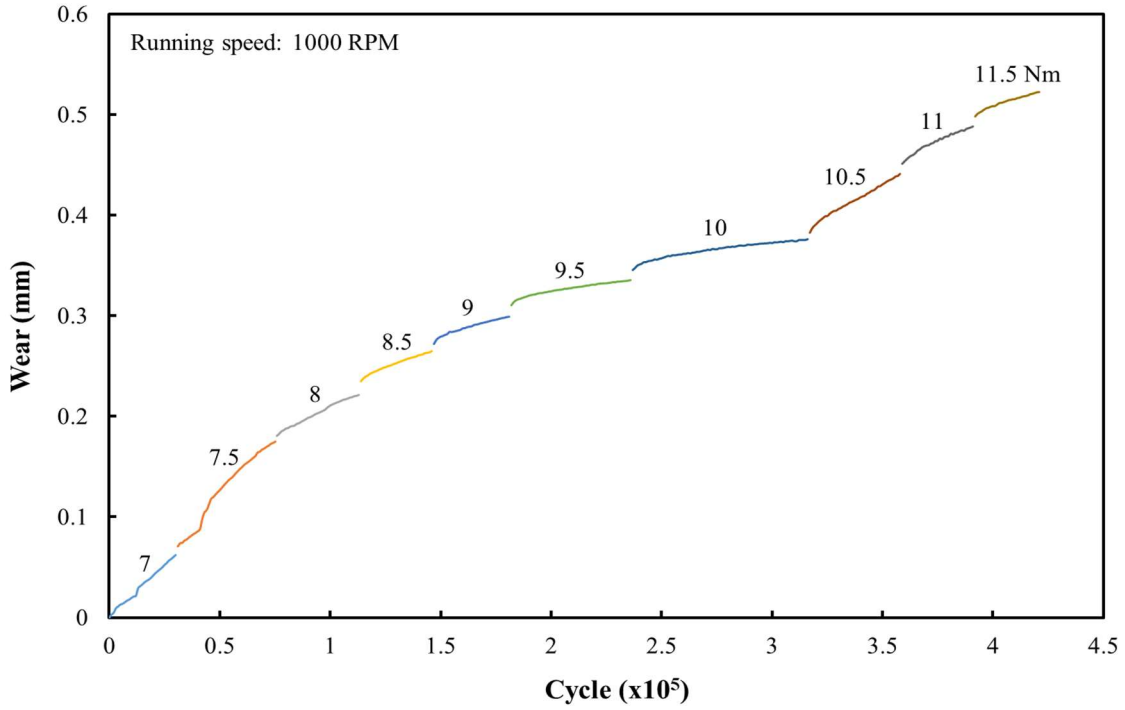

Figure 6.1 Wear of machine cut nylon gear running at the speed of 1000 RPM, in oil lubrication medium and step-loading condition (part 1 of 4: from 7 Nm to 11.5 Nm)

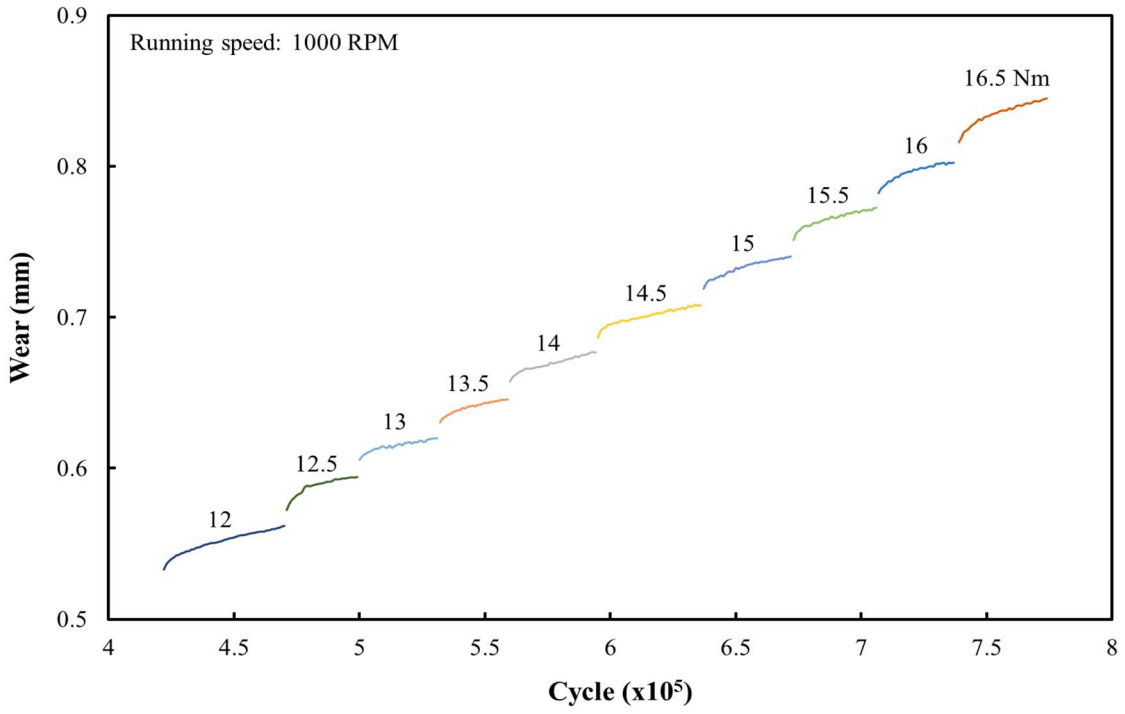

Figure 6.2 Wear of machine cut nylon gear running at the speed of 1000 RPM, in oil lubrication medium and step-loading condition (part 2 of 4: from 12 Nm to 16.5 Nm)

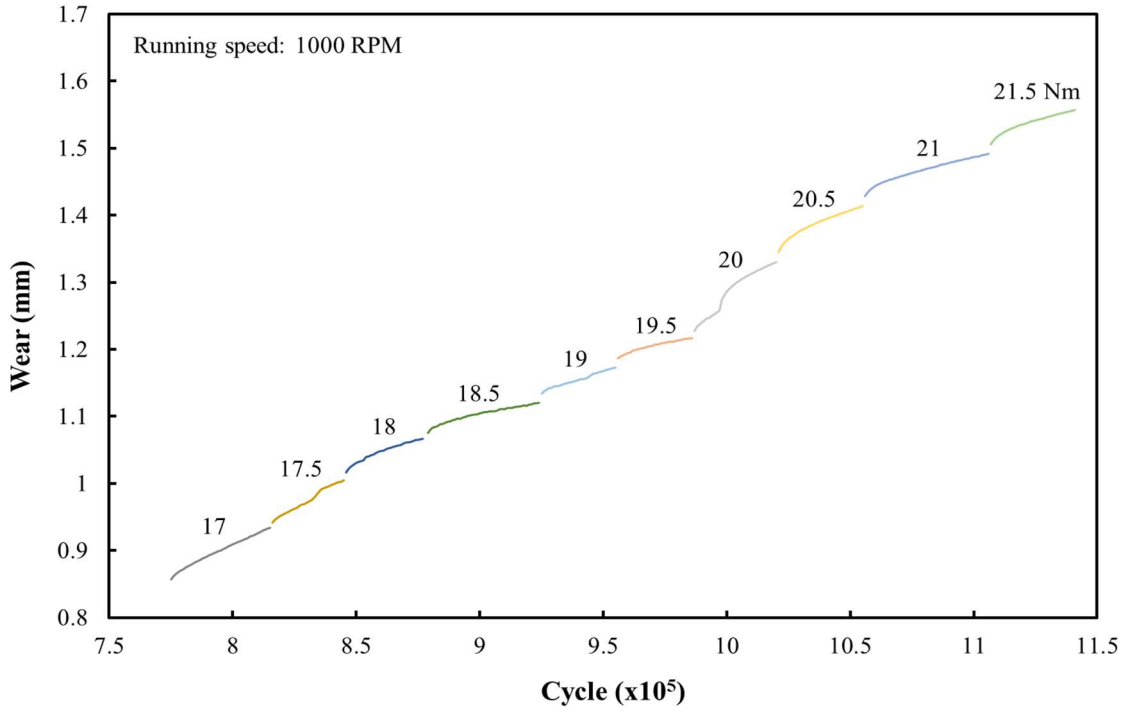

Figure 6.3 Wear of machine cut nylon gear running at the speed of 1000 RPM, in oil lubrication medium and step-loading condition (part 3 of 4: from 17 Nm to 21.5 Nm)

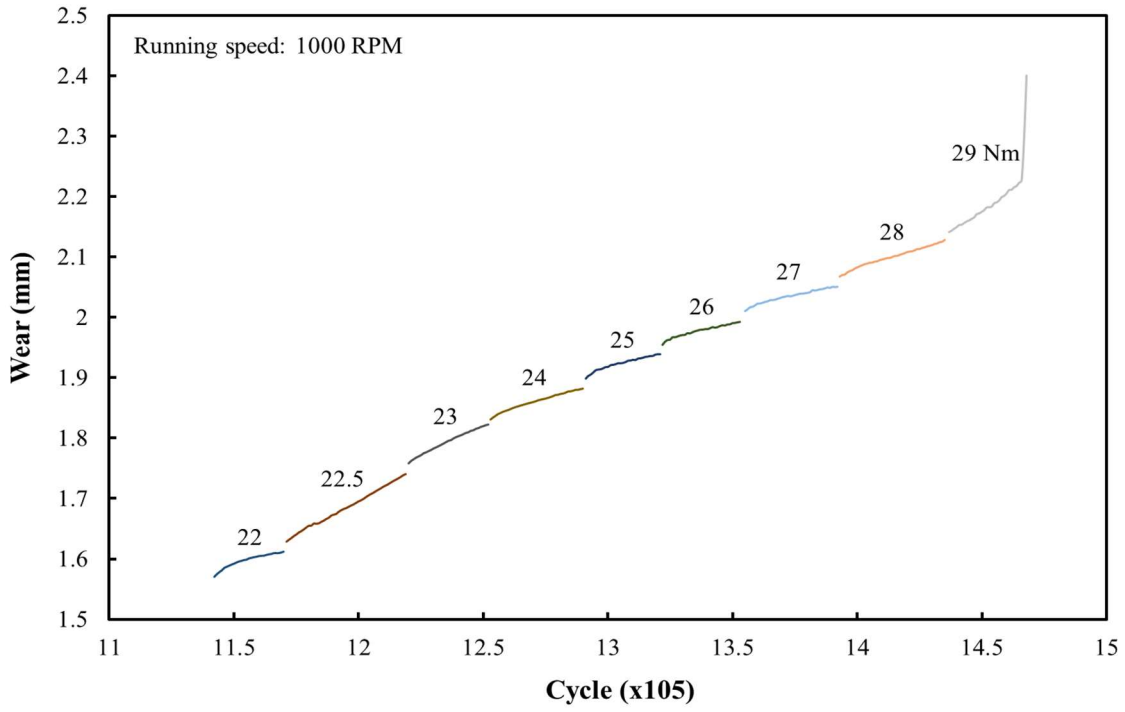

Figure 6.4 Wear of machine cut nylon gear running at the speed of 1000 RPM, in oil lubrication medium and step-loading condition (part 4 of 4: from 22 Nm to 29 Nm)

It can be seen that the wear rate was relatively high at the early steps (from 7 Nm to 8.5 Nm). This indicates that the running-in period of nylon gear in the lubricant takes a longer time than the dry running condition. The expected nearly-linear wear behaviour started to establish itself from the step-load of 9 Nm, where wear rate can be calculated more precisely.

The high increase in the curve at the final load of 29 Nm indicates the gear teeth fracture. In this test some the driving gear teeth were fractured at the root point leading to the drop of the loading arm and the automatic stop of the test rig (by touching the cut-off switch). Therefore, the maximum load capacity of this gear, in oil lubrication, is defined to be at this highest step-load of 29 Nm. This rapid estimation of a nominal load capacity is likely to be acceptable for initial evaluation but, therefore, should be subject to larger-scale validation. Hence more test, designed in accordance to the scoping trials of these results, were done and results are illustrated and discussed at the following two sections (6.3 and 6.4).

For each load, the wear rate was calculated as a function of number of cycles by defining the slope of the straight trend line for the last one-third sequence of wear data (last ten minutes of each step). In all steps, the trend line was a high quality fit, with the lowest squared correlation coefficient (R^2) above 96%. Figure 6.5 shows the wear rate of the machine cut nylon gear for the step-loading test in oil lubricant and at the speed of 1000 RPM. The wear rate axis is plotted in log format with the base of ten; this is because of the high variation in values between the dry running test results and the oil lubrication test results, although the oil lubrication test itself did not show high variation in wear rate, with values mostly between 1.5×10^{-6} mm/cycle and 2×10^{-7} mm/cycle.

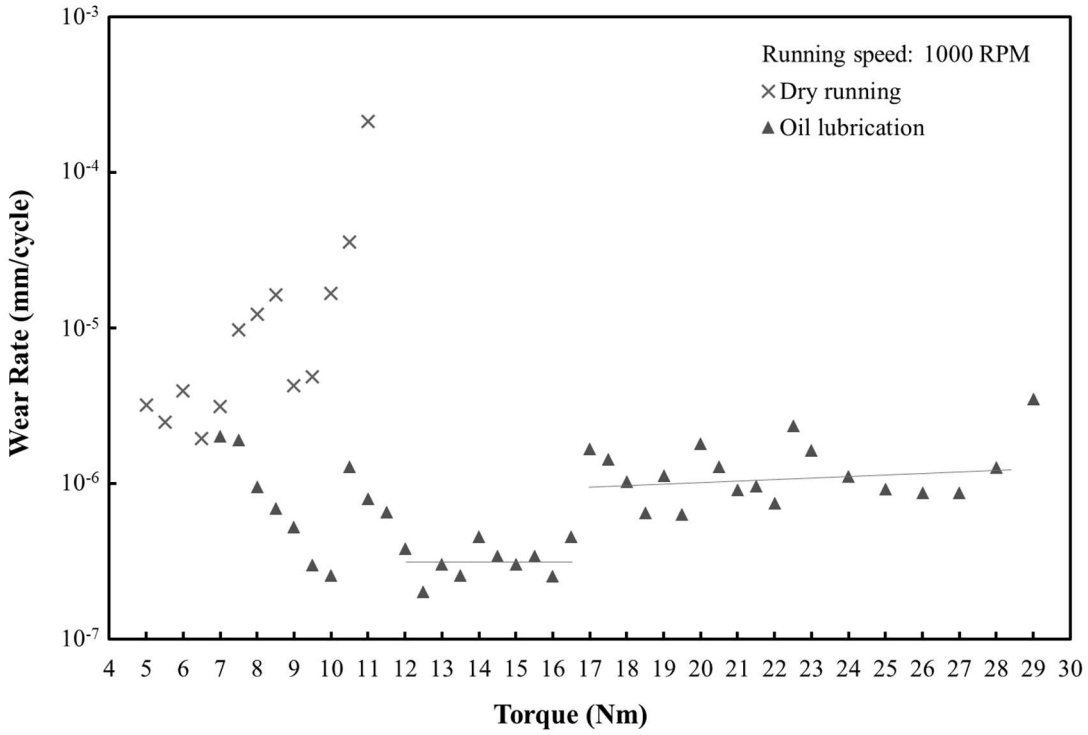

Figure 6.5 Wear rate of the machine cut nylon gear for the step-loading test in oil lubricant and at the speed of 1000 RPM (with typical regional trend lines shown for illustration)

Machine cut nylon gears showed different wear rate trends compared to the dry-running step-loading test for the same gears. Starting at a relatively high wear rate of 2.01 x 10^{-6} mm/cycle at the load of 7 Nm, the wear rate with oil lubrication showed continuous decrease with torque increase up to the load of 10 Nm, where the wear rate reached the value of 2.5 x 10^{-7} mm/cycle. One of the reasons of this high wear rate values was thought to be the long period of running-in stage in nylon gears with oil lubricant. The wear rate then suddenly jumped to the value of 1.27 x 10^{-6} mm/cycles at the torque of 10.5 Nm. This was followed by a second decreasing trend up to the load of 12.5 Nm, where the wear rate reached the lowest value of 2.02 x 10^{-7} mm/cycle. The wear rate was then fluctuating around this range with the torque increase up until the load of 17 Nm, where the wear rate dramatically increased to the value of 1.67 x 10^{-6} mm/cycle. The wear rate was then decreasing, for the third time, to the value of 6.45 x 10^{-7} mm/cycle at 18.5 Nm. The wear rate trend then

entered a region of larger fluctuations, with apparently systematic increases and decreases, until reaching the larger value of 1.79 x 10^{-6} mm/cycle at 20 Nm. The wear rate was then showed a fourth generally decreasing trend to the value of 7.46 x 10^{-7} mm/cycle at 22 Nm, before it was again dramatically increased to the wear rate of 2.36 x 10^{-6} mm/cycle at 22.5 Nm. This was followed by a fifth decreasing trend with the torque increase up until 27 Nm, where the wear rate reached 8.68 x 10^{-7} mm/cycle. Nylon gear wear rate then dramatically increased again, reaching the value of 3.48 x 10^{-6} at the load of 29 Nm, where the driving gear teeth were fractured at the root side of each gear. In general, there were two groups of wear rate that could be classified as relatively low wear rate and relatively high wear rate. The first lies between the torques of 12 Nm to 16.5 Nm, while the second could be between the torques of 17 Nm to 29 Nm. For more investigations, the first group of loads was called low load range and the second as high load range, which will be more investigated and illustrated in the next two sections (6.3 and 6.4).

Largely ignoring the highest war rate at the fracture point, the second highest wear rate was at the load of 22.5 Nm and was about 2.3 x 10^{-6} mm/cycle. This can be compared with the lowest wear rate of the machine cut nylon gears in the dry-running condition, which was at the load of 6.5 Nm and was 1.9 x 10^{-6} mm/cycle. This shows the large reduction in wear rate that occurred when using the oil lubricant.

Oil lubricant changed the wear rate phenomena of the machine cut gears in two ways. Firstly, wear rate dramatically decreased in nylon gears with oil lubricant, compared with the nylon gears in dry-running condition at the same amount of torque. Secondly, wear rate remained relatively low throughout the whole load increase sequence compared to the high increase in wear rate at the high loads range for the dry running test.

6.3 Tribology and wear behaviour at low load range

A number of tests were then carried out to further understand gear tooth wear behaviour and to examine tribologically the tested gear teeth using the different investigation methods discussed in Chapter 3.

Figure 6.6 shows the wear trend of machine cut nylon gears running at the speed of 1000 RPM in oil lubrication medium and under different applied loads of 10.5 Nm, 12.5 Nm and 16 Nm. It can be seen that all the wear trends for the three tests showed generally similar behaviour, with two types of wear, namely running-in and nearly-linear wear trend. All tests were stopped during the nearly-linear period in order to have the gear teeth in the running condition for further investigations. It is clear from the graph that the running-in periods for all three tests were relatively longer compared to the dry running tests. The nearly-linear stage for all tests was smooth with relatively small fluctuations, and therefore provided nearly constant wear rate across the period.

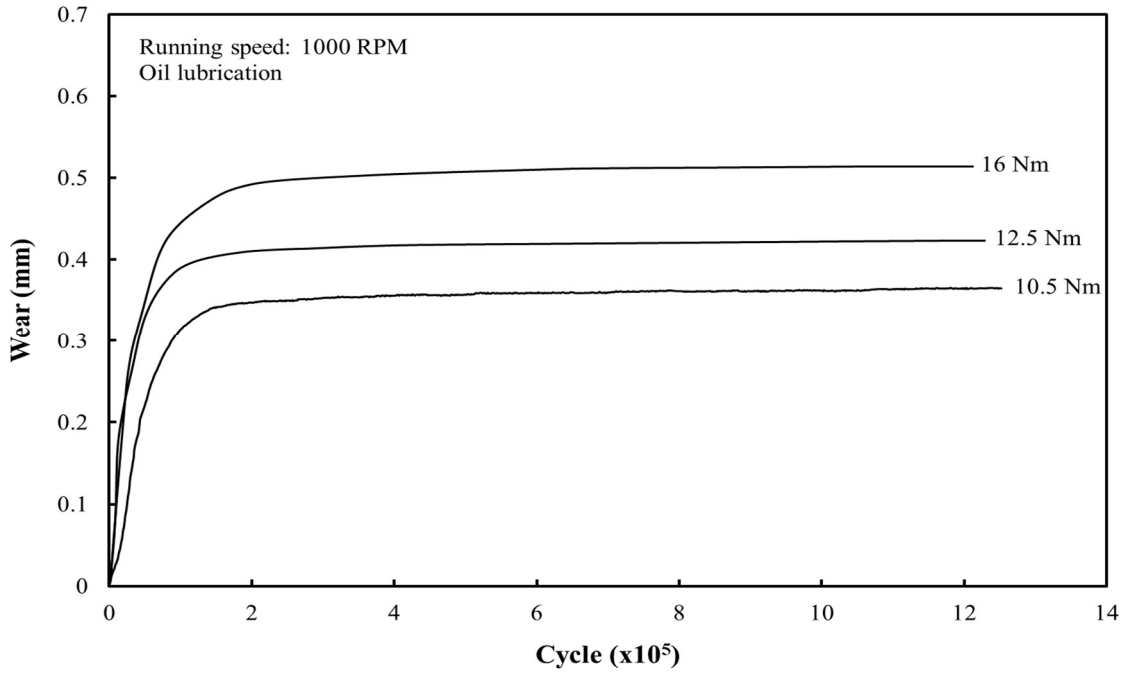

Figure 6.6 Wear of machine cut nylon gears in oil lubrication medium, at the speed of 1000 RPM, and under different applied loads

Table 6.1 shows the defined wear rate of the machined cut nylon gear pair running at the speed of 1000 RPM in oil lubrication and loaded by different torques (tests in Figure 6.6). It can be seen that wear rate showed no nearly difference (to the defined accuracy) between the two tests with the value of 0.8×10^{-8} mm/cycle for both loads of 10.5 Nm and 12.5 Nm, while 16 Nm test showed some increase in wear rate, with a value of 1.1×10^{-8} mm/cycle. This very low wear rate may indicate the occurrence of the EHL phenomenon, where a layer of oil is formed between the two surfaces that prevents their contact. Investigations included measuring the gear the gear tooth surface maximum temperature to better understand this wear rate change phenomena.

Table 6.1 Wear rate of machine cut nylon gear pair running at 1000 RPM in an oil lubricant for the low range loads

Torque (Nm)	Wear rate (mm/cycle)
10.5	0.8×10^{-8}
12.5	0.8×10^{-8}
16	1.1×10^{-8}

Figure 6.7 shows the tooth flank maximum temperature for the machine cut nylon gears that was running at the speed of 1000 RPM and under the applied torque of 10.5 Nm. The test was in oil lubrication medium. Temperature readings were fluctuating by about 10°C for the reason of the gear movement. The surface temperature rose from 31°C at the start of the test to 90°C after around 10^5 cycles. This increase in temperature fits in the running-in wear period in Figure 6.6. The temperature was then increasing more slowly until reaching 98°C at 5×10^5 cycle, when it stabilized for the next 4×10^5 cycles. The values then showed a slightly increase during the rest of the running cycles for about 6°C, where the highest temperature of 104°C was recorded. Throughout the nearly-linear stage, driven gear showed higher temperature readings than the driving

gears with a difference of up to 10°C. In general, it can be seen that the maximum surface temperature of the nylon gear in this test did not reached the glass transition temperature (98°C, from Figure 4.15) in either the running-in wear stage or the first half of the nearly-linear wear stage, while the later half of that stage showed it rise slightly towards the glass transition point with a relatively higher amount of fluctuation. This small raise did not affect the wear behaviour and wear rate trend, because of the high variation of the surface temperature across the gear rotation. The maximum temperature here may occur instantaneously and mostly at the pitch line (as illustrated in the literature), but cool down very rapidly to a temperature below the critical point.

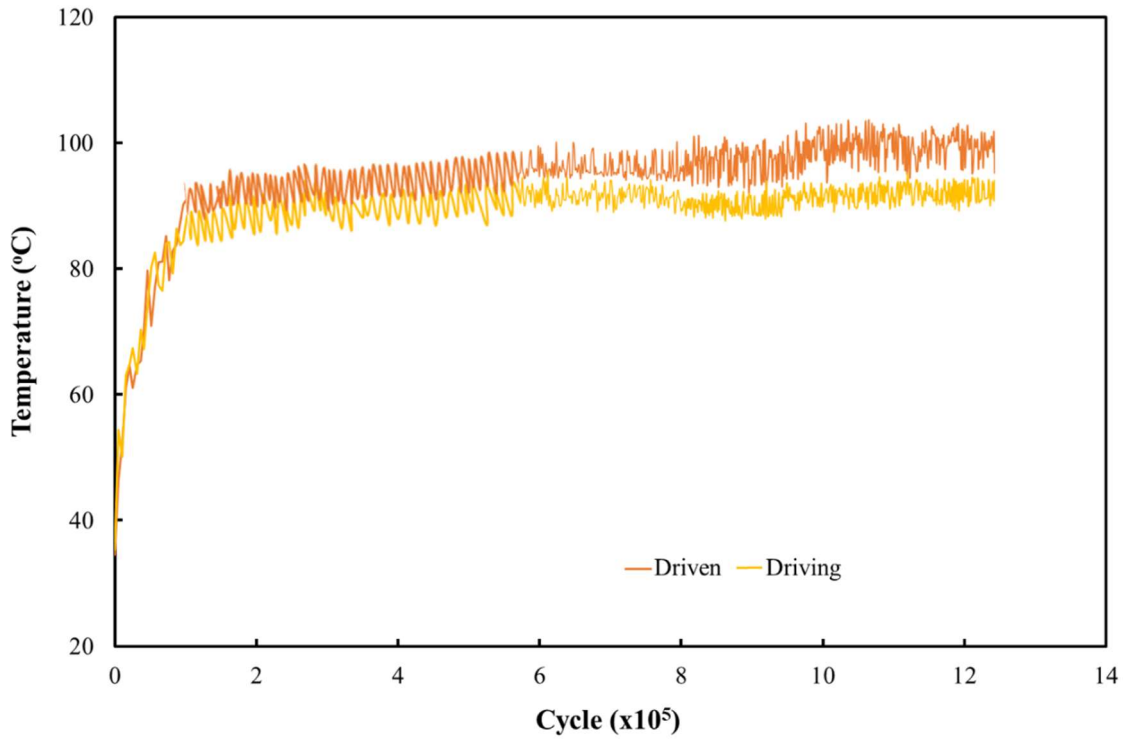

Figure 6.7 Maximum tooth surface temperature for machine cut nylon gears running at 1000 RPM, under the torque of 10.5 Nm and in oil lubricant medium

In this oil lubrication test, the driving gear showed a lower maximum temperature than the driving gear. This result is in close agreement with the dry-running tests, but with the difference between the driving and the driven surface temperature slightly higher in this oil lubrication test. This is because the polymer gears were dipped into the oil for about 7 mm and re-lubricated each cycle straight after coming out of the mesh (Figure 3.15).

Figure 6.8 shows the maximum surface temperature for the machine cut nylon gear teeth. Gears were running in an oil lubricant medium, at the speed of 1000 RPM and under the torque of 12.5 Nm. Surface temperature phenomena showed initial increase at the early running-in wear stage from the start of the test up to 2 x 10^5 cycles, where it reached the maximum temperature of 97°C on the driven gear. It then experienced a slight increase for the next 1.5 x 10^5 cycles, until reaching the value of 100°C on the same gear. This was followed by a stable maximum temperature all across the followed running time. The maximum surface temperature showed small fluctuations throughout the test with the highest of around 8°C. It can be seen that the maximum temperature value did not reach the glass transition point of the tested material, except instantly, which helped in maintaining the level of wear rate at the nearly-linear wear stage.

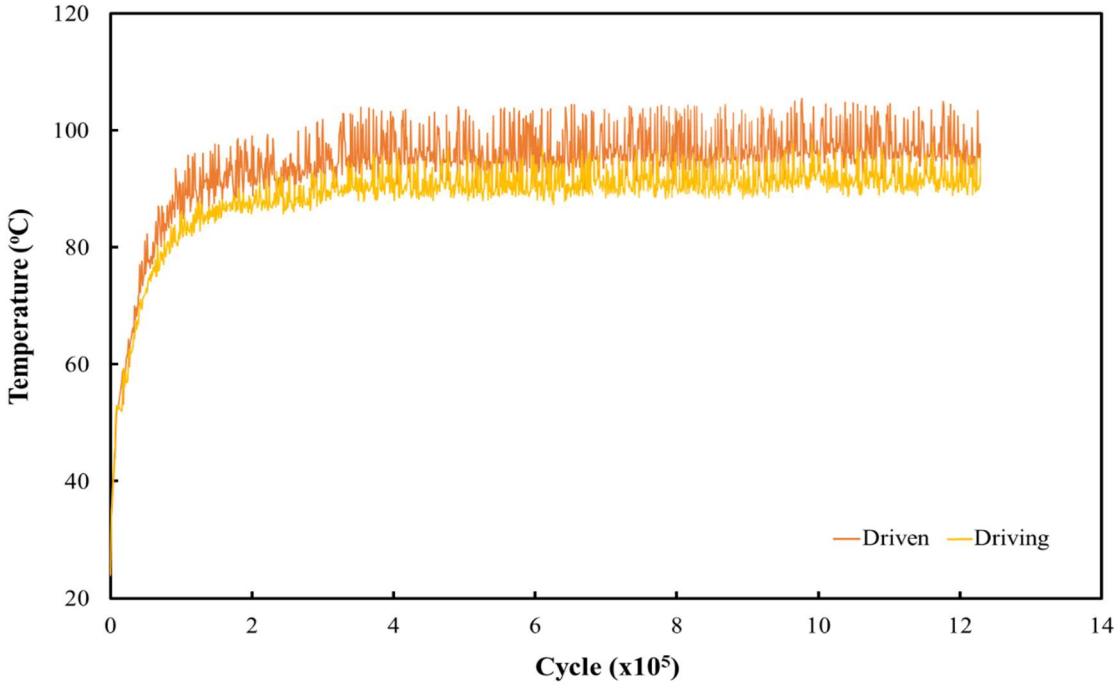

Figure 6.8 Maximum tooth surface temperature for machine cut nylon gears running at 1000 RPM, under the torque of 12.5 Nm and in oil lubricant medium

Figure 6.9 shows the maximum surface temperature for machine cut nylon gear teeth. The gear pair was running at the speed of 1000 RPM, loaded at 16 Nm torque and lubricated using oil lubrication. Tooth surface maximum temperature behaviour showed a high increase at the early running stage of the test between 0 and 1.7 x 10^5 cycles, where the values increased from 35°C to nearly 110°C. This rapid increase was followed by nearly stabilized values throughout the remaining running time. The data showed relatively small temperature fluctuation all across the test of around 10°C, because of the continuously moving objects. Gear surface temperature showed relatively higher values in this test as the load increased, reaching higher than the glass transition point of the tested material. This may reveals one of the reasons for the increase in wear rate and gear teeth deflection during this test (Figure 6.6 and Table 6.1).

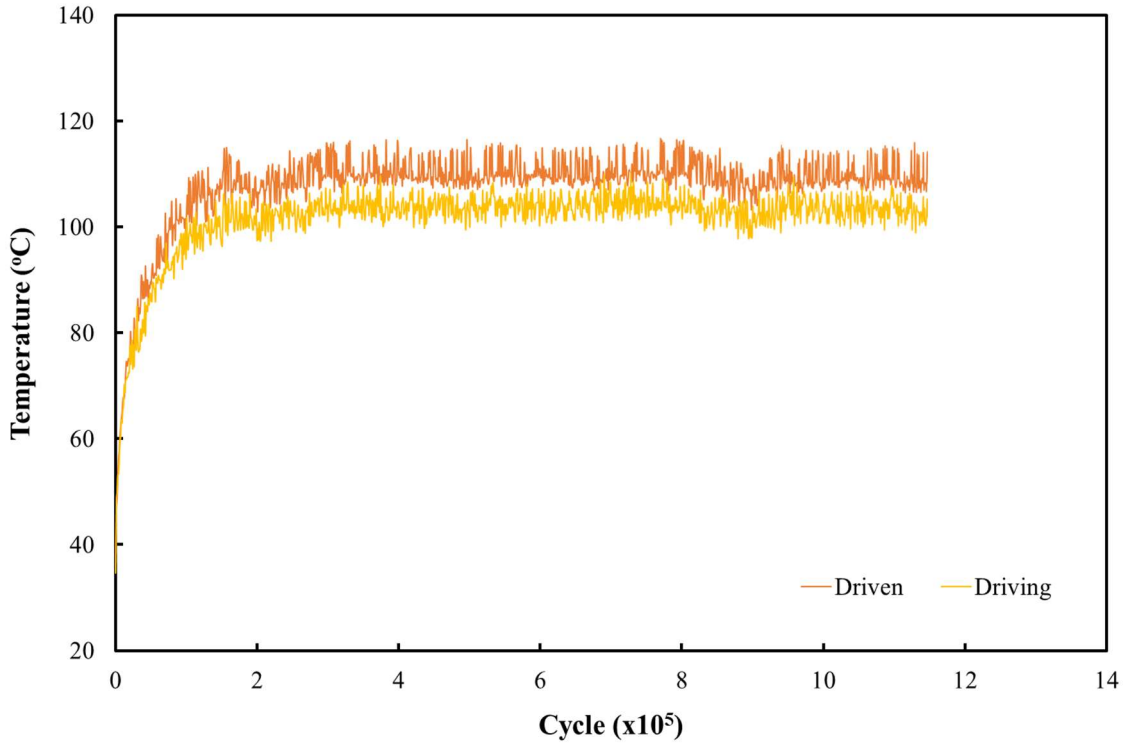

Figure 6.9 Maximum tooth surface temperature for machine cut nylon gears running at 1000 RPM, under the torque of 16 Nm and in oil lubricant medium

Figure 6.10 to Figure 6.12 show general overview of the after-test gears. Further investigations were carried out for all the three gears tested. Figure 6.13 shows the SEM pictures for a tooth of the machine cut nylon driving gear that was tested at the speed of 1000 RPM, under the applied torque of 10.5 Nm and in an oil lubrication medium.

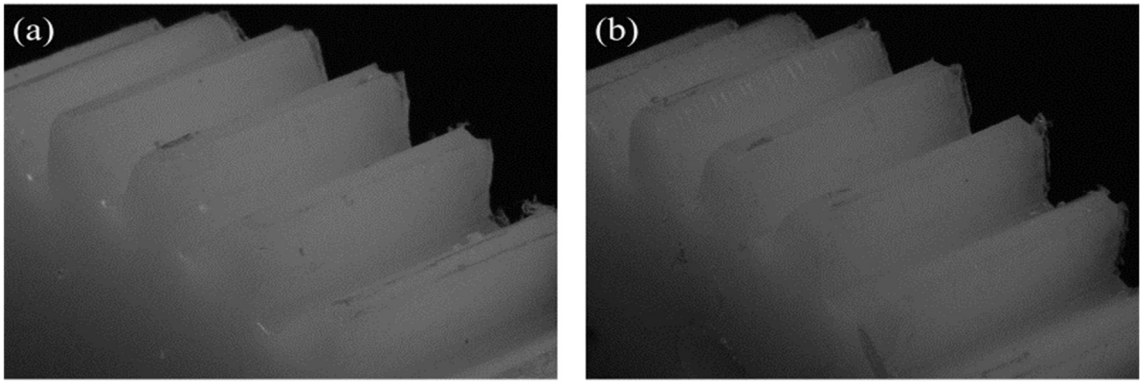

Figure 6.10 (a) The driving and (b) the driven machine cut nylon gear after testing at 1000 RPM, under 10.5 Nm torque and in oil lubrication

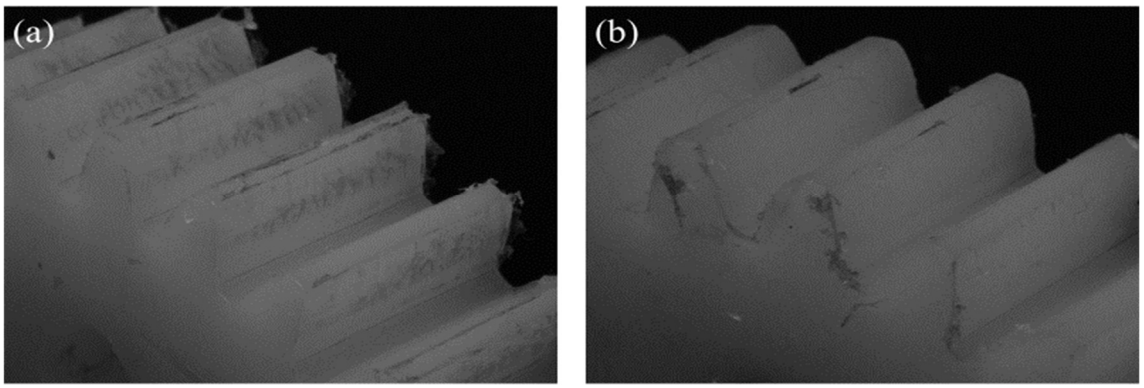

Figure 6.11 (a) The driving and (b) the driven machine cut nylon gear after testing at 1000 RPM, under 12.5 Nm torque and in oil lubrication

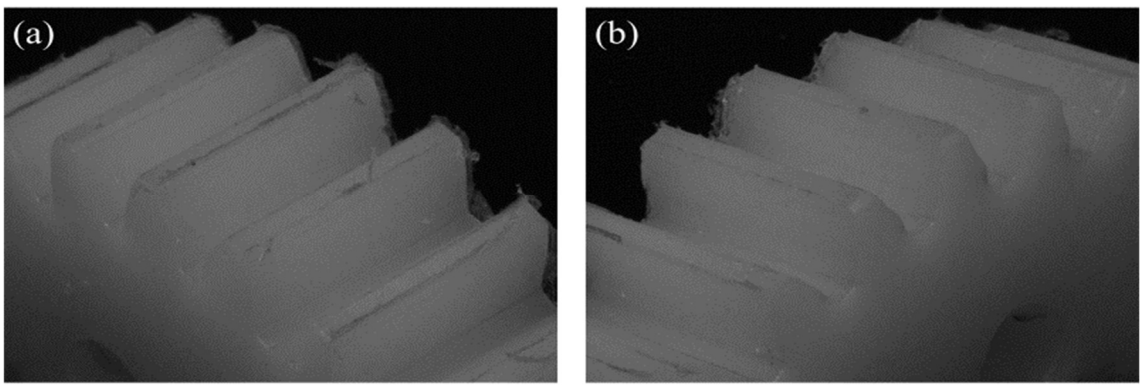

Figure 6.12 (a) The driving and (b) the driven machine cut nylon gear after testing at 1000 RPM, under 16 Nm torque and in oil lubrication

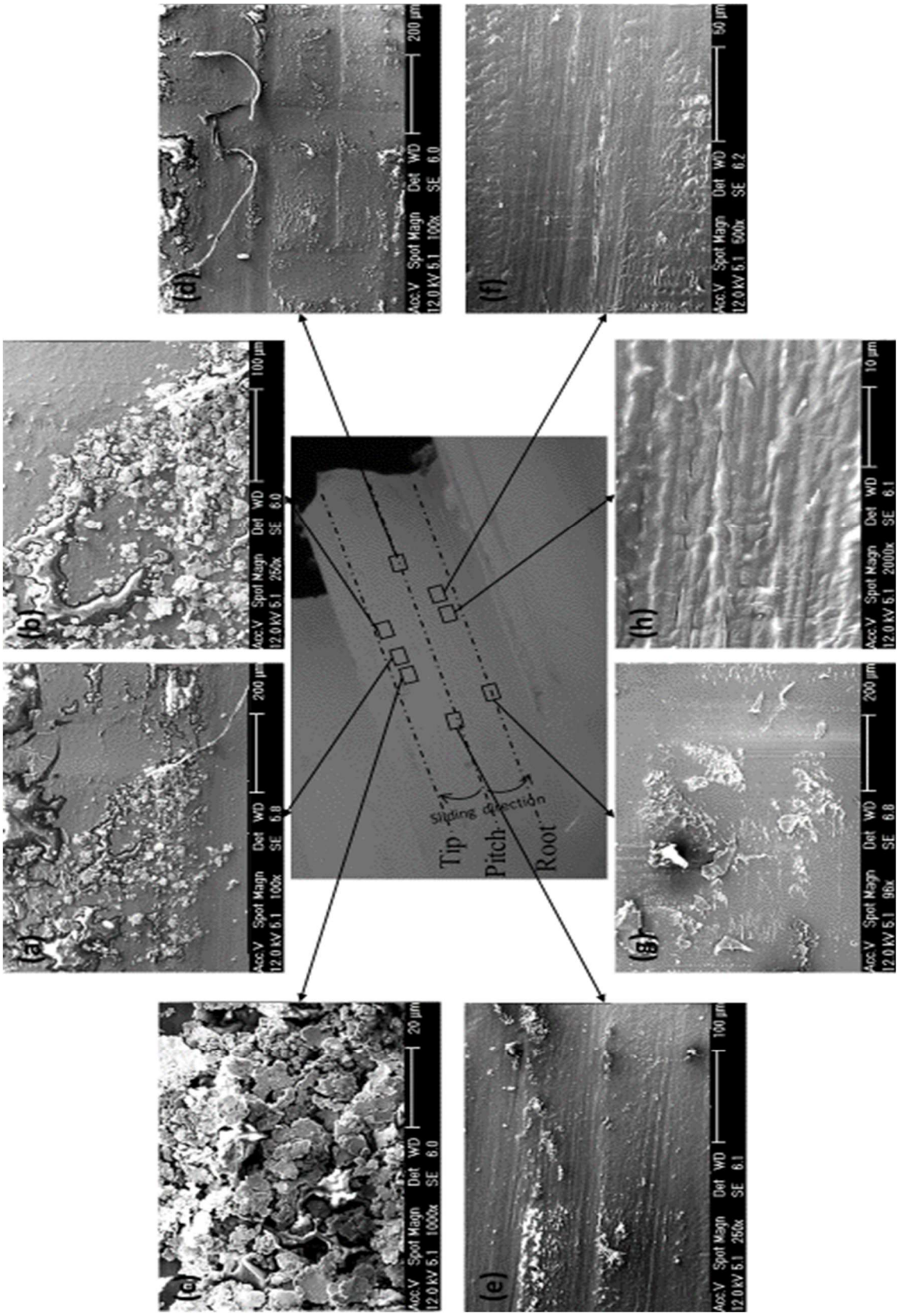

Figure 6.13 SEMs of machine cut nylon driving gear tooth (10.5 Nm, 1000 RPM and oil lubrication)

The SEM pictures of the driving gear focus on the three most important areas of the tooth surface flank, namely root to pitch, pitch line and pitch to tip. Figure 6.13 (a), (b) and (c) cover part of the pitch to tip area. They revealed that this area was the one most full of wear debris, especially towards the tip side, where the sliding direction ends. In contrast to the dry-running tests, debris here was not shaped in long-rounded fibres, but as very small pieces of chips, because of the oil lubrication effect, which prevents the rubbing of these small pieces between the two surfaces. Adhesive wear was found to be the most type of wear in this area.

Figure 6.13 (d) and (e) show the two SEM pictures that were taken at the pitch line of the driving gear. In this area, the tooth showed some long cross scratches aligning across edge-to-edge of the tooth surface. These are thought to be because of firstly the sliding direction, which starts from this point along two opposite directions and secondly the high pressure applied by the tip of the driven gear at the start of each mesh period.

Figure 6.13 (f), (g) and (h) reveal the surface for the area from root to pitch. It can be seen that this part of the tooth surface contained some surface microcracks all across the surface from edge-to-edge. This form of microcracks for nylon materials was discovered in other research, as discussed in Chapter 2. One of the reasons of this phenomena could be the high-stresses of the Hertzian pressure.

Figure 6.14 shows the SEM of the driven gear tooth for the machine cut nylon material, at the speed of 1000 RPM, 10.5 Nm torque and in oil lubrication. The SEM covers all three tooth surface regions.

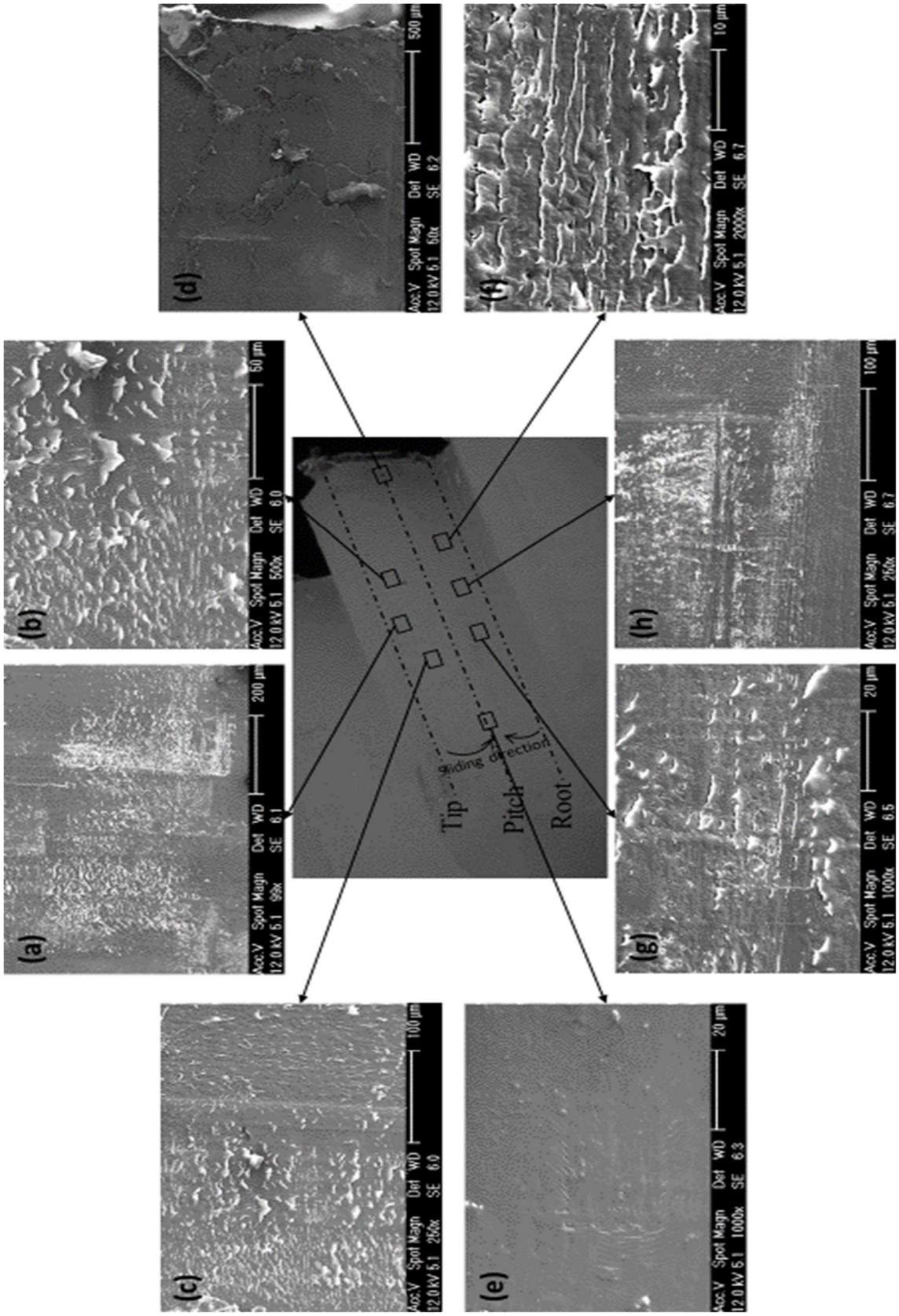

Figure 6.14 SEMs of machine cut nylon driven gear tooth (10.5 Nm, 1000 RPM and oil lubrication)

Figure 6.14 (a), (b) and (c) show SEMs of the pitch to tip area, where the sliding direction is from the tip to the pitch line of the tooth. Surface tribology revealed that the wear behaviour in this area follows a shape that could be imagined as frozen sea waves, where part of the material was reformed out of the surface and pushed over it (surface deformation). This type of damage is known as abrasive wear.

Figure 6.14 (d) and (e) show the two sides of the surface flank at around the pitch line. Because the sliding direction on the driven gear that leads to pushing the materials from root and tip towards the pitch line, in addition to the higher pressure at the pitch line (compared to the root and tip sides) and the surface temperature that was reaching the glass transition point, which makes the surface softer, the material was pressed and pushed to the two sides of the tooth. This process redistributed the nylon throughout the surface of the tooth, which is known as the surface plastic flow.

Figure 6.14 (f), (g) and (h) revealed that the area between the root and pitch line was showing some surface microcracks. These microcracks were again attributed to the occurrence of the high-stresses at this area from the Hertzian pressure. In addition, this region showed some abrasive wear that was similar to the pitch-to-tip wear behaviour, which could be attributed to the same reasons.

Figure 6.15 shows the SEM for a driving gear tooth of the machine cut nylon gear tested at the speed of 1000 RPM under 12.5 Nm torque in oil lubrication.

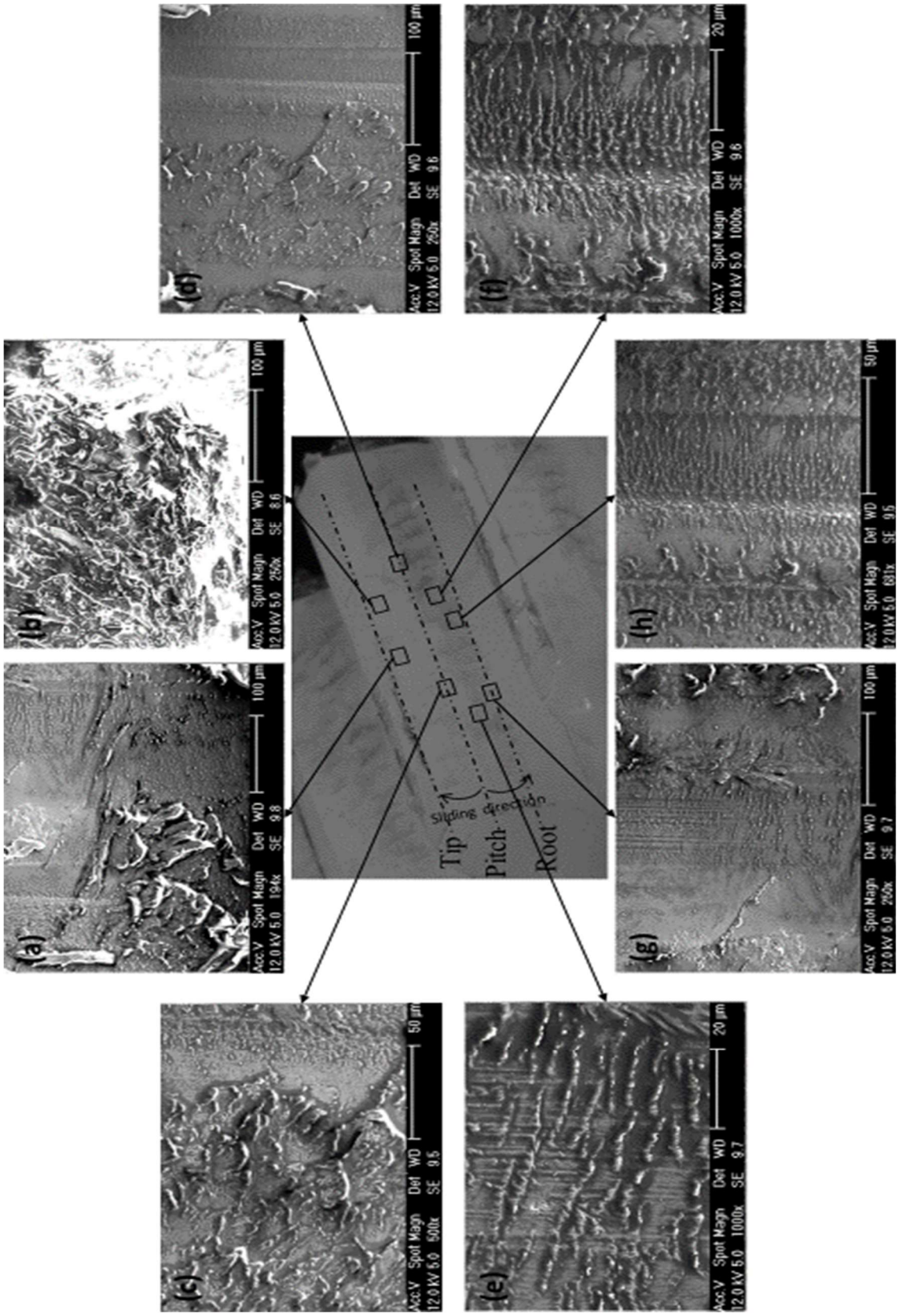

Figure 6.15 SEMs of machine cut nylon driving gear tooth (12.5 Nm, 1000 RPM and oil lubrication)

At the addendum side of the tooth (Figure 6.15 (a) and (b)), the surface showed some softened materials towards the tip edge. This might be dragged from around the pitch line area, where the temperature was expected to be the highest, especially with the effect of the flash temperature. In addition, some other parts showed an adhesive wear behaviour, where the material at the surface was pushed radially.

Moving toward the pitch line (Figure 6.15 (c) and (d)), more areas of adhesive wear can be seen, with more severe damage because of the relatively higher pressure at this area. The SEM revealed that this area of the driving gear tooth was one of the main sources of initial debris, which, when dragged towards the two opposite ends, could lead to more debris generation and, in consequence, more wear damages.

The dedendum side of the tooth (Figure 6.15 (e), (f), (g) and (h)) showed more evidence of adhesive wear. More debris can be seen in this area of the tooth because of the building-up along the contact area and the curved end that prevents the material from leaving the surface. In general, smaller amounts of microcracks were found in the dedendum side.

Figure 6.16 shows the SEM of the machine cut nylon driven gear tooth, which was tested at the speed of 1000 RPM, under the applied torque of 12.5 Nm and was running in an oil lubrication medium.

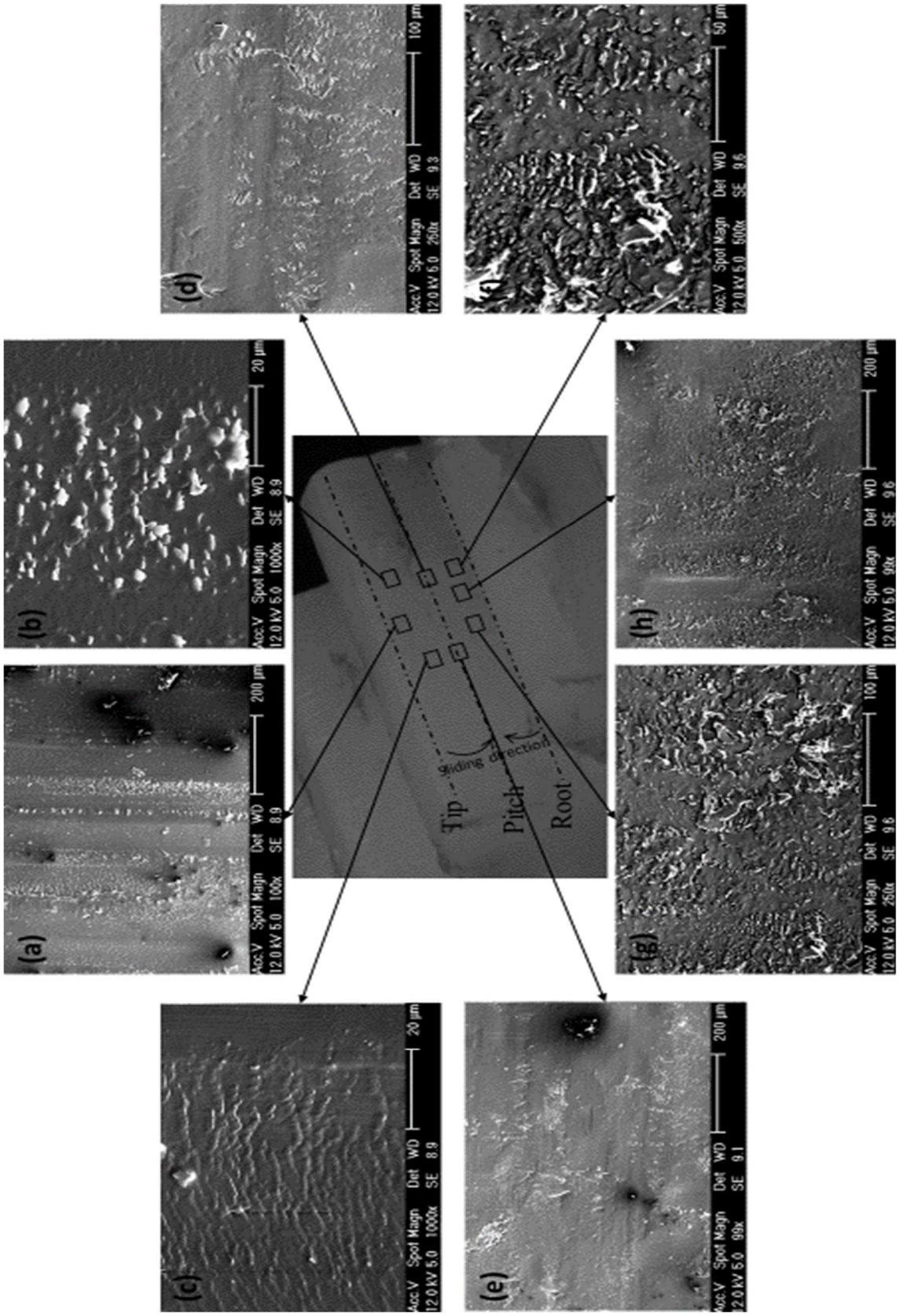

Figure 6.16 SEMs of machine cut nylon driven gear tooth (12.5 Nm, 1000 RPM and oil lubrication)

At the area of the tooth between the pitch line and the tip (Figure 6.16 (a), (b) and (c)), images showed the effect of the high pressure contact on the tip side of the tooth at the beginning of the gear mesh. With the effect of the high pressure, this side of the tooth was subjected to two types of wear, namely pitting and adhesive wear.

Around the pitch line (Figure 6.16 (d) and (e)), the tooth showed a formation of surface bulges as a result of the effect of the sliding direction. A small amount of debris was found in this area. There are some very small and shallow formations of microcracks, which could be the result of the high and sudden changes in the sliding direction at this particular area because of the low elasticity of the nylon material.

Moving towards the dedendum side of the tooth surface (Figure 6.16 (f), (g) and (h)), one can see the occurrence of adhesive wear all across the surface from the root to the pitch line. Some material was dragged radially and parallel to the surface before it was separated forming a debris with a flat shape. Opposite to the dry-running tests, the debris here did not rotate between the two surfaces to form long fibres. This is most likely because of the oil lubricant.

Figure 6.17 shows the SEM of the tooth surface of the final tested machine cut nylon driving gear from the low load range. The test was carried out at the speed of 1000 RPM, in an oil lubrication and under the applied torque of 16 Nm.

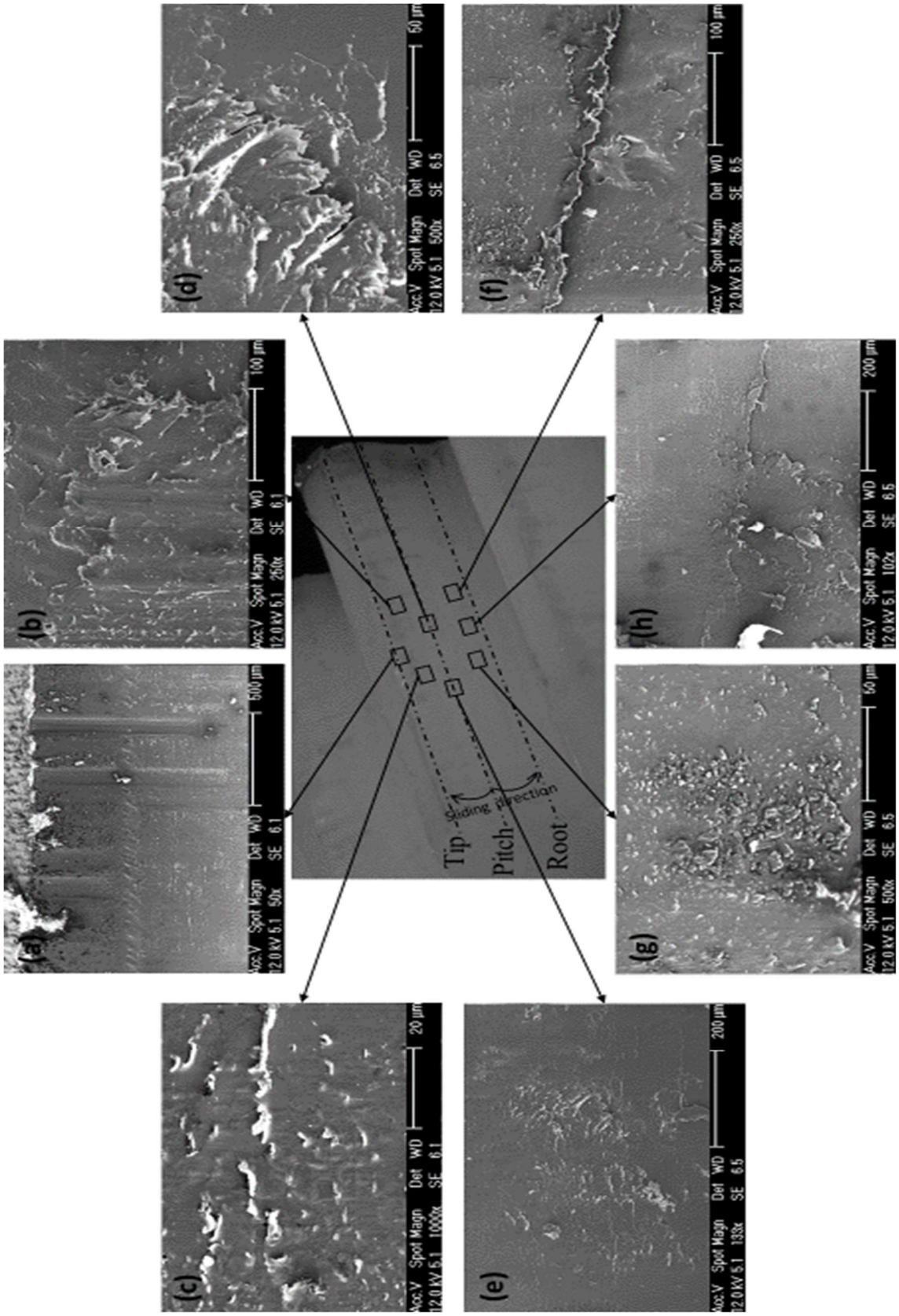

Figure 6.17 SEMs of machine cut nylon driving gear tooth (16 Nm, 1000 RPM and oil lubrication)

Figure 6.17 (a), (b) and (c) reveal the occurrence of abrasive wear at the addendum side of the driving gear, because of the increased load compared to the two previous tests. This abrasive wear is more prevalent towards the tip of the tooth. While moving toward the pitch line within the same area, adhesive wear could be seen in small amounts at few places. Some of the area includes both types of wear at the same time.

Investigating the pitch line area of the driving gear tooth, Figure 6.17 (d) and (e), revealed that a very limited number of microcracks could be found here. Also, the area was suffering from the rapid change in sliding direction as the surface showed multidirectional adhesive wear.

Figure 6.17 (f), (g) and (h) shows the surface tribology behaviour of the dedendum side of the tooth. Here, one large crack was found, but with no signs of any initial microcracks. This crack was not around the pitch line, where more microcrack could be expected to occur, suggesting it arose as a result of a thermal effect or as a result of tooth material expansion that led to jamming the tooth between two teeth of the driven gear. Some adhesive wear can be seen at the root side of the dedendum area, with some softened surfaces identified.

Figure 6.18 illustrates some tooth surface SEMs for the machine cut nylon driven gear that was tested at the speed of 1000 RPM, under the effect of 16 Nm applied torque and in an oil lubricant medium.

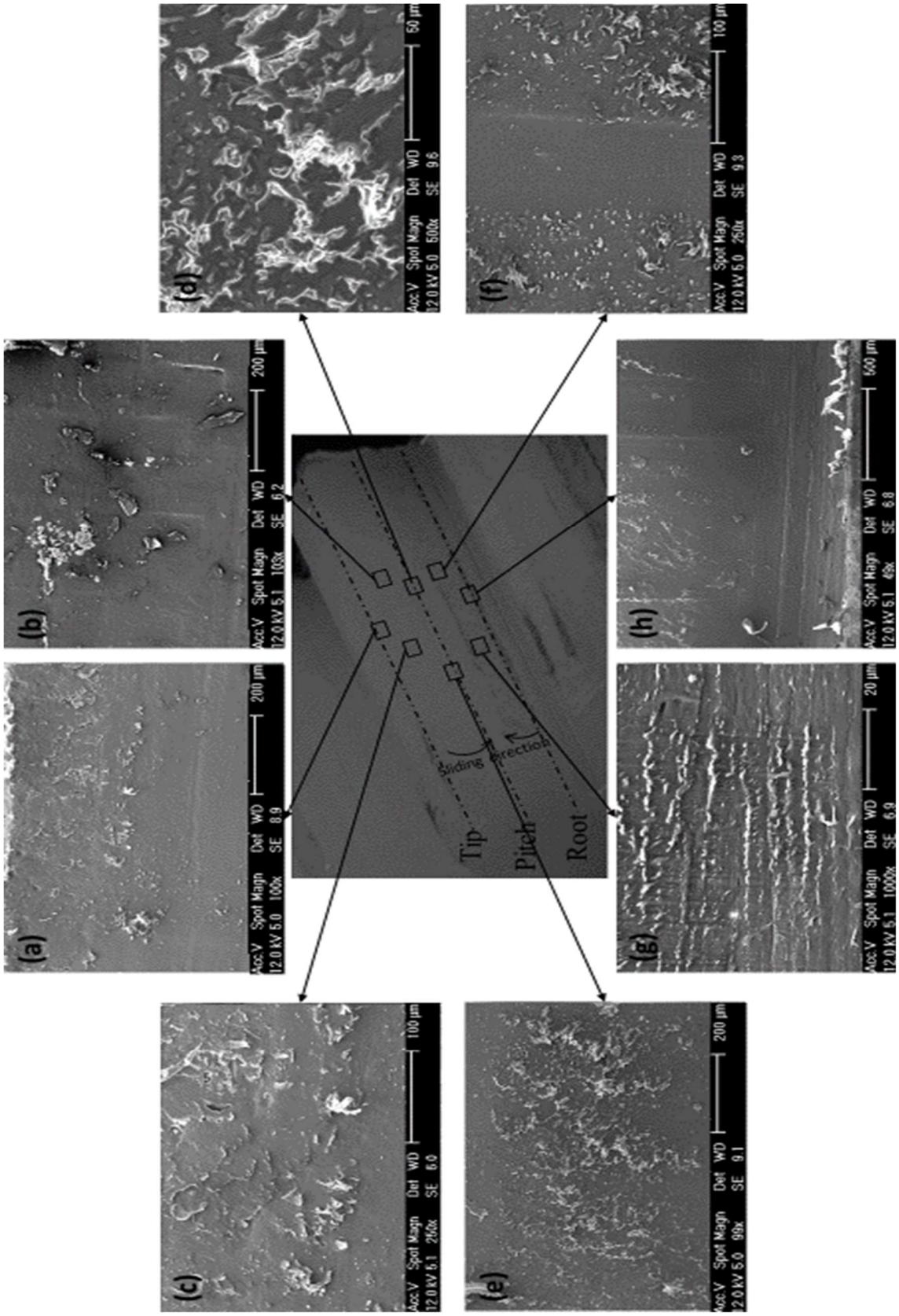

Figure 6.18 SEMs of machine cut nylon driven gear tooth (16 Nm, 1000 RPM and oil lubrication)

It can be seen that the addendum side of the driven gear (Figure 6.18 (a), (b) and (c)), show the high impact pressure on this side of the driven gear, as it enters the mesh. Some high abrasive wear was recognised in the area, with some surfaces being polished with clear scratching marks. Very little debris was found on this side of the tooth, but any seen was of molten clots. Pitting wear was also evident in some places.

Towards the pitch line, Figure 6.18 (d) and (e) reveal that large amount of debris gathered here as a result of the sliding direction. The debris was formed in both chip and fibre shapes. Debris was still relatively light, compared to the dry running tests, because of the oil lubricant effect.

Figure 6.18 (f), (g) and (h) show the SEMs of the dedendum side of the driven gear tooth. Both abrasive and adhesive wear can be classified as two of the surface damage behaviours for this side of the tooth. In addition, many surface microcracks were discovered at this area. One reason for this increase could be the increase in the surface contact pressure and the Hertzian pressure. Lastly, one large crack at the root of the tooth was found, which is explained by the anology high by loaded cantilever.

To conclude, when running the machine cut nylon gears, in an oil lubricant, at low load ranges, the wear behaviour of gear teeth was be mostly of the nearly-linear type. Wear rate was not highly affected by the increase in torque within these low load ranges. In all tests, although applying relatively higher torques, compared to the dry-running tests, gear teeth did not fracture or become completely damaged, even after relatively high numbers of cycles, again because of the use of oil lubrication.

One of the main factors to maintain long running of machine cut nylon gears could be the control of the maximum surface temperature at levels below the glass transition of this material. This could be guaranteed by the use of oil lubricant and so prevent the tooth surfaces from transferring to more severe wear and damage mechanisms.

The surface tribology of the tooth surface for both the driving and driven gears revealed that, for at machine cut nylon gears running in an oil lubricant at low load ranges, the most common types of damage were adhesive and abrasive wear. Other types of wear were discovered, like pitting, but in lesser amounts. In addition, surface microcracks were more common here, probably because of the high surface contact pressure and Hertzian pressure.

6.4 Tribology and wear behaviour at high load range

After investigating the effect of low loads on the wear rate of nylon gears in the oil lubrication, it is important to investigate the effect of high loads under the same conditions. Three wear tests were instigated to more deeply understand nylon gear wear behaviour.

Figure 6.19 shows the wear curves of the teeth of a pair of machine cut nylon gears running at the speed of 1000 RPM and in an oil lubrication medium. Each tested gear pair was loaded at a constant torque of 22.5 Nm, 26 Nm or 29 Nm. It can be seen that the wear trend of these three curves showed typically similar general behaviour, with the recognition of three different wear stages, namely: running-in wear, nearly-linear wear and very rapid wear and fracture stage.

Test durations were shorter than for the low loaded tests, so the onset of the final stage was not so predictable and therefore no tests were deliberately stopped during the nearly-linear stage to supply teeth for further investigations. However, after the tests were stopped automatically, some teeth were found in reasonably good shape for the SEM investigations. It can be seen from the curves that the running-in stages were shorter than in the low load tests, with the period decreasing as load increased. All curves showed acceptably smooth shapes with small

amounts of fluctuations, which is very helpful for the defining of gear tooth wear rates.

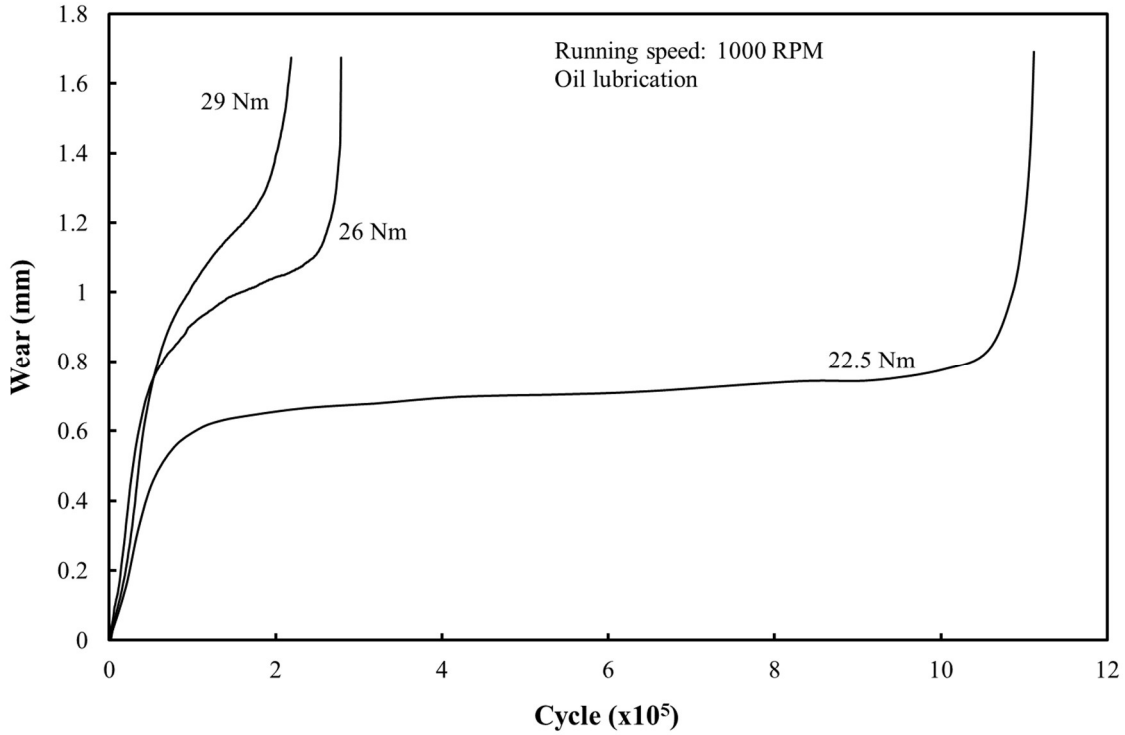

Figure 6.19 Wear of machined cut nylon gears in oil lubrication medium, at the speed of 1000 RPM, and under different applied loads

Table 6.2 illustrates the wear rates for the machine cut nylon gear tests in Figure 6.19. The wear rate was relatively low at the torque of 22.5 Nm (at the value of 1.2×10^{-7} mm/cycle) before it was increased nearly ten times, with a torque increase of 3.5 Nm, to the load of 26 Nm, when the value reached 1.2×10^{-6} mm/cycle. The wear rate was then doubled to 2.65×10^{-6} mm/cycle with a 3 Nm load increase to 29 Nm.

Table 6.2 Wear rate of machine cut nylon gear pair running at 1000 RPM in an oil lubricant for the high range loads

Torque (Nm)	Wear rate (mm/cycle)
22.5	1.2×10^{-7}
26	1.04×10^{-6}
29	2.65×10^{-6}

Figure 6.20 shows the tooth surface maximum temperature for both driving and driven machine cut nylon gears running at 1000 RPM, in oil lubricant medium and under the applied torque of 22.5 Nm. The maximum surface temperature dramatically increased during the running-in wear stage from around 27°C to around 110°C at the driven gear, during the period from 0 to 2×10^5 cycle. This was followed by a nearly stable temperature values of around 110°C at the driven gear, with some temperature fluctuation. Gear maximum surface temperature then dropped down dramatically after the fracture of the teeth and the stopping of the test rig, reaching the early running values in about 30 minutes.

During the test, the driven gear showed higher surface temperature than the driving gear with an average difference of 13°C. Maximum surface temperature measurements showed some reading fluctuation of around the average of 7°C, because of the continuously moving gears. All in all, the surface maximum temperature was fluctuating around the glass transition point and therefore this could be one of the reasons of the high gear teeth wear rate at this load. Gear teeth were fractured, before completely worn, at the root side of the teeth for both the driving and the driven gears.

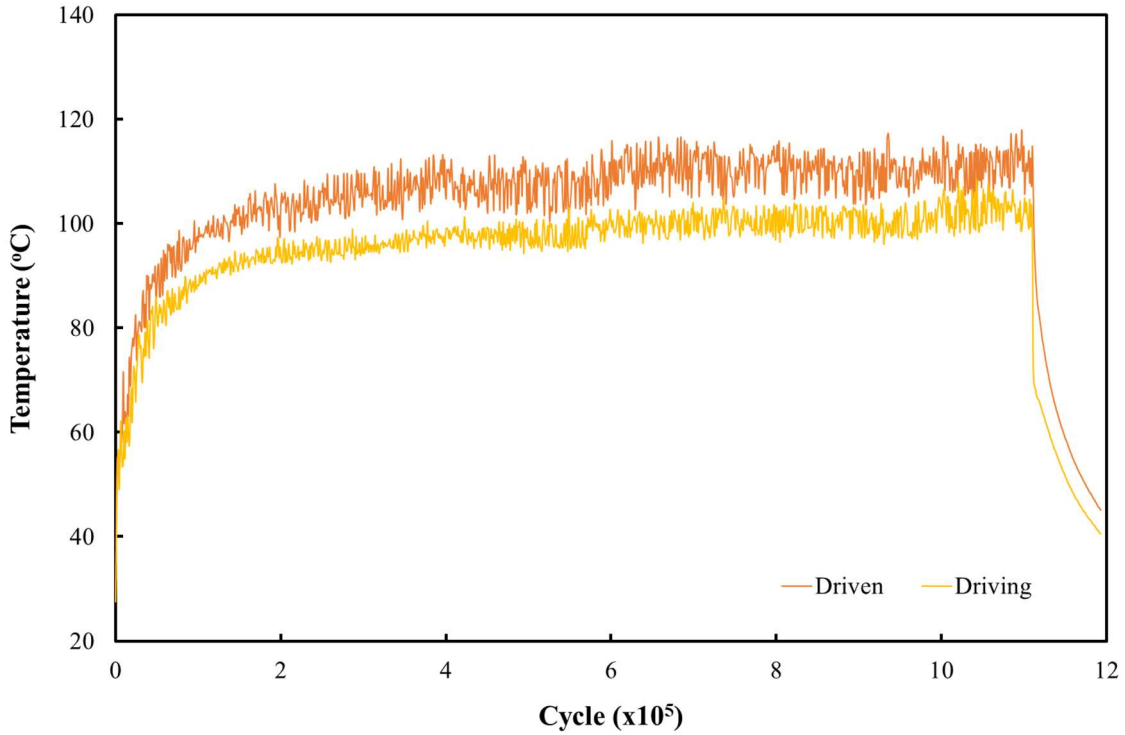

Figure 6.20 Maximum tooth surface temperature for machine cut nylon gears running at 1000 RPM, under the torque of 22.5 Nm and in oil lubricant medium

Figure 6.21 shows the gear teeth maximum surface temperature for both the driving and the driven of the machine cut nylon gear pair that was loaded by the torque of 26 Nm while running at 1000 RPM in an oil lubricant medium. It can be seen here that the maximum surface temperature is different to that in the low load tests, with three stages of increases. The first stage was the dramatic increase of maximum surface temperature during the running-in wear from 0 to 0.5 x 10^5 cycles, where the value reached 100°C. This was followed by the second small and steady increase of 30°C over the next 2 x 10^5 cycles. The third increase was also dramatically high, with the temperature reaching nearly 152°C at 2.8 x 10^5 cycles, where the gears were fractured, and the test rig was automatically stopped. Gear surface temperatures then cooled down, reaching the early running values in 30 minutes.

In this test, the gear surface maximum temperature reach values that exceeded the glass transition point in the second stage of increase, which may explain the increase in wear rate between this test and the 22.5 Nm test of nearly ten times.

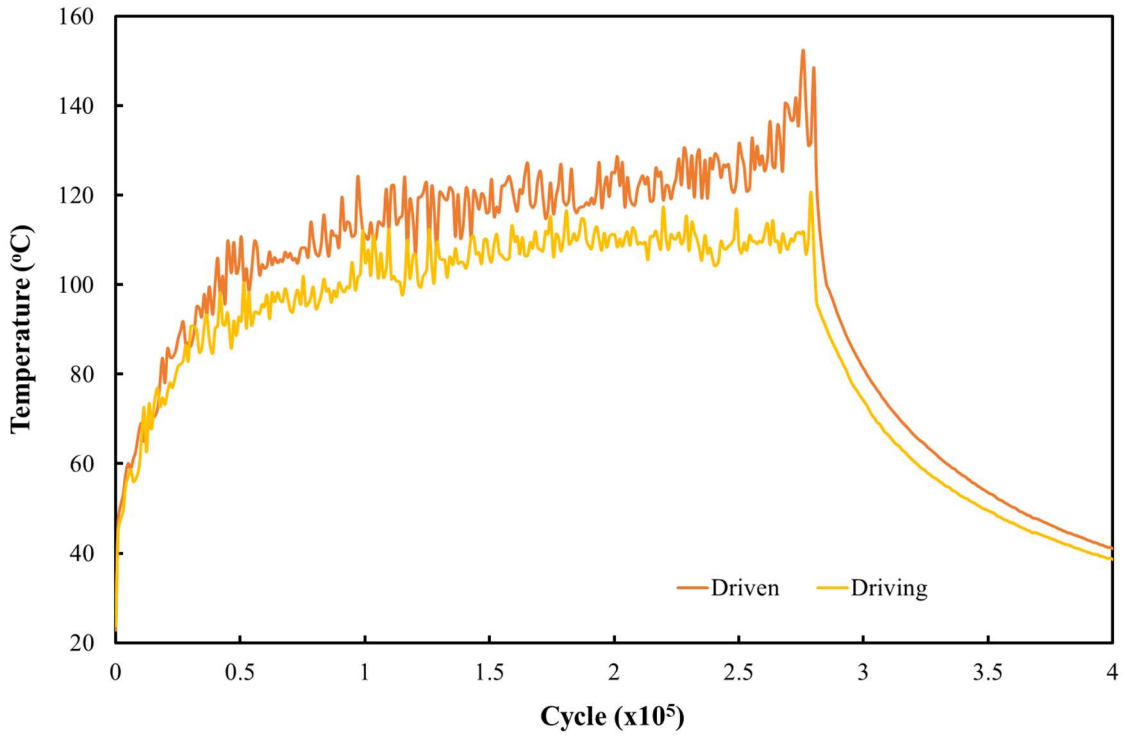

Figure 6.21 Maximum tooth surface temperature for machine cut nylon gears running at 1000 RPM, under the torque of 26 Nm and in oil lubricant medium

Figure 6.22, Figure 6.23 and Figure 6.24 show general overviews of the after-test gears. All the tested gears had their teeth fractured at the root side of the gear. Mostly, the fracture happened at the driven gear first. This type of fracture was thought to follow the loaded cantilever concept.

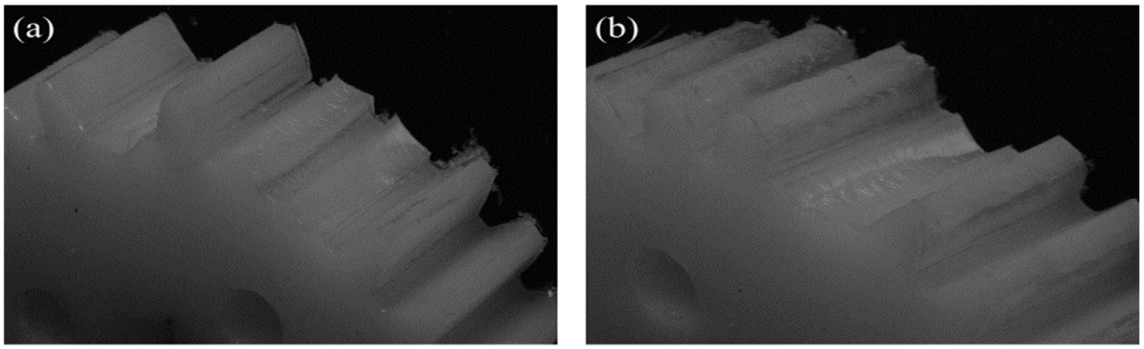

Figure 6.22 (a) The driving and (b) the driven machine cut nylon gear after testing at 1000 RPM, under 22,5 Nm torque and in oil lubrication

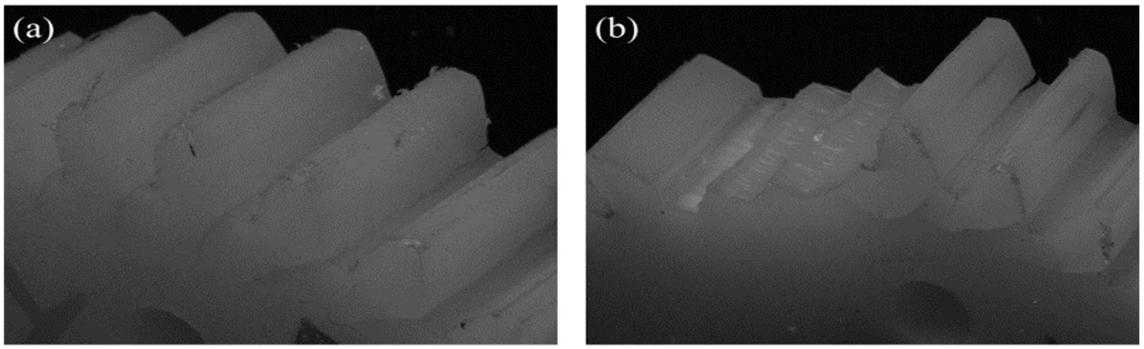

Figure 6.23 (a) The driving and (b) the driven machine cut nylon gear after testing at 1000 RPM, under 26 Nm torque and in oil lubrication

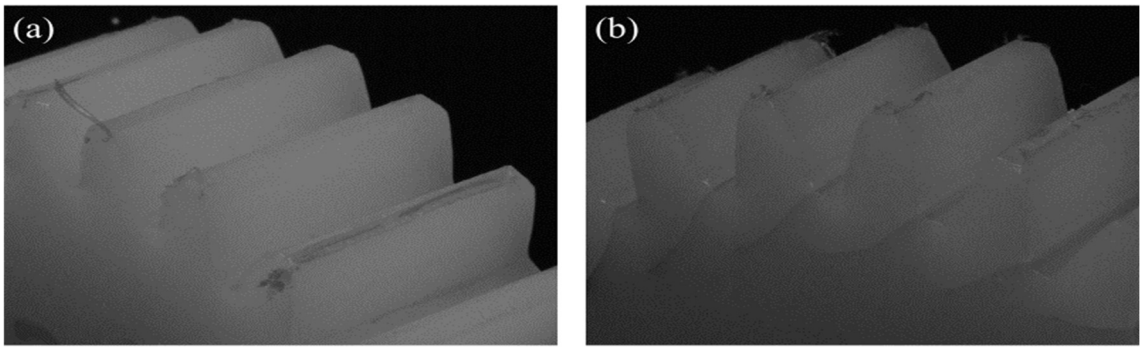

Figure 6.24 (a) The driving and (b) the driven machine cut nylon gear after testing at 1000 RPM, under 29 Nm torque and in oil lubrication

Figure 6.25 shows the SEM for the tooth surface of the machine cut nylon driving gear that was tested at the speed of 1000 RPM, under the applied torque of 22.5 Nm and in oil lubricant medium.

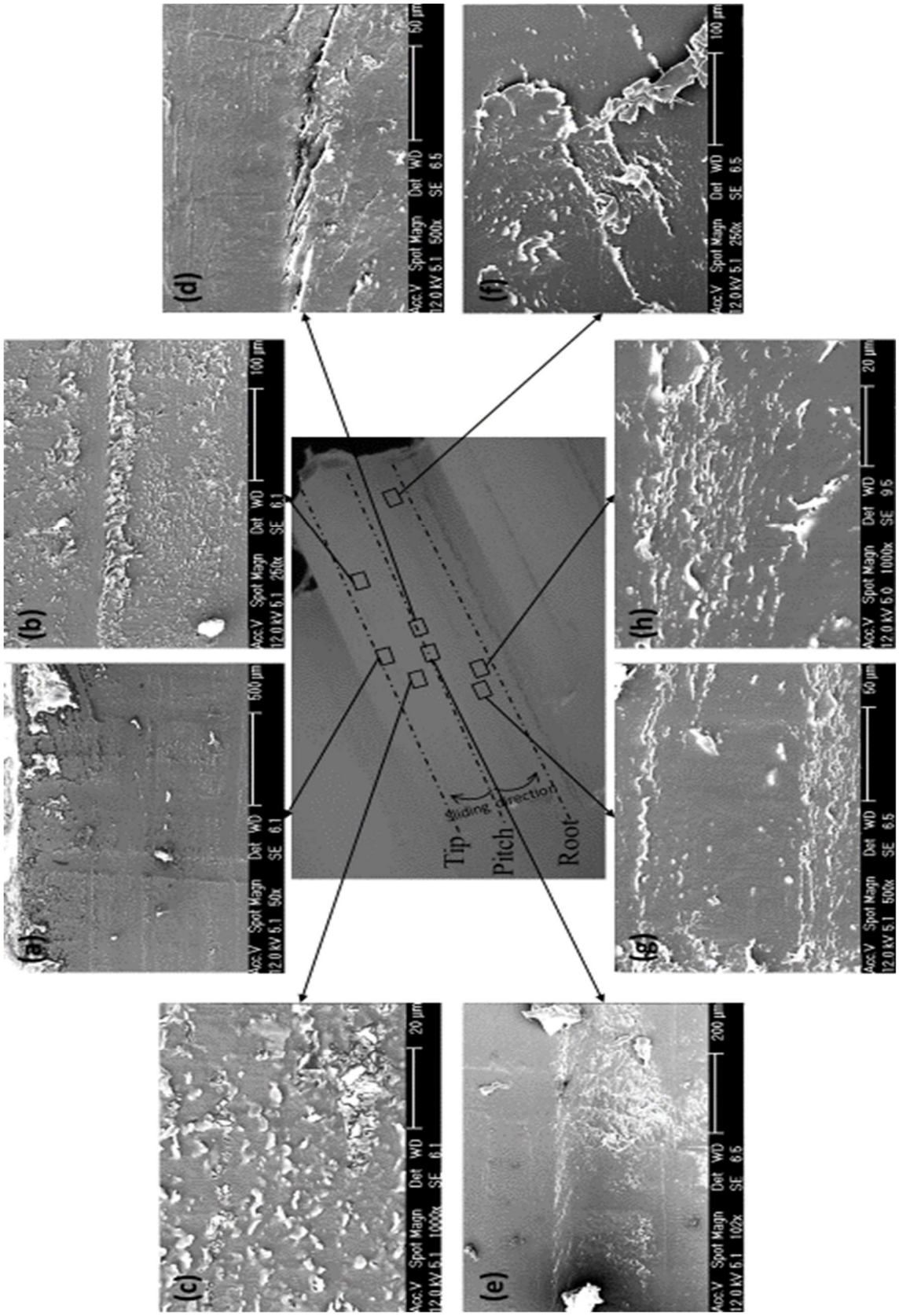

Figure 6.25 SEMs of machine cut nylon driving gear tooth (22.5 Nm, 1000 RPM and oil lubrication)

The area between the pitch line and the tip of the tooth (Figure 6.25 (a), (b) and (c)) showed the occurrence of both adhesive and abrasive wears. Due to being highly loaded, the tooth addendum was polished at some parts of the surface with long line grooves. Other parts show adhesive wear, where surface material was dragged along the surface and formed chips debris. Micro pits were also discovered in some places.

Moving towards the pitch line (Figure 6.25 (d) and (e)), both microcracks and large cracks were found all along the face width of the tooth. These could occur became of the high surface contact pressure and Hertzian pressure in this area, in addition to the effect of the sliding direction that leads the two sides to turn apart. Also, some plastic flow was discovered around the pitch line, guiding the surface material to the two sides of the tooth because of the relatively high pressure in this test.

At the dedendum side of the tooth, from root to pitch line (Figure 6.25 (f), (g) and (h)), adhesive wear behaviour was more common than abrasive wear. Plastic flow was also discovered at different areas, which tended to move some surface material towards the edges. Also, microcracks were seen in some areas towards the root of the tooth.

Figure 6.26 illustrates the SEM for the tooth surface of the machine cut nylon driven gear that was tested at the speed of 1000 RPM, under the applied load of 22.5 Nm and in an oil lubrication medium.

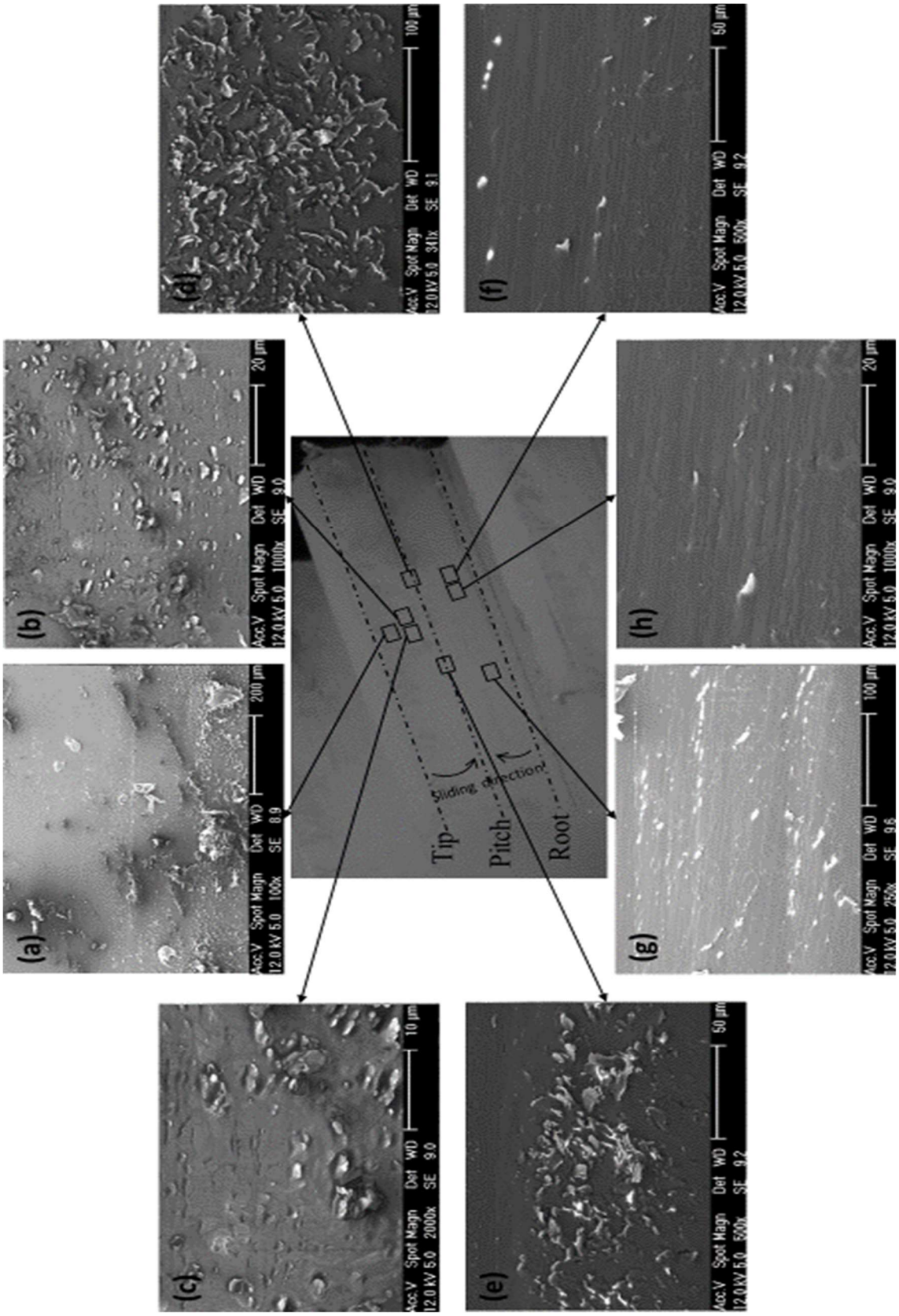

Figure 6.26 SEMs of machine cut nylon driven gear tooth (22.5 Nm, 1000 RPM and oil lubrication)

The area from the pitch line to the tip of the tooth (Figure 6.26 (a), (b) and (c)), showed more softening and clotted debris in an oval shape as a result of the high surface temperature. Abrasive wear was evident in some areas, but, interestingly, a great number of micro pits were discovered on the surface. This could be because of the large increase of pressure compared to the previous low load tests. A very small amount of adhesive wear was also observed.

Figure 6.26 (d) and (e) cover some areas at the pitch line of the tooth. Here, adhesive wear was the most common, with the extra effect of multi-direction sliding that eliminates the trace of wear. Also, more debris was found in this area, it is more generally thought that debris collects preferentially in this are of driven teeth.

Towards the dedendum side of the tooth surface (Figure 6.26 (f), (g) and (h)), more abrasive wear was discovered, with much polishing of surfaces because of the high pressure. Surface microcracks were also forming in this area, but more as micro scales shallow to the surface. They are thought to be the result of the high surface pressure caused by the tip of the driving gear. Hardly any debris was found on the dedendum side of this tooth because mostly it was pushed to the end of the two surface contacts, as one of the abrasive wear functions.

Figure 6.27 shows the SEM images for the tooth surface of the driving machine cut nylon gear. The sample was tested for 2.5×10^5 cycles, at the speed of 1000 RPM, in an oil lubrication medium and under the applied torque of 26 Nm.

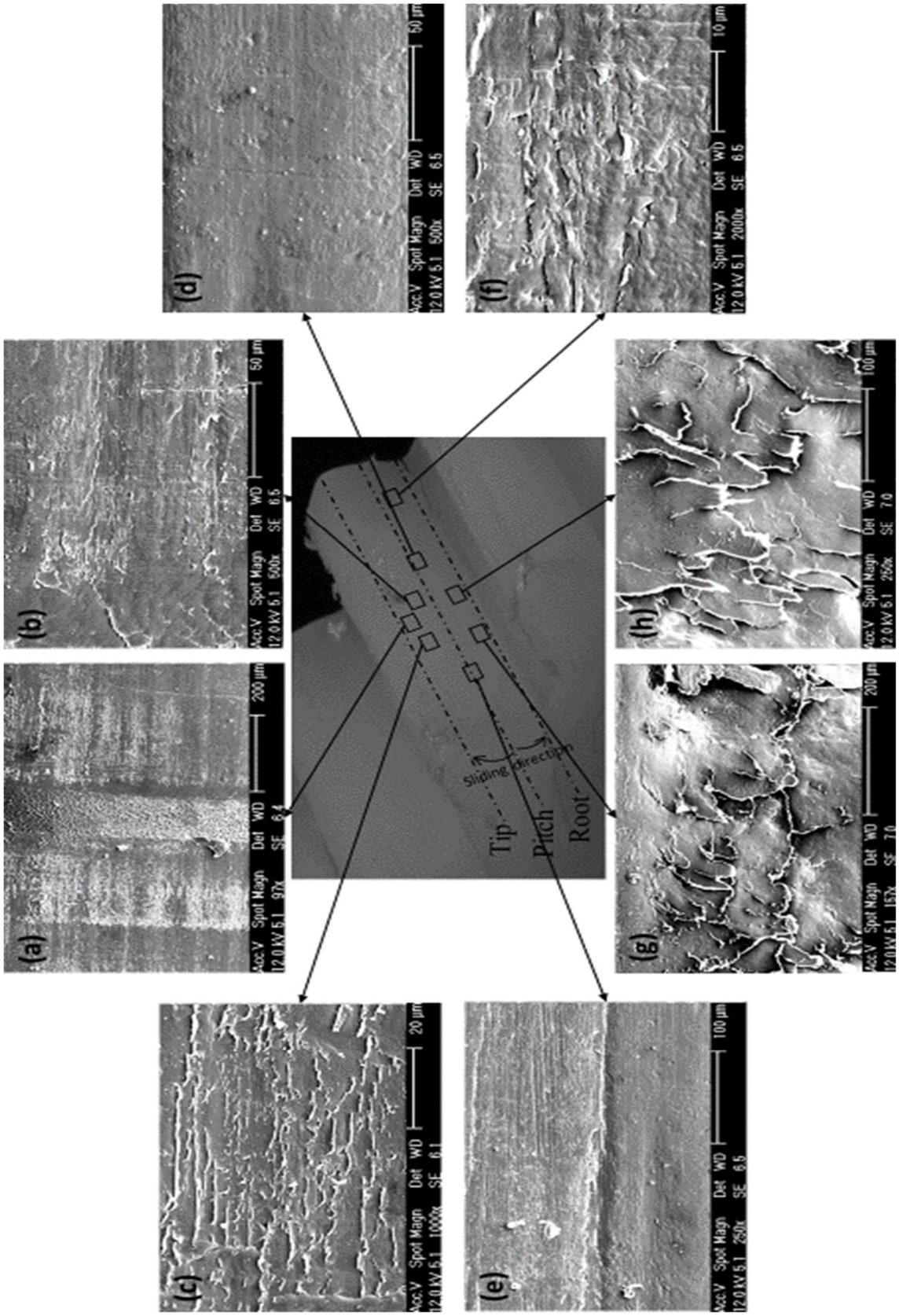

Figure 6.27 SEMs of machine cut nylon driving gear tooth (26 Nm, 1000 RPM and oil lubrication)

At the addendum side of the tooth surface (Figure 6.27 (a), (b) and (c)), the effect of the high surface pressure is even more recognisable, compared to the low load ranges. Both abrasive and adhesive wear are found in this area of the tooth surface. With the contact frequency of gear meshing, both types of wear could occur at a particular point alternately. This could explain what is observed here with some detached surfaces that were pressed and welded hard again on to the surface. Their appearance could be thought at first to be microcracks, but with more through investigations, this phenomenon could be identified.

Around the pitch line (Figure 6.27 (d) and (e)), a surface bump was forming at some parts of the tooth face width, which might be because of the sliding direction behaviour at this area. Other areas were flat and showed just normal abrasive contact, which demonstrates the change of the location of sliding direction transition because of the low material elasticity. Some microcracks were discovered also, but with limited size and depth.

On the dedendum side of the tooth surface (Figure 6.27 (f), (g) and (h)), the area suffers from a very high adhesive wear, with larger amounts of surface materials were dragged radially to the edges and for longer distance. This could be because of the higher surface temperature (reaching up to 120^{o}C at the driving gear) and pressure at this test, compared to the other tests. Some plastic flow could be discovered at this area.

Figure 6.28 illustrates the surface SEMs for the machined cut nylon driven gear tooth running at 1000 RPM, under 26 Nm torque and in oil lubrication.

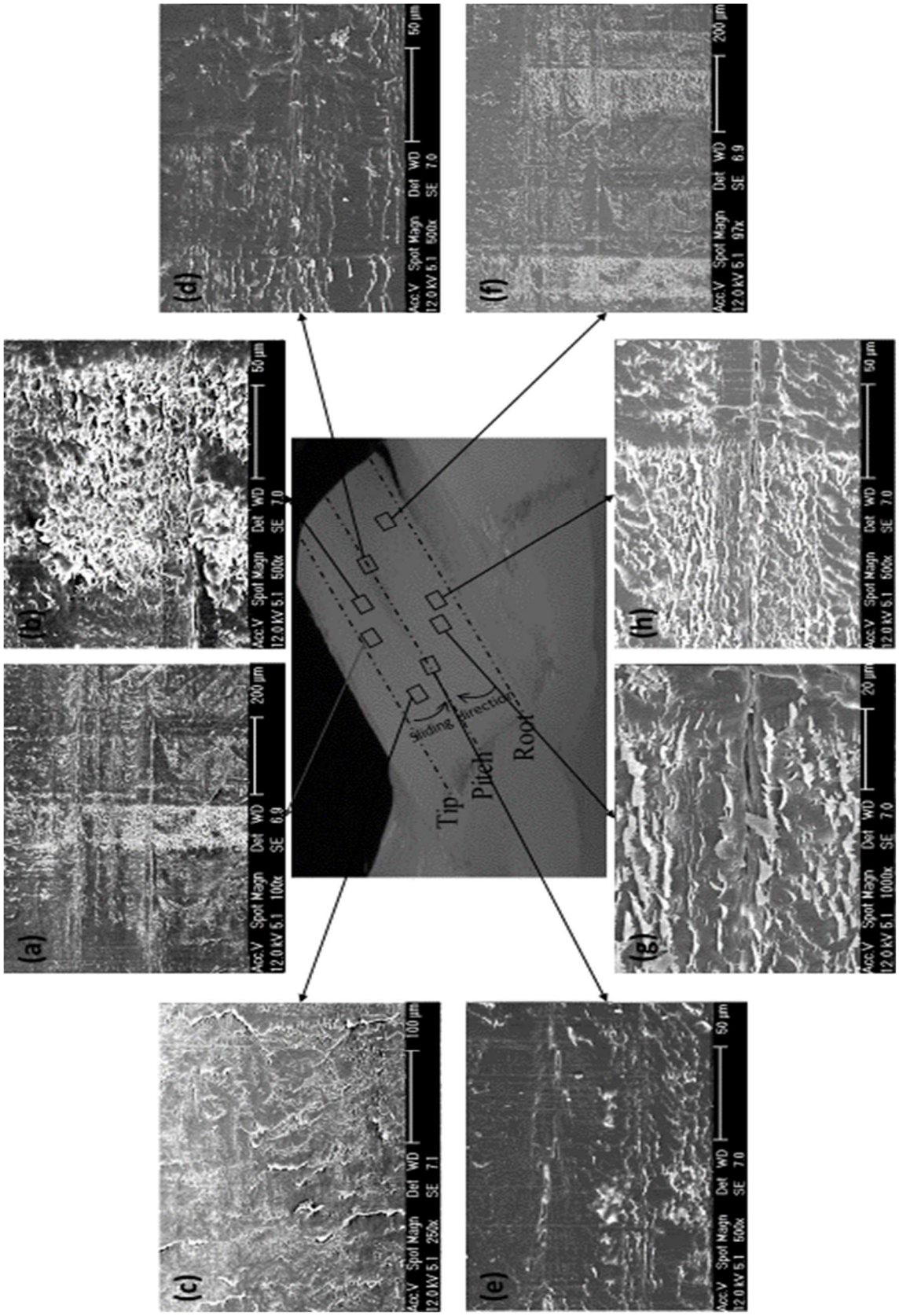

Figure 6.28 SEMs of machine cut nylon driven gear tooth (26 Nm, 1000 RPM and oil lubrication)

At the addendum side of the tooth surface (Figure 6.28 (a), (b) and (c)), there was a high surface pressure with the effect of sudden impacts in this area of the tooth at the beginning of the mesh. These led to a high abrasive wear to the area in addition to the clear surface plastic flow. A small amount of adhesive wear was seen in some limited places.

Figure 6.28 (d) and (e) showed some microcracks around the pitch line of the tooth surface. Also, adhesive wear was one of the main types in this area. Debris was hardly found at all around the pitch line of the tooth.

Moving towards the dedendum side of the tooth surface flank (Figure 6.28 (a), (b) and (c)), more adhesive wear could be recognised, with relatively larger size features of dragged surfaces. Interestingly, no wear debris was found at the end of the contacting zone as a result of this large adhesive wear. Some microcracks were discovered at the dedendum side of the tooth surface. Also, high plastic flow was found (similar to the addendum surface side) when moving towards the two edges of the tooth.

To summarise, running the machine cut nylon gears at high loads in an oil lubrication revealed that the gear wear mostly exhibited similar behaviour, with three stages of wear: running-in stage, nearly-linear stage and high wear and tooth fracture stage. The wear rate during the nearly-linear stage was defined for all tests and found to be highly affected by load change. Up to ten fold increases in wear rate could be experienced when increasing the applied torque by reasonably small amounts. In all the tests gear teeth were fractured mostly at the driven gears, but sometimes at the driving gear, with the fracture happening always at the tooth root.

Increasing the torque in these tests leads to an increase in the gear tooth surface temperature, reaching up to, and above, the glass transition point of the machine cut nylon gear, which leads to the high increase in wear rates.

Surface tribology studies of tooth surfaces revealed that, for machined cut nylon gears at high loads and in an oil lubrication, both adhesive and

abrasive wear were common on tooth surfaces. Small amounts of micro pitting was discovered in some areas. Microcracks mostly occurred at the pitch line and dedendum side of the tooth surfaces, but they did not appears to be one of the major causes of tooth damage. Mostly, the teeth were damaged by the high stresses on tooth root, which follows the loaded cantilever analogy.

6.5 Long run test

To further understand the behaviour and endurance of nylon gears in long term running with oil lubrication, a long running test of the machined cut nylon gears was initiated using one of the low range torques. Figure 6.29 shows the gear tooth wear trend of these gears running continuously for around one week (115×10^5 cycles) at a speed of 1000 RPM, under the applied torque of 12.5 Nm and in an oil lubrication medium. It can be seen that the wear reached the value of 0.4 mm at the running-in wear stage. This was followed by a long period of the nearly-linear wear stage, with in total a very small amount of additional wear of around 0.03 mm. The test was stopped, and the gears were left to cool down before they were taken out for further investigations. The driving gear had one tooth fractured at the pitch line, while the driven gear had three teeth fractured between the tip and the pitch line. The wear rate of this nylon gear was defined by measuring the slope of the trend line that was fitted to the nearly-linear wear stage with a squared correlation of 97% and was found to be around 0.8×10^{-8} mm/cycle.

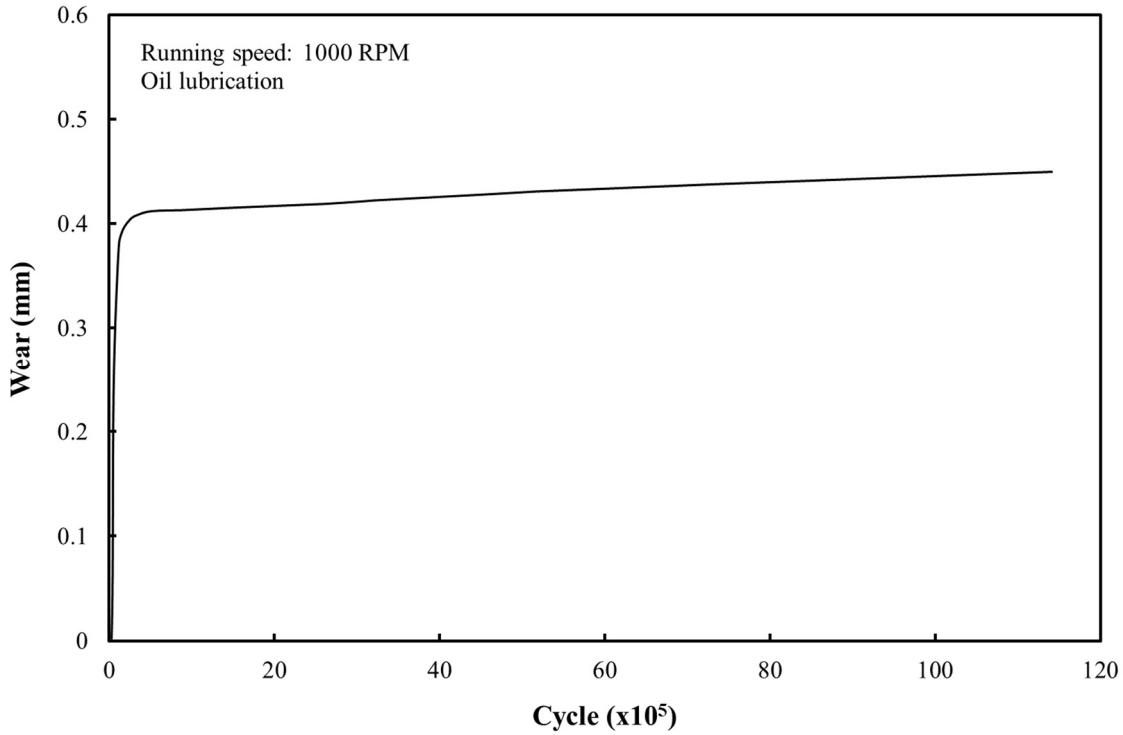

Figure 6.29 Wear of machine cut nylon gears for long run test (one week) in oil lubrication medium, at the speed of 1000 RPM, and 12.5 Nm torque

Figure 6.30 shows the after-test machined cut nylon gear pair that was tested in a long run, at the running speed of 1000 RPM, under the load of 12.5 Nm and in oil lubrication medium.

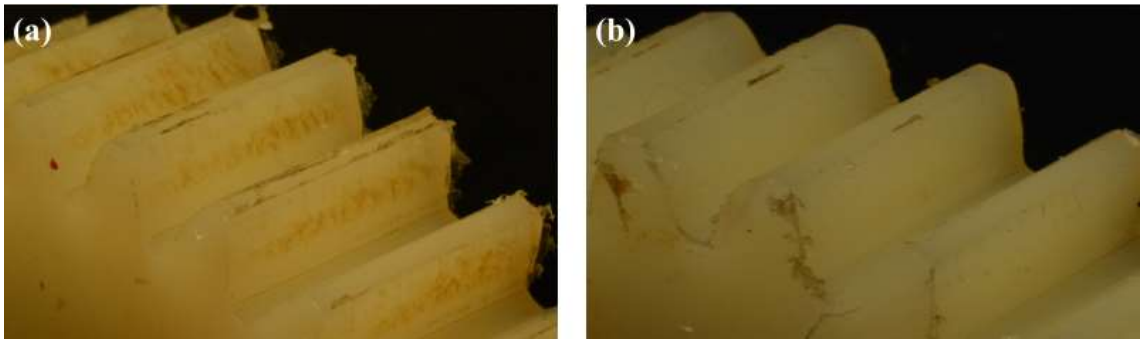

Figure 6.30 (a) The driving and (b) the driven machine cut nylon gear after testing at 1000 RPM, under 12.5 Nm torque, for a long run and in oil lubrication.

Because of the long running time and limitations of the camera memory storage capacity, the gear maximum surface temperature was recorded for only a third the test period. Figure 6.31 shows the tooth maximum surface temperature for both the driving and driven machine cut nylon gears that was running at the speed of 1000 RPM, under the applied torque of 12.5 Nm and in an oil lubrication medium. The maximum surface temperature increased from the beginning of the test to the end of the running-in wear stage (2 x 10^5 cycle), where it reached the value of 97°C. The temperature then increased slightly to reach the value of 103°C after 5 x 10^5 cycles. The readings were then stabilized for the next 7 x 10^5 cycles before they were slow fluctuation of typical around 7°C for the rest of the record. This small amount of fluctuation could be one of the reasons for very small fluctuations observed (but not readily visible in Figure 6.29) in the long nearly-linear wear stage. In addition, the maximum surface temperature was fluctuates around the glass transition point of this material, with some useful cooling down periods that were enough to maintain the wear rate.

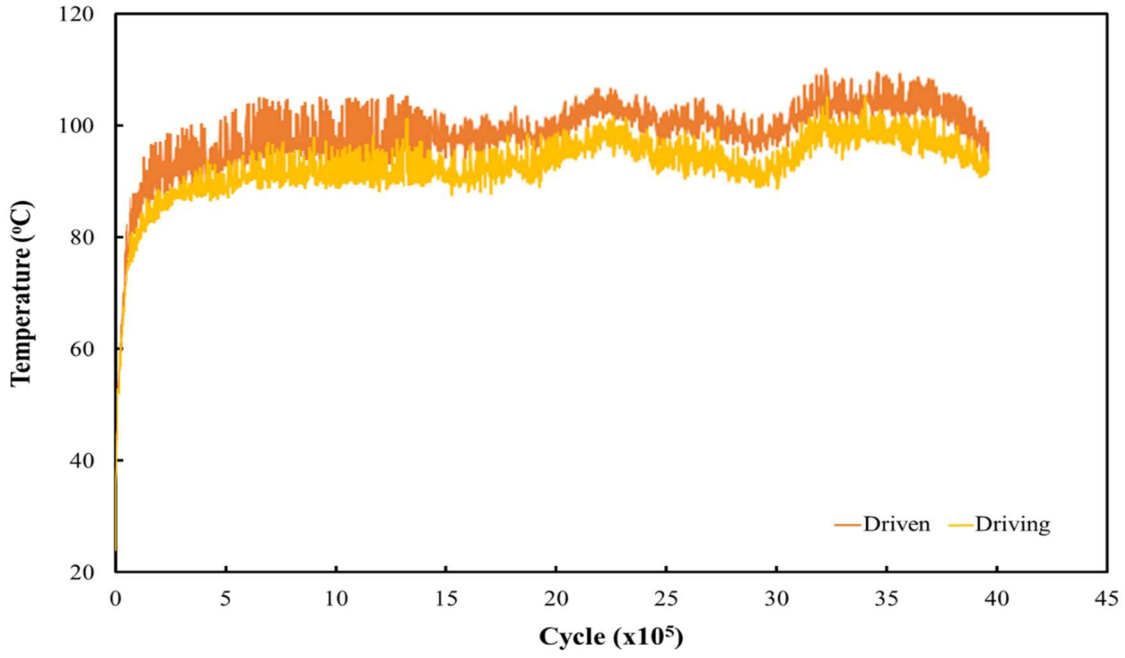

Figure 6.31 Maximum tooth surface temperature for machine cut nylon gears running at 1000 RPM, under the torque of 12.5 Nm and in oil lubricant medium (long run endurance test)

6.6 Summary

The effect of oil lubrication on nylon gear running has been investigated in this chapter. Some tests were designed and carried out using test rig II and gear wear and wear rate were established. These started with the gear load capacity scoping using the custom designed step-loading test and ended with some long-run tests to further investigate the machined cut nylon gears behaviour.

It was found that using an oil lubricant with the machine cut nylon gears would improve the load capacity of these devices to about 2.5 times the load capacity of the dry running condition. Additionally, the gear wear rate was reduced about ten times, which could lead to an increase of the gear running life.

Measuring the surface maximum temperature for both the driving and the driven gear pair revealed the relationship between this parameter and the gear tooth surface wear rate. Because of the relatively low glass transition temperature of the nylon (PA66), it can be reached easily by the high speed running and rubbing of the driving and driven tooth surfaces, which has a large effect in tooth surface wear rates. The gear tooth maximum temperature can be controlled in low load ranges by using an external lubricant in addition to the control of load limits. It was found that the maximum surface temperature can easily reached at high load ranges over in oil lubrication.

The tribological behaviour of the driving and driven gear tooth surfaces was investigated and linked to the wear and surface temperature behaviour. It was found that at the low load ranges, wear behaviour was largely limited to abrasive wear, with sometimes adhesive wear when higher temperatures were reached. Microcracks were discovered, but with limited sizes and depth, and therefore unlikely to highly affect the wear behaviour of the machine cut nylon gears in oil lubrication. On the other hand, at the high load ranges, both adhesive and abrasive wears were recognised as

having important effects on performance because of the high surface contact pressure. Some microcracks were found around and below the pitch line, but mostly did not propagate into large cracks or fractures. In contrast, all fractures occurred at the tooth root side and followed the loaded cantilever concept.

Chapter 7
THE EFFECT OF MISALIGNMENT ON POLYMER GEARS

7.1 Introduction

Gear misalignment can occur as a result of many different causes, such as shaft or case distortions and instabilities of gear dimensions. Although, there is very limited literature about nylon gear misalignment (as discussed in Chapter 2), this could be one of the most important effects for the increase of polymer gear wear rate and failure. Exploring this important aspect here is highly worthwhile bring together the most critical factors that affect polymer gear life and endurance. In this chapter the effect of misalignment on the wear rate of machine cut nylon gears will be studied. In addition, more thorough investigations will be undertaken during and after these tests.

There are four different types of misalignments that can be modelled using the polymer gear test rig I, namely yaw, pitch, radial and axial misalignment (see Chapter 2). Here, because time and cost limitations, we focus on the two most important types, which are yaw and pitch misalignments. Tests were designed to study how misalignment angle increased wear and wear rate by stabilizing torque and running speed and increasing the targeted misalignment angle. All tests were run in dry-running condition.

7.2 Yaw misalignment

Yaw misalignment can be modelled to test a pair of polymer gears using test rig I by tilting and fixing one of the holding blocks to a certain angle as represented in Figure 3.3. Yaw angle will be represented as α (degrees).

Figure 7.1 shows the wear of the machine cut nylon gears running at 1000 RPM, under the applied load of 9 Nm and at different angles of yaw misalignment. The wear curve of the 9 Nm test at α = 0.0° (from section 5.4) was plotted here for comparison. All the wear curves for the yaw misalignment tests showed the two main stages of wear, namely running-in stage and nearly-linear stage. Also, teeth in all tests experienced the final gear teeth fracture stage.

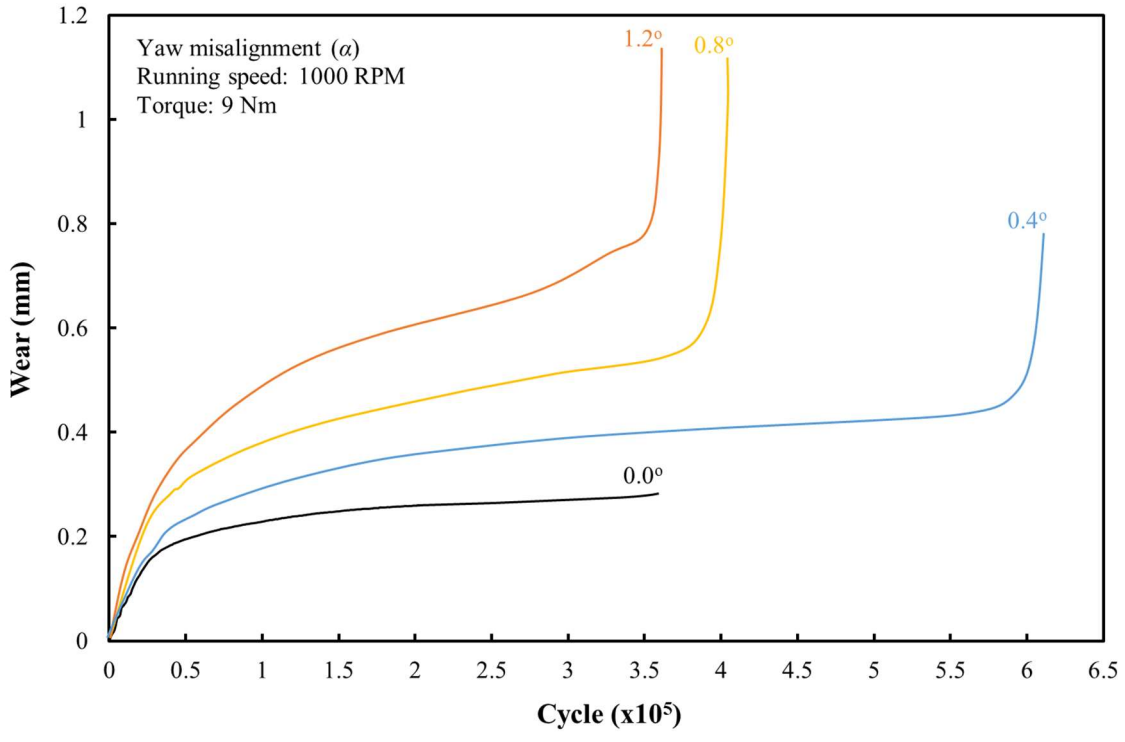

Figure 7.1 Wear of machine cut nylon gears, running at 1000 RPM, under the applied torque of 9 Nm and at different angles of yaw misalignments

Table 7.1 and Figure 7.2 illustrate the wear rate of the machine cut nylon gear teeth, which were running at 1000 RPM, under the applied torque of 9 Nm and at different angles of yaw misalignment (α = 0.0°, 0.4°, 0.8° and 1.2°). The values were defined at the nearly-linear wear stage by calculating the slope of the linear trendline. Compared to the aligned test discussed in section 5.4, the wear rate showed a relatively small increase at a yaw angle of 0.4°. This wear rate was dramatically increased by more than three times when the α angle was increased by another 0.4°. Finally, gear tooth wear rate was more than doubled for the next 0.4° increase in yaw angle. This gives a general conclusion that a very small amount of yaw misalignment angle (around 0.4°) may not have a high effect on gear tooth wear rate. In contrast, a higher amount of yaw misalignment angle could lead to a practically serious increase in gear tooth wear rate. Non-active surfaces may go in contact, which may lead to and increase in the contact pressure on the active surfaces.

Table 7.1 Wear rate of the machine cut nylon gear teeth, running at 1000 RPM, under the applied torque of 9 Nm and at different angles of yaw misalignment

Yaw angle (α) (degrees)	Backlash (mm)	Wear rate (mm/cycle x 10^5)
0	0.16	0.02
0.4	0.11	0.0333
0.8	0.06	0.108
1.2	0.01	0.247

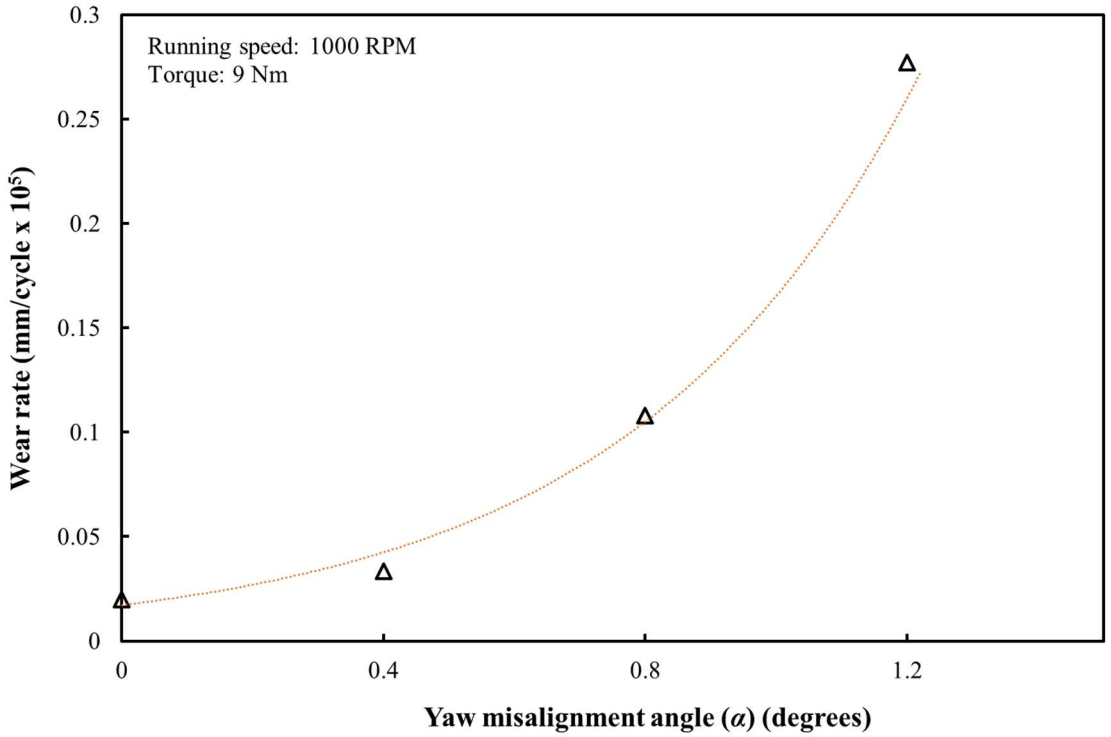

Figure 7.2 Wear rate of the machine cut nylon gear teeth, running at 1000 RPM, under the applied torque of 9 Nm and at different angles of yaw misalignment (with an exponential trendline).

To gain more understanding on the wear behaviour of the tested gears, maximum surface temperature of gear teeth was measured for both the driving and driven gears. Each one of the three tests showed broadly similar patterns in this gear surface maximum temperature records.

Figure 7.3 shows the gear tooth maximum surface temperature for both the driving and the driven machine cut nylon gears, which was tested at the speed of 1000 RPM, under the applied load of 9 Nm and with yaw misalignment of α = 0.4°. There was a sudden increase in the maximum surface temperature during the early running-in wear stage, from 23°C to around the maximum of 70°C. This was followed by a steady increase in the maximum surface temperature between 0.25 x 10^5 cycle and 1.75 x 10^5 cycle, reaching a peak maximum of 140°C. This increasing stage corresponded to a relatively high wear rate trend at the same period. Between the 1.75 x 10^5 cycle and the 2.25 x 10^5 cycle, there was a

maximum surface temperature decrease to around 120°C. This was followed by a nearly stable maximum surface temperature for the next 3 x 10^5 cycles of the test. This stable surface temperature was corresponded to a relatively low wear rate trend over the same time interval. By the last 1 x 10^5 cycles, the maximum surface temperature was increasing dramatically, reaching the maximum value of 180°C. Because of the high speed moving gears, the maximum surface temperature result was fluctuating across the running time, with an average change of around 29°C. After the test was stopped, the gears were left to cool down and the maximum surface temperature decreased rapid reaching 40°C in about half an hour.

Comparing to the aligned running test at 9 Nm, the maximum surface temperature here reached higher levels from the early stage of the test. This was thought to be because of the decrease of the contact area between the two gears because of the misalignment.

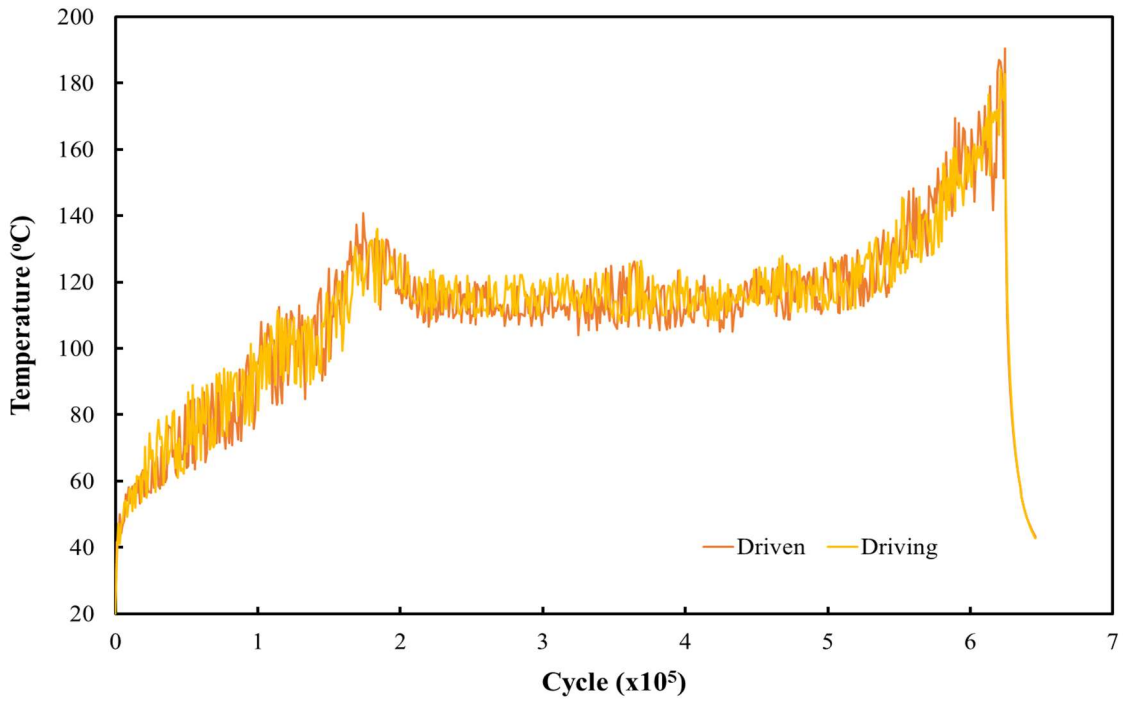

Figure 7.3 Maximum surface temperature of machine cut nylon gear pair (9 Nm, 1000 RPM and yaw misalignment α = 0.4°)

By linking the wear result and the maximum surface temperature result, we can find that the (early stage) of surface temperature increase corresponded to the running-in wear stage and the high wear rate stage. During the early stage, the gear teeth contact area was relatively smaller than the ideal gear mesh because of the misalignment. After the teeth had experienced a certain amount of wear, the contact area was thought to be slightly increased, allowing the maximum surface temperature to be reduced by around 20°C. The wear rate then also decreased and stabilized for the next 3 x 10^5 cycles, where surface temperature was stable at 120°C. Because of the large reduction of tooth thickness at the final stage, with the help of the high temperature (higher than the glass transition point of the tested material), the contact area was thought to be more increased, leading to the high increase in surface temperature, which in consequence lead up to the tooth fracture and the stopping of the test.

Figure 7.4 shows the maximum surface temperature of the pair of machine cut nylon gears that were tested at the speed of 1000 RPM, under 9 Nm torque and at α = 0.8° misalignment. In general, the maximum surface temperature trend is similar to what was recorded in the α = 0.4° misalignment test. The surface temperature increased in the early stage, reaching a peak at around 1 x 10^5 cycles before decreasing slightly by around 20°C over the next 0.5 x 10^5 cycles. What is different here is that the next 2 x 10^5 cycles did not experiencing a stable surface temperature, but there was a steady increase of about 20°C. This was followed by the final rapid increase in surface temperature, reaching the maximum of 180°C, where the gear teeth were fractured and the test was stopped. The maximum surface temperature then recorded a rapid cool down rate, reaching 60°C after about 20 minutes. Because of the high speed running and the high instability of gear meshing as a result of the high angle misalignment, the recorded maximum surface temperature exhibited a higher amount of fluctuation, typically around 25°C.

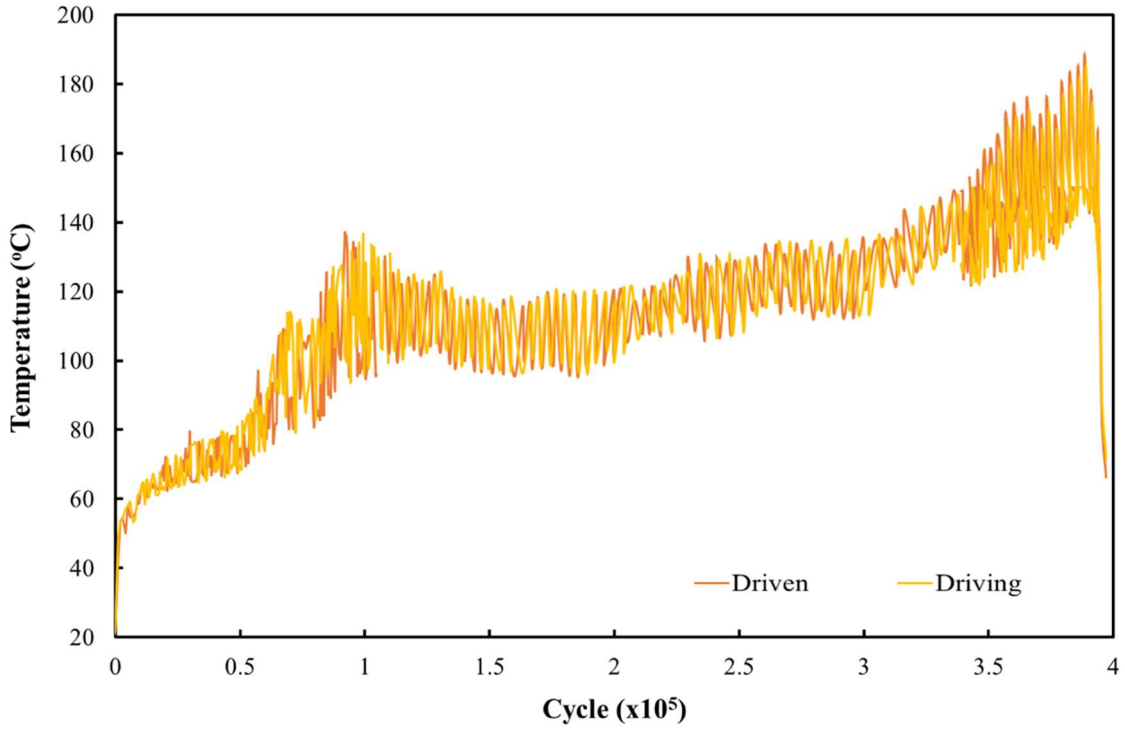

Figure 7.4 Maximum surface temperature of machine cut nylon gear pair (9 Nm, 1000 RPM and yaw misalignment α = 0.8°)

Similar to the α = 0.4° misalignment test, the high increase at the beginning of the test, reaching values higher than the ideal 9 Nm test, was thought to be because of the smaller area of contact between the two gears. In addition, doubling the angle of misalignment has reduced the time for this temperature increase by about half (1 x 10^5 cycles, comparing to 2 x 10^5 cycles at α = 0.4°). The second increase in the surface temperature here was thought to be because of the further increase on the contact area, as the larger angle leads to more area to cover with the faster reduction in tooth thickness.

Figure 7.5 shows the maximum surface temperature of the gear teeth surfaces for the machine cut nylon gear pair that were tested at the speed of 1000 RPM, under the applied torque of 9 Nm and the effect of yaw misalignment α = 1.2°. Quite a similar maximum temperature trend to the α = 0.8° misalignment test was found here. Therefore, similar analyses and conclusions could be inferred for this test. The gear teeth experienced two

surface temperature increases, both of which are thought to be caused by the continuous increase in the gear pair contact area. By increasing the yaw angle from α = 0.8° to α = 1.2°, tooth fracture stage was reached around 0.5 x 10^5 cycles earlier.

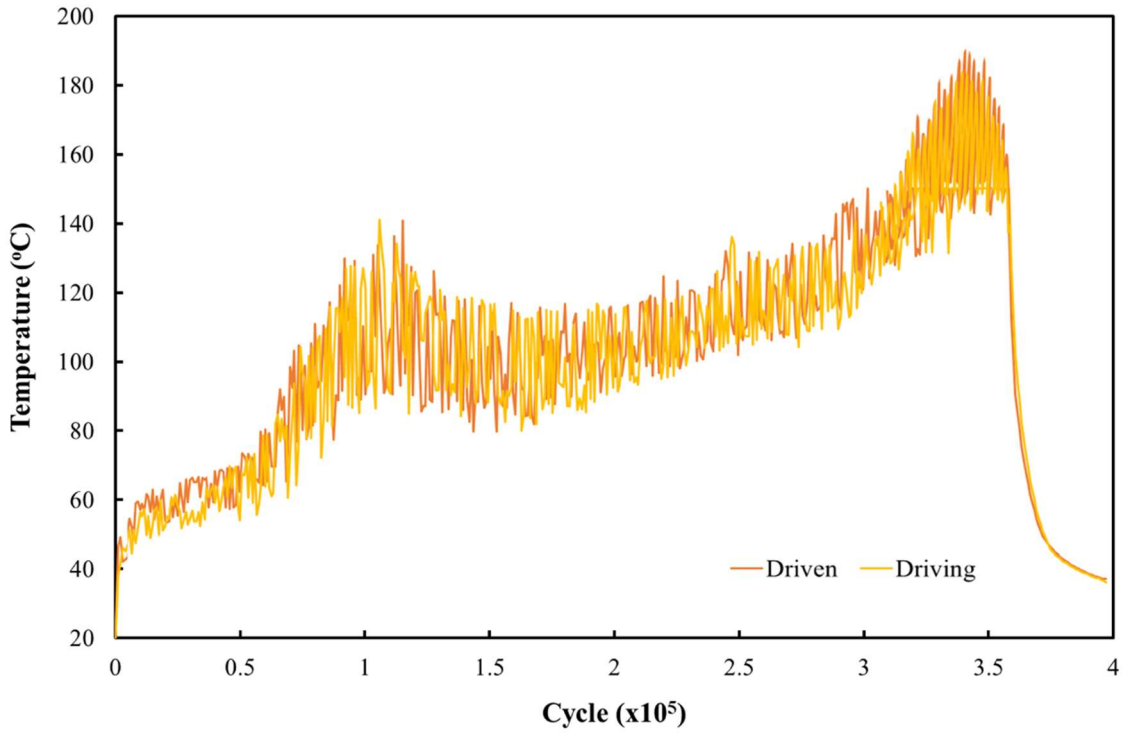

Figure 7.5 Maximum surface temperature of machine cut nylon gear pair (9 Nm, 1000 RPM and yaw misalignment α = 1.2°)

Figure 7.6 to Figure 7.8 show a general overview of the after-test gears.

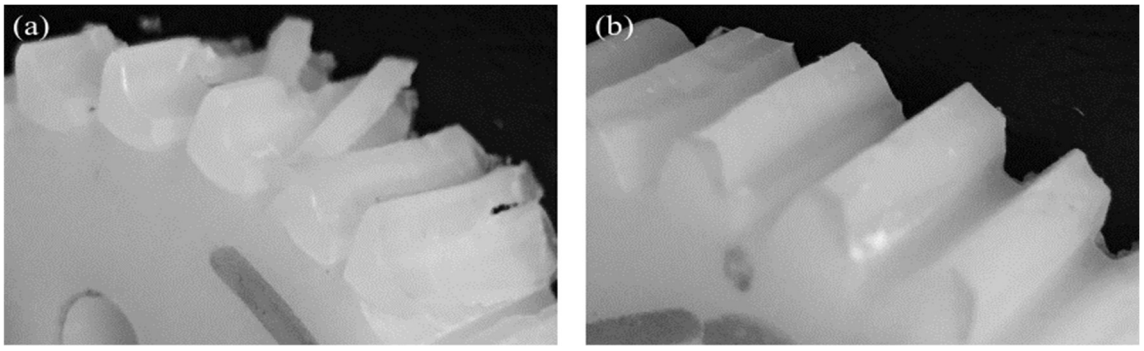

Figure 7.6 (a) The driving and (b) the driven machine cut nylon gear after testing at 1000 RPM, under 9 Nm torque and 0.4° yaw misalignment

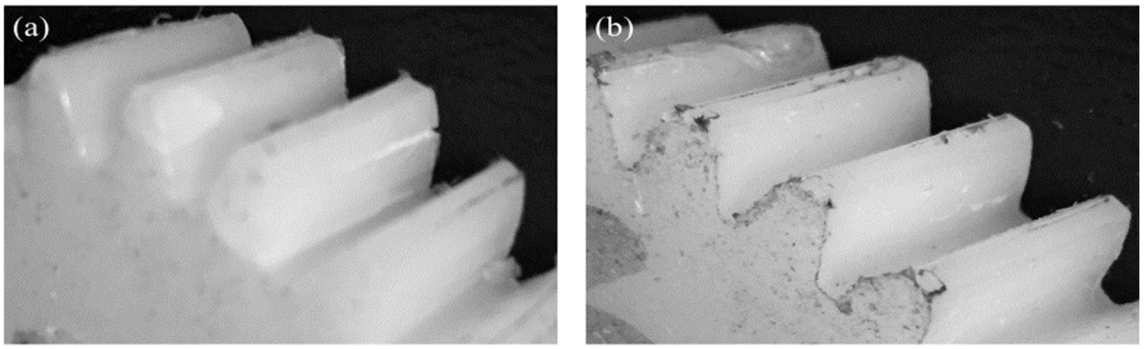

Figure 7.7 (a) The driving and (b) the driven machine cut nylon gear after testing at 1000 RPM, under 9 Nm torque and 0.8° yaw misalignment

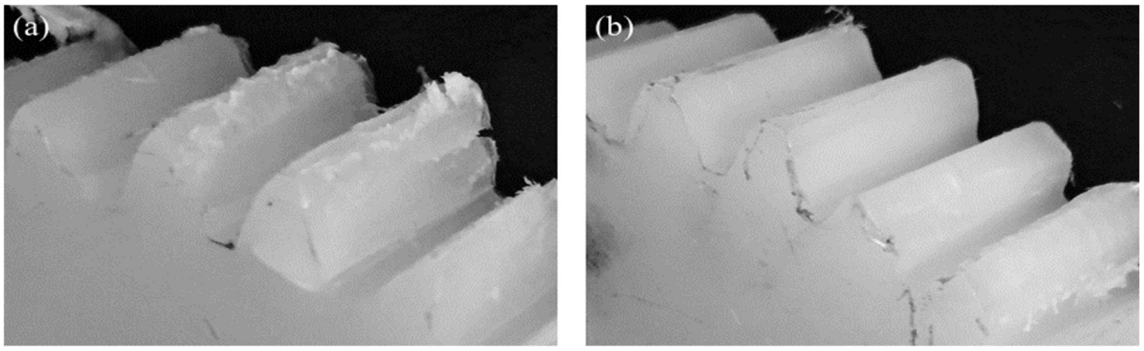

Figure 7.8 (a) The driving and (b) the driven machine cut nylon gear after testing at 1000 RPM, under 9 Nm torque and 1.2° yaw misalignment

Further gear tooth surface investigation was carried out to all the tested gear pairs using the SEM to understand the wear and failure mechanisms of those gears under the effect of the yaw misalignment. Because the gear

teeth experienced a Hertzian pressure and friction conditions at each side, SEM examination was done for both sides of each tooth for general comparisons.

Figure 7.9 shows the SEM images for the machine cut driving gear that was tested with a yaw angle of 0.4º misalignment, at the speed of 1000 RPM and under 9 Nm torque. The right side of the tooth was experiencing the higher amount of load and friction, as shown by the crack initiation at this area. The addendum side of the tooth surface was subject to a sliding direction from the pitch line to the tip side of the tooth. Figure 7.9 (a) shows some surface plastic flow, which is concentrated more to the left side of the image than the right side. Moving towards the right (Figure 7.9 (b)), we can see more pitting wear, whereas the other side (Figure 7.9 (c)) has more normal types of wear. Also, the gear teeth were fractured around the pitch line, where a clear crack can be seen in Figure 7.9 (d) and (e). The crack was wider towards the right side. No microcracks were found around the pitch line that might have caused this large crack to initiate, suggesting, that it formed because of the high load at one side of the tooth. On the dedendum side of the tooth surface (Figure 7.9 (f), (g) and (h)), there was normal wear across the area. Generally, there were no large differences in surface tribology between the left and right sides of the tooth, as the misalignment angle is relatively small.

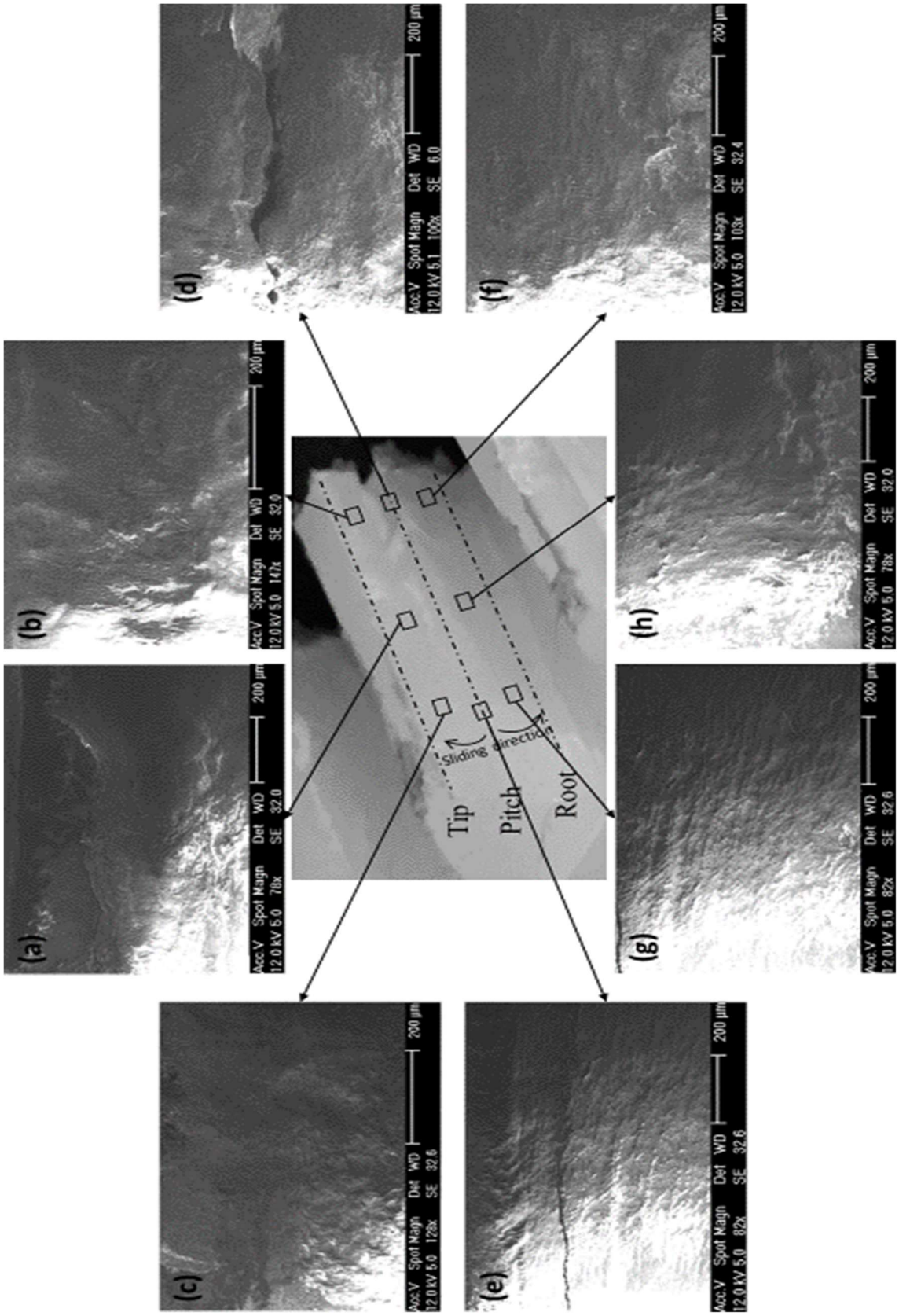

Figure 7.9 SEMs for the driving machine cut nylon gear, tested at 1000 RPM, under 9 Nm torque and with yaw misalignment of α = 0.4°

Quite similar wear behaviour and surface tribology were seen on the driven gear tooth. Figure 7.10 shows the SEM plates for the driven machine cut nylon gear tooth, which was tested to model a yaw misalignment angle of 0.4º, at the speed of 1000 RPM and under the applied load of 9 Nm. At the addendum side of the tooth surface (Figure 7.10 (a), (b) and (c)), the effect of the high initial pressure contact, at the start of the mesh, was clear, with some uneven surface. Pitting wear was the common on this part of the tooth, with some plastic flow concentrated at the left side, as it is a relatively lower loaded area.

Around the pitch line area (Figure 7.10 (d) and (e)), there was no debris collection as explored in the aligned tests. This may be because the misalignment effect initiates sideways movements, which lead the debris to the side of the teeth. Wear behaviour at this part of the tooth was of two types, normal wear and micro pitting forms to the right, and plastic flow to the left. Again, no formation of microcracks was found in the area.

Figure 7.10 (f), (g) and (h) show the surface tribology of the dedendum side of the tooth. In this area, normal wear was common at both sides of the tooth, with some form of plastic flow starting to appear from the middle to the left side of the tooth. Microcracks were not present anywhere in the area.

In general, the effect of the 0.4º yaw misalignment was relatively small, as proven by small increase in wear rate. The early fracture of teeth might occur because of the higher load and Hertzian pressure at one side of the tooth compared to the other side, which cause some focused fatigue to that part of the gear.

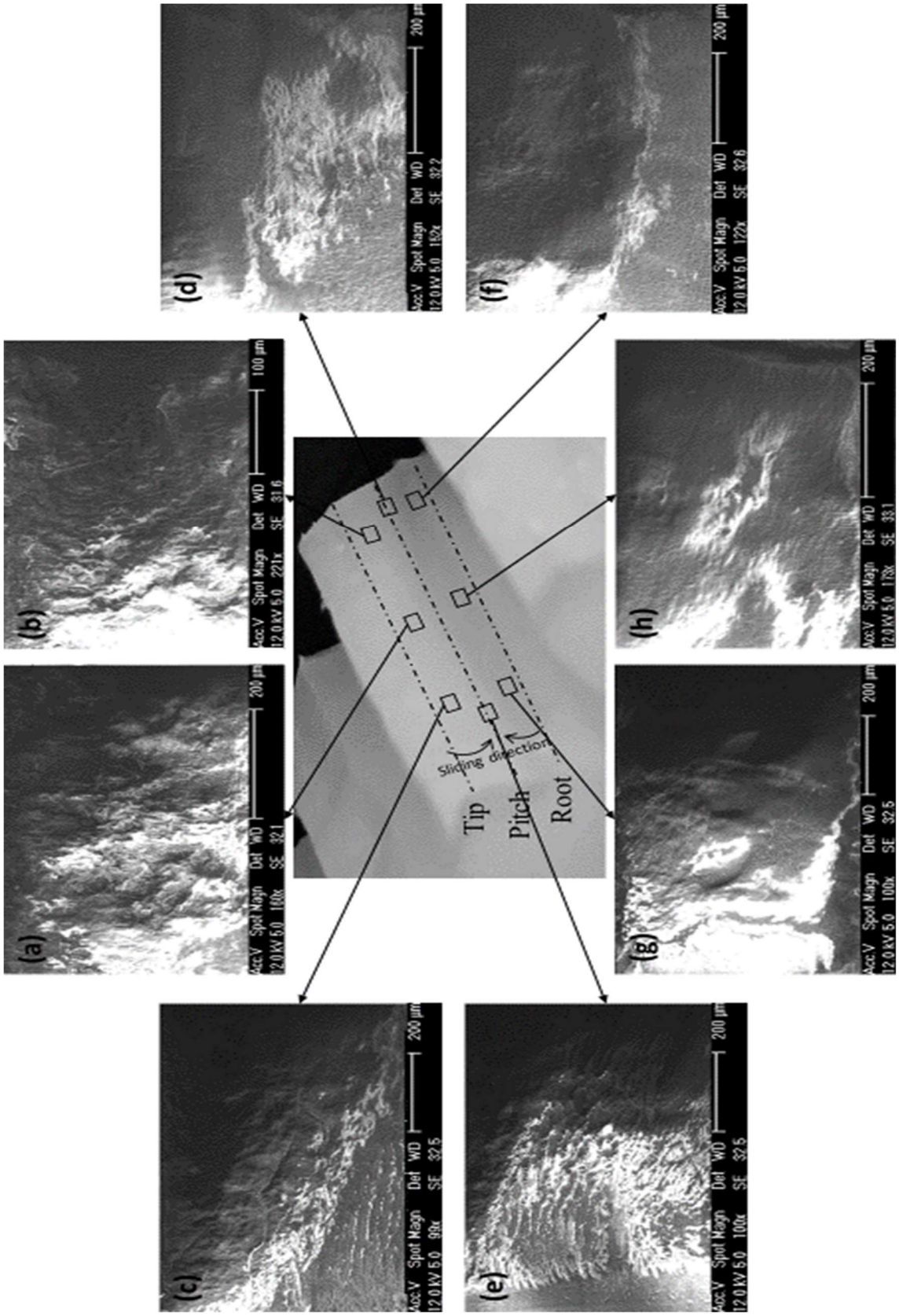

Figure 7.10 SEMs for the driven machine cut nylon gear, tested at 1000 RPM, under 9 Nm torque and with yaw misalignment of α = 0.4°

With the increase of yaw misalignment angle, more effects started to appear on tooth surfaces. Figure 7.11 shows the SEM investigation for the tooth surface of the machine cut nylon gear. The driving gear was tested at the speed of 1000 RPM, under the applied torque of 9 Nm and with yaw misalignment at an angle of $\alpha = 0.8^{o}$. More load variance effects was over found here than with the previous lower angle misalignment.

Between the pitch line and tip of the tooth surface (Figure 7.11 (a), (b) and (c)), the surface experienced two types of wear varying across the surface from edge to edge. To the right side of the tooth, high abrasive wear was more active, leading to larger amounts of material removal and causing more surface damage to the area. To the left side of the tooth, there was more of plastic flow, with relatively smaller surface damage.

To the pitch line area (Figure 7.11 (d) and (e)), a large crack started from the right side of the tooth, where the misalignment angle is leading to a relatively higher local load. This crack reached the middle of the tooth but did not appear anywhere to the left side of the gear, although some microcracks were starting to form in the area. The general wear phenomena in this area tended to have some micro pitting, especially at the right side. The dedendum side of the tooth surface (Figure 7.11 (f), (g) and (h)) shows some abrasive wear to the right and plastic flow to the left of the gear. Some wear debris had collected at left side of the tooth root, which is further evidence to confirm the side movement theory of misaligned gear engagement, where debris is pushed towards the lower loaded side of the tooth.

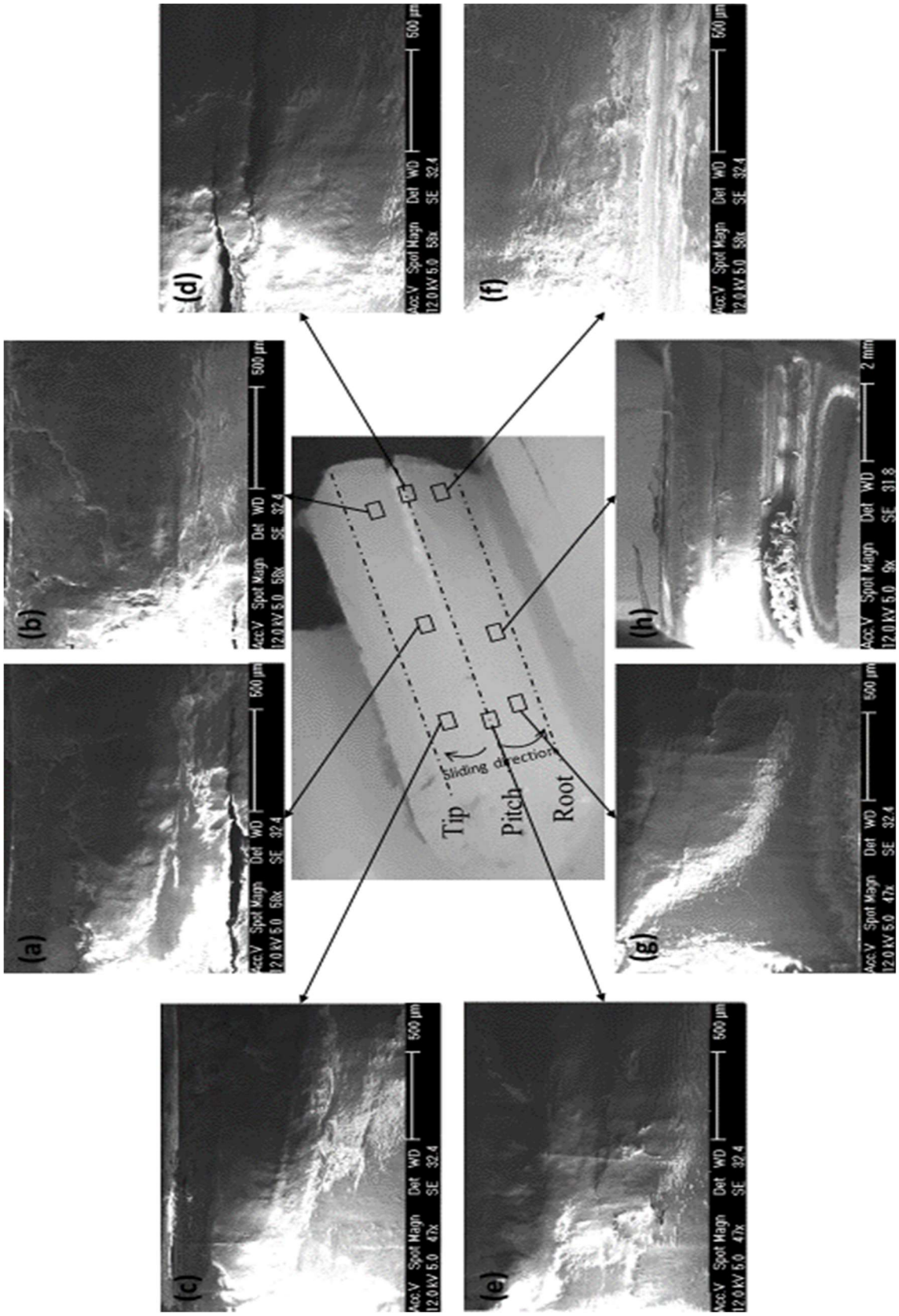

Figure 7.11 SEMs for the driving machine cut nylon gear, tested at 1000 RPM, under 9 Nm torque and with yaw misalignment of α = 0.8°

Figure 7.12 shows the SEMs of the tooth surface for the machine cut driven gear, which was tested at the speed of 1000 RPM, under 9 Nm torque and with 0.8° yaw misalignment angle. No microcracks were found throughout the whole surface of the tooth. This indicates why tooth fracture and gear failure occurred only in the driving gear. Small differences of surface tribology were found between the two sides of the tooth.

On the addendum side of the tooth (Figure 7.12 (a), (b) and (c)), the SEMs show general abrasive wear across the surface, with high severity towards the right side. Some micro pitting was observed in that area. The effect of the high load impacting at the start of the gearing mesh can be clearly discovered here.

Moving to the pitch line area (Figure 7.12 (d) and (e)), the form of wear that can be seen here tends to be more of non-directed plastic flow, due to the variation of the sliding direction in the area. More severe wear can be found near the right side of the tooth. No microcrack formation was found in the driven gear.

Between the tooth root and the pitch line (Figure 7.12 (f), (g) and (h)), surface abrasive and pitting wear were observed to the right side of the tooth. From the middle to the left side, the surface started to experience a small amount of plastic flow, in addition to the abrasive wear. In general, the form of wear across the whole tooth surface was mostly abrasive wear, with some changes from right to left because of the load changes caused by the misalignment. However, the variations in surface behaviour here is relatively low, compared to the driving gear of the same test.

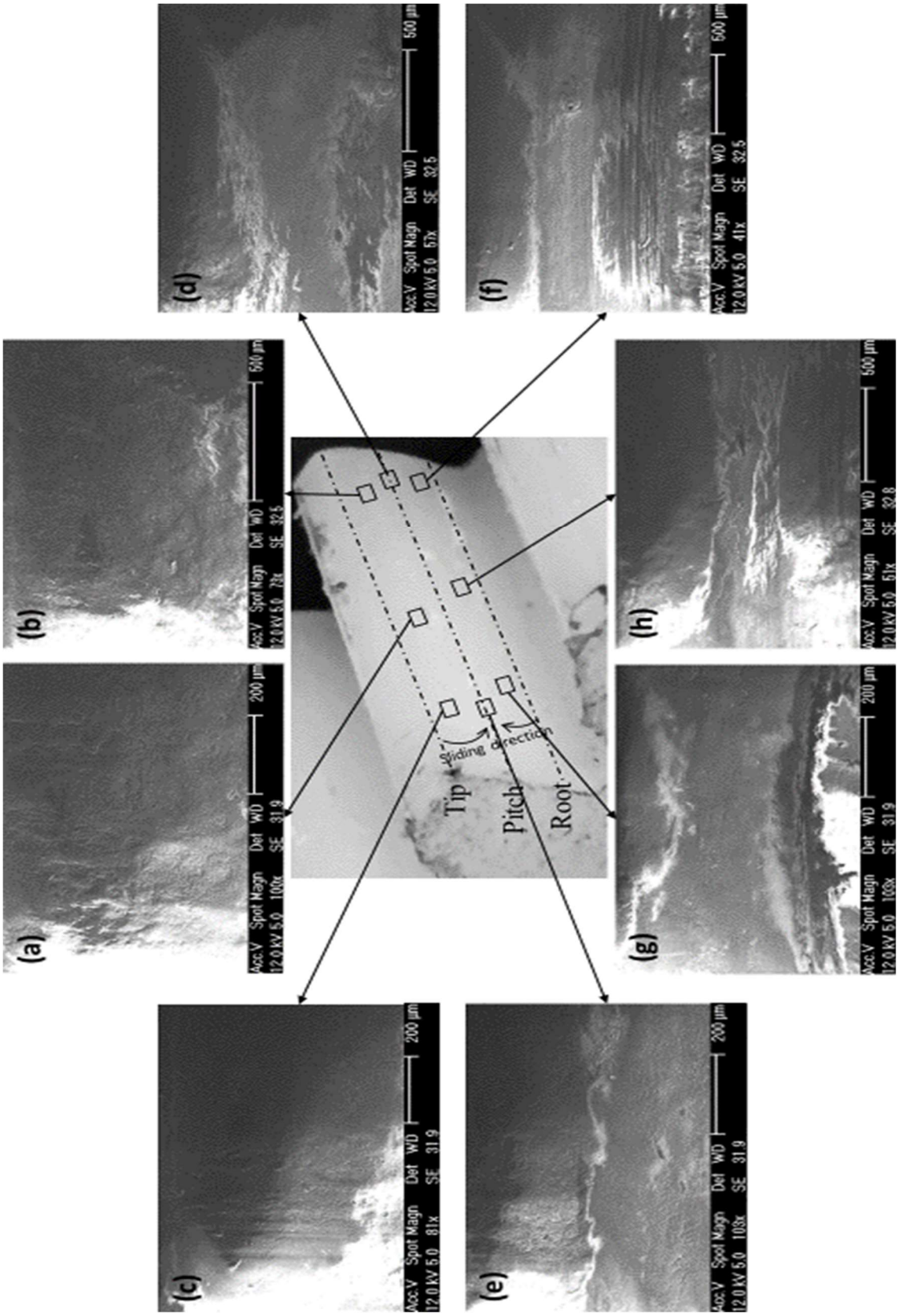

Figure 7.12 SEMs for the driven machine cut nylon gear, tested at 1000 RPM, under 9 Nm torque and with yaw misalignment of α = 0.8°

The higher yaw misalignment angle of 1.2º led to a massive increase in the wear rate of the machine cut nylon gear. Figure 7.13 shows the SEMs for the driving gear tooth surface that was tested at 1000 RPM, under 9 Nm torque and at 1.2º yaw misalignment. The middle image of the tooth shows the severe effects of the high misalignment angle on the surface, especially on the right side.

Some softened material can be observed, on the addendum side of the tooth surface (Figure 7.13 (a), (b) and (c)). This could be because of the increase in surface temperature in that area. The common surface damage here is abrasive wear, with some plastic flow concentrated only to the left side of the tooth. Wear debris was not found at this area.

Moving to the pitch line (Figure 7.13 (d) and (e)), some small cracks were observed across the tooth. They get wider towards the right side because of the higher load effects from the misalignment. Abrasive wear was more active to the right side, while plastic flow and some adhesive wear were found more to often the left side.

On the dedendum side of the tooth (Figure 7.13 (f), (g) and (h)), some microcracks were found to the right side. In this area, abrasive wear was the most prevalent. Moving towards the middle and the left side, more plastic flow wear can be seen. A side sliding direction was observed to the left side of the tooth. More variance could be observed between the two sides of the tooth than in the previous test.

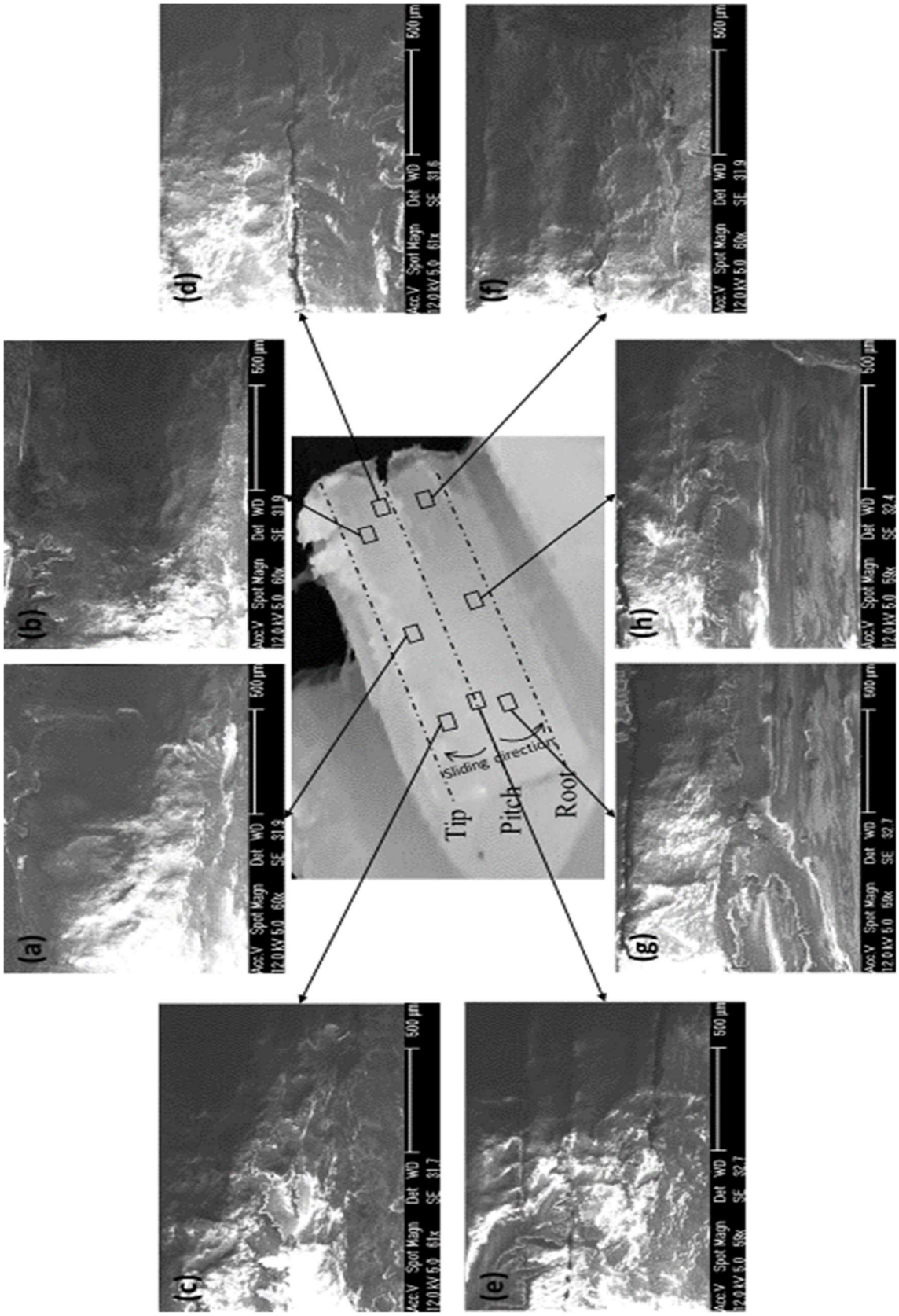

Figure 7.13 SEMs for the driving machine cut nylon gear, tested at 1000 RPM, under 9 Nm torque and with yaw misalignment of α = 1.2°

Figure 7.14 shows the SEMs for the machine cut driven gear tooth. The gear was tested at the speed of 1000 RPM, under the applied load of 9 Nm and with a yaw misalignment of 1.2º. The driven gear tooth showed less surface damage than the driving gear tooth. No tooth fracture was observed in the driven gear.

The addendum side of the tooth surface (Figure 7.14 (a), (b) and (c)) showed large amounts of surface wear, especially at the tip edge, where the tooth was experiencing high load impact at the start of the mesh. The right side of the tooth experienced more abrasive wear, with some pitting. On the other hand, the left side of the gear was under a combination of abrasive and plastic flow wear.

Around the pitch line of the tooth (Figure 7.14 (d) and (e)), the surface showed more abrasive wear to the right side and plastic flow wear to the left side. A surface peak was formed as a result of the sliding direction, which was clearer to the right side. No microcracks were found at this area. In addition, debris did not collect here, as in aligned tests, because of the side sliding that takes it out of the contact area towards the side of the gears.

On the dedendum side of the tooth (Figure 7.14 (f), (g) and (h)), the surface experienced more plastic flow wear, with some adhesive contact at the root of the tooth. More adhesive wear was found at the left side of the gear.

Generally, there were some surface failure differences across the tooth surface. Abrasive wear was observed more to the right of the tooth, while plastic flow and adhesive wear were found to the left side of the tooth.

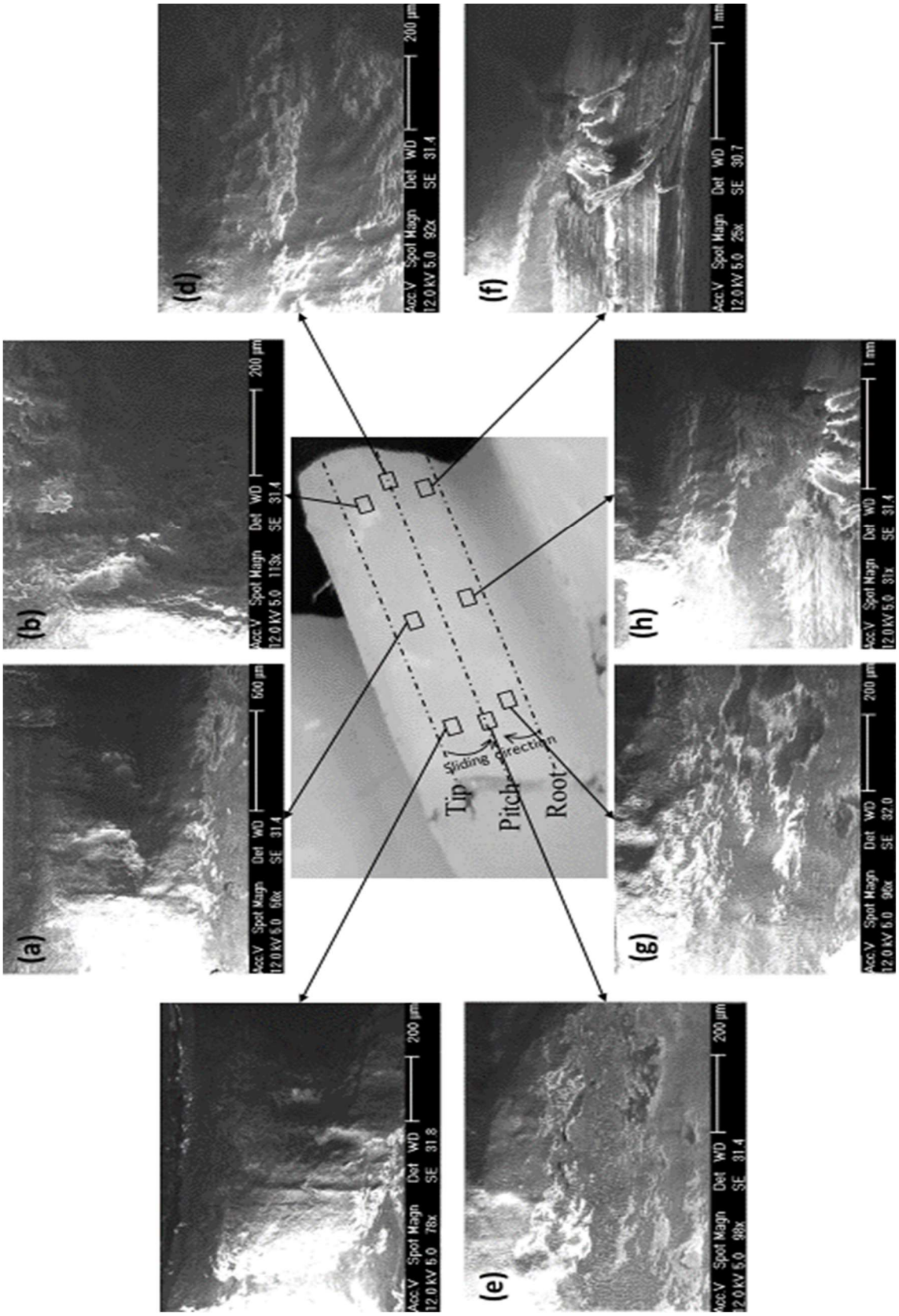

Figure 7.14 SEMs for the driven machine cut nylon gear, tested at 1000 RPM, under 9 Nm torque and with yaw misalignment of α = 1.2°

To summarise, yaw misalignment of machine cut nylon gears has a varying ariable effect on tooth wear rate, depending on the misalignment angle. At low yaw misalignment angle (α = 0.4°), the wear rate was slightly increased, compared to the aligned test. Doubling that angle leads to a three times increase in wear rate and another similar increase of 0.4° leads to a further similar increase in wear rate. This means that there is a critical point beyond which the wear rate and tooth damage are seriously affected. This point lies between the yaw misalignment of α = 0.4° and α = 0.8°.

The tooth wear phenomena were better understood from measuring the running tooth maximum surface temperature. This measurement reveals the tooth behaviour with yaw misalignment. When the load was applied, and the misaligned gear pair started to run, there was a high initial increase in surface maximum temperature, which then cooled down slightly. This was related to the surface temperature reaching above the glass transition point of the tested material, which leads to a high tooth wear and deflection. This change in gear tooth shape leads to increase the surface contact area between the two teeth, leading to the surface temperature decrease that was observed in the measurements.

The after-test tooth surface investigation using the SEM revealed two common types of wear, namely abrasive wear and plastic flow. The abrasive wear occurs mostly at the side of the tooth highly loaded because of the misalignment meshing. The plastic flow occurs mostly to the other, less loaded, side of the tooth, for the same reason. Some other types of surface wear were found in different places, but in much smaller amounts compared to the two common types. Tooth microcracks were found always on the driving gear, for which teeth failed before those of the driven gear. These microcracks occur around the pitch line of the tooth and initiate first at the highly loaded side of the tooth. Side sliding was found to function in all misalignment tests, with increasing effect as yaw angle increases. In general, the tooth damage was found to be more severe with the increase in the yaw misalignment.

7.3 Pitch misalignment

Test rig I is able to model four types of misalignments, as illustrated in section 3.2.3 (Figure 3.3), one of which is pitch misalignment. This can be modelled by tilting and fixing the driven holding block to the required angle. The pitch angle discussed in this section will be represented as β (degrees).

Figure 7.15 illustrates the wear of the machine cut nylon gear pairs that were tested at three different angles of pitch misalignment, at the running speed of 1000 RPM and under the applied torque of 9 Nm. The wear result of the aligned test (β = 0.0°) and 9 Nm was represented here for comparison purposes. The wear curves showed different trends compared to the common previously defined wear trend.

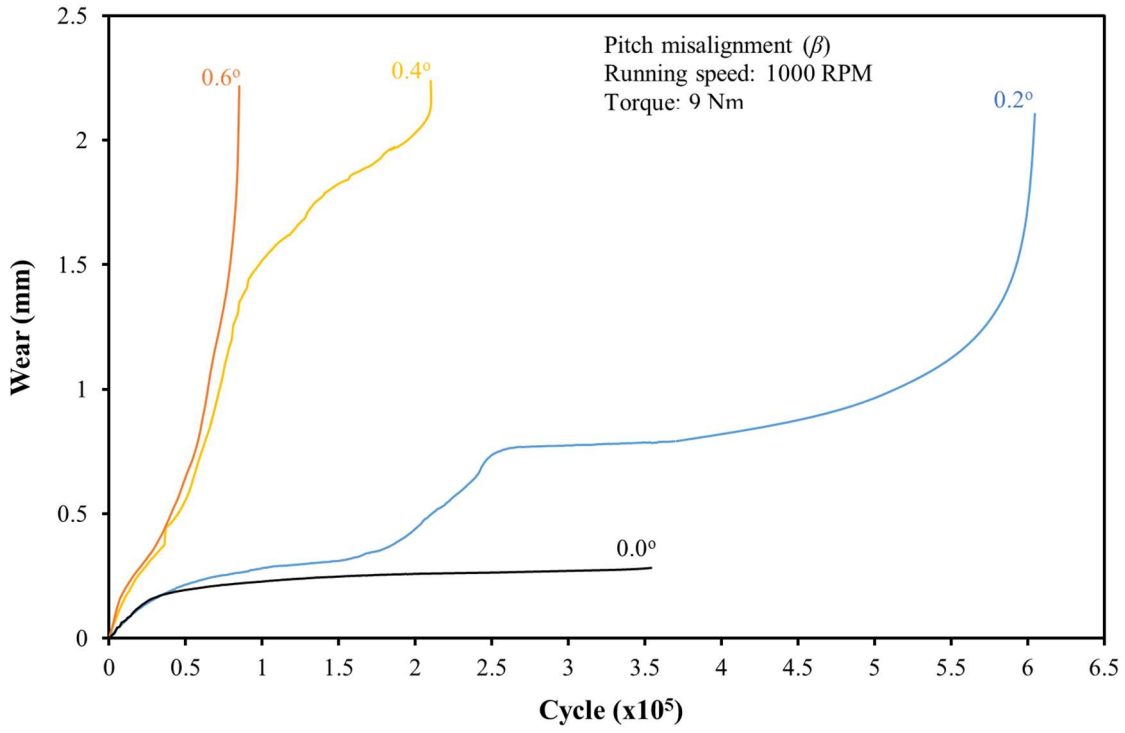

Figure 7.15 Wear of machine cut nylon gears, running at 1000 RPM, under the applied torque of 9 Nm and at different angles of pitch misalignments

At β = 0.2°, the tooth wear experienced five stages of wear. Starting with the running-in stage with high increase in wear, it moved to a nearly-linear stage, where the wear rate settled down. This was followed by a second stage of high wear increase and then a second nearly-linear wear stage. Finally, the wear increased greatly, reaching the tooth fracture stage where the test was automatically stopped.

Increasing the pitch misalignment to β = 0.4° gives another sequence of gear tooth wear stages. It started with the running-in wear stage with a high increase in wear. This was followed by a sudden jump in wear before rapidly increasing again. A nearly-linear wear stage (although with quite high wear rate) then functioned for about 1 x 10^5 cycles before the gear teeth experienced the fracture stage and the end of the test.

At the pitch misalignment angle of β = 0.6°, only three stages of wear were shown. The wear was started with the running-in stage. This was followed by a dramatically high wear stage. Finally, the tooth reached the fracture stage, where the test rig stopped.

The wear rate of each wear curve was defined at the nearly-linear stage of β = 0.2° and β = 0.4°, and at the high wear stage of β = 0.6° by calculating the slope of the linear trendline. Table 7.2 and Figure 7.16 illustrate the wear rate of the machine cut nylon gear pairs that were tested at different pitch misalignment (β = 0.0°, 0.2°, 0.4° and 0.6°), at the running speed of 1000 RPM and under the applied load of 9 Nm. The wear rate showed a relatively small increase for a pitch angle increase to 0.2°, especially during the second nearly-linear wear stage. This wear rate was dramatically increased, nearly seven-fold, with β increased to 0.4°. When the pitch angle was increased to β = 0.6°, the wear rate was dramatically increased nearly eight-fold over that β at 0.4°. Therefore, it can be concluded that a small amount of pitch misalignment, to the maximum of 0.2°, may have a small effect on the nylon gear tooth wear behaviour, while in case of slightly higher pitch misalignment, the tooth may experience high wear rate behaviour and severe damage.

Table 7.2 Wear rate of the machine cut nylon gear teeth, running at 1000 RPM, under the applied torque of 9 Nm and at different angles of pitch misalignment (NB: Two nearly-linear regions exist at B=0.2°)

Pitch angle (β) (degrees)	Backlash (mm)	Wear rate (mm/cycle x 10^5)	
0	0.16	0.0200	
0.2	0.08	0.0553	0.0269
0.4	0.04	0.478	
0.6	0.00	3.247	

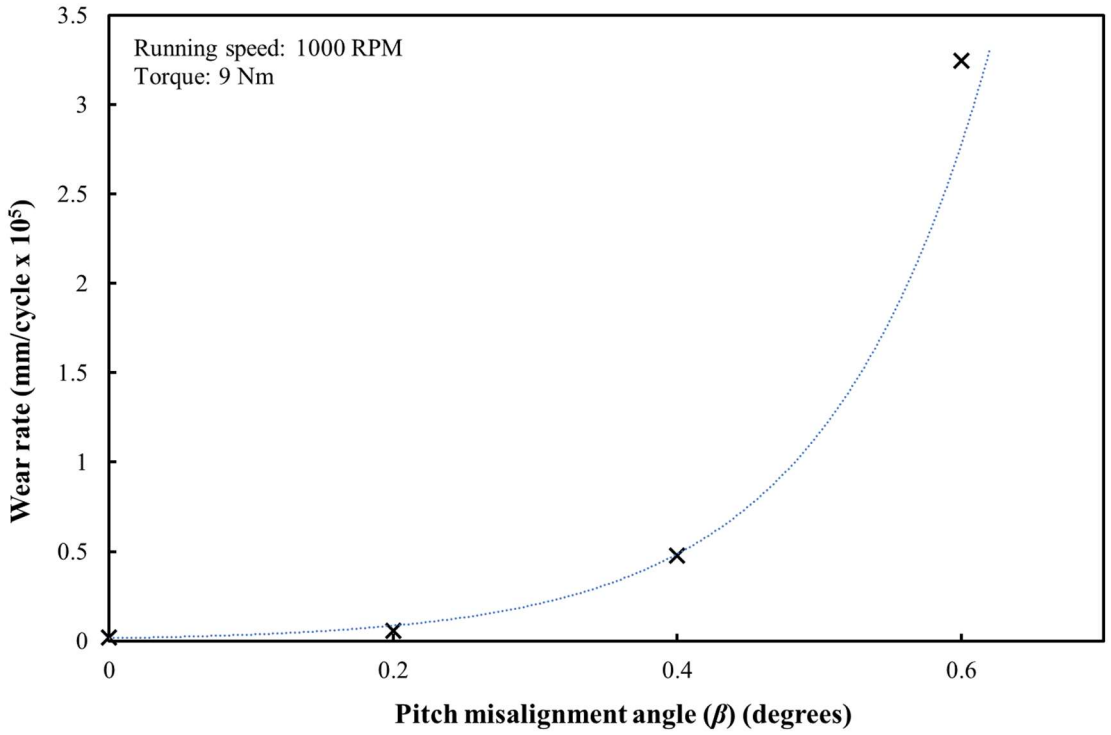

Figure 7.16 Wear rate of the machine cut nylon gear teeth, running at 1000 RPM, under the applied torque of 9 Nm and at different angles of pitch misalignment (with an exponential trendline).

With the aim of better understanding the wear and wear rate behaviour with respect to the pitch angle misalignment, the tooth surface maximum temperature was measured for all tested gear pairs, using the IR thermal imaging camera. The low pitch angle test showed a maximum surface temperature pattern that was different to the other two higher pitch angle tests.

Figure 7.17 illustrates the maximum tooth surface temperature for a gear pair of machine cut nylon gears. The gears were tested at the running speed of 1000 RPM, under the applied torque of 9 Nm and with a pitch misalignment of 0.2°. The curves showed an increase in the maximum surface temperature during the running-in stage of wear and the early part of the nearly-linear wear stage (1.5 x 10^5 cycles), reaching a maximum of 70°C. This was followed by a rapid increase in the maximum surface temperature over the next 1 x 10^5 cycles, reaching a peak maximum of 180°C. In this period, the gear was experiencing the second stage of the high wear. Between 2.5 x 10^5 cycles and 3.5 x 10^5 cycles, the maximum surface temperature decreased to around 135°C. This corresponded to the second stage of nearly-linear tooth wear. Gear tooth maximum temperature then increased again, reaching the peak of 180°C at 5.5 x 10^5 cycles. This was followed by a relatively small temperature decrease of 20°C for the next 0.5 x 10^5 cycles. The gear teeth then fractured at around 6 x 10^5 cycles and the test was stopped. Gears were then left to cool down and the surface maximum temperature reached 35°C in around half an hour. Because of the high speed moving gears, the maximum surface temperature result was fluctuated throughout the running time, with an average change of around 20°C.

The large increase in tooth surface temperature between 1.5 x 10^5 cycles and 2.5 x 10^5 cycles was thought to be one of the reasons for the second high wear increase stage in this specific test. During and before this period, the gear misalignment was causing reached engaged contact area, which is thought to be one of the causes of this high temperature increase. After reaching these high temperature values (higher than the glass transition point of the tested material, Figure 4.15), the tooth surfaces were highly worn, especially on the more highly loaded side, reaching the fully engaged state, where teeth contact area was increased to the maximum, which was thought to be the reason for the decreasing stage of the maximum surface temperature, as load sharing across the surfaces was increased. Similarly, this increase in the contact area leads to the second

stage of increase in maximum surface temperature to high values, which increases the wear rate again and causes the final tooth fracture.

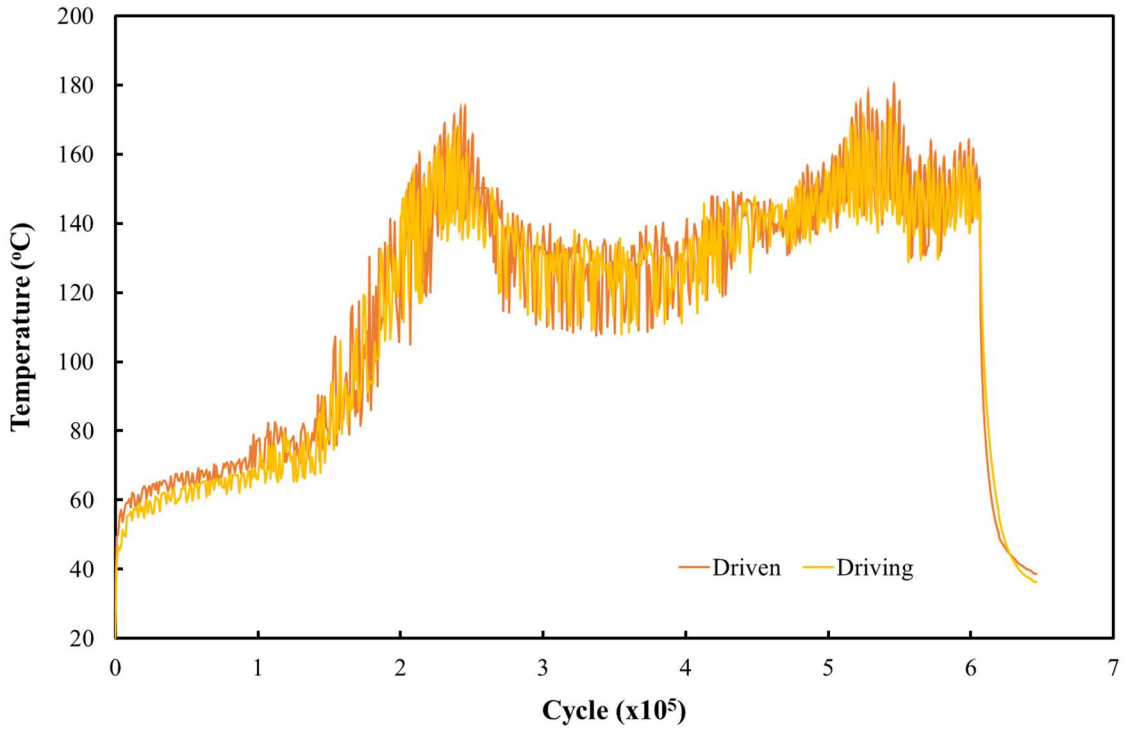

Figure 7.17 Maximum surface temperature of the machine cut nylon gear pair (9 Nm, 1000 RPM and pitch misalignment β = 0.2°)

Figure 7.18 shows the tooth surface maximum temperature of the pair of machine cut nylon gears that were tested at the speed of 1000 RPM, under 9 Nm torque and at a pitch misalignment β = 0.4°. Here, the maximum surface temperature trend is different to what was recorded in the β = 0.2° test. At the running-in wear stage (0 cycles to 0.4 x 10^5 cycles), the surface maximum temperature was increasing, reaching a maximum of 100°C. This was followed by a peak (at around 0.5 x 10^5 cycles) reaching the value of 140°C, before returning back to 125°C. The gear surface maximum temperature then increased to 160°C during the next 0.3 x 10^5 cycles. This was followed by a stable period for the next 0.7 x 10^5 cycles, before starting to increase again for the next 0.4 x 10^5 cycles reaching the

maximum temperature of 210°C. Gear teeth were fractured at 2.2 x 10^5 cycles and the test was stopped. The surface temperature then cooled down with a high rate, reaching 35°C in about 40 minutes. Because of the high speed running and the high instability of gear meshing as a result of the pitch misalignment, the recorded maximum surface temperature consistently experienced a high amount of fluctuation, typically around for 20°C.

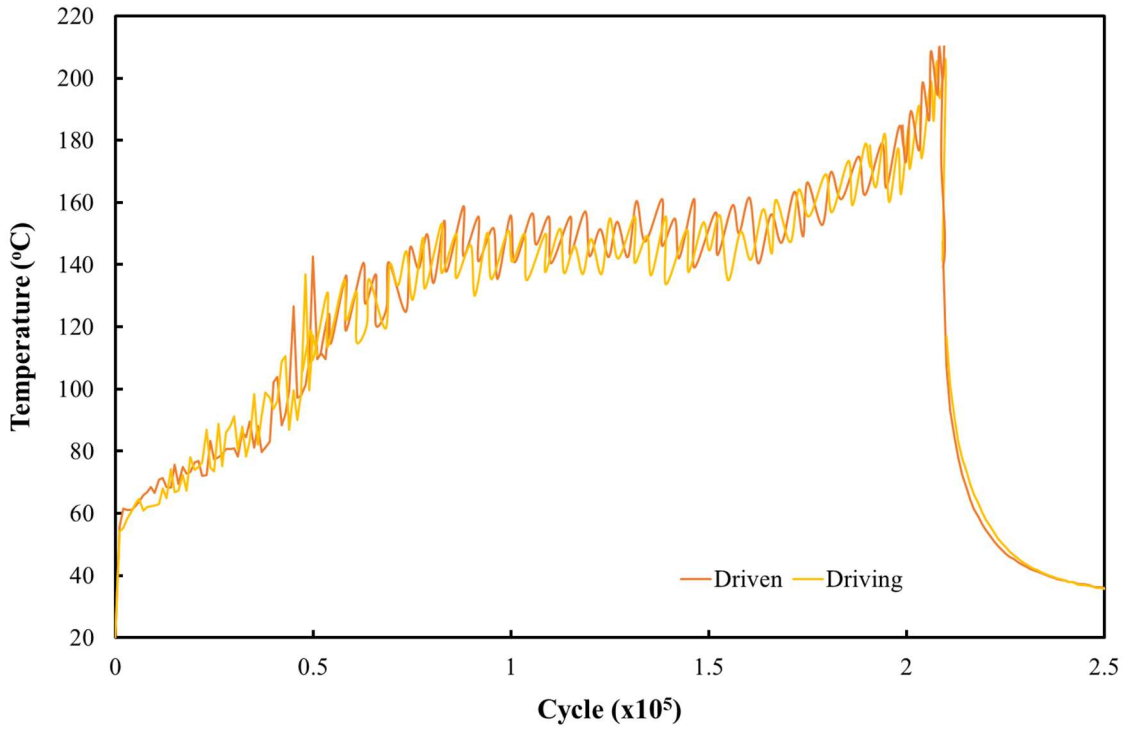

Figure 7.18 Maximum surface temperature of the machine cut nylon gear pair (9 Nm, 1000 RPM and pitch misalignment β = 0.4°)

The running-in wear stage in Figure 7.15, at β = 0.4°, can be linked to the early stage of increasing maximum temperature in Figure 7.18. At this stage, the gear teeth were not in a full conjugate contact, due to the pitch misalignment. The sudden increase in the surface temperature, reaching a value that was higher than the glass transition point, may explain the high jump in wear phenomena at the same period of running time. This jump in

wear may previously affect the highly loaded side of the teeth, which may then increase the contact zone area between the driving and driven gears. This may explain the sudden decrease in temperature before it started to increase again for the same reason as previously discussed. The second increase in surface temperature corresponds to the second high increase in the wear curve. This period was followed by a stable surface temperature period, which corresponds to the nearly-linear wear stage. This decrease in wear rate at this period could be because of the softened material that may function as an internal lubricant. Finally, the last surface temperature increase explains the high increase in wear and teeth fracture.

Figure 7.19 shows the tooth surface maximum temperature of the machine cut nylon gear pair that was tested at the running speed of 1000 RPM, under the applied load of 9 Nm and the effect of pitch misalignment of β = 0.6°. The temperature curve trend here is different to those in the two previous tests. During the running-in wear stage (the first 0.2 x 10^5 cycles), the maximum surface temperature was increasing, reaching of 100°C. This high temperature increase rate, reaching the glass transition point of the tested material, could lead to the fast wear of the more highly loaded side of the teeth, in turn leading to an increase in the area of contact between the two gears. This was followed by another stage of increasingly maximum surface temperature between 0.2 x 10^5 cycles and 0.7 x 10^5 cycles, reaching the value of 190°C. The following 0.1 x 10^5 cycles were experienced a stable period of maximum surface temperature before it dramatically increased to around 210°C at 0.88 x 10^5 cycles, where the teeth were fractured, and the test was stopped. The gears were than left to cool down and the maximum surface temperature reached that at the start within half an hour.

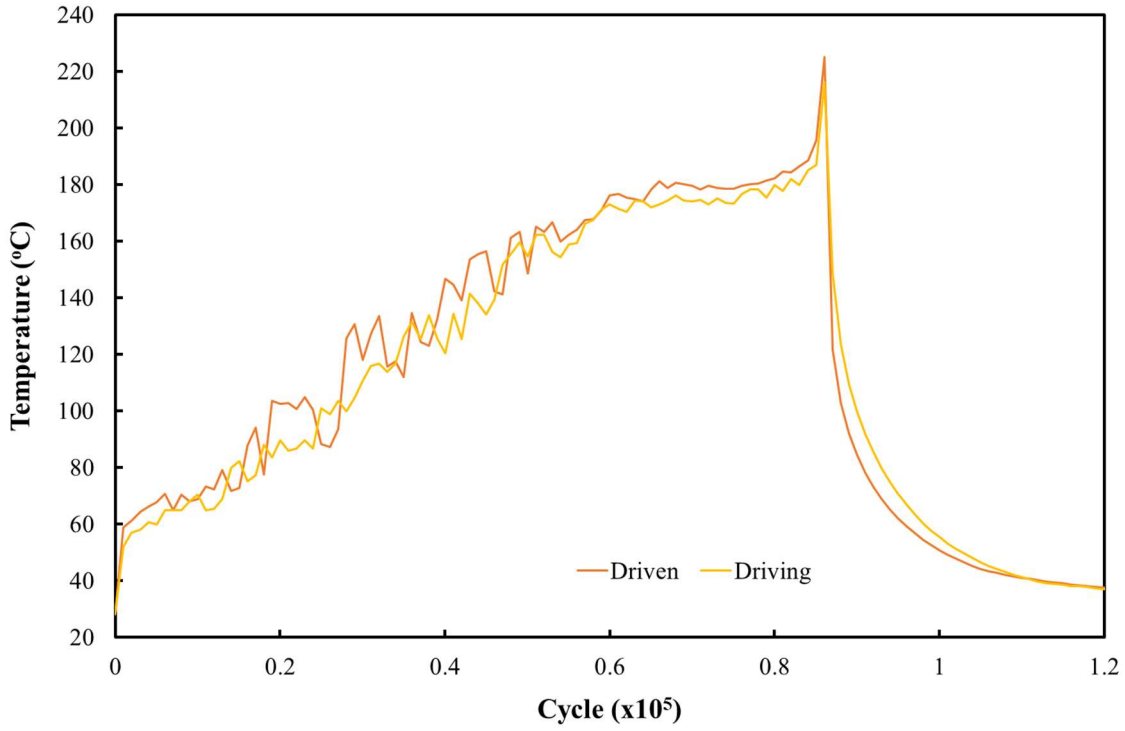

Figure 7.19 Maximum surface temperature of the machine cut nylon gear pair (9 Nm, 1000 RPM and pitch misalignment β = 0.6°)

Figure 7.20, Figure 7.21 and Figure 7.22 show a general overview of the after-test gears.

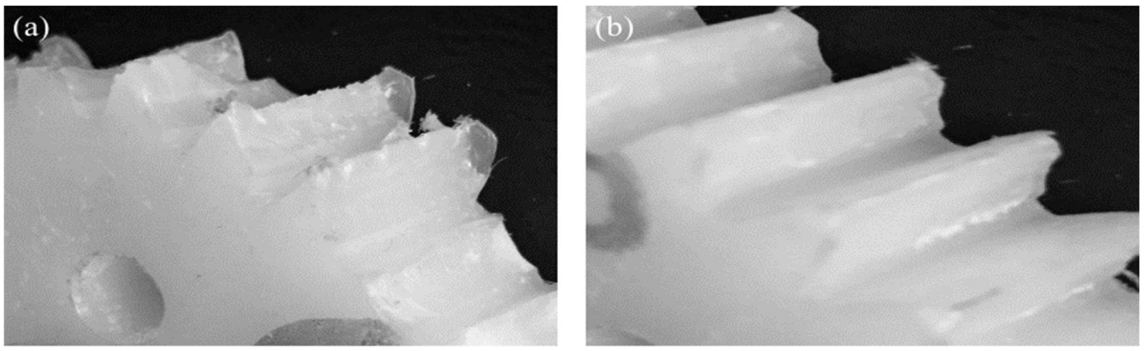

Figure 7.20 (a) The driving and (b) the driven machine cut nylon gear after testing at 1000 RPM, under 9 Nm torque and 0.2° pitch misalignment

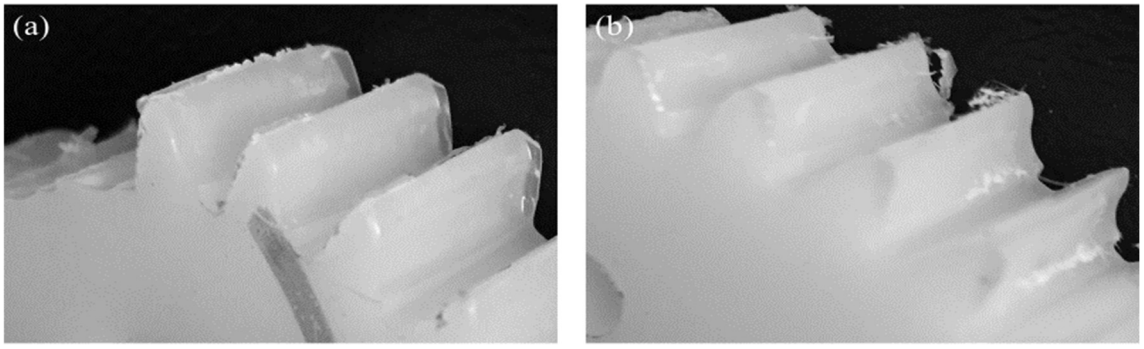

Figure 7.21 (a) The driving and (b) the driven machine cut nylon gear after testing at 1000 RPM, under 9 Nm torque and 0.4° pitch misalignment

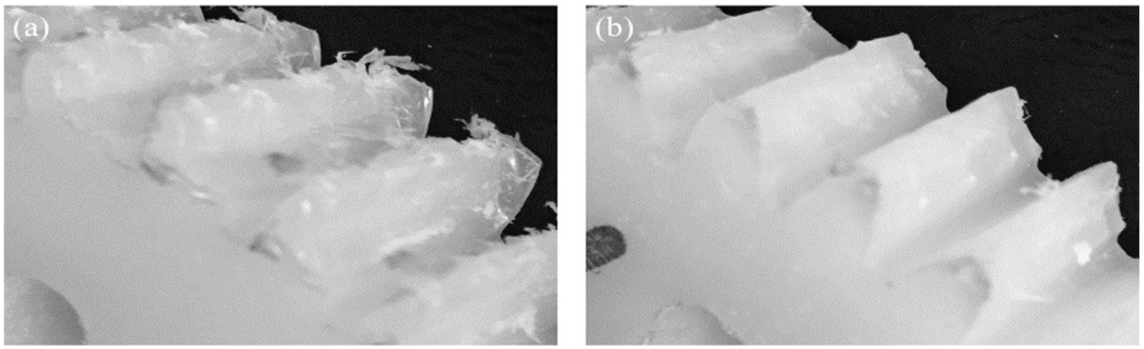

Figure 7.22 (a) The driving and (b) the driven machine cut nylon gear after testing at 1000 RPM, under 9 Nm torque and 0.6° pitch misalignment

All the tested gear pairs were further investigated using the methods discussed section 3.8. Gear tooth surface investigation was carried out using the SEM to further understand the wear and failure mechanisms under the effect of the pitch misalignment. Because the gear teeth experienced pressure and friction conditions differently at each side, the SEM examination was done for both sides of each tooth to allow general comparisons.

Figure 7.23 illustrates the SEM plates for the machine cut driving gear that was tested at the speed of 1000 RPM, under 9 Nm torque and with a pitch misalignment angle of 0.2°. Different surface tribology was observed between the left side and the right side of the tooth, because of the

differences in load and mesh characteristics, as an effect of the pitch misalignment.

The sliding direction at the addendum side of the tooth surface was from the pitch line to the tip. Figure 7.23 (a), (b) and (c) show a common abrasive wear type across that area of the tooth surface. Moving towards the right side of the tooth, we can see more pitting wear, whereas the left side has more the form of plastic flow wear. Neither microcracks nor debris were found in this area.

Moving towards the pitch line (Figure 7.23 (d) and (e)), a clear groove right across the tooth surface can be seen, which is the result of the opposite sliding directions. This groove appears to be the initial propagation of the surface crack, which, after development, leads to tooth pitch line fracture. Abrasive wear can be found at this area of the tooth. No microcracks were found here.

Or the dedendum side of the tooth surface (Figure 7.23 (f), (g) and (h)), the form of abrasive wear can be seen. More intensive wear was observed to the right side, where the higher load was active, whereas comparably lower wear effect can be seen to the left. The uneven surface observed from left to right could be directly because of the pitch misalignment.

Generally, the differences between the left and right sides of the tooth surface is low here, because of the low misalignment angle.

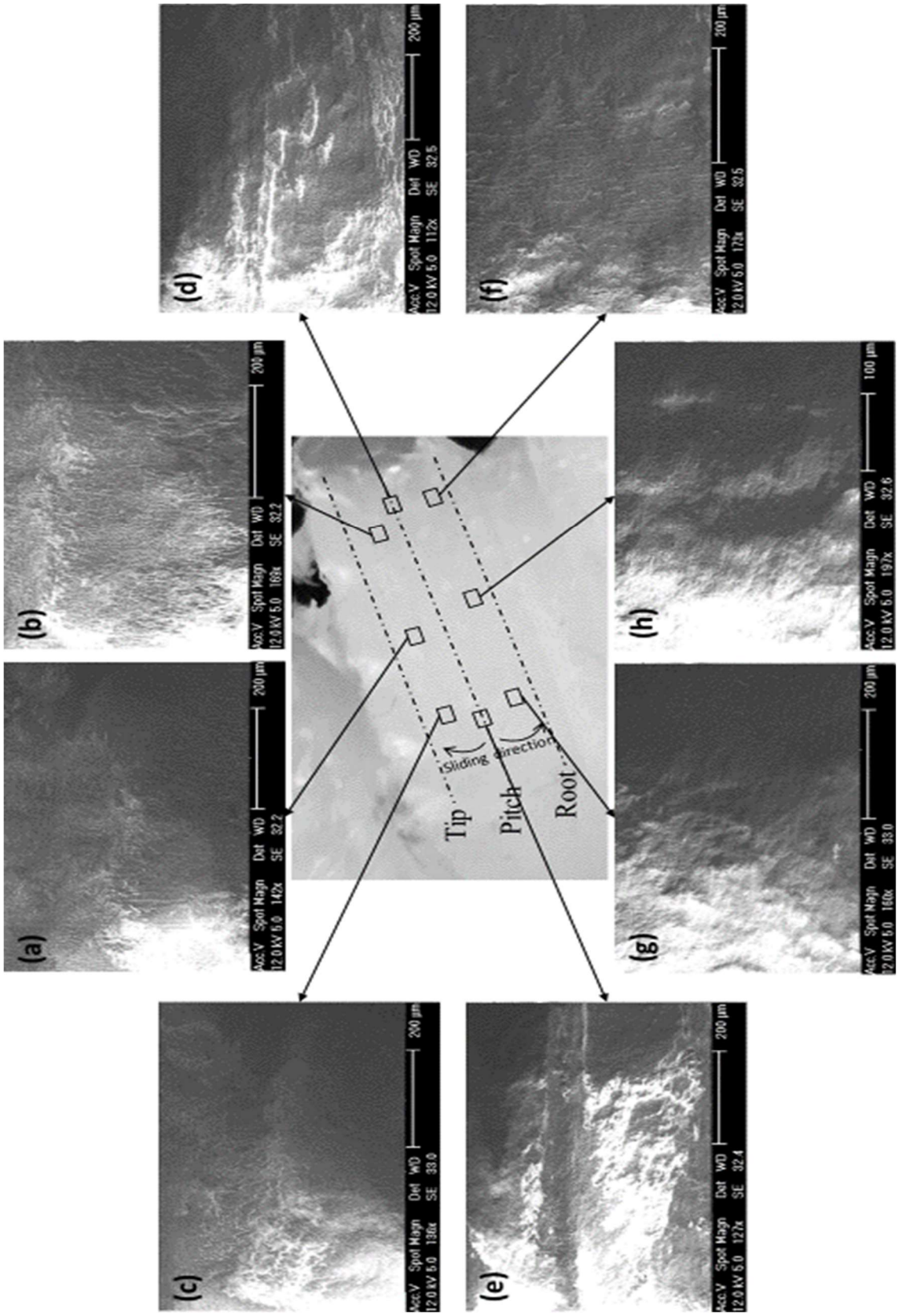

Figure 7.23 SEMs for the driving machine cut nylon gear, tested at 1000 RPM, under 9 Nm torque and with pitch misalignment of β = 0.2°

Figure 7.24 shows the SEM images for the driven machine cut nylon gear tooth surface that was tested at the speed of 1000 RPM, under the applied torque of 9 Nm and to model a pitch misalignment angle of 0.2º. The addendum side of the tooth surface (Figure 7.24 (a), (b) and (c)) showed more evidence of abrasive wear, with a higher amount to the right side, where higher loads were expected. The phenomenon associated with side sliding directions was clear in this area and more active to the left side. This is one of the consequences of the pitch misalignment. Some form of plastic flow can be seen to the left side of the tooth.

Around the pitch line area (Figure 7.24 (d) and (e)), a highly pitted surface can be observed. Change of the sliding direction leads to some surface peaks. Extra surface damage occurred to the right side, whereas some surface microcracks were discovered at the left side of the tooth. No wear debris was found here as a result of the sliding direction, which supports the idea of the occurrence of the sideways sliding because of the pitch misalignment.

Figure 7.24 (f), (g) and (h) show the surface tribology of the dedendum side of the tooth. In this area, abrasive wear can be recognised across the surface. Heavier wear, with some abrasive wear can be seen to the right. Some plastic flow wear was found to the left side of the tooth. Microcracks were not present anywhere in the area.

In general, the effect of the 0.2º pitch misalignment was relatively small, which material with the low increase in wear rate.

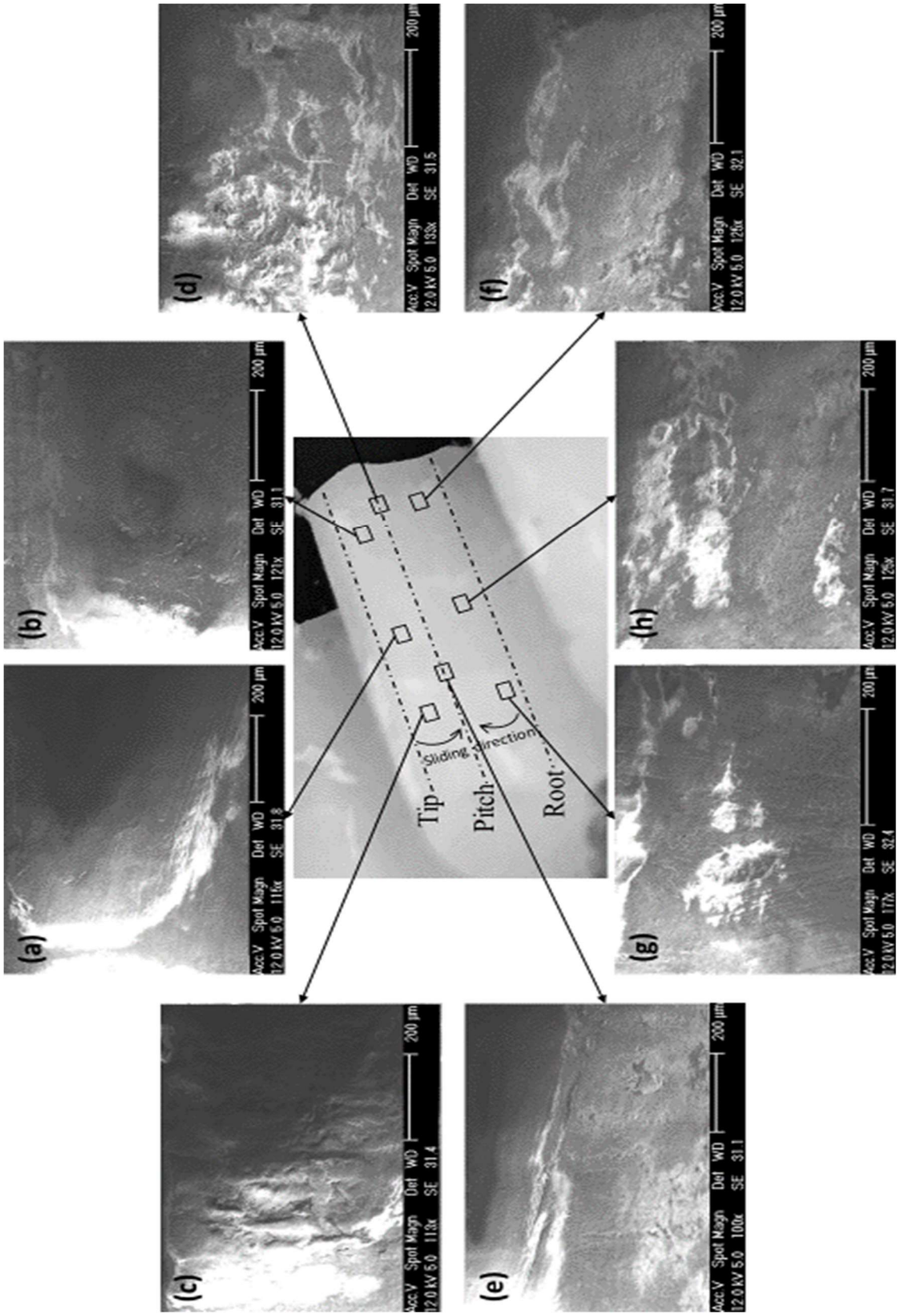

Figure 7.24 SEMs for the driven machine cut nylon gear, tested at 1000 RPM, under 9 Nm torque and with pitch misalignment of β = 0.2°

More effects started to appear on the tooth surfaces with the increase of pitch misalignment angle. Figure 7.25 shows the SEM plates for the tooth surface of the machine cut nylon driving gear that was tested at the speed of 1000 RPM, under the applied load of 9 Nm and modelling a pitch misalignment at an angle of $\alpha = 0.4^{o}$.

Between the pitch line and tip of the tooth surface (Figure 7.25 (a), (b) and (c)), abrasive wear was common across the area. Higher wear damage was found to the right side, where the load is higher, than the left side. Some surface pitting was observed at the middle and right side of the tooth surface. No microcracks were found at this area of the tooth.

Within the pitch line area (Figure 7.25 (d) and (e)), a surface groove similar, to the previous test was discovered. This groove becomes wider when moving to the right side of the tooth surface. As in the previous test, this groove could be because of the sliding direction, which was acting from the pitch line towards the tip and root sides of the tooth. More indications of plastic flow wear were found in this area.

The dedendum side of the tooth surface (Figure 7.25 (f), (g) and (h)) showed some adhesive wear to the right and plastic flow to the left of the gear. Surface microcracks rarely formed to the right side of the tooth surface. No debris was found anywhere in the area.

In general, relatively higher wear variety was found here, compared to the previous test, between the two sides of the tooth surface.

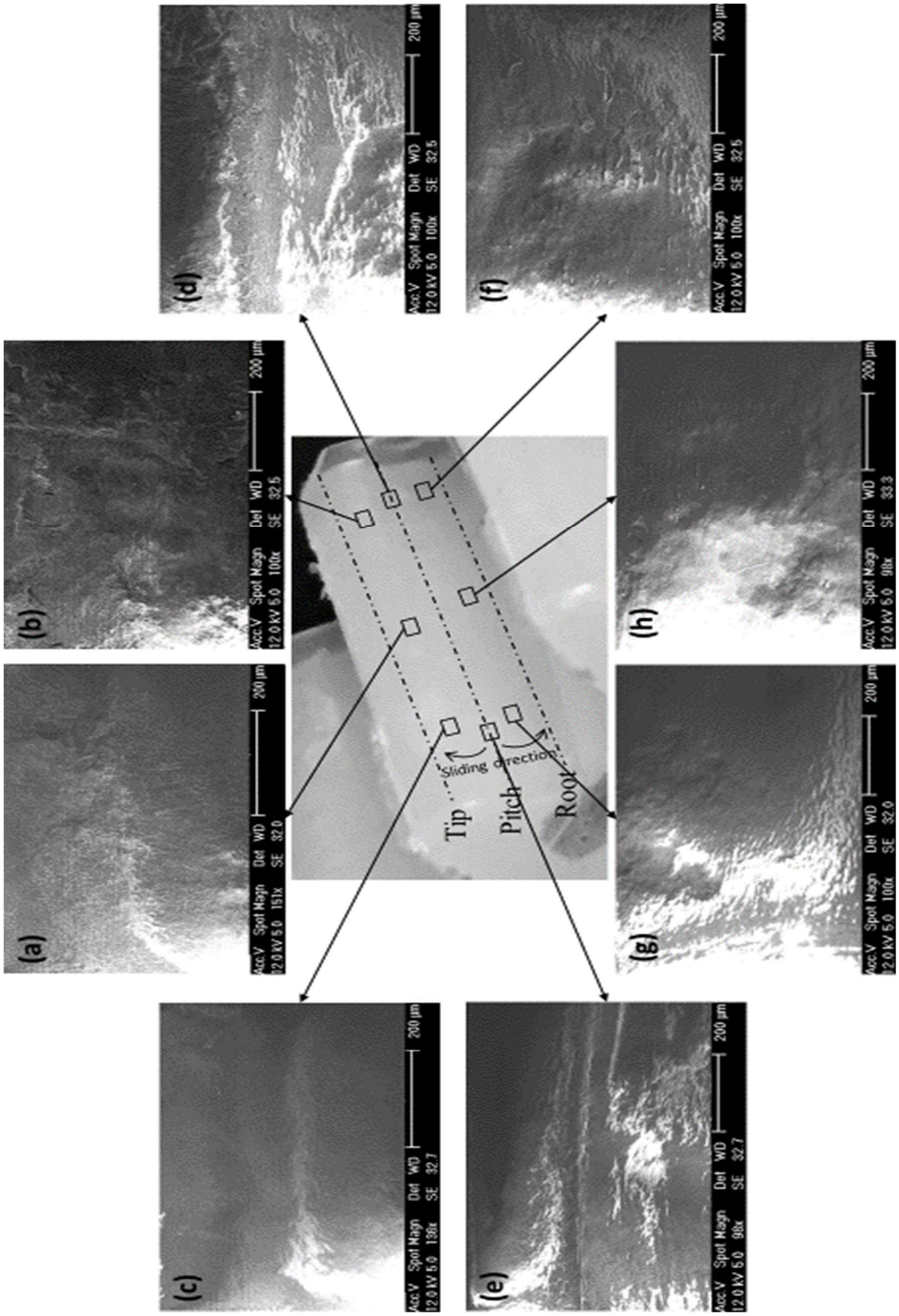

Figure 7.25 SEMs for the driving machine cut nylon gear, tested at 1000 RPM, under 9 Nm torque and with pitch misalignment of β = 0.4°

Figure 7.26 shows the SEM of the tooth surface for the machine cut driven gear, which was tested to model a pitch misalignment angle of $\beta = 0.4^{o}$, at the speed of 1000 RPM and under the applied torque of 9 Nm.

At the addendum side of the tooth (Figure 7.26 (a), (b) and (c)), the SEM showed a general abrasive wear across the surface, with more severity towards the right side. Some adhesive wear was found to the left side of the tooth. No microcracks were found at this area of the tooth. A Sideways sliding direction can be recognised more at the left side.

Moving to the pitch line area (Figure 7.26 (d) and (e)), the form of wear that can be seen here is tending to be more of non-directed adhesive wear, due to the variation of the sliding direction in the area, and the low material modulus of elasticity. Microcracks were hardly seen around the pitch line of the driven gear.

Between the tooth root and the pitch line (Figure 7.26 (f), (g) and (h)), surface adhesive wear was observed to the middle and right side of the tooth. The left side surface was predominately undergoing plastic flow wear. No debris was found in this area.

In general, with the increase of the pitch misalignment, the form of wear for both the driving and driven gears started to change from a concentration of abrasive wear to a concentrating adhesive wear. At both teeth, the wear form was changing between the left and right side of the surface due to the gear pitch misalignment.

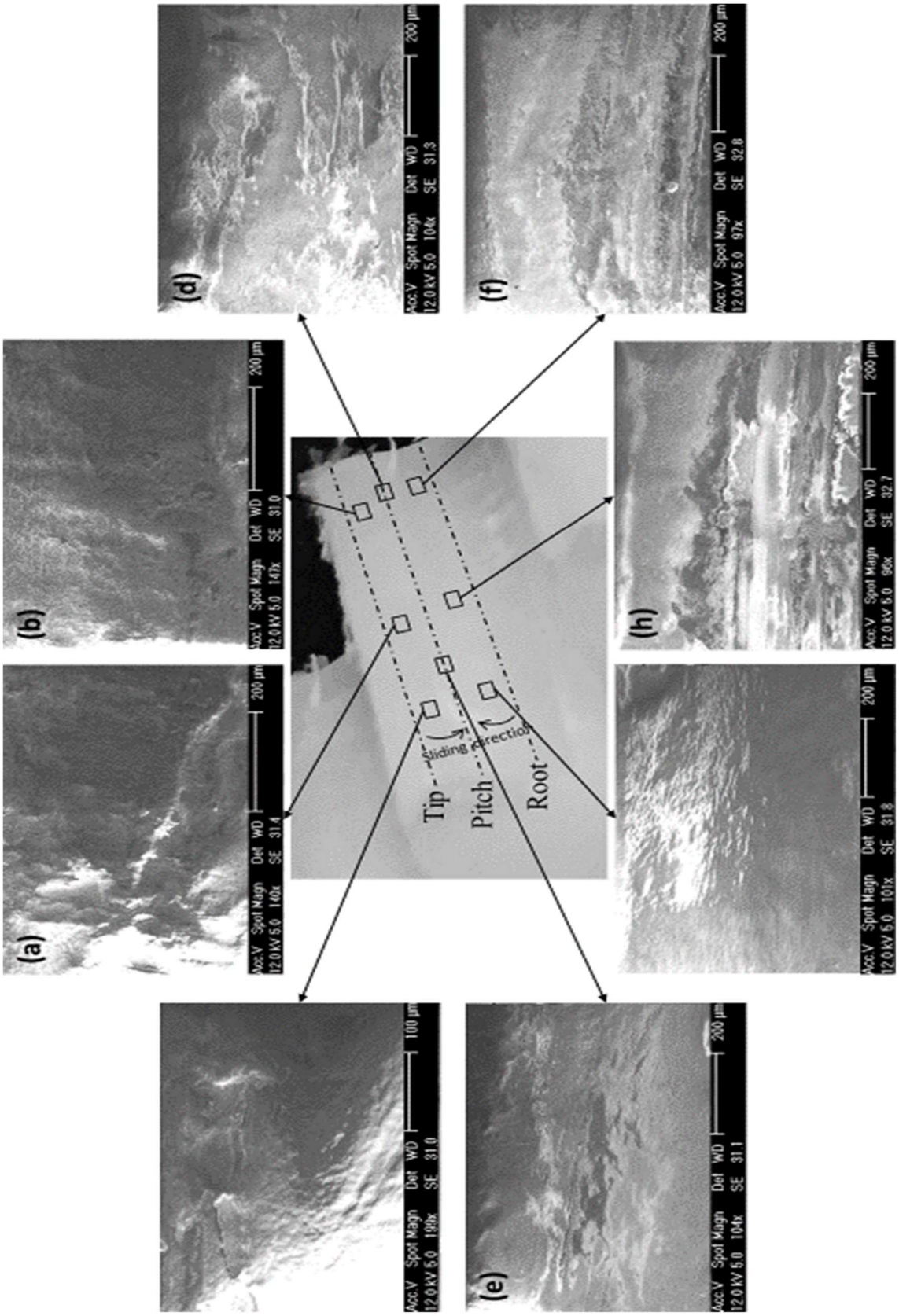

Figure 7.26 SEMs for the driven machine cut nylon gear, tested at 1000 RPM, under 9 Nm torque and with pitch misalignment of β = 0.4°

A higher pitch misalignment angle of 0.6º leads to six folds increase in wear rate of the machine cut nylon gear. Figure 7.27 shows the SEM for the driving gear tooth surface that was tested at 1000 RPM, under the applied load of 9 Nm and at the pitch misalignment of β = 0.6º.

The addendum side of the tooth surface (Figure 7.27 (a), (b) and (c)), has some softened material, which could arise because of the large increase in surface temperature in that area. Adhesive wear could be seen more to the middle and right side of the tooth, while abrasive wear was common to the left. The softened material chips were taken off the surface in the direction of sliding.

Moving to the pitch line (Figure 7.27 (d) and (e)), one small crack was found across the right side of the tooth. Adhesive wear was common in this part of the tooth. The chips taken out did not indicate a consistent sliding direction because it rapidly changes in this.

To the dedendum side of the tooth (Figure 7.27 (f), (g) and (h)), abrasive wear was active to the right side of the tooth. One small crack was observed at the right edge. More evidence of micro pitting was found near the middle and some plastic flow wear was discovered to the left side. Neither debris nor microcracks were found at this area.

The tooth experienced a greater variety of surface damage than was found in the previous test.

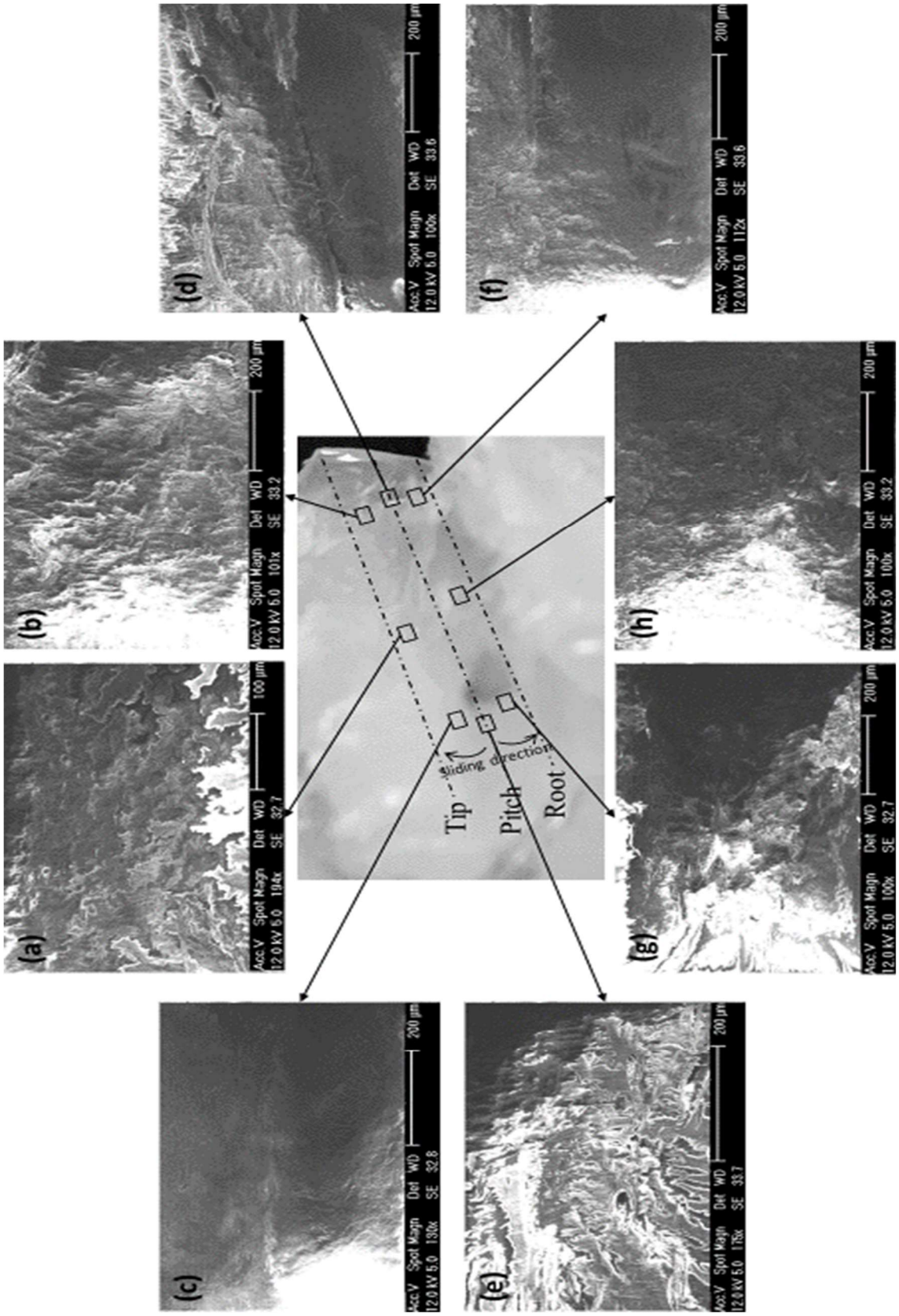

Figure 7.27 SEMs for the driving machine cut nylon gear, tested at 1000 RPM, under 9 Nm torque and with pitch misalignment of β = 0.6°

Figure 7.28 shows the SEM for the machine cut driven gear tooth that gear was tested at the speed of 1000 RPM, under the applied torque of 9 Nm and with a pitch misalignment of 0.6º. The driven gear tooth showed less surface damage than the driving gear tooth. No tooth fracture was observed in the driven gear.

The addendum side of the tooth surface (Figure 7.28 (a), (b) and (c)) showed a highly softened and damaged surface with some surface micro pitting. In this area, the tooth was experiencing high load impacts at the start of the mesh. The right side of the tooth experienced more adhesive wear. On the other hand, the left side of the gear was undergoing abrasive wear.

Around the pitch line of the tooth (Figure 7.28 (d) and (e)), the surface showed more adhesive wear and a softened surface to the right side and plastic flow wear to the left side. No microcracks were found at this area. In addition, debris was not collected here, as in aligned tests, because of the side sliding that takes it out of the contact area towards the edges of the gears.

To the dedendum side of the tooth (Figure 7.28 (f), (g) and (h)), the surface experienced more abrasive wear, with some plastic flow towards the left side of the tooth. The side sliding direction can be seen in some parts of this area.

Generally, there were some surface wear differences across the tooth surface. Softened tooth surfaces were observed more to the right of the tooth, while abrasive wear was found to the left side of the tooth.

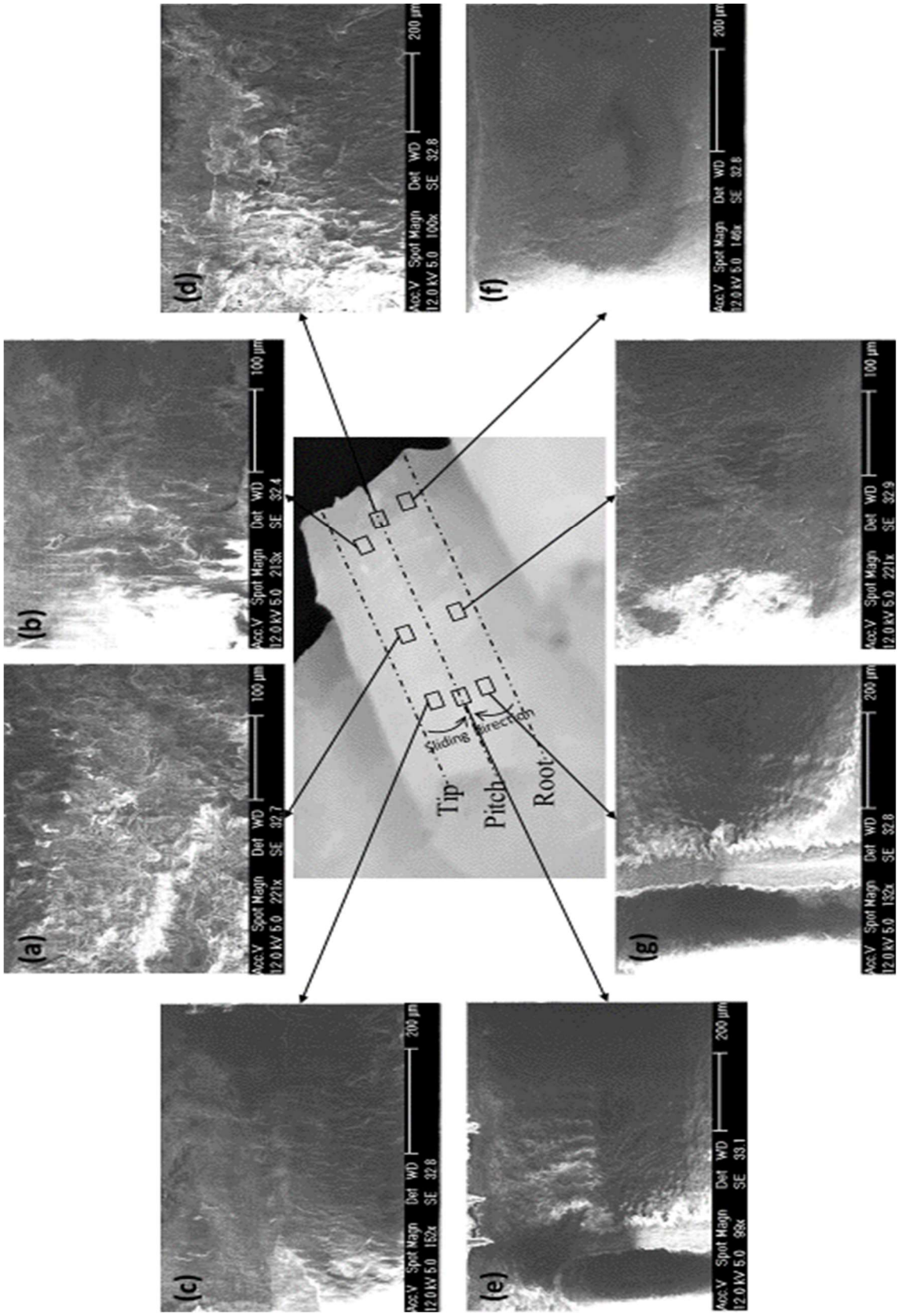

Figure 7.28 SEMs for the driven machine cut nylon gear, tested at 1000 RPM, under 9 Nm torque and with pitch misalignment of β = 0.6°

To summarise, the pitch misalignment for machine cut nylon gear has a variable effect on tooth wear rate, depending on the misalignment angle. At low pitch misalignment angle (β = 0.2°), the wear rate experienced a small increase, compared to the aligned test. Doubling that angle leads to a seven times increase in wear rate and a further similar increase in the angle leads to a nearly similar increase in wear rate. This means that there is a critical point of which the wear rate and tooth damage are extremely affected afterwards. Pitch misalignment critical angle could be around β = 0.2°. In general, the wear curves with pitch misalignment showed different trends than the common one regularly seen in the tests.

The tooth wear phenomena were more readily understood when measuring the running tooth maximum surface temperature. This measurement reveals the tooth behaviour with pitch misalignment. When the load was applied, and the misaligned gear pair started to run, there was a large increase in surface maximum temperature, which cooled down slightly afterwards. This was related to the surface temperature reaching above the glass transition point of the tested material, which leads to a high tooth wear and deflection. This change in gear tooth shape leads to an increase in the surface contact area between the two teeth, leading to the surface temperature decrease that was observed in the measurements.

The after-test tooth surface investigations using the SEM revealed two common types of wear, namely adhesive wear and softened surfaces. The softened surface wear occurs mostly at the more highly loaded side of the tooth, which occur because of the misaligned meshing. A abrasive wear occurs mostly to the other, less loaded, side of the tooth, for the same reason. Some other types of surface wear were found at different places, but in much smaller amounts compared to these two major types. Tooth microcracks were not common in the pitch misalignment tests, but some small cracks were found on the driving gear, for which teeth failed before these or the driven gear. Side sliding was found to function in all misalignment tests, with increased effect on the pitch angle increased. The

phenomena of side sliding was confirmed in all tests, with more intensity as the pitch misalignment angle increased. In general, the tooth damage was found to be more severe as the pitch misalignment increased.

7.4 Summary

In this chapter, the effect of some types of gear misalignment was tested. Some modelled misalignments were designed using test rig I. The tested gear teeth wear and wear rate wear defined and related to the aligned tests. Continuous wear rate increase was found with the increase of yaw and pitch misalignment angles. Gear surface temperature was measured during the continuous run of the tests. And further gear tooth surface investigations were carried out to understand the effect of different gear misalignments on the tooth surface tribology.

It was found that the small increase of yaw misalignment angle slightly increases the wear rate of the nylon gear. This wear rate was dramatically increased with the reach of a critical point of yaw misalignment angle. Pitch misalignment showed higher effect on wear rate, with dramatical increase even at small angle increase.

Measuring the surface maximum temperature for both the driving and the driven gear pair revealed special gear surface temperature phenomena with the relation of the tooth wear behaviour. The gear surface temperature reached the glass transition early, helping the gear to wear out quickly at the mostly loaded side and increases the contact area, which, in consequence, decreases the surface temperature again.

The tribological behaviour of the gear tooth surfaces was investigated and linked to the gear wear behaviour. It was found that surface tribology varies at each side of the teeth. High effect severe wear was found mostly to the highly loaded side of the gear, as a result of the gear misalignment. Different types of surface wear can be found in the two sides of a single tooth.

Chapter 8
CONCLUSION AND FUTURE WORK

8.1 Conclusions

The wear behaviour against load and speed variables of polymer gears has been tested using enhancements of test rigs uniquely designed for this purpose. Gear pairs made from four different materials and by two manufacturing methods were monitored continuously for their wear and wear rate at speeds typical of smaller power applications and different loads that allow practical working ranges to be determined. Dry running and oil lubrication were studied and gear misalignment effects were modelled. The experimental data were analysed and compared with the available literature. Good agreements were found in overlapping regimes, providing confidence that the new data obtained here is of value for guiding design. The following sections consider each major experimental sequence individually.

8.1.1 Step-loading tests (Chapter 4)

Step-loading tests were carried out on polymer gears made of different materials in a dry-running condition. The samples were manufactured using two different methods, namely injection moulded and machine cut. The amount of tooth thickness reduction with time was recorded at each increment of step-load. Consequently, the wear rate of polymer gear teeth with respect to the number of cycles was found at each load, with an initially agreed accuracy. This technique was introduced as a rapid and

inexpensive approach for initial scoping trials, for routine quality assurance tests and other such needs.

The increase in acetal gear wear rate with respect to load increase was mostly stable and nearly linear at low loads, but this trend ended suddenly with a high increase at a specific torque, defined as the transition point. It was found that the transition point of the machined cut acetal gear is at 7 Nm. Further investigations revealed that this sudden increase in wear rate was linked to the gear surface temperature, which reaches critical values, near the melting point of the tested material. Theoretical evaluations related to the maximum surface temperature of a dry-running polymer gear revealed a good agreement with these findings.

The wear rate trend with load for nylon gears was found to be more complicated than for acetal gears. This wear rate varied both up and down over some successive torque increments in both injection moulded and machine cut samples. Similar findings appear in the literature. The phenomenon was further investigated as the higher-level wear rate trend of nylon gears is quite different from the nearly linear trend of acetal gears. It may be concluded that this high change in wear rate trend for nylon gears was caused by a tribological phenomenon whereby a thin film of molten material (arising for reasons of high temperature or pressure) was formed at some load ranges, and then acts as an internal lubricant. Further investigations using SEM carried out as part of the work discussed in Chapter 5 validate these polymer gear wear rate results. The injection moulded nylon gears had a load capacity between 9 Nm and 9.5 Nm, where the wear showed a large value transition. On the other hand, the load capacity of machine cut nylon gears was between 9.5 Nm and 10 Nm.

It was found that acetal and nylon gears had wear rates essentially independent of the manufacturing process, as both materials' wear showed close agreement despite of the production technique. Machine cut processing provides slight extra load capacity to nylon gears, but with

some increase in wear rates. This change could be because of material microstructure differences that were formed by the manufacturing process.

Injection moulded polycarbonate gears showed relatively similar patterns of wear rate to the other tested materials. One of the limitations found in this material is that its load capacity is considerably lower compared to other polymer gears. This could be partly because of the high friction in tooth surfaces that leads to high increases in surface temperature to values that exceed the glass transition point of that material. Some molten material was found at the root of the gear teeth.

8.1.2 Dry running testing (Chapter 5)

After establishing the general load capacity and wear behaviour of each polymer gear material using step-loading methods, larger-scale endurance tests were carried out under selected dry-running conditions. Each endurance test was designed to run at a continuously constant load and speed, using the purpose-designed test rig. The wear (as gear tooth thickness reduction) of each gear pair was recorded and logged against the number of running cycles. Gear tooth surface temperature was continuously measured during the test running. Further investigations, mostly with optical and electron microscopes, were carried out during and after the tests.

For the machine cut acetal gears, a gear pair was tested at the critical load of 7 Nm to reveal the wear and tribology phenomena at this point. The wear rate of this pair of gears showed reasonably good agreement between the endurance test and the step-loading test, which supports the suitability of the step-loading test as an initial polymer gear evaluation method. Further SEM investigations revealed some indications about the tooth surface tribology phenomena of the driving and driven gears. Scratch wear was found to be active in machine cut acetal gears, with the help of the

debris that was moving along the sliding directions between the two surfaces.

For the injection moulded nylon gear, two separate endurance tests were run at the initial and final loads considered in the step-loading test. These tests revealed that the accuracy of wear rate value could be increased at the step-loading test by somewhat increasing the amount of time for each loading period, for the reason that this material requires longer time than acetal to establish a nearly-linear wear stage. The SEM investigation for the lower load revealed that scuffing wear and surface plastic flow were the most common types of surface tribology behaviour in this material, with less debris held between the two rubbing surfaces. The collected debris was mostly shaped as micro-chips. On the other hand, for the higher loaded test SEM revealed that abrasive wear was more active, with debris formed as small fibres and acting as an abrasive material.

For the machine cut nylon gear, the two critical loads around where the wear rate decreases before increasing again (8.5 Nm and 9 Nm) were considered for endurance tests. The two long-run tests confirmed the wear rate decrease phenomenon that was discovered during the step-loading tests, especially in the early part of the nearly-linear wear stage. Gear surface maximum temperature was continuously measured while running tests. It showed a large decrease in tooth surface temperature with the load increase at these particular critical loads. Both wear rate and surface temperature decreases were thought to be because, with the load increase, there in an increase in surface pressure that affects the surface of the teeth. Some surface layers were observed on the tooth surface that are thought to be functioning as an internal lubricant. SEM investigations for the gear pairs in both tests provided similar conclusions. Softened material was found to cover different parts of the tooth surfaces for the gears that wear loaded by 9 Nm. Adhesive wear and plastic flow was found to be common in both tests, with more severity at 8.5 Nm load.

The effect of polymer gears' rotational speed change on wear rate was investigated. The results showed an increasing relation between the nylon gear wear rate and the running speed. In addition, load capacity showed high decrease with the increase in gear running speed.

8.1.3 Oil-lubricated testing (Chapter 6)

The effect of oil lubrication on the surface tribology and wear behaviour of polymer gears was investigated and discussed. Firstly, step-loading tests were run to define the gear load capacity and wear rate behaviour in comparison to dry running. It was found that gear load capacity was increased nearly three times with the use of oil lubricant. In addition, the wear rate was significantly decreased. Two regions of load were defined depending on the corresponding wear rate values, as low load range and high load range. Each range was further investigated by long-run tests.

Within the low load range, the tested gears ran continually at the nearly-linear wear stage, with very low wear rate, and no wear increase or fracture was experienced. Gear surface temperatures showed reasonably low values that reached to around, but did not exceeded, the glass transition point. Adhesive wear was most commonly found on tooth surfaces in the SEM investigation. Some surface plastic flow was also found. This was thought to be the reason for the increase in the surface temperature to near the glass transition point.

At the high load range, gears were mostly ran for a short time in the nearly-linear wear stage before they experienced a relatively sudden and large increase in wear rate and gear tooth fracture. In all tests, the wear rates were relatively high compared to those in the low load range. Gear surface temperature was measured to increase more in this case, reaching to values higher than the glass transition point. This higher temperature increase is directly implicated in the large jump in wear rate and tooth fracture. The

SEMs revealed that adhesive and abrasive wear were the dominant mechanisms in all these tests.

A continuous long-run test, lasting for one week, was instigated at a low load value to investigate the endurance of the gears under the effect of oil lubricant. It revealed a long nearly-stable and nearly-linear stage. The wear rate was relatively low and, throughout, the gears did not experience any increase in wear rate or gear tooth fracture. The tooth surface temperature fluctuated somewhat over the running time, with values mostly around, but the extremes not exceeding, the glass transition point.

8.1.4 Testing under misalignment (Chapter 7)

The effect of gear misalignment on the surface tribology and wear behaviour of polymer gears was studied and analysed by using special features of the test rigs to introduce small, controlled deviations from the ideal geometric arrangement of gear pairs. The majority of the effort was concentrated on pitch and yaw effects, which appear to be the most critical ones in practice.

For yaw misalignment, gear tooth surfaces showed the typical three stages of wear that were observed in the aligned gear tests, namely running-in, nearly-linear phase and then severe wear and tooth fracture. The wear rate showed a rapidly increasing correlation with yaw misalignment angle increase. Relatively high wear rate and tooth damage were seen at yaw misalignment angles above 0.8°, but the effect on practical lifetimes was tolerable up to 0.4°. At all tests, the gear maximum surface temperature showed two stages of increase that were separated by a decreasing stage. From the first increase, the surface temperature reached levels that exceeded the glass transition point of the material. The middle decreasing stage was thought to be because of changes in the area of the tooth contact surfaces. SEMs showed different tribological behaviour between the left and right sides of the gear because of the yaw misalignment effect.

For the pitch misalignment, the wear behaviour showed different pattern with respect to running cycles. Five wear stages were recognised. Similar to yaw misalignment, the wear rate showed rapid increase with increase in pitch misalignment angle. A very high wear rate occurred at the at pitch misalignment angles above 0.4°, but the effect on practical lifetimes was tolerable up to 0.2°. The surface temperature measurement revealed some variation with the running cycles. It rose to a high level from the early stages, reaching the glass transition point of the tested material. The final stage of the running experienced a dramatic increase in surface temperature, which causes the final gear teeth fractures. Further investigations using SEM revealed different surface tribology between the two sides of the gear tooth surface, because of the pitch misalignment angle.

8.1.5 Final comments

All test findings here can be considered in the light of polymer gear rating. Depending on the conditions and requirements, polymer gear wear can be controlled to the lowest amount using the revealed wear rate results. In addition, the observations of gear tooth surface tribology help understanding of the surface behaviour under different running conditions, which in consequence helps increase polymer gear running time and endurance. Also, gear surface temperature can be controlled to some acceptable limits that are governed by the glass transition temperature and melting temperature of the used polymer material.

8.2 Recommendations for future work

The polymer gear testing and tribological investigations undertaken here have revealed some interesting new data and understanding of such mechanical devices while running under different conditions. This information could improve the usability of polymer gears in more

standardized way. However, although different materials were used and variable conditions were examined, there are still be more undiscovered aspects that require more time, facilities and focused effort to be properly accounted. This section covers some of these aspects, with recommendations for the most immediate needs in future work.

Some improves to the testing methods could improve the accuracy of the tooth surface wear measurements. This improvement includes the development of the current used two test rigs. In addition, the after-test investigations could involve more accurate gear thickness measurements for more wear reading validation.

8.2.1 Testing optimisation

The test rigs used here have the significant advantage that they continually measure the gear tooth wear as a function of the running cycles. However, one limitation of the current rigs is that the measured reduction in tooth thickness is interfered with by any change in tooth deflection that is caused by the applied load. One current method to partially isolate the wear was to also measure the tooth thickness after the test. Another solution was to measure the wear rate as a function of rotation cycles, by defining the wear curve slope, which improved the accuracy of measurements and removed the effect of gross tooth deflection. For further improvement to the wear measurement accuracy, it is suggested that the current test rig design should be modified to eliminate this intervention in a way to satisfy the precise measurement of gear tooth surface wear. Carefully sited additional displacement sensors might achieve this.

8.2.2 Polymer materials

This research work covered three different polymer materials, namely acetal, nylon and polycarbonate. To gain more understanding of the mechanical and tribological behaviours of polymer gears relevant to a

wider range of potential applications, it is recommended to use similar methods to study other polymer materials. Further focus on polymer composite materials would be particularly beneficial. In addition, investigation into using different materials for the driving and driven gears could reveal improvements to the contact behaviour of the polymer gears and could lead to more applications.

8.2.3 Gear manufacturing methods

The tested gears wear produced using machine cut and injection moulding manufacturing techniques. While these are commonly used processes, some other manufacturing methods are used to produce polymer gears, which may have their own specific advantages and limitations. To understand the effect of each production method, there is need for similar research applied to each one of those processes.

8.2.4 Gear shape parameters

This research was carried out on standardized gear shape parameters. In addition, the gear dimensions were left constant in all experiments. Other gear shape parameters can affect the mechanical and tribological behaviour of the polymer gears. Further research is required to cover a widely representative range (ideally, all) of the different gear designs.

8.2.5 Gearing ratio

Because all tests wear done on driving and driven gears that have the similar properties, the gear contact ratio was always 1:1 in this current work. Therefore, it is recommended to study the effect of different gearing ratios on the surface contact behaviour of polymer gears, especially that the contact frequency will then be different by a significant factor between the driving and the driven gear.

BIBLIOGRAPHY

[1] White J. The Design and Evaluation of Polymer Composite Spur Gears. University of Birmingham, UK, 1998.

[2] Yousef SS. Performance and Design of Thermoplastic Gears. University of Waterloo, Canada, 1974.

[3] Drago RJ. Fundamentals of Gear Design. Boston: Butterworths; 1988.

[4] Mao K. The Performance of Dry Running Non-metallic Gears. The University of Birmingham, UK, 1993.

[5] American Gear Manufacturers Association. ANSI/AGMA 1006-A97: Tooth Proportions for Plastic Gears. Alexandria, VA: 1997.

[6] British Standards Institution. BS6168: Specification for non-metallic spur gears. 1987.

[7] Verein Deutscher Ingenieure Standards. VDI 2736 Part2: Thermoplastic gear wheels - Cylindrical gears - Calculation of the load-carrying capacity. 2014.

[8] Mott RL. Machine Elements in Mechanical Design. Pearson Education; 2013.

[9] Elmquist J. Deciding When to Go Plastic. Gear Technol 2014;July:46–7.

[10] Corus Plc. corporate governance. London: 2006.

[11] Rosato D V, Schott NR, Rosato MG. Plastics Institute of America Plastics Engineering, Manufacturing & Data Handbook. Springer Science & Business Media; 2001.

[12] Dasari A, Njuguna J. Functional and Physical Properties of Polymer

Nanocomposites. John Wiley & Sons; 2016.

[13] Ticona PLC. A guide to polymer gearing. Telford: 2006.

[14] Snyder L. At the “PEEK” of the Polymer Food Chain. Gear Technol June 2010:26–8.

[15] Dvorak PJ. More Bite for Plastic Gears. Mach Des 1988;60:75–80.

[16] Kono S. Increase in power density of plastic gears for automotive applications. University of Birmingham, 2002.

[17] Li Z, Mao K. Frictional effects on gear tooth contact analysis. Adv Tribol 2013;2013. doi:10.1155/2013/181048.

[18] Yelle H, Burns DJ. Calculation of contact ratios for plastic/plastic or plastic/steel spur gear pairs. J Mech Des 1981;103:528–42.

[19] Gauvin R, Girard P, Yelle H. Investigation of the Running Temperature of Plastic/Steel Gear Pairs. ASME Pap 1980;80.

[20] Radzevich SP. Theory of gearing: kinematics, geometry, and synthesis. CRC Press; 2013.

[21] Walton D, Shi YW. A comparison of ratings for plastic gears. Proc Inst Mech Eng Part C Mech Eng Sci 1989;203:31–8.

[22] Hooke CJ, Mao K, Walton D, Breeds AR, Kukureka SN. Measurement and Prediction of the Surface Temperature in Polymer Gears and Its Relationship to Gear Wear. J Tribol 1993;115:119–24. doi:10.1115/1.2920964.

[23] Evans SM, Keogh PS. Efficiency and running temperature of a polymer-steel spur gear pair from slip/roll ratio fundamentals. Tribol Int 2016;97:379–89. doi:10.1016/j.triboint.2016.01.052.

[24] Johnney Mertens A, Kumar P, Senthilvelan S. The effect of the mating gear surface over the durability of injection-molded

polypropylene spur gears. Proc Inst Mech Eng Part J J Eng Tribol 2016;230:1401–14.

[25] Yousef S, Osman TA, Abdalla AH, Zohdy GA. Wear Characterization of Carbon Nanotubes Reinforced Acetal Spur, Helical, Bevel and Worm Gears Using a TS Universal Test Rig. JOM 2015;67:2892–9. doi:10.1007/s11837-014-1268-5.

[26] Senthilvelan S, Gnanamoorthy R. Damage mechanisms in injection molded unreinforced, glass and carbon reinforced nylon 66 spur gears. Appl Compos Mater 2004;11:377–97.

[27] Pogačnik A, Tavčar J. An accelerated multilevel test and design procedure for polymer gears. Mater Des 2015;65:961–73. doi:10.1016/j.matdes.2014.10.016.

[28] Rider MJ. Design and Analysis of Mechanisms: A Planar Approach. Wiley; 2015.

[29] Juvinall RC, Marshek KM. Fundamentals of Machine Component Design, 5th Edition. Wiley; 2011.

[30] Walton D, Goodwin AJ. The wear of unlubricated metallic spur gears. Wear 1998;222:103–13. doi:https://doi.org/10.1016/S0043-1648(98)00291-9.

[31] Singh AK, Siddhartha, Singh PK. Polymer spur gears behaviors under different loading conditions: A review. Proc Inst Mech Eng Part J J Eng Tribol 2017:1350650117711595.

[32] Menezes P, Nosonovsky M, Ingole S, Kailas S, Lovell M. Tribology for scientists and engineers : from basics to advanced concepts. New York: Springer; 2013.

[33] Walton D, Cropper a B, Weale DJ, Meuleman PK. The efficiency and friction of plastic cylindrical gears Part 1: Influence of materials. Proc Inst Mech Eng Part J J Eng Tribol 2002;216:75–8.

doi:10.1243/1350650021543915.

[34] Mao K, Hooke C, Walton D. The wear behaviour of polymer composite gears. J Synth Lubr 1996;12:337–45.

[35] Mao K, Langlois P, Alharbi K, Hu Z, Xu X, Milson M, et al. The wear and thermal mechanical contact behaviour of machine cut polymer gears. Wear 2015;332–333:822–6. doi:10.1016/j.wear.2015.01.084.

[36] Kukureka SN, Chen YK, Hooke CJ, Liao P. The wear mechanisms of acetal in unlubricated rolling-sliding contact. Wear 1995;185:1–8. doi:10.1016/0043-1648(94)06575-6.

[37] Hooke CJ, Kukureka SN, Liao P, Rao M, Chen YK. The friction and wear of polymers in non-conformal contacts. Wear 1996;200:83–94. doi:10.1016/S0043-1648(96)07270-5.

[38] Dearn KD, Kukureka SN, Walton D. ENGINEERING POLYMERS AND COMPOSITES FOR MACHINE ELEMENTS. Polym. Tribol., IMPERIAL COLLEGE PRESS; 2009, p. 470–505. doi:doi:10.1142/9781848162044_0014.

[39] Hoskins TJ, Dearn KD, Chen YK, Kukureka SN. The wear of PEEK in rolling-sliding contact - Simulation of polymer gear applications. Wear 2014;309:35–42. doi:10.1016/j.wear.2013.09.014.

[40] Breeds AR, Kukureka SN, Mao K, Walton D, Hooke CJ. Wear behaviour of acetal gear pairs. Wear 1993;166:85–91. doi:10.1016/0043-1648(93)90282-Q.

[41] Mao K, Li W, Hooke CJ, Walton D. Friction and wear behaviour of acetal and nylon gears. Wear 2009;267:639–45. doi:10.1016/j.wear.2008.10.005.

[42] Li W, Wood A, Weidig R, Mao K. An investigation on the wear behaviour of dissimilar polymer gear engagements. Wear

2011;271:2176–83. doi:10.1016/j.wear.2010.11.019.

[43] Mao K. A numerical method for polymer composite gear flash temperature prediction. Wear 2007;262:1321–9. doi:10.1016/j.wear.2007.01.008.

[44] Mao K, Li W, Hooke CJ, Walton D. Polymer gear surface thermal wear and its performance prediction. Tribol Int 2010;43:433–9.

[45] Li S, Anisetti A. On the flash temperature of gear contacts under the tribo-dynamic condition. Tribol Int 2016;97:6–13. doi:10.1016/j.triboint.2016.01.027.

[46] Anifantis N, Dimarogonas AD. Flash and bulk temperatures of gear teeth due to friction. Mech Mach Theory 1993;28:159–64. doi:10.1016/0094-114X(93)90054-Y.

[47] André-Pascal R. Glossary of terms and definitions in the field of friction, wear and lubrication (tribology). Wear 1970;6:456.

[48] Abdelbary A. Wear of polymers and composites. Woodhead Publishing; 2015.

[49] Chen YK, Kukureka SN, Hooke CJ, Rao M. Surface topography and wear mechanisms in polyamide 66 and its composites. J Mater Sci 2000;35:1269–81.

[50] Crippa G, Davoli P. FATIGUE RESISTANCE OF GEARS. KUNSTSTOFFE-GERMAN Plast 1991;81:147–50.

[51] Hall KW, Alvord HH. Capacity of nylon plastic gears. Mach Des 1956:120–2.

[52] Merritt HE. Gears. Pitman; 1954.

[53] The British Standards Institution. The benefits of using standards n.d. https://www.bsigroup.com/en-GB/standards/benefits-of-using-standards/ (accessed February 8, 2017).

[54] Hogan O, Sheehy C, Jayasuriya R. The Economic Contribution of Standards to the UK Economy. Cent Econ Bus Res Ltd 2015:106.

[55] ETSI. Why we need standards 2017. http://www.etsi.org/standards/why-we-need-standards (accessed February 8, 2017).

[56] Sheridan D, Smith Z. Plastic Gear Standards: A Balancing Act. GEAR Technol 2007;March/Apri:14–5.

[57] Verein Deutscher Ingenieure Standards. VDI 2545: Gear Wheels Made From Thermoplastics 1981.

[58] German National Standard. DIN 3990: Calculation of load capacity of cylindrical gears; introduction and general influence factors 1987.

[59] The British Standards Institution. BS 6168:1987 Specification for non-metallic spur gears. BSI Stand 1987:50.

[60] Hachmann H, Strickle E. Design of nylon gears. SPE J., vol. 24, 1968, p. 39.

[61] Hachmann H, Strickle E. Polyamide als Zahnradwerkstoffe. 1966.

[62] Pogačnik A, Tavčar J. Accelerated Testing and Temperature Calculation of Plastic Gears. Gear Solut 2016;December:35–40.

[63] American Gear Manufacturers Association. AGMA 920-A01: Materials for Plastic Gears. 2001.

[64] American Gear Manufacturers Association. AGMA 920-B15: Materials for Plastic Gears. 2015.

[65] United States of America Standards Institute, American Gear Manufacturers Association. AGMA 201.A2: Tooth Proportions for Coarse-pitch Involute Spur Gears. (Inactive). American Gear Manufacturers Association; 1968.

[66] American Gear Manufacturers Association. ANSI/AGMA 1003-G93: Tooth Proportions for Fine-Pitch Involute Spur and Helical Gears. 1992.

[67] American Gear Manufacturers Association. ANSI/AGMA 1106-A97: Tooth Proportions for Plastic Gears (Metric Edition). 1997.

[68] American Gear Manufacturers Association. AGMA 909-A06: Specifications for Molded Plastic Gears. 2006.

[69] American Gear Manufacturers Association. ANSI/AGMA 2000-A88: Gear Classification and Inspection Handbook - Tolerances and Measuring Methods for Unassembled Spur and Helical Gears (Including Metric Equivalents). 1988.

[70] Goldfarb V, Trubachev E, Barmina N, editors. Advanced Gear Engineering. vol. 51. Cham: Springer International Publishing; 2018. doi:10.1007/978-3-319-60399-5.

[71] Merritt HE. Gear engineering. Pitman; 1971.

[72] Cornelius EA, Budich IW. Investigation of gears of acetal resins. Konstruktion 1970;22:103–16.

[73] Karimpour M, Dearn KD, Walton D. A kinematic analysis of meshing polymer gear teeth. Proc Inst Mech Eng Part L J Mater Des Appl 2010;224:101–15. doi:10.1243/14644207jmda315.

[74] van Melick HGH. Tooth-bending effects in plastic spur gears. Gear Technol 2007:58–66.

[75] Mao K. A new approach for polymer composite gear design. Wear 2007;262:432–41.

[76] Mao K, Hooke C, Walton D. The wear behaviour of polymer composite gears. J Synth Lubr 1996;12:337–45. doi:10.1002/jsl.3000120405.

[77] Bravo A, Koffi D, Toubal L, Erchiqui F. Life and damage mode modeling applied to plastic gears. Eng Fail Anal 2015;58:113–33. doi:10.1016/j.engfailanal.2015.08.040.

[78] Cropper A. The failure mode analysis of plastic gears. University of Birmingham, 2003.

[79] Düzcükoğlu H, Düzcükoğlu H. PA 66 spur gear durability improvement with tooth width modification. Mater Des 2009;30:1060–7. doi:10.1016/j.matdes.2008.06.037.

[80] Imrek H, İmrek H. Performance improvement method for Nylon 6 spur gears. Tribol Int 2009;42:503–10. doi:10.1016/j.triboint.2008.08.011.

[81] American Gear Manufacturers Association. Nomenclature of gear-tooth wear and failure 1964;110.03.

[82] Stachowiak GW. Wear: materials, mechanisms and practice. John Wiley & Sons; 2006.

[83] Marshek KM, Chan PKC. Qualitative analysis of plastic worm and worm gear failures. Wear 1981;66:261–71.

[84] Dearn K. An investigation into tribological and performance related aspects of polymeric gearing. University of Birmingham, 2008.

[85] Luscher A, Houser DR. An investigation of the geometry and transmission error of injection molded gears. J Inject Molding Technol 2000;4:177.

[86] Kurokawa M, Uchiyama Y, Nagai S. Performance of plastic gear made of carbon fiber reinforced poly- ether-ether-ketone. Tribol Int 2000;32:491–7.

[87] Friedrich K. Friction and wear of polymer composites. Elsevier; 1986.

[88] Lancaster JK. Estimation of the limiting PV relationships for thermoplastic bearing materials. Tribology 1971;4:82–6. doi:10.1016/0041-2678(71)90136-9.

[89] Archard JF. Contact and rubbing of flat surfaces. J Appl Phys 1953;24:981–8. doi:10.1063/1.1721448.

[90] Friedrich K, Reinicke P. Friction and wear of polymer-based composites. Mech Compos Mater 1998;34:503–14. doi:10.1007/BF02254659.

[91] Senthilvelan S, Gnanamoorthy R. Effect of rotational speed on the performance of unreinforced and glass fiber reinforced Nylon 6 spur gears. Mater Des 2007;28:765–72.

[92] Kukureka SN, Hooke CJ, Rao M, Liao P, Chen YK. The effect of fibre reinforcement on the friction and wear of polyamide 66 under dry rolling–sliding contact. Tribol Int 1999;32:107–16. doi:10.1016/S0301-679X(99)00017-1.

[93] Takanashi S, Shoji A. On the Temperature Risc in the Teeth of Plastic Gears. Int. Power Transm. Gearing Conf. San Fr., 1980.

[94] Wright N., Kukureka S. Wear testing and measurement techniques for polymer composite gears. Wear 2001;251:1567–78. doi:10.1016/S0043-1648(01)00793-1.

[95] Mertens AJ, Senthilvelan S. Surface durability of injection-moulded carbon nanotube–polypropylene spur gears. Proc Inst Mech Eng Part L J Mater Des Appl 2016:1464420716654308.

[96] Blok H. The flash temperature concept. Wear 1963;6:483–94. doi:10.1016/0043-1648(63)90283-7.

[97] Archard JF. The temperature of rubbing surfaces. Wear 1959;2:438–55.

[98] Gianattasio R. Engineering Essentials: Lubrication Tips for Plastic Gears and More (Part 2). Mach Des 2000. http://www.machinedesign.com/mechanical-drives/engineering-essentials-lubrication-tips-plastic-gears-and-more-part-2 (accessed March 5, 2018).

[99] Gordon DH, Kukureka SN. The wear and friction of polyamide 46 and polyamide 46/aramid-fibre composites in sliding–rolling contact. Wear 2009;267:669–78.

[100] Düzcükoğlu H. Study on development of polyamide gears for improvement of load-carrying capacity. Tribol Int 2009;42:1146–53. doi:10.1016/j.triboint.2009.03.009.

[101] Terashima K, Tsukamoto N, Nishida N. Development of plastic gears for power transmission: design on load-carrying capacity. Bull JSME 1986;29:1326–9.

[102] TEC. Motor Datasheet. 2013.

[103] ABB. Low voltage motors: Motor guide. 3rd ed. 2014.

[104] RDP Electronics. DCV Series Isolated 0 to 10V Output Displacement Transducer Data Sheet 2015.

[105] DuPont Thermoplastics Data. Delrin® 500P NC010 (POM) (Acetal resin) datasheet 2017.

[106] DuPont Thermoplastics Data. Delrin® HTNFE8200 NC010 (High performance PA resin) 2018.

[107] DSM Engineering Plastics. Stanyl® TW341 (High-performance PA 46) data sheet 2018. https://plasticsfinder.com/en/datasheet/Stanyl® TW341/V67x4 (accessed April 14, 2018).

[108] FLIR Systems Inc. User's manual FLIR T4xx series. 2016.

[109] Ensinger. Polyamide 66 Data Sheet. 2014.

[110] DuPont Engineering Polymers. Acetal 500P Data Sheet. 2008.

[111] DSM Engineering Plastics. Polyamide 46 Data Sheet. 2011.

[112] Bayer Material Science LLC. Polycarbonate Data Sheet. 2008.

[113] Nikon Corporation. Digital camera D5200 reference manual. Tokyo: 2012.

[114] NOKIA Corporation. Nokia stereoscopic microscope SMZ-2T Instructions. Tokyo: n.d.

[115] Reichert. Reichert-Jung POLYVAR Manual. Vienna: n.d.

[116] Reichert. Reichert-Jung ULTRACUT Manual. n.d.

[117] FEI. Philips XL30 TMP Scanning Electron Microscope: Product Data Sheet. Eindhoven: n.d.

[118] Hooke CJ, Kukureka SN, Liao P, Rao M, Chen YK. Wear and friction of nylon-glass fibre composites in non-conformal contact under combined rolling and sliding. Wear 1996;197:115–22. doi:10.1016/0043-1648(95)06828-7.

[119] DuPont Thermoplastics Data. Delrin® 500P NC010 (POM) (Acetal homopolymer resin) datasheet 2016. http://dupont.materialdatacenter.com/profiler/e0GK0/standard/main/ds/11831/4097 (accessed November 29, 2016).

[120] ULPROSPECTOR. Polyamide 66 datasheet 2016. https://materials.ulprospector.com/Profile.aspx?I=34&E=234394#DV_DS (accessed November 28, 2016).

[121] Voss H, Friedrich K. On the wear behaviour of short-fibre-reinforced peek composites. Wear 1987;116:1–18. doi:10.1016/0043-1648(87)90262-6.